PHENANTHROPIPERIDINE ALKALOIDS: METHODOLOGY DEVELOPMENT, SYNTHESIS AND BIOLOGICAL EVALUATION

BY

Micah James Niphakis

Submitted to the graduate degree program in Medicinal Chemistry and the
Graduate Faculty of the University of Kansas
in partial fulfillment of the requirements for the degree of
Doctor of Philosophy.

_____
Chair

Committee:_____

_____

_____

_____

Date defended:_____

This Dissertation Committee for Micah J. Niphakis certifies
that this is the approved version of the following dissertation:

PHENANTHROPIPERIDINE ALKALOIDS: METHODOLOGY DEVELOPMENT, SYNTHESIS AND BIOLOGICAL EVALUATION

_____
Chair

Committee:_____

_____

_____

_____

Date defended:_____

This work is dedicated to my parents, Stavros and Holly.

ACKNOWLEDGEMENTS

The past five years of research would have been impossible without the gracious support my mentors, coworkers, friends and family. Firstly, I wish to thank Professor Gunda Georg who has been an exemplary doctoral research advisor and has introduced me to the multifaceted nature of Medicinal Chemistry. She has been a constant source of guidance and encouragement in the midst of my blunders and struggles to become an independent scientist and I am immeasurably grateful.

I am also greatly indebted to the faculty of the department of Medicinal Chemistry and Chemistry at the University of Kansas who have indelibly shaped my understanding of the molecular world and kindled a sense of wonder that has been the impetus of my own research. Professor Jeffrey Aubé, in particular, has been an outstanding model of an academic scientist and has provided invaluable guidance and support for my scientific career. Professors Gunda Georg, Jeffrey Aubé, Gary Grunewald and Paul Hanson are especially thanked for their strong letters of support which have played a pivotal role in fellowship and post-doctoral applications. I also thank Professors Georg, Aubé, Hanson, Carlson and Dutta for graciously serving as members of my oral examination committee.

The majority of my graduate career has been spent at the University of Minnesota (UMN) where I have greatly benefited from the support of the faculty and coworkers in the Institute for Therapeutics Discovery and Development (ITDD). As such, I must thank the department of medicinal chemistry at the UMN for infusing me into their program despite my foreign status. Specifically, I wish to thank Dr. Michael Walters, who has become indispensable to

the Georg group, for many enlightening discussions and for guidance in my research. I also thank Dr. Derek Hook, Dr. Jonathan Solberg and Dr. Harry Tian for carrying out cytotoxicity and metabolic studies on short notice. My work has been supported by the service of the National Institute of Health-Psychoactive Drug Screening Program under Director Bryan Roth, M.D., Ph.D. whom I thank. Victor G. Young, Jr. of the University of Minnesota X-Ray Crystallographic Laboratory is thanked for determining the X-ray crystal structure of compound **2.38**.

Thanks is given to financial supporters: National Institutes of Health (Grants CA90602, GM069663, GM076302 and GM081267), the Kansas Masonic Cancer Research Institute, the University of Minnesota through the Vince and McKnight Endowed Chairs and ACS Division of Medicinal Chemistry (Predoctoral fellowship).

The Georg group and my fellow graduate students have been vital for supporting my graduate studies as well. Those who have made a substantial impact include Brandon Turunen and Haibo Ge whom I thank for their foundational work that made much of my research possible. I owe much thanks to Matthew Leighty, Oliver Hutt and Keith Ellis for their mentorship and advice, right my the start of my graduate studies. Also, I am grateful to Andrea Knickerbocker for her extensive and essential role in the Georg group and for her friendship.

My parents deserve my utmost thanks. They have made immense sacrifices to provide an education for me and have shown unrivaled support throughout my life. Last, and certainly not least, I wish to thank my wife and best friend, Easten, whose love, patience and support has been my sustenance through the most difficult times of my graduate career.

ABSTRACT

Phenanthropiperidine Alkaloids: Methodology Development, Synthesis and Biological Evaluation

Micah J. Niphakis, Ph. D.
The University of Kansas, 2010

The phenanthropiperidines are remarkably potent anti-proliferative alkaloids. Only one member of this class has been tested in the clinic, but the trials were terminated shortly thereafter due to adverse neurological side-effects. This work is directed towards the development of safe phenanthropiperidines for the treatment of cancer. It focuses on synthetic methodologies that facilitate their preparation and biological studies to better understand their neurological effects.

The preparation of cyclic enaminones in high enantiomeric purity is made possible through a one-flask, two-step protocol that uses mild Boc-deprotection conditions to suppress racemization. This reaction enables the preparation of monocyclic and bicyclic, six- and seven-membered enaminones, some of which can be used as precursors to phenanthropiperidine alkaloids.

Elaboration of the enaminone scaffold was made possible with a direct palladium(II)-catalyzed arylation using aryltrifluoroborates as coupling partners. Combined with the enaminone methodology this approach gives rapid access to enantiomerically pure 3-

arylpiperidines. The utility of these scaffolds were demonstrated in the synthesis of two natural products: (+)-ipalbidine and (+)-antofine.

A short and high-yielding synthetic route has also been devised to provide tylocrebrine, the only phenanthropiperidine to enter clinical trials. We report the first enantioselective synthesis of tylocrebrine which uses a novel aryl-alkene oxidative coupling reaction that surmounts the historical challenge of obtaining a single phenanthrene regioisomer. A small collection of tylocrebrine analogs were prepared and studied along with tylocrebrine to elucidate the cause of tylocrebrine's neurological side-effects. Although the causes remain elusive, tylocrebrine and several of its analogs were found to bind to key biogenic amine receptors, disclosing another potential risk factor for their therapeutic use. The phenanthrene substitution pattern, however, had an marked influence on binding and could be used to minimize these off-target interactions.

TABLE OF CONTENTS

Chapter 2

Synthesis of Six- and Seven-Membered Cyclic Enaminones: Optimization, Scope and Mechanistic studies

Chapter 3

Palladium(II)-Catalyzed Cross-Coupling of Cyclic Enaminones and Organotrifluoroborates

LIST OF FIGURES

CHAPTER 1

CHAPTER 2

CHAPTER 3

CHAPTER 4

CHAPTER 5

List of Tables and Graphs

Chapter 1

Chapter 2

CHAPTER 3

CHAPTER 4

CHAPTER 5

LIST OF COMPOUNDS

CHAPTER 2

CHAPTER 3

CHAPTER 5

ABBREVIATIONS

Ac	acetyl
ACN	azobis-cyclohexanecarbonitrile
AFP	alpha-fetoprotein
AIBN	azobisisobutyronitrile
Ar	aryl
araC	arayinoside cytosine
BBB	blood-brain barrier
Bn	benzyl
Boc	*tert*-butoxycarbonyl
BQ	benzoquinone
br	broad
CAN	ammonium cerium (IV) nitrate
Cbz	carbobenzyloxy
CDK	cyclin-dependent kinase
CNS	central nervous system
Cp	cyclopentadienyl
CPT	camptothecin
d	doublet
d.r.	diastereomeric ratio
DA	dopamine
DAT	dopamine active transporter
dCK	deoxycytidine kinase
DIAD	diisopropyl azodicarboxylate
DIBAL-H	diisobutylaluminium hydride
DMAP	4-dimethylaminopyridine
DME	dimethoxyethane

DMF	dimethylformamide
DMSO	dimethyl sulfoxide
DNA	deoxyribonucleic acid
DNFB	dinitrofluorobenzene
dppf	1,1'-bis(diphenylphosphino)ferrocene
DTH	delayed-type hypersensitivity
e.r.	enantiomeric ratio
EDCI	1-ethyl-3-(3-dimethylaminopropyl) carbodiimide
EtOAc	ethyl acetate
EtOH	ethanol
FEV_1	forced expiratory volume in 1 second
fod	6,6,7,7,8,8,8-heptafluoro-2,2-dimethyl-3,5-octanedionate
GPCR	G-protein coupled receptor
h	hour
HASPO	4,4,5,5-tetramethyl-1,3,2-dioxaphospholane 2-oxide
HBD	hydrogen bond donor
HIF-1	hypoxia-inducible factor I
HIR	humoral immune response
HPLC	high performance liquid chromatography
HRP	horseradish peroxidase
HU	hydroxyurea
i-Pr	isopropyl
i.p.	intraperitoneal
i.v.	intravenous
IR	infrared
K_D	dissociation constant
LAH	lithium aluminum hydride
LDA	lithium diisopropyl amide

LPS	lipopolysaccharide
m	multiplet
MAO	monoamine oxidase
MBC	maximum breathing capacity
MDR	multidrug resistant
Me	methyl
MeOH	methanol
μW	microwave
min	minutes
MPP+	1-methyl-4-phenylpyridinium
MPPP	1-methyl-4-phenyl-4-propionoxypiperidine
MPTP	1-methyl-4-phenyl-1,2,3,6-tetrahydropyridine
MRP	multidrug resistance protein
Ms	mesyl
MW	molecular weight
NADH	nicotinamide adenine dinucleotide
NBS	*N*-bromosuccinamide
NCI	National Cancer Institute
NET	norepinephrine transporter
NMM	*N*-methylmorpholine
NMR	nuclear magnetic resonance
PDSP	psychoactive drug screening program
PEFR	peak expiratory flow rate
P-gp	P-glycoprotein
Ph	phenyl
PIFA	(bis(trifluoroacetoxy)iodo)benzene
PK	pharmacokinetic
PMP	p-methoxyphenyl

PNS	peripheral nervous system
PPA	polyphosphoric acid
PSA	polar surface area
rac	racemic
RNA	ribonucleic acid
RR	ribonucleotide reductase
rt	room temperature
s-Bu	*sec*-butyl
S-Phos	dicyclohexyl(2',6'-dimethoxy-[1,1'-biphenyl]-2-yl)phosphine
SAR	structure-activity relationship
SERT	serotonin transporter
SN-38	7-ethyl-10-hydroxycamptothecin
SRBC	sheep red blood cells
t	triplet
t-Bu	*tert*-butyl
TBAF	tetra-*N*-butylammonium fluoride
TBS	*tert*-butyldimethylsilyl
TEA	triethylamine
Tf	trifluoromethanesulfonyl
TFA	trifluoroacetic acid
TFAA	trifluoroacetic anhydride
THF	tetrahydrofuran
TMS	trimethylsilyl
TMV	tobacco mosaic virus
Topo I	topoisomerase I
Topo II	topoisomerase II
TsOH	toluenesulfonic acid
VEGF	vascular endothelial growth factor

VC	vital capacity
VP-16	etoposide
XRCC1	X-ray repair cross-complementing gene I

CHAPTER 1

INTRODUCTION TO PHENANTHROPIPERIDINE ALKALOIDS

1.1 Introduction

With the historical success of pharmacognosy, nature continues to be scoured for new drug leads. The discovery of a medicinally active natural product, however, is only the beginning of the arduous venture of drug development. Nature-derived drug leads often require considerable optimization before they are of any instrumental value and the phenanthropiperidines, the subject of this work, are a case in point. These alkaloids have been pursued as leads for the treatment of cancer and immune-related diseases for over 50 years yet not a single member has emerged for clinical use. Some have abandoned the effort, while others tenaciously pursue next generation phenanthropiperidines with hope that this class is still redeemable. The reasons that undergird both of these positions will be explored in the following pages.

Like many bioactive natural products, the phenanthropiperidines were isolated from plants that had been used in folk medicine for untold centuries.[1] The reputed therapeutic value of *Tylophora indica* (*asthmatica*) spurred early scientific activity that sought to validate and characterize its biological effects. In spite of periodic lapses of interest over the past six decades, these alkaloids are now receiving more attention than ever. This renewed interest is

attributable to recent advances in biotechnology that have just begun to uncover the profound biochemical remodeling induced by these alkaloids in living systems that could be harnessed to treat disease. Herein, we give an extensive review of the literature related to the chemistry and biology of the phenanthropiperidine class. This review differs from previous ones[2-5] in that it is not limited to recent findings, and its scope extends deeper into the pharmacology of these alkaloids. The purpose of this work is to consolidate the widely dispersed literature on this subject to encourage a holistic understanding of what contributes to their potential use as medicinal agents. In this regard, special attention will be given to pharmacologically relevant details in order to comprehend better the poorly understood mechanism of action to assess therapeutic value. Considering that drug or lead accessibility is a major contributor to the success of natural product- and naturally-derived medicinal agents, we will also discuss precedent for the preparation of these alkaloids. Ideally, this compendium will expose impediments to clinical success and will encourage and guide the refinement process in a preclinical environment.

1.2 Background

1.2.1 Discovery of tylophorine, tylophorinine, cryptopleurine and tylocrebrine

Folk medicines are a rich source of incipient drugs that are laden with clues for therapeutic use. The phenanthropiperidines owe their discovery to an Indian household remedy, now called *T. indica* that was brought to the attention of Western scientists in the late

19th century.[6] The roots and leaves of this perennial climbing plant have been used for a broad spectrum of medical conditions, and it is listed as an important member of the Indian materia medica.[7] In 1935, with the aim of isolating the active constituents of this natural remedy, Ratnagiriswaran *et al.* extracted and purified two alkaloids, naming them tylophorine and tylophorinine (Fig. 1–1).[7] The structure of tylophorine was not determined until 1960 after several years of degradation studies and comparison with the synthetically-derived natural product.[8-12] The proposed structure contained an indolizidine heterocycle fused to a symmetrically substituted phenanthrene.[13] The stereochemistry, which had been mistakenly assigned earlier,[14] was unambiguously assigned as *R* following a total synthesis and comparison of the optical rotation with the isolated alkaloid.[15] Although tylophorine was the first member of its class to be isolated, another phenanthropiperidine had been characterized several years before its structure was determined.

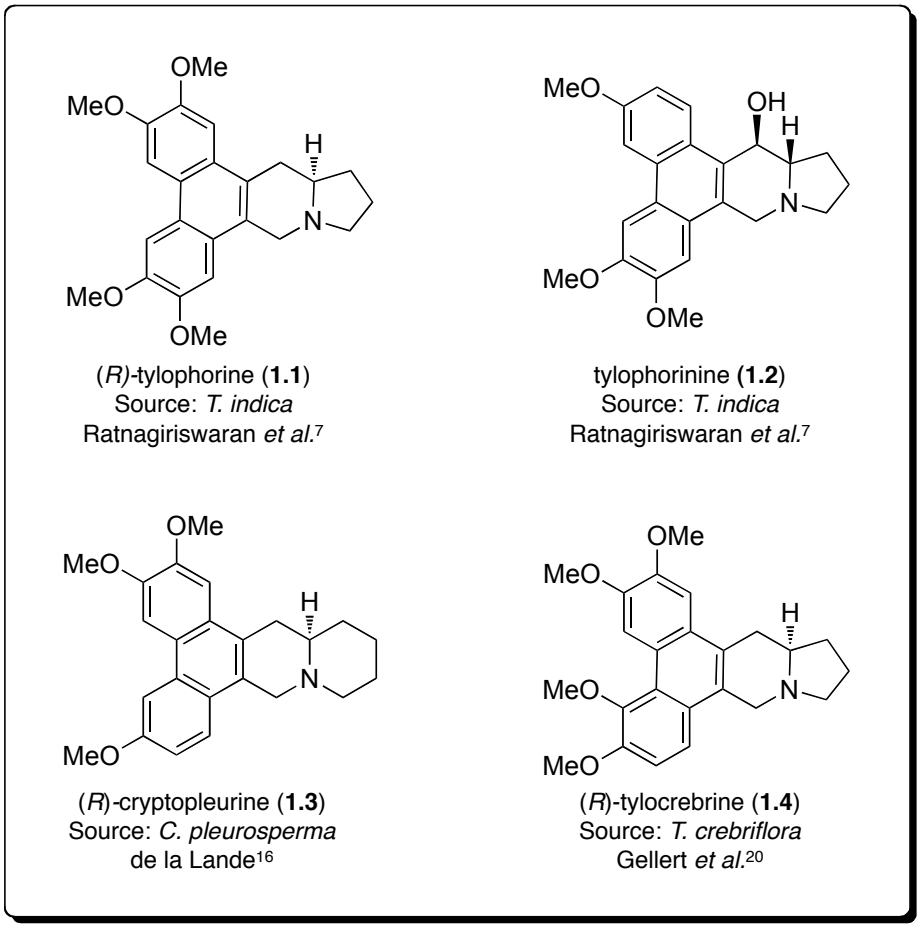

Fig. 1–1. Structure of first discovered phenanthropiperidines.

In 1948 de la Lande reported the isolation of a highly toxic substance named cryptopleurine that had been extracted from *Cryptocarya pleurosperma*, a walnut tree indigenous to Austrailia.[16] Seminal pharmacological studies demonstrated that cryptopleurine was lethal in rat, mouse, rabbit, dog and cat models (LD_{50} 1.5 to 5 mg/kg). It also became apparent that the alkaloid was a potent skin irritant. Upon oral administration, rats developed blisters on the face and feet. Furthermore, topical administration in human volunteers produced vessication on the arm and face that lasted over two weeks. Moreover, gastrointestinal inflammation and ulceration were found in histological studies of rabbits that

had received oral dosages of the alkaloid. In 1954, the structure of cryptopleurine was determined through X-ray diffraction studies of its methiodide congener making it the first member in its class with a known structure.[17-19]

In any discussion of the history of phenanthropiperidines a fourth member of this class, tylocrebrine, is worthy of note. This alkaloid was isolated in 1962 from a North Queensland vine, *T. crebriflora* which also had vesicant properties.[20] The major alkaloid, tylocrebrine, was found to be a regioisomer of tylophorine. With accumulating evidence that phenanthropiperidine alkaloids have anti-cancer properties, tylocrebrine was tested and found to be considerably more effective than tylophorine, tylophorinine and crytopleurine in the several cancer models.[21] Clinical testing began in 1965, only three years after its isolation.[2] Unfortunately, there were unforeseen problems with the alkaloid and the clinical trials were terminated before tylocrebrine's therapeutic efficacy could be established. Suffness reported that the studies were terminated due to CNS side-effects.[2] It is of no surprise that medicinal interest in these alkaloids waned in the years to follow. Cryptopleurine was an undiscriminating poison, tylophorine and tylophorinine had only mediocre activity, and worse yet, tylocrebrine, the most promising candidate, was potentially neurotoxic.

1.2.2 Phenanthropiperidine isolation and structural features

Since 1965, over 60 phenanthropiperidines and closely related analogs have been isolated and characterized. To date, they have been found primarily in two plant families, the Asclepiadaceae and Moraceae. Five genera (*Tylophora*, *Cynanchum*, *Vincetoxicum*,

Pergularia, and *Antitoxicum*) out of the 300 genera in the Asclepiadacea family are known to contain these alkaloids compared with only one genus (*Ficus*) from the Moraceae family.[5] These plants are found throughout Asia, Africa, Australia and the Pacific Islands (*e.g.* Taiwan, Japan and the Philippines). The details of the isolation studies fall outside of the scope of this work. Fortunately, there are several reviews on this subject already.[2, 4]

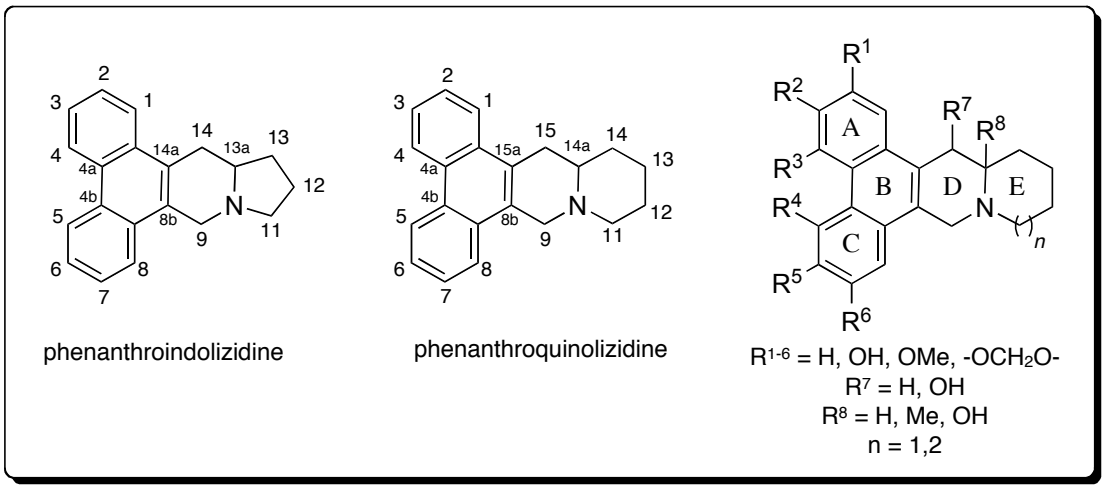

Fig. 1–2. General structural features of the phenanthropiperidines.

The general structural features of these alkaloids are a bicyclic nitrogenous heterocycle and a polyoxygenated phenanthrene system (Fig. 1–2). The phenanthrene portion is generally substituted with three to five methoxy or hydroxy groups, although methylenedioxy substituents have been isolated as well.[22, 23] A pyrrolidine or a piperidine make up the terminal aliphatic heterocycle (ring E), hence the names phenanthro*indolizidine* and phenanthro*quinolizidine*. (4a,4b)-Seco- and dehydro-derivatives (Fig. 1–3)—where ring D is fully aromatized—are frequently isolated along with their phenanthropiperidine parent

compounds showing a spectrum of oxidation states that exist within the plant.[3, 4] Oxygenation can also occur as evidenced by indolizidines and quinolizidines bearing a hydroxyl functionality at C14 or C15, respectively. Moreover, an oxygen atom can be introduced at the nitrogen resulting in phenanthroindolizidine *N*-oxides.[24] Johns *et al*. isolated a rare phenanthroquinolizidine alkaloid, cryptopleuridine, which possesses a C12-hydroxyl group.[25] To date, this is the only known, natural phenanthropiperidine that has a functionalized ring E system.

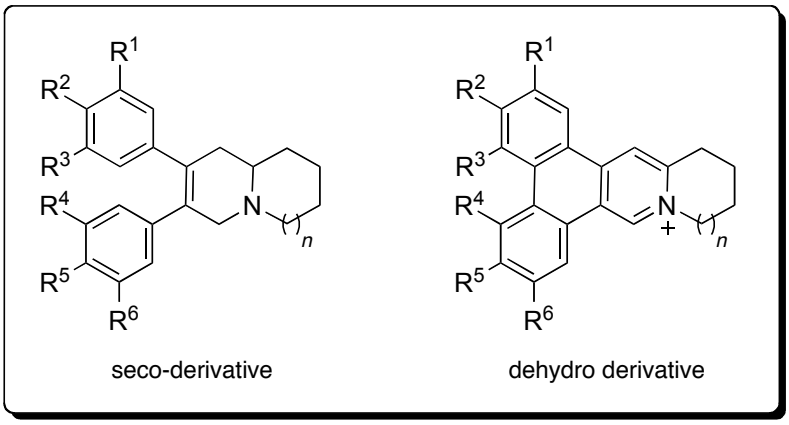

Fig. 1–3. Under- and over-oxidized scaffolds.

In 1984, another structural anomaly was observed in the alkaloids of cultivated *T. hirsuta.* [26, 27] These natural products were essentially identical to several phenanthroindolizidines already isolated except they had a 13a-methyl substitution (R^8 = Me). Recently, Pettit and coworkers isolated and characterized several more of these alkaloids from *Hypoëstes verticillaris*.[28] Interestingly, in wild populations of *T. hirsuta,* the principal alkaloidal constituent bears a hydroxyl group at the ring juncture (R^8 = OH) in lieu of an angular methyl group.[29] This labile hemiketal functionality has since been identified in several tyloindicines

isolated in 1991 by Ali and coworkers (Fig. 1–4).[30] Besides the rare 13a-hydroxy group that appears in tyloindicine F and G, these anomalous members also have a precariously positioned olefin (15, 15a) that is out of conjugation with ring C.

The natural variety that is found within this class has aided an understanding of structure-activity relationships (SARs) and provided swathes of targets for synthetic organic chemists. These will be discussed in detail later on. For our current purposes it is important to point out that practical synthetic routes have provided a sustainable source of many of these alkaloids and, in those cases, total syntheses have supplanted isolation efforts.

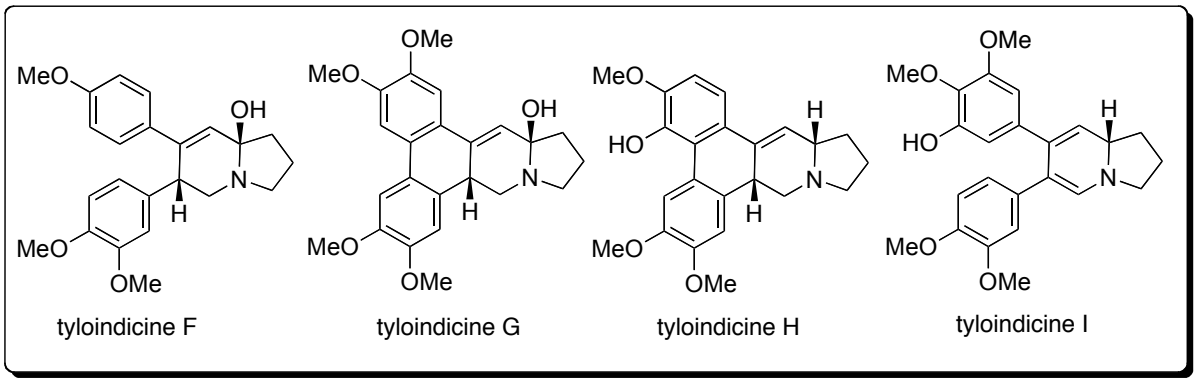

Fig. 1–4. Unusual structures of tyloindicines F–I.

1.2.4 Biosynthesis

Although the biosynthesis of the phenanthroindolizdines is better understood than that of the phenanthroquinolizidines, it is likely that the pathways are analogous.[31] A representative biosynthetic pathway is outlined in Scheme 1–1. It should be noted that the extent of phenolic methylation of each intermediate is uncertain and is most likely liberally regulated

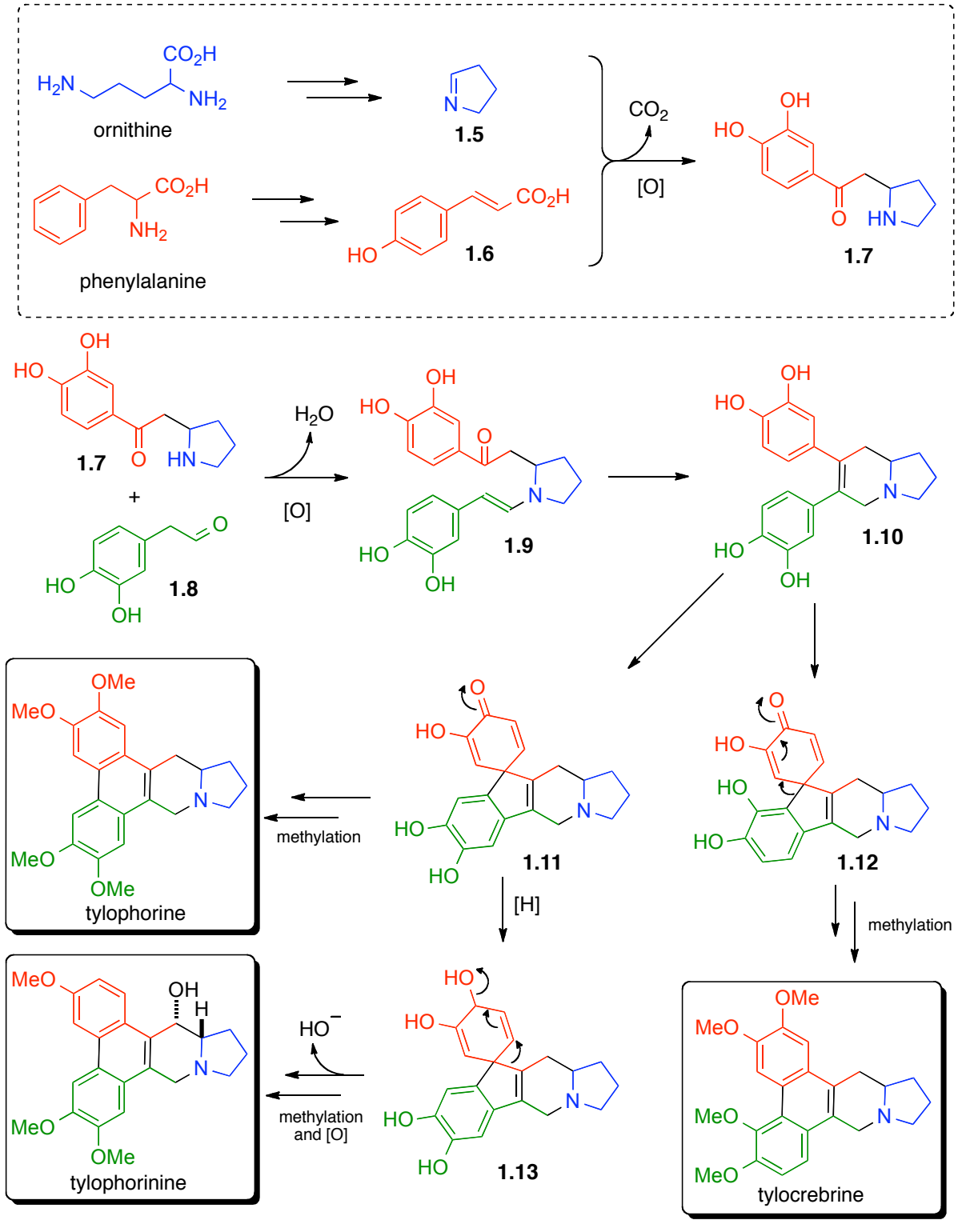

Scheme 1–1. Proposed biosynthesis of phenanthropiperidines.

as evidenced by the diversity seen in the natural products, the representative structures in Scheme 1–1 notwithstanding. These pentacyclic alkaloids are thought to be derived from tyrosine,[32] phenylalanine[33] and ornithine.[32] The phenanthroquinolizidine biosynthesis varies only with respect to the latter precursor, which is derived from lysine instead. In the indolizidine class, the pyrrolidine carbons originate from ornithine which decarboxylates, deaminates and cyclizes to pyrroline (**1.5**). This cyclic imine further reacts with cinnamic acid **1.6**[34]—synthesized from phenylalanine—affording a carboxylic acid intermediate (not shown). Following decarboxylation and alcohol oxidation, amine **1.7** undergoes condensation with 3,4-dihydroxyphenylacetaldehyde (**1.8**) which is derived from tyrosine.[35] The resultant enamine (**1.9**) cyclizes and upon dehydration yields the seco-derivative **1.10**. As already discussed, isolation of the seco-derivatives is relatively facile and gives support to this biosynthetic pathway. The final transformation is thought to proceed through an oxidative coupling and subsequent rearrangement,[34] but no direct evidence has been garnered to support or contradict this hypothesis.

Mulchandani *et al.* suggest that this process is initiated with the formation of dienones **1.11** or **1.12** through ortho- or para-phenolic couplings. The strained spirocycles then undergo a 1,2-alkyl shift to consummate the biosynthetic sequence of tylophorine or tylocrebrine. Another fate for spirocyle **1.11** was also proposed to explain the formation of tylophorinine. In this scenerio, dienone **1.11** is reduced to dienol **1.13** prior to rearrangement resulting in the elimination of hydroxide upon phenanthrene formation. Despite the remaining ambiguities of the latter sequence, this mechanistic hypothesis is plausible when considering its resemblance to the phenolic couplings seen in the biogenesis of morphine.[36]

Furthermore, this hypothesis has considerable explanatory power, needing minimal revision to explain the biogenetic origins of multiple naturally occurring phenanthropiperidines.

1.3 Biology of *Tylophora indica*

Tylophora extracts have gained considerable attention for the treatment of inflammatory diseases and, to a much lesser extent, cancer. Chitnis *et al*. investigated the cytotoxic properties of leaf and plant extract of *T. indica* in mice presenting transplantable leukemia tumors (either L1210 or P388).[37] Notably, mice receiving daily doses of extract survived longer than those treated with a placebo. Since the anti-cancer properties of *T. indica* have been attributed primarily to specific phenanthropiperidine alkaloids, most investigations have focused on the pharmacology of the purified alkaloids rather than on plant-derived mixtures and hence will be discussed later. On the other hand, the efficacy and mode of action of *T. indica* for the treatment of immune disorders, such as asthma, have been extensively investigated.

1.3.1 Clinical studies

Six clinical studies have been conducted using the extracts of *T. indica* for the treatment of asthma (Table 1–1). Shivpuri *et al.* conducted two double-blind clinical investigations of *T. indica.*[38, 39] In these studies, the leaves of *T. indica* were administered to over 100 patients with asthma and allergic rhinitis. After a six-day regimen, patients experienced significant

symptomatic relief that lasted for several weeks. In a follow-up study, ethanolic extracts were administered to 195 asthmatics.[40] Over 50% experienced moderate to complete symptomatic cessation compared with 31% of patients taking a placebo. Four other clinical investigations have been conducted with either extracts or powdered plant material.[41-43] Two studies showed appreciable symptomatic remission, while the other reported no statistically significant difference between patients receiving the treatment and placebo. In pursuit of a physiological explanation for the apparent symptomatic relief, Gore *et al.* demonstrated that dried leaf powder had immunosuppressive properties.[44] Interestingly, the immunosuppression, as judged by an eosinophil count, coincided with elevated 17-ketosteroid secretion, suggesting an indirect effect through stimulation of the adrenal cortex. Notably, increased levels of eosinophils in the sputum of asthmatics have a strong correlation with bronchial inflammation.[45]

Table 1–1. Clinical studies with *T. indica* for the treatment of asthma.

reference	source	# of participants	study length	results
Shivpuri[39]	leaves	166	6 days	50–100% Symptomatic relief
Shivpuri[38]	leaves	110	12 weeks	62% vs. 28% (control) Improvement at 6 days; 16% Improvement at 12 weeks
Shivpuri[40]	EtOH extract	195	12 weeks	50% of participants experienced symptomatic relief vs. 31% of placebo
Mathew[43]	alkaloid extract	123	12 weeks	Improvement in symptomatic relief and FEV_1 Effects peak at 4 weeks
Gupta[41]	powdered plant	135	3 weeks	No significant improvement of symptoms
Thiruvengadam[42]	dried leaf powder	30	16 days	Nocturnal dyspnea symptoms improved Sustained rise in MBC, VC and PEFR
Gore[44]	dried leaf powder	29	4 weeks	Decreased eosinophile count; Increased 17-ketosteroid secretion

FEV_1 = forced expiratory volume (in 1 second); MBC = maximum breathing capacity; VC = vital capacity; PEFR = peak expiratory flow rate.

An assessment of the methodologies used in five of these clinical trials has recently been reported by Huntley and Ernst.[46] Although positive effects of *T. indica* in asthmatics are clear, the authors conclude that the clinical relevance of several of these studies was undermined by poorly designed experiments or the omission of important details (*e.g.* age range of participants, dropouts/withdrawals, *etc.*). Considering the prevalence of asthma and the appeal of complementary medicine,[47] there is a great need for further characterization of the efficacy and safety of *T. indica*, which is currently marketed in products such as AsmaAide™, Ultra Asthmatica and T. Asthmatica Plus.

1.3.2 *In vitro* and *in vivo* studies with *T. Indica*

Preclinical studies have been instrumental in uncovering the intricacies of the anti-asthmatic effects of *Tylophora* extracts. A summary of these investigations is presented in Table 1–2. Haranath and Shyamalakumari studied the effect of *T. indica* on *in vivo* immunosuppression.[48] Aqueous extracts administered intraperitoneally prevented anaphylaxis in guinea-pigs 10 days after its administration and caused leucocytosis and leucopenia—indicative signs of immunosuppression—in dogs upon *i.v*. administration. Atal *et al.* later reported the immunomodulating properties of ethanolic extracts of *T. indica*.[49] Significant inhibition of the humoral immune response (HIR), stimulation of phagocytic function and a significant increase in survival time for a foreign skin graft were reported. Adrenergic effects were noted by Udupa *et al.*[50] Upon treatment of male albino rats with the extracts of *T. indica*, the adrenals increased in weight and decreased in cholesterol and vitamin C content indicating direct stimulation of the adrenal cortex. These findings are illuminating considering the use of β_2-agonists as bronchodilators in asthmatics.

Table 1–2. *In vivo* and *in vitro* studies with *T. indica* extracts.

reference	extract	route/dose	model	result
Haranath[48]	*aqu*eous	*i.p.*	guinea pig	prevented anaphylaxis
		i.v.	dog	leucocytosis and leucopenia
Atal[49]	ethanolic	oral	mouse	↓ DTH ↓ HIR ↑ survival time in skin allograft rejection
Udupa[50]	multiple	oral, *i.p.*	rat	stimulation of adrenal cortex
Ganguly[51]	alkaloidal	oral	rat	↓ DTH
			mouse	↓ DNFB-contact sensitivity ↓ IgM response
Ganguly[52]	alkaloidal	> 300 pg/mL	T cells	↓ IL-2, ↓ proliferation
		19-300 pg/mL	macrophage	↑ IL-2, ↑ proliferation
		39 ng/mL	macrophage	↑ IL-1, macrophage activation

i.p. = intraperitoneal; *i.v.* = intravenous; DTH = Delayed-type hypersensitivity; HIR = Humoral immune response; DNFB = dinitrofluorobenzene.

With evidence that *T. indica* can be used for the treatment of pathologies arising from aberrant immune responses (*i.e.* asthma, anaphylaxis, arthritis, *etc*.) Ganguly and Sainis sought to further characterize the immunogenic effects of the alkaloids in *T. indica*.[51] They found that the alkaloid mixture mitigated delayed-type hypersensitivity (DTH) to sheep red blood cells (SRBC) and contact sensitivity to dinitrofluorobenzene (DNFB), indicating a suppression of T cell-mediated response. Additionally, the alkaloids inhibited mast cell degranulation and suppressed the discharge of pro-inflammatory mediators. Lending further credence to their therapeutic value, prophylactic and remedial benefits were noted in the

sensitized rodent models. Contrary to previous findings,[49] however, the alkaloids did not suppress primary humoral (IgM) immune response to SRBC.

The effect of the extracts was also investigated in rodent splenocytes.[52] Concanavalin A, a mitogen, was used to induce splenocyte proliferation as a model for the cellular immune response. Interestingly, a biphasic response was observed where proliferation was inhibited at high concentrations (> 300 pg/mL) and stimulated at lower concentrations (19–300 pg/mL). Both T cells and macrophages were shown to be perturbed by the alkaloid extracts. As an aside, this result is reminiscent of cryptopleurine's dual effect on motor nerve sprouting reported by Hoffman in 1952.[53] In addition to T cell mitogenic inhibition, IL-2 secretion was independently inhibited whereas IL-1 production increased. Furthermore, the alkaloids activated macrophages and hence were thought to exert their immunosuppressive activity via production of reactive oxygen and nitrogen species.

The molecular basis for *T. indica*'s anti-inflammatory effects is clearly not straightforward. These preclinical and clinical studies have provided insight into the pharmacologic mechanisms by which *T. indica* alleviates asthma. The use of raw plant material or plant extracts, however, muddies the water in discussions of the mechanism of action. The chemical composition of any given plant is a complex mixture of biomolecules, and although the most profound effects are often attributed to a primary active constituent, it is conceivable that a few components, if not many, contribute to the overall physiological outcome. A second major challenge arises from the variation among plants of the same species. It is well-known that subtle environmental factors can dramatically change the

biochemical landscape within a given plant species, thus, reproducibility may be difficult to attain.

1.4 Biology of phenanthropiperidine alkaloids

Investigation of the pure alkaloidal constituents of *T. indica* has resolved some of the ambiguities that arise from studying complex botanical mixtures. Tylophorine, perhaps due to its relatively high abundance (0.015–0.036%),[7, 30, 54] early discovery, and ease of synthesis, has received the greatest attention in this regard. The physiological effects of tylophorine are not subtle. The earliest isolation attempts report severe contact dermatitis and blistering upon exposure to the alkaline extracts of *T. indica.*[7] Notably, other plant species containing phenanthropiperidines and, indeed, the alkaloids themselves are notorious for their vesicant properties.[16, 20] These noxious effects, however, have not deterred scientists from exploring their therapeutic potential. With the already established anti-inflammatory, immunosuppressive and cytotoxic properties of the plant extracts it was fitting that the pure alkaloids should be appropriated in the same therapeutic areas. The following section will discuss their biological effects and mechanism of action.

1.4.1 Anti-cancer activity

1.4.1.1 *In vivo* studies

The phenanthropiperidines have long been touted as promising anti-cancer agents due to their broad-spectrum and potent cytotoxicity. As seen already, tylophorine, tylocrebrine and cryptopleurine were the first members to enter the limelight. Out of these three alkaloids, cryptopleurine was found to be the most toxic and tylophorine the least. The general toxicity of cryptopleurine was studied in guinea-pig, rat, mouse, rabbit, cat and dog.[16] The alkaloid proved to be lethal at doses as low as 1 mg/kg with little regard for species or the mode of administration.

A non-selective toxin is obviously a poor drug. Nevertheless, fatal diseases such as cancer have greater leeway with respect to selectivity if the final outcome with the drug is more desirable than that of the untreated disease. In spite of its potent cytotoxicity, low doses of cryptopleurine (1 mg/kg *i.p.*, twice daily for 8 days) inhibited the growth of Ehrlich ascite tumors in mice without killing the host.[55] Preclinical studies at the NCI (Table 1–3), however, showed that cryptopleurine had only marginal activity *in vivo*.[2] Tylocrebrine, on the other hand, was a more promising lead and became a clinical candidate soon after its discovery. Still, this alkaloid was found to be inactive in sarcoma 180, adenocarcino 755, B16 melanoma, Lewis lung, P1534 leukemia and Walker 256 carcinosarcoma models. It was tylocrebrine's structural novelty and superior efficacy to tylophorine and cryptopleurine[21] in lymphoid leukemia L1210 mouse models that justified its entry into clinical trials.[2] In 1966,

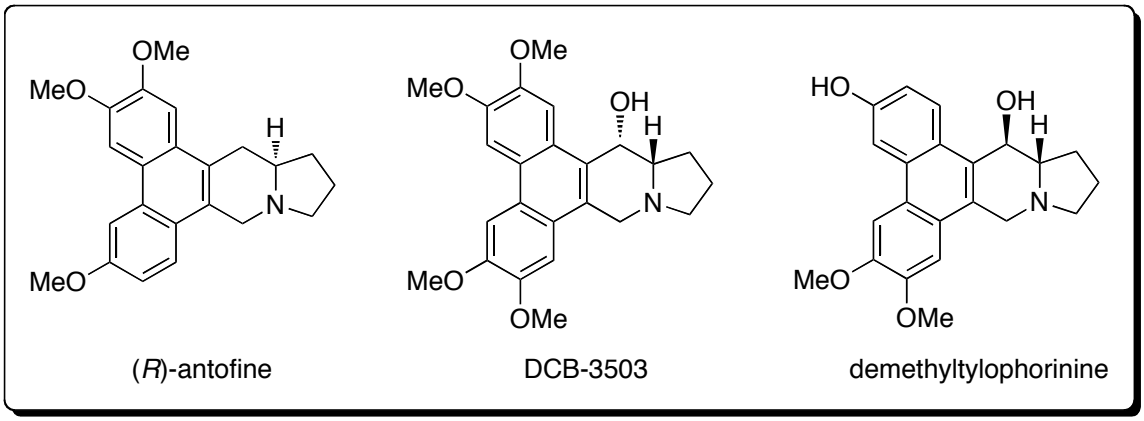

Fig. 1–5. Structures of several NCI-tested phenanthropiperidines.

less than a year after the clinical trials began, the studies were aborted before its therapeutic value could be determined. Suffness reported that this was because of central nervous system (CNS) toxicity evidenced by ataxia and disorientation.[2] Unfortunately, the original clinical data from these studies could not be obtained.

Table 1–3. Best NCI *in vivo* results for L1210 leukemia model.

compound	NSC #	dose (mg/kg)	life extension (%)
(*R*)-cryptopleurine	19912	1.0	140
(*R*)-tylocrebrine	60387	20.0	155
(*S*)-tylophorine	717335	30.0	150
tylophorinine	100055	6.0	130
demethyltylophorinine	94739	15.0	153

1.4.1.2 *In vitro* studies

Over the next few decades, medicinal interest in tylocrebrine and other phenanthropiperidines waned. Recently, however, there has been a resurgence of activity with regard to these natural products. This can be traced back to a NCI 60 human tumor cell-line screen in the early nineties that included several phenanthropiperidines. To date, eleven naturally occurring members of this class have been tested in this screen. The structures of these can be found in Fig. 1–1, 1–4 and 1–5. Contrary to earlier speculation, many of these alkaloids were found to have potent and broad-spectrum cytotoxicity. Salient members of this class inhibited tumor growth with GI_{50} values in the low nanomolar to picomolar range, on par with currently used anticancer drugs.

Since the disclosure of this finding, the phenanthropiperidines have been intensely pursued as anti-cancer drug leads. Thus far, a vast majority of these studies have been limited to *in vitro* anti-proliferative experiments, and the NCI has acquired the majority of the data. A cross-section of the 60-tumor cell line panel screen results is shown in Table 1–4. From this, it should be clear that the alkaloids endowed with activity show little discrimination between cell lines. This is exemplified by the fact that the GI_{50} ranges over the 60-tumor cell line panel show moderate selectivity between the most and least susceptible cell lines. To put this in perspective, paclitaxel, under the same assay, has a GI_{50} range of 2 to 1000 nM, a 500-fold difference. Although this is not direct evidence, selectivity within the 60-cell line panel may be indicative of selectivity between malignant and normal tissue.

Table 1–4. Growth inhibitory activity for antofine and NCI tested phenanthropiperidines.

		60-cell line panel GI_{50} (nM)		individual cell line GI_{50} (nM)			
compound	NSC #	mean	range	CEM	A549	MCF-7	HCT 116
tylophorine	717335	17.5	10–400	10, 15[a]	10	10	10
antofine	NA	ND	ND	5.2[a]	10.4,[b] 0.44[c]	12.4[c]	9.9[b]
cryptopleurine	19912	5.1	1.3–50	5.0, 2[a]	5.0	5.0	5.0
tylocrebrine	60387	29.5	10–126	25	25	50	25
DCB-3503	716802	29.1	10–160	25	25	16	20
tylophorinine	100055	57.6	10–500	40	63	63	40
demethyltylophorinine	94739	1.13	1.0–16	1.0	1.0	1.0	1.0
tyloindicine F	650393	0.10	0.1–0.1	0.10	0.10	0.10	0.10
tyloindicine G	650394	0.10	0.10–0.16	0.10	0.10	0.10	0.10
tyloindicine H	650395	0.50	0.10–20	0.40	0.63	3.98	0.50
tyloindicine I	650396	4.40	1.6–20.0	3.16	3.98	5.01	2.00

CEM = leukemia, A549 = non-small cell lung carcinoma, MCF-7 = breast carcinoma, HCT 116 = colon carcinoma, NA = Not applicable, ND = No data. Unless otherwise specified, data were gathered from NCI-DTP Database. [a] Gao *et al.*[62] [b] Fu *et al.*[63] [c] Su *et al.*[56]

A second observation that can be made from the collective data is that these alkaloids retain their potency in drug-sensitive and multidrug-resistant (MDR) cell lines (Table 1–5).[24, 56-58] Antofine and several closely related analogs, for instance, have equipotent growth-inhibitory activity against common and MDR cell lines.[56, 57] Furthermore, in a KB cell line panel containing strains resistant to many of the conventional anti-cancer drugs, tylophorine and its hydroxylated analog, DCB-3503, showed no bias in their anti-proliferative effects.[58] Besides the obvious pertinence to therapeutic utility, this suggests that these alkaloids have a different mechanism of action from drugs that are ineffective in these refractory cancers. To add to this, an earlier evaluation of tylophorine in the NCI's COMPARE analysis bears further witness to the unique mechanism of action and potentially novel cellular target(s).[59]

Table 1–5. Growth inhibitory activity in drug-resistant cell lines (Gao *et al.*).[58]

cell line	biochemical changes	resistance	GI_{50} (nM) tylophorine	DCB-3503	antofine
KB (parental)	-	-	12, 214[a]	28	16[a], 1.2[b]
KB-MDR	gp 170 ↑	VP-16, taxol, adriamycin, vincristine	14	26	–
KB-7D	Topo II ↓, MRP ↑	VP-16, adriamycin, vincristine	12	45	–
KB-7D-Rev	Topo II ↓	VP-16, adriamycin	11	25	–
KB-Ha-R	RR ↑, dCK ↓	HU, araC, gemcitabine	25	36	–
KB-Ha-Rev	dCK ↓	araC, gemcitabine	16	28	–
KB-100	Topo I ↓, XRCC1 ↑	CPT, topotecan, SN-38	20	38	–
KB-100-Rev	Topo I ↓	CPT, topotecan, SN-38	10	41	–
KB-VI	P-gp ↑	adriamycin, vinblastine, colchicine	173[a]	–	14[a], 2.3[b]

[a]Stærk *et al.*[57] [b]Su *et al.*[56] MRP, multidrug resistance protein; VP-16, etoposide; HU, hydroxyurea; RR, ribonucleotide reductase; dCK, deoxycytidine kinase; Topo II, topoisomerase II; Topo I, topoisomerase I; XRCC1, X-ray repair cross-complementing gene I protein; araC, aravinoside cytosine; CPT, camptothecin; SN-38, 7-ethyl-10-hydroxycamptothecin; P-gp, P-glycoprotein.

1.4.1.3 Structure-activity relationships

The size of the phenanthropiperidines class has grown significantly since the discovery of tylophorine. There are over sixty members in this class, including seco-analogs and closely related isomers, from which SARs have begun to emerge. For the purpose of this discussion, fifty-one natural and unnatural analogs belonging to eleven scaffolds will be considered. In Table 1–6, the compounds are ordered from the most to the least potent according their average GI_{50} activity in up to fourteen of the most commonly used cell lines or, for those that have been tested by the NCI, the mean GI_{50} value in the 60-tumor cell line is used. It should be cautioned that compounds in Table 1–6 may not have been tested in the same assay or even in the same cell lines. Furthermore, since internal standards were rarely used,

Table 1–6. Structure and average GI_{50} over select cell lines.

entry	common name	code[a]	scaffold[b]	R^1	R^2	R^3	R^4	R^5	R^6	R^7	R^8	n	Avg GI_{50} (nM)[c]
1	tyloindicine F	43	F	H	OMe	H	H	OMe	OMe	H	OH[d]	1	0.1
2	tyloindicine G	44	E	OMe	OMe	H	H	OMe	OMe	H	OH[d]	1	0.1
3	–	38	A	H	OH	OMe	H	OMe	OMe	*S*-OH	*S*-H	1	0.2
4	tyloindicine H	45	E	H	OMe	OH	H	OMe	OMe	H	H[d]	1	0.5
5	demethyltylophorinine	39	A	H	OH	H	H	OMe	OMe	*R*-OH	*S*-H	1	1.1
6	(±)-cryptopleurine	±-11	A	OMe	OMe	H	H	OMe	H	H	*rac*	2	2.0
7	6-demethylantofine	37	A	OMe	OMe	H	H	OH	H	H	*rac*	1	4.1
8	tyloindicine I	46	G	OMe	OMe	OH	H	OMe	OMe	H	H[d]	1	4.4
9	(*R*)-cryptopleurine	R-11	A	OMe	OMe	H	H	OMe	H	H	*R*-H	2	5.1
10	boehmeriasin A	16	A	H	OMe	H	H	OMe	OMe	H	*rac*	2	5.2
11	(*R*)-antofine	R-6	A	OMe	OMe	H	H	OMe	H	H	*R*-H	1	10.1
12	(±)-antofine	±-6	A	OMe	OMe	H	H	OMe	H	H	*rac*	1	14.0
13	–	2	A	OMe	OMe	H	H	OMe	OH	H	*R*-H	1	16.0
14	(*S*)-tylophorine	S-1	A	OMe	OMe	H	H	OMe	OMe	H	*S*-H	1	17.2
15	–	34	A	OMe	OMe	H	H	*i*-PrO	H	H	*rac*	1	27.8
16	tylocrebrine	18	A	OMe	OMe	H	OMe	OMe	H	H	*rac*	1	29.5
17	DCB-3503	22	A	OMe	OMe	H	H	OMe	OMe	*S*-OH	*S*-H	1	29.5
18	–	36	A	OMe	OH	H	H	OMe	H	H	*rac*	1	30.3
19	deoxytylophorinidine	27	A	H	OMe	H	H	OH	OMe	H	*R*-H	1	35.7
20	–	33	A	OMe	*i*-PrO	H	H	OMe	H	H	*rac*	1	38.7
21	isotylocrebrine	20	A	H	OMe	OMe	H	OMe	OMe	H	*S*-H	1	41.0
22	deoxypergularine	19	A	H	OMe	H	H	OMe	OMe	H	*rac*	1	64.3
23	demethoxyantofine	7	A	OMe	OMe	H	H	H	H	H	*rac*	1	69.5
24	–	35	A	OH	OMe	H	H	OMe	H	H	*rac*	1	80.3
25	tylophorine-*N*-oxide	5	B	OMe	OMe	H	H	OMe	OMe	H	*R*-H	1	97.0
26	DCB-3501	21	A	OMe	OMe	H	H	OMe	OMe	*R*-OH	*S*-H	1	108.0
27	(*R*)-tylophorine	R-1	A	OMe	OMe	H	H	OMe	OMe	H	*R*-H	1	109.7
28	–	3	A	OMe	OMe	H	H	OMe	OMe	H	*rac*	2	117.3
29	–	10	A	OMe	OMe	H	H	OMe	H	*R*-OH	*R*-*H*	1	130.0
30	antofine-*N*-oxide	9	B	OMe	OMe	H	H	OMe	H	H	*R*-*H*	1	135.0
31	tylophorinine	28	A	H	OMe	H	H	OMe	OMe	*R*-OH	*S*-H	1	160.1
32	(±) -tylophorine	±-1	A	OMe	OMe	H	H	OMe	OMe	H	*rac*	1	254.7
33	(*R*)-ficuseptine C	R-12	A	–OCH_2O–		H	H	OMe	H	H	*R*-H	1	283.3
34	(±) -ficuseptine C	±-12	A	–OCH_2O–		H	H	OMe	H	H	*rac*	1	521.4
35	DCB-3506	23	A	OMe	OH	H	H	OMe	OMe	*S*-OH	*S*-H	1	600.0
36	–	32	A	*i*-PrO	OMe	H	H	OMe	H	H	*rac*	1	927.7
37	–	13	H	OMe	OMe	H	H	OMe	H	H	*R*-H	1	1064.7
38	tylophorinidine	29	A	H	OMe	H	H	OH	OMe	*S*-OH	*S*-H	1	1832.7
39	dehydroantofine	17	D	OMe	OMe	H	H	OMe	H	H	*rac*	1	2360.0
40	(*R*)-secoantofine	8	C	OMe	OMe	H	H	OMe	H	H	*R*-H	1	2535.0
41	tylophoridicine E	24	A	H	OH	H	H	OMe	OMe	*S*-OH	*S*-H	1	3336.7
42	–	30	A	H	H	H	H	H	H	H	*rac*	1	3571.2
43	tylophoridicine F	26	B	H	OMe	H	H	OMe	OMe	*R*-OH	*S*-H	1	6378.0
44	tylophoridicine C	25	B	H	OMe	H	H	OH	OMe	*S*-OH	*S*-H	1	8388.3
45	–	31	A	H	H	H	H	H	H	H	*rac*	1	9460.0
46	–	15	I	OMe	OMe	H	H	OMe	H	H	*R*-H	1	9645.0
47	–	14	I	OMe	OMe	H	H	OMe	H	H	*S*-H	1	9685.0
48	–	40	J	OMe	OMe	H	H	OMe	OMe	H	*rac*	1	15600.0
49	–	42	K	OMe	OMe	H	H	OMe	OMe	H	*rac*	2	42000.0
50	dehydrotylophorine	4	D	OMe	OMe	H	H	OMe	OMe	H	*rac*	1	> 50000
51	–	41	K	OMe	OMe	H	H	OMe	OMe	H	*rac*	1	> 50000

[a] Refers to number in Graph 1–1. [b] See Fig. 1–6. [c] Average GI_{50} in HepG2, Panc-1, CEM, A549, MCF-7, KB, KB-VI, KB-3-1, HCT 116, HT-1080, MDA-MB-231, COLO-205, NUGC-3 and HONE-1. [d] Unknown stereochemistry

Graph 1–1. Anti-proliferative activity of phenanthropiperidines in fourteen select cell lines.

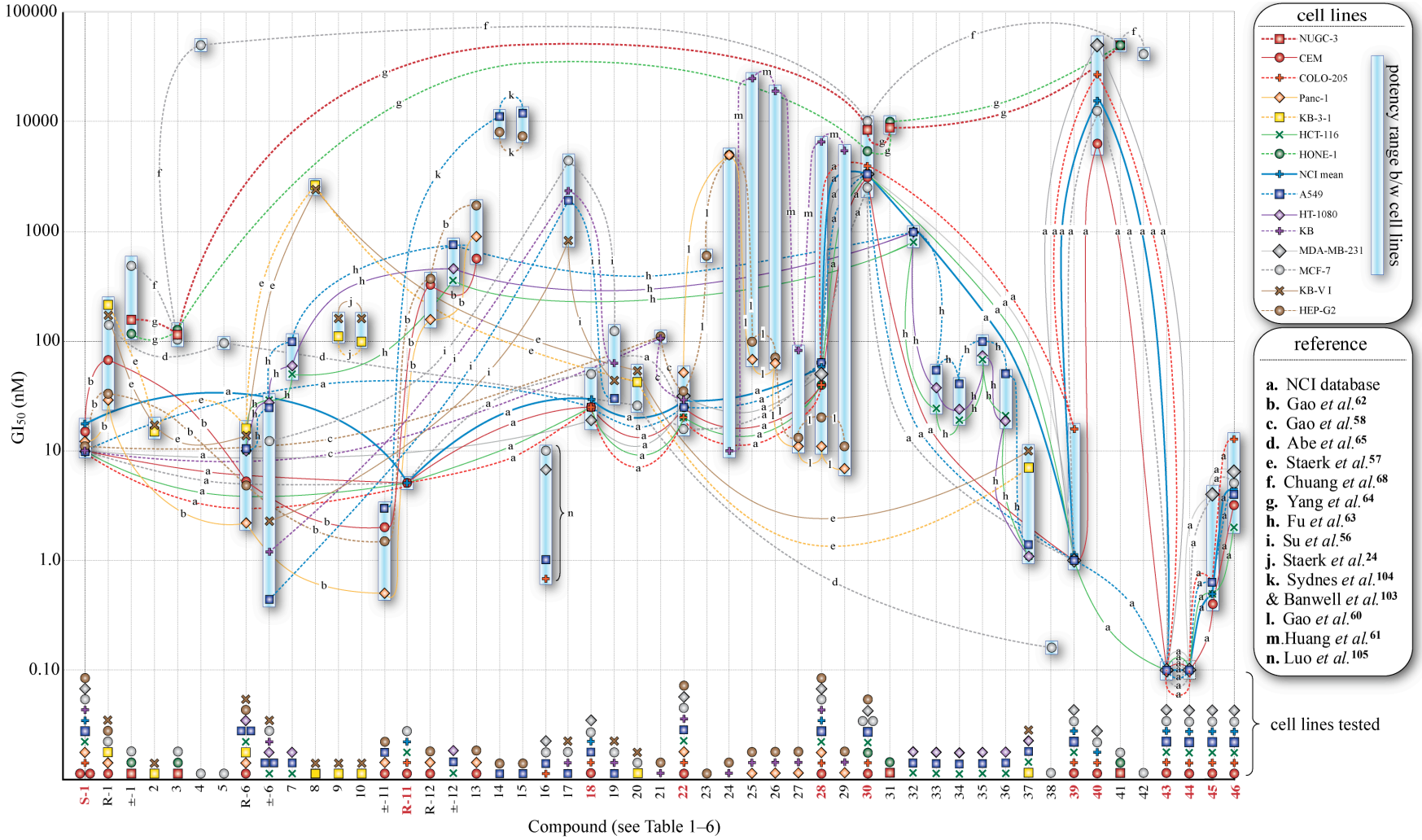

Note: A line that connects two or more data points refers to a comparative study between the compounds that are connected by that line. The letter on each line indicates the literature reference where this data is reported. Compounds tested in the NCI tumor cell line panel are shown in red.

normalization of these results is virtually impossible. Because of this lack of standardization, a more detailed understanding of the variables specific to each anti-proliferative assay is required to assess the reliability of activity ranking across this class.

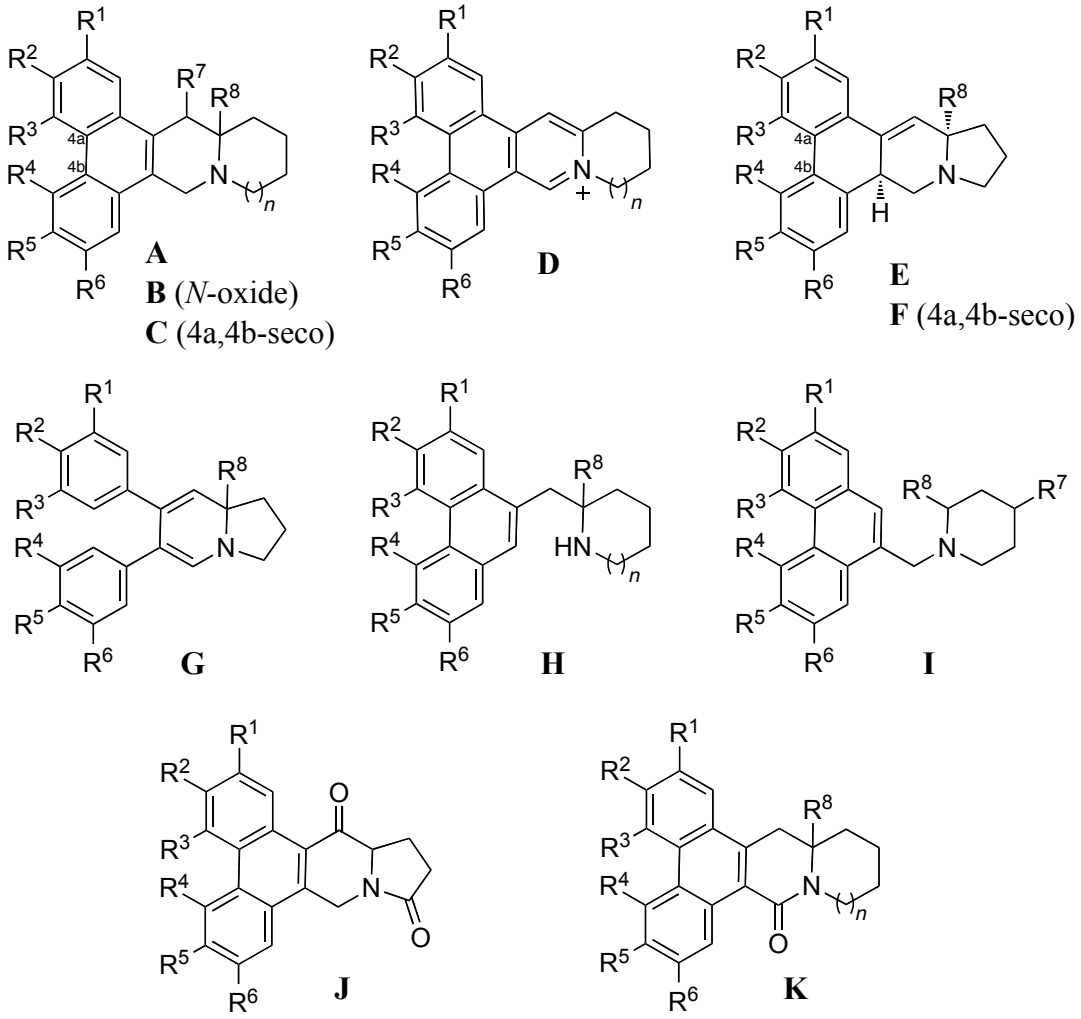

Fig. 1–6. Scaffolds of phenanthropiperidines and analogs.

Graph 1–1 accounts for a number of these variables by incorporating information about each compounds anti-proliferative activity in relation to the specific cell line and assay (*i.e.* which compound have been tested simultaneously in the same assay). A crude comparison of each compounds activity can be accrued by the range (represented by a blue bar) and mean

activity (the center of the blue bar which corresponds to the "Avg. GI_{50}" column in Table 1–6) of each compound. The innate differences between the cell lines, however, make this type of ranking rather inaccurate. An extreme example of this is seen with reported data for compounds 24 and 25. In HepG2 and Panc-1 cells, compound 25 exhibits more than 50 fold greater activity compared with compound 24,[60] whereas in KB cells compound 24 is at least 25,000 times more active than compound 25.[61] Whether this dramatic difference is a function of the particular cell lines or the different sources of each compound remains unknown, but is clear that simply averaging the GI_{50} values obscures this peculiar finding. In order to address this, the activity of the individual cell lines are presented in Graph 1–1 and are distinguished based on the color and shape of each point.

Another concern is that even among common cell lines there can be a significant amount of variation between assays. In A549 cells, racemic antofine (±-6) was reported to have a GI_{50} value of 25 nM in one report and 0.44 nM in another, over a 50 fold difference. This discrepancy demonstrates the wide variation that can exist between independently acquired data in anti-proliferative assays. In this regard, we have indicated the compounds that have been tested in the same assay by linking them with a line, where the color and stroke (*i.e.* solid or dashed) of the line refers to the cell line, and the lowercase letter corresponds to the reference for a particular comparative study. In other words, all points that fall along a line of the same style (cell line) and letter (reference) were tested simultaneously. This not only allows the most accurate comparisons between each compound but provides a means to assess the relative activity of compounds that have not been compared in the same assay by finding commonalities between data sets. For instance, (*R*)-tylophorine (R-1) and (*R*)-

cryptopleurine (R-11), which have not been tested together, can be compared, because both compounds have been tested along with (*S*)-tylophorine (S-1) in CEM cell lines which can be used as the standard. On the other hand, a comparison of boehmeriasin A (16) with other compounds should be taken with reservation since it has not been tested along with any other members of this class. Nevertheless, by piecing together GI_{50} values for particular cell lines that have been reported in the literature, we gain a better, albeit incomplete, understanding of structural features that contribute to the phenanthropiperidine's anti-cancer activity.

The phenanthrene system (rings A, B and C) has been studied most extensively. The seco-analogs are almost universally less active (*e.g.* Table 1–6, entries 11 and 40). There may, however, be other ways to compensate for this loss in activity as evidenced by tyloindicine F and I (entry 1 and 8) which are extremely cytotoxic in spite of their rings A and C being disconnected. Disrupting the aromaticity of ring B as in DCB-3502 (not shown) can also reduce activity.[58, 62] Furthermore, the location and type of substituents on the phenanthrene has a profound effect on its activity.[57, 61, 63] From Table 1–6, it should be apparent that formulating strict phenanthrene SARs without considering the rest of the scaffold inevitably leads to irreconcilable data. From the fact that when methoxy or hydroxy substituents are removed completely, the naked scaffold is significantly less active (entries 42 and 45), it can be surmised that the presence of these substituents substantially boosts activity.[64] Although this may be due to the requirement of an electron-rich arene, the incorporation of surrogate electron donators, such as amines, has not been investigated.

The position of the substituents is also important but data gathered from different sources and cell lines make it difficult to discern precise correlations. Nevertheless, some

generalizations can be made. First, the 2,3,6-trisubstituted system seems to be favorable as evidenced by the remarkable potency of antofine and cryptopleurine (entries 6, 9, 11 and 12). A hydroxyl group at C6 can increase potency as in 6-desmethoxyantofine[63] (entry 7 and 12). Depending on the scaffold, C3-hydroxy groups will either increase (entries 5 and 43)[65] or decrease activity[57, 63] (entries 12 and 18). Fu *et al.* reported a systematic study of antofine's (entry 12) phenanthrene substituents and found that the C2 position was particularly sensitive to alteration. Replacement of the methoxy group with either a methylenedioxy bridge (entry 34), hydroxy (entry 24) or an isopropoxy group (entry 36) resulted in a significant loss of potency.[62, 66] On the other hand, replacing the methoxy groups at C3 and C6 with hydroxy (entries 7 and 18) or isopropoxy (entries 15 and 20) was well-tolerated.

There are several piperidine (ring D) modifications that can be made without losing activity. A 14-hydroxy group (R^7 = OH) seems to be tolerated with only a several-fold loss of activity (entries 14 and 17),[24, 58, 60, 65] but the stereochemistry of C14 does seem to affect the activity (entries 3 and 41; 17 and 26). There are probably multiple factors determining the most active diastereomer.[58, 60, 67] Despite the slightly diminished activity of C14-hydroxyl analogs, demethyltylophorinine (entry 5) is among the most potent members of this class to be tested in the 60-tumor cell line screen (see Table 1–4 also).[67] Interestingly, Gao *et al.* discovered that a hydroxylated DCB-3503 (entry 17) showed superior activity *in vivo* compared with its non-hydroxylated parent, tylophorine (entry 14), thus, hydroxylation may ultimately prove to be beneficial.[58, 60]

Several groups have constructed *N*-oxide analogs which, surprisingly, produced only a 2–10-fold reduction in activity (entries 25 and 27; 11 and 30).[24, 65] Amide analogs, however, are

almost completely inactive (entries 48, 49 and 51).[64, 68] Dehydro-analogs, where the piperidine is aromatized to a pyridinium, are also inactive (entries 12 and 39; 32 and 50).[64]

It is worth mentioning that several tylophorine-based analogs have been designed that do not contain an intact ring D piperidine (entries 37, 46 and 47). Multiple-bond scissions have been investigated but all permutations of this type have reduced the alkaloid's anti-proliferative effects. Nevertheless, the ease of preparing these simplified analogs has enabled extensive SAR studies and, through these, the discovery of moderately potent analogs such as PBT-1 (Fig. 1–7) which have IC_{50} values of 200–400 nM.[69, 70] Despite their close structural-relatedness, evidence suggests that these unnatural derivatives are mechanistically distinct.[62, 71]

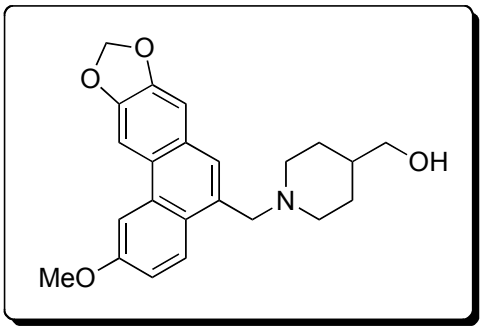

Fig. 1–7. Structure of PBT-1.

There is evidence that the stereochemistry of the bridgehead carbon does contribute to the activity. Only a few labs, however, have tested two enantiomers in the same assay. Gao *et al.* were able to acquire both enantiomers of tylophorine and found the (*S*)-isomer (entry 14) to be 3–5-fold more active than the (*R*)-isomer (entry 27) in HepG2, Panc-1 and CEM cells.[62] Moreover, the anti-proliferative activities of each enantiomer paralleled their inhibitory

effects on key transcription factors. In a separate study, (*R*)-antofine (entry 11) was tested with its racemate (entry 12) in A549, HCT 116 and HT-1080 cells showing the former to be three-fold more active in all three cell lines.[63] From this it may be inferred that, in contrast to tylophorine, the (*R*)-enantiomer is most active. If this is true, the phenanthrene substituents have differing effects on the activity of each enantiomer and, therefore, the absolute stereochemistry of the eutomer is not uniform across this class. Anecdotal evidence suggests that substitution requirements for C2- and C7- substituents are reversed upon changing the stereochemistry of the indolizidine, but this is still to be borne out in comparative studies.[3]

Indeed, there is still a superficial understanding of SARs that, if better understood, could be profitable for the design of improved therapeutic agents. One reason for our poor understanding of SARs is that the available data are disjointed. Over fifty members of this class have been tested in anti-proliferation assays, but most of the results are compiled using specialized cell lines or lack an internal standard resulting in tenuous comparisons between most analytes. Another part of the problem is that SAR studies have been confined to a somewhat homogenous collection of alkaloids. Although the effect of substituent location has been explored, the type of substitution has not strayed beyond hydroxy or alkoxy groups. Surprisingly, even the incorporation of an additional nitrogen atom or halogen has yet to be investigated. There is also a paucity of SAR studies on ring E (Fig. 1–2) other than the observation that indolizidine and quinolidine analogs appear to be comparable in activity.[64, 68] Many of these limitations are understandable in light of the challenge of preparing such analogs.[3]

1.4.2 Mechanism of action

The effect of phenanthropiperidines on living systems has been investigated at the biochemical level. From these studies, several targets have been proposed, but none ratified. Notwithstanding the likelihood that these alkaloids interact with multiple targets, some of the alleged targets are needlessly invoked, only being perturbed at concentrations far above those required to exert the desired effect. Others that are supported by compelling experimental evidence, are unduly overlooked. Accordingly, this discussion will attempt to unify the body of work aimed at identifying the mechanism of action of the phenanthropiperidines with the aim of facilitating a critical analysis of the putative biological targets.

1.4.2.1 Protein, DNA and RNA biosynthesis inhibition

The most extensively studied mechanism for the phenanthropiperidine's anti-cancer activity is protein biosynthesis inhibition. Beginning in 1968, Donaldson *et al.* reported that tylophorine, tylocrebrine and cryptopleurine inhibited protein synthesis in Ehrlich ascites-tumor cells but did not markedly affect RNA synthesis (entry 1, Table 1–7).[72] Paralleling the order of their anti-proliferative effects, cryptopleurine exhibited the most potent inhibition whereas tylophorine was the least active. (–)-Antofine has recently been shown to inhibit protein biosynthesis with remarkable potency (entry 2).[62] In spite of its potency in eukaryotic systems, cryptopleurine did not inhibit protein synthesis in *E. coli* (entry 1).[72] It was hypothesized that phenanthropiperidines were exerting their growth inhibitory activity via

80S ribosomal inhibition thus explaining their inactivity in prokaryotes that have instead 70S ribosomes. To confirm this hypothesis, a systematic study explored the activity of the three phenenanthropiperidines in *S. cerevisiae*, a model eukaryote, and *E. coli* (entry 3).[73] The order of cytostasis was identical to that in the previous studies with cryptopleurine again being the most potent. Ribosomal inhibition studies clearly showed that the alkaloids inhibited protein synthesis with a noticeable preference for yeast cytoplasmic ribosomes over mitochondrial and *E. coli* ribosomes. Furthermore, cryptopleurine was shown to irreversibly inhibit ribosomal protein synthesis.

Table 1–7. Inhibition of protein, DNA and RNA synthesis.

entry	reference	model	compound	IC_{50} (nM) PS	RS	DS
1	Donaldson[72]	Ehrlich ascites-tumor cells	CP	20	> 100000	-
		Ehrlich ascites-tumor cells	TC	200	> 100000	-
		Ehrlich ascites-tumor cells	TP	1000	> 100000	-
		E. coli	CP	> 10000	-	-
2	Gao[62]	HepG2 cells	AF	12	> 50	8
			FS	2500	2500	1000
3	Haslam[73]	*S. cerevisiae; E. coli*	CP	< 1000; > 100000	-	-
			TC	1000; > 100000	-	-
			TP	20000; > 100000	-	-
4	Huang[74]	HeLa cells	TC	50	300	60
		reticulocytes	TC	< 1000	-	-
5	Entner[78]	reticulocytes; reticulocyte lysate	CP	150; 700	-	-
			TC	300; 800	-	-
6	Skogerson[76]	*S. cerevisiae; cry* mutant ribosomes	CP	180; 18000	-	-
7	Gupta[80]	CHO cell wild type; Emt^R mutant	CP	330; 660	-	-
			TC	400; 1800	-	-

CP = cryptopleurine, TC = tylocrebrine, TP = tylophorine, AF = antofine, FS = ficuseptine C, PS = Protein synthesis, RS = RNA synthesis, DS = DNA synthesis, Emt^R = emetine resistant.

Delving deeper into the mechanism of inhibition, Huang *et al.* examined the effects of tylocrebrine in HeLa cells and rabbit reticulocytes, a cell-free model for protein biosynthesis (entry 4).[74] Tylocrebrine, like cryptopleurine, irreversibly inhibited protein biosynthesis. Studies of several phenanthropiperidines corroborate that the inhibition takes place during the translocation step of chain elongation.[74-77] When tylocrebrine was compared with a small collection of emetine-like alkaloids, its ameobocidal activity closely correlated with the activity of compounds that inhibited cell-free protein synthesis to the same extent (entry 5).[78]

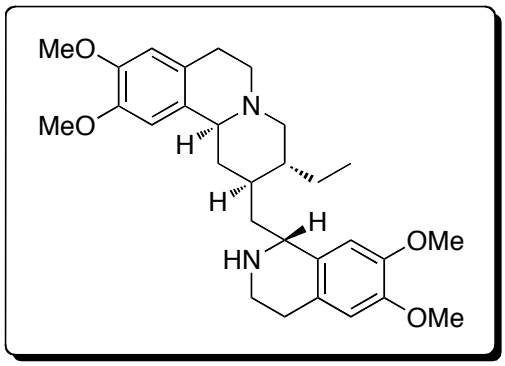

Fig. 1–8. Structure of emetine.

The juxtaposition of emetine (Fig. 1–8) and the *Tylophora* alkaloids is not arbitrary. Emetine's natural source, ipecacuanha, and *T. indica* have both been used in traditional medicine as natural emetics. Their similar therapeutic properties even earned *T. indica* the name "Indian ipecacuanha." On a chemical level, there are also some similarities that have caused speculation about common binding sites on the ribosome.[79]

In 1973, mounting evidence for ribosomal inhibition emerged from the identification of the *cry* gene that conferred resistance in *S. cerevisiae* (entry 6).[76] Ribosomes isolated from *cry* mutants required 100 fold more cryptopleurine to produce the same inhibitory response as parent ribosomes. Interestingly, the normal (uninhibited) activity of 40S ribosomal subunits in *cry* mutants was impaired revealing the biochemical outcome of the mutation.[76, 77] This finding, however, did not elucidate the ribosomal subunit selectivity of these alkaloids, nor does it identify a specific binding site.

Evidence for this was gathered from genetic studies that found the cryptopleurine (Cry^R) and tylocrebrine (Tyl^R) resistant CHO cells bore a remarkably similar cross-resistance profile to emetine-resistant (Emt^R) mutants (entry 7).[80] The fact that Emt^R cell's resistance could be

traced to a modified 40S ribosomal subunit and that emetine bore structural resemblance to the phenanthropiperidines was adduced as analogical evidence that these protein synthesis inhibitors shared a common binding site.[79, 80] The proposed common pharmacophore of the emetine and cryptopleurine, however, was not predictive of biological activity in synthetic analogs endowed with the alleged essential structural features.[81]

Addressing this, evidence for a ribosomal binding site was finally provided by Dolz *et al.* in 1982.[82, 83] Displacement assays with tritiated cryptopleurine confirmed the existence of a single high-affinity binding site on the 40S and 80S subunits that are shared with tylocrebrine and tylophorine. Emetine and tubulosine, however, only displaced cryptopleurine at very high concentrations, suggesting separate binding locations in spite of their similar effects on translocation. These experiments also showed that non-specific, low-affinity interactions exist on the 40S, 80S and 60S subunits, explaining cryptopleurine's discrete (peptide bond formation *vs*. translocation) inhibitory effects at high concentrations.

Besides protein synthesis, tylocrebrine-induced inhibition of RNA and DNA synthesis in HeLa cells (entry 4).[74] It should be emphasized that protein and DNA synthetic pathways are interdependent and, consequently, inhibitors of protein synthesis. For example, anisomycin, cycloheximide and emetine, which are potent protein synthesis inhibitors, inhibit DNA synthesis as well. Antofine, a closely related analog, has recently been shown to simultaneously inhibit protein and DNA biosynthesis as well (entry 2).[62] Thus, the effect on DNA synthesis is likely a secondary consequence of tylocrebrine's and antofine's ribosomal inhibition.

These studies as a whole provide compelling evidence not only for a mechanism of action —namely protein biosynthesis inhibition—but also for the specific molecular target, the 40S ribosome. The question naturally arises: Is this explanation sufficient to explain the pharmacological effects of these alkaloids? This is difficult to answer since protein synthesis is an integral part of a cells normal growth and division and, as such, perturbation of the normal ribosomal function has vast repercussions. To borrow Pestka's analogy, inhibiting protein synthesis is like sticking a wrench into a very complicated gearbox, "almost anything can happen."[84] Therefore, it is not unfounded that protein synthesis inhibitors like the phenanthropiperidines are cytostatic to the cells they target.

Another important stipulation for anti-cancer therapeutics must also be met. That is, they must exhibit an appropriate level of selectivity for tumor cells. There is accumulating evidence that this can be achieved with protein synthesis inhibitors.[85] First, aberrantly regulated protein synthesis is highly contributive to tumorigenesis[86] and metastatic progression.[87] Second, there is a higher critical threshold for protein synthesis in transformed cells than in normal cells that grow more slowly. Indeed, the rate of cell proliferation positively correlates with the level and rate of translation. Clinical studies have already borne witness to the therapeutic potential of several such inhibitors despite being limited by cardiovascular and other complications[88-90]—hypotension, ventricular tachycardia, atrial irritability, ST-T wave changes and premature ventricular contractions, for example.[90] Still, there is significant interest in developing more selective agents.[85]

That multiple phenanthropiperidines potently inhibit protein synthesis and that their anti-proliferative effects correlate with this inhibition evinces the notion that these alkaloids exert

their cytotoxic effect, primarily but not exclusively, through protein biosynthesis inhibition. Moreover, as evidenced from studies with tritiated cryptopleurine, one molecular targets of the phenanthropiperidines is the 40S ribosome.

1.4.2.2 Apoptosis and cell cycle arrest

Characterizing cellular events associated with anti-cancer lead molecules provides a window into their mechanism of action. Protein biosynthesis inhibitors will, by their nature, abate cell growth, but they are not inherently cytotoxic. Even though cytostatic agents can effectively treat malignancies by subverting the accelerated proliferation in neoplastic growth, cancer cell death or differentiation is required for complete remission. In 2002, it was reported that an alkaloidal extract of *T. indica*, containing mainly tylophorine, tylophorinine and tylophorinidine, completely inhibited cell growth in K562 (human erythroleukemic) cells at 0.1 μg/mL (entry 1, Table 1–8).[91] Interestingly, when the alkaloidal concentration was increased by ten-fold, the cells underwent apoptosis. Indeed, apoptotic agents engage a strategic battlefront for chemotherapeutic intervention, but the higher concentrations used here to achieve cell death may not be therapeutically practicable. Moreover, since an alkaloidal mixture was used, synergy cannot be ruled out. Lee *et al.* simplified analysis by using a single alkaloid: antofine (entry 2).[92] Antofine showed potent inhibition of growth and colony formation in A549 and Col2 cancer cells. No evidence of apoptosis or necrosis was observed at these low concentrations suggesting that antofine is primarily cytostatic. In Col2

cells, morphological changes and G2/M cell cycle arrest were noted at concentrations as low as 0.1 nM.

Table 1–8. Apoptosis and cell cycle arrest by phenanthropiperidine alkaloids.

entry	reference	cell line	compound	concentration	result at cytostatic concentrations
1	Ganguly[91]	K562	*T. indica* extract	0.1 μg/mL	no apoptosis
				1 μg/mL	apoptosis
2	Lee[92]	A549, Col2	AF	< 30 nM	no apoptosis
		Col2	AF	0.1 nM	G2/M phase arrest; morphological changes
3	Gao[58]	KB	TP, DCB-3503	0.03-1 μM	S phase accumulation
		HepG2	TP, DCB-3503	0.3-3 μM	no DNA damage; sustained growth inhibition
4	Wu[93]	HONE-1 NUGC-3 HepG2	TP	2 μM	sustained growth inhibition G1 phase arrest
5	Yan[94]	MDA-MB-231	BA	19 nM	G1 phase arrest, no apoptosis

TP = tylophorine, AF = antofine, BA = boehmeriasin A, DCB-3503 = 14-hydroxytylophorine.

The Cheng group observed that tylophorine and DCB-3503 did not cause DNA damage as concluded from the fact that p53 was not induced during treatment with either of these alkaloids (entry 3).[58] Both alkaloids (0.03-1 μM) induced S-phase accumulation in KB cells, whereas in HepG2 cells, the cells did not accumulate at any particular phase. Notably, analog DCB-3503 does not induce apoptosis or necrosis at up to 3 μM concentrations, and both tylophorine and DCB-3503 produced complete and sustained growth inhibition in HepG2 cells over 8 days. This persistency of activity was also demonstrated for tylophorine in HONE-1 and NUGC-3 cell lines (entry 4).[93] These long lasting effects are noteworthy considering these alkaloids induce *irreversible* protein synthesis inhibition.

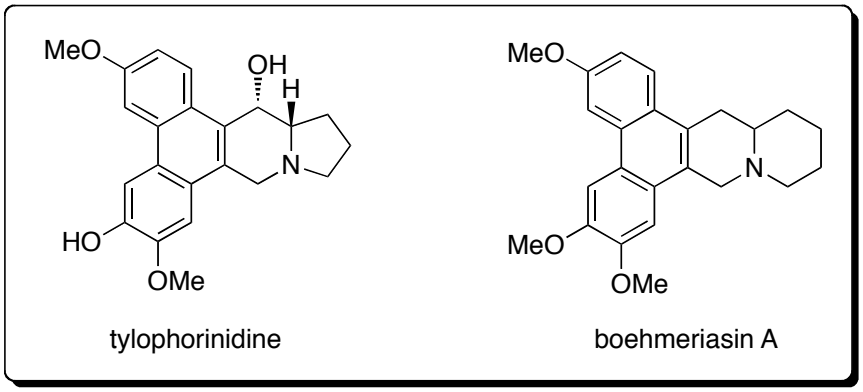

Fig. 1–9. Structures of tylophorinidine and boehmeriasin A.

In HepG2, HONE-1 and NUGC-3 carcinoma cells, tylophorine induced G1-phase arrest that was linked to a suppression of cyclin A2 expression (entry 4).[93] Furthermore, DCB-3503 and tylophorinidine (Fig. 1–9) were shown to down-regulate cyclin D1.[60] It was noted that cyclin D1 suppression correlated with each compound's growth inhibitory effects. In breast cancer cell line MDA-MB-231, boehmeriasin A (Fig. 1–9) exerts its potent anti-proliferative effects via G1 cell cycle arrest and not by apoptosis (entry 5).[94] In this study, cyclins D1 and E2 were found to be under-expressed in the treated cells. Given the role of cyclin-dependent kinases (CDKs) in the governance of cell cycle progression, modulators of CDK pathways could potentially correct the faulty regulation that leads to unmitigated cell division in cancer.[95-98] From these data, it is apparent that the archetypal phenanthropiperidines are not apoptotic agents but rather induce cytostasis by overriding a cancer cell's replicative potential.

1.4.2.3 Angiogenesis

Another hallmark of cancer is "sustained angiogenesis".[99] Highly metabolically active cells, such as those in many types of tumors, require sufficient vasculature to meet their exorbitant aerobic demands. Even slow-growing and anaerobic tumors rely on a blood supply for their basic sustenance. This need is met by actively recruiting blood vessels through the release of growth factors such as VEGF which is triggered by hypoxia. Targeting angiogenesis is, therefore, a highly effective way to suppress tumor growth. Cai *et al.* investigated cryptopleurine's and 15*R*-hydroxycryptopleurine's effects on hypoxia-inducible factor-1 (HIF-1),[100] a key regulator of a cell's response to hypoxia and a promising drug target.[101, 102] Both alkaloids potently inhibit HIF-1-mediated gene expression under anaerobic conditions (IC_{50} = 8.7 and 48.1 nM, respectively). Furthermore, VEGF expression is also suppressed in a dose-dependent manner. Unfortunately, attempts to determine cryptopleurine's anti-angiogenic properties *in vitro* were hampered by its poor solubility.[103] A number of seco-analogs did, however, inhibit angiogenesis in rat aorta blood vessel fragments at low micromolar concentrations.[103, 104] It is still unclear if the anti-angiogenic effects of these alkaloids are independent of their anti-proliferative properties.

1.4.2.4 Cell differentiation

When considering the pervasive impact within a cell resulting from protein synthesis inhibition, it is not surprising that the phenanthropiperidines elicit patent phenotypic changes

in transformed cells. The possibility that tylophorine induced cell differentiation was investigated through monitoring the expression levels of two tumor biomarkers, alpha-fetoprotein (AFP) and albumin.[58] Treatment with tylophorine (1 μM) resulted in a suppression of AFP expression and an increase in albumin expression which is consistent with cell differentiation. Boehmeriasin A also induced cell differentiation that manifested as morphological changes, lipid droplet accumulation and modulation of gene expression.[94, 105, 106]

1.4.2.5 NF-κB Signaling pathway

A recent effort has led to the discovery that tylophorine potently inhibits NF-κB–promoted transcription (IC_{50} = 30 nM) and, to a lesser extent, that of AP-1 and CRE (IC_{50} = 500 nM).[58] Several closely related analogs, including DCB-3503, were also discovered with similar effects.[60] It is unclear if these events are related through overlapping signaling networks but it does provide deeper insight into the root cause of tylophorine's pharmacological effects. NF-κB–signaling pathways are an integral part of normal cell growth and immunological function.[107-109] A large cohort of cytokines, growth factors and effector enzymes associated with immune responses are strictly regulated by this transcription factor. Furthermore, a growing body of evidence has linked the dysregulation of NF-κB to the onset of cancer and immune-related disorders.[107-109] Thus, the discovery that tylophorine inhibits NF-κB provides a hypothetical link between tylophorine's seemingly

disparate pharmacologies—namely, anti-cancer and anti-inflammatory/immune—and demonstrates therapeutic potential through a validated target.

1.4.2.6 DNA and RNA

Other targets for the phenanthropiperidines that have been explored recently are DNA and RNA. Xi *et al.* prepared a small library of DNA oligonucleotides containing a variety of secondary structures, such as hairpin bends and bulges, and studied antofine's associative properties.[110] Antofine showed clear preference for duplex oligonucleotides as measured by dissociation from and stability of the DNA-alkaloid complex. Moreover, the alkaloid binds with moderate selectivity for DNA bulges in a 1:1 stoichiometry (Fig. 1–10) and shows slight sequence selectivity. The significance of antofine's selectivity toward bulged DNA and RNA lies in the fact that these abnormalities are implicated in the etiology of numerous diseases.[111, 112] Docking studies with the bulged structures give reason to conclude that this association is intercalative. It is worth reiterating here that tylophorine does not induce DNA damage as DNA-bulge–selective agent neocarzinostatin does. Tylophorine's affinity for DNA, however, has yet to be investigated. In addition to DNA binding, antofine has also shown high affinity for the assembly origin of Tobacco Mosaic Virus (TMV) RNA.[113] This RNA motif contains hairpin loop structures with several bulges. Antofine was found to bind to with a K_D of 9 nM and a 1:25 stoichiometry.

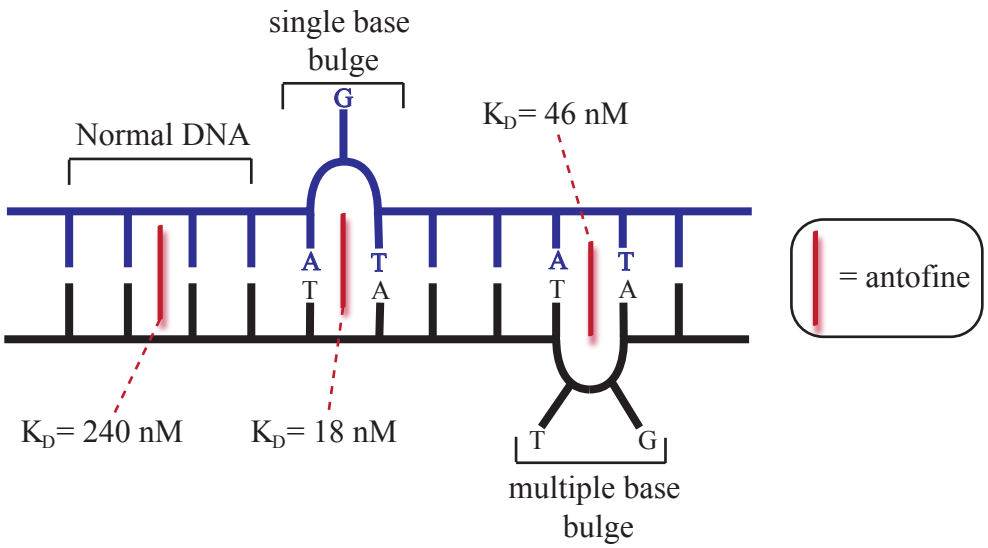

Fig. 1–10. Antofine's affinity for DNA structures.

The high affinity of antofine for DNA and RNA structures impels consideration in discussions of its mechanism of action and warrants further characterization in more complex systems such as cells. Furthermore, in view of the homogeneity within this class, these interactions should be determined for other members and correlated with their anti-proliferative activities. Considering the planarity of the phenanthrene system and structural similarity to other DNA intercalators (*e.g.* ethidium bromide), the question of intercalation is an obvious one and should be addressed.

1.4.2.7 Other molecular targets

In addition to the 40S ribosomal subunit and polynucleotides, several other molecular targets have been proposed for the phenanthropiperidines. Thymidylate synthase[114, 115] and dihydrofolate reductase[116] inhibition have been observed at high concentrations (IC_{50} > 30

μM) of tylophorinidine. Since the phenanthropiperidine's activity is in the low nanomolar range, invoking these targets to explain its anti-cancer activity is seemingly gratuitous.

1.4.3 Anti-inflammatory activity

Like anti-cancer properties, the basis for the anti-inflammatory and immunosuppressive effects is not straightforward. The plant extracts were clearly shown to suppress the inflammatory response in cell, animal and human models. With this in mind, the first task was to demonstrate that the pure alkaloids retained the anti-inflammatory effects of *T. indica* and its extracts. This was borne out in several studies that confirmed that pure tylophorine allayed immunopathological and inflammatory reactions *in vitro* and *in vivo*.[117, 118]

In pursuit of a novel anti-rheumatic agent, Yin and coworkers identified the promising tylophorine analog, DCB-3503.[119] The compound was chosen based on its inhibitory effects on TNFα-induced NF-κB activity (IC_{50} = 100 nM). Although the reason for choosing this analog over tylophorine, in spite of its inferior NF-κB activity, was not disclosed, it is noteworthy that this hydroxylated analog outperformed tylophorine in animal studies, presumably due to improved pharmacokinetics.[58] Mice injected with collagen or lipopolysaccharide (LPS) to induce arthritis were treated with DCB-3503 and closely monitored for signs of efficacy. It was found that the development, onset and severity of LPS- and collagen-induced arthritis were abated with no signs of toxicity. TNFα and IL-1β, two important pro-inflammatory cytokines, were down-regulated at the systemic and local level. Furthermore, immune-cell production of key inflammatory signaling molecules, such

as TNFα, IL-12, IL-6, MCP-1, iNOS and COX-2, was significantly impaired, demonstrating DCB-3503's multifaceted approach to suppressing the arthritic immune response.

Indeed, inhibition of NF-κB transcription is a plausible explanation for these extensive biological effects, but this conclusion may be reductionistic. Earlier work in LPS/IFNγ-induced RAW264.7 cells (a murine macrophage cell line), found that tylophorine significantly reduced TNFα, iNOS and COX-2 production at 3-10 μM without causing NF-κB inhibition.[120] AP1 activation, however, was significantly inhibited. This result was accounted for by measuring the levels of upstream signaling factors MEKK1, Akt and c-Jun. Although tylophorine blocked MEKK1 activation, which normally inhibits NF-κB, concurrent Akt activation counteracted its effect. While the relation of these events to the attenuation of inflammatory responses is discernible, the molecular basis for such a response remains elusive. Indeed, the complex network of biochemical processes within this pathway that are constitutively interlaced with feedback loops and other regulatory events makes the search for molecular target an immense challenge.

1.4.4 Miscellaneous activity

In addition to their anti-cancer and anti-inflammatory effects, the phenanthropiperidines have been investigated for activity in several other systems. In some of the earliest biological studies with these alkaloids, Barnard reported that cryptopleurine had colchicine-like c-mitotic activity in the root tips of germinating onion seeds.[121] In oyster embryos and yeast, in spite of inhibiting growth, its activity at 10^{-6} to 10^{-3} M did not seem to resemble that of

colchicine.[122] Anti-fungal activity was also observed for cryptopleurine and some closely related analogs.[123] Amoebicidal,[78, 124] insecticidal[125] and anti-feedant[126] properties have also been reported.

Anti-viral effects have also been noted. When kidney cells were exposed to crytopleurine and subsequently inoculated with herpes virus hominis, viral growth was stunted.[127] The alkaloid did not, however, have any antiviral activity in coxsackie B-5 or polio-type I viruses. Antofine was also found to exhibit anti-TMV activity in the low micromolar range, presumably due to its affinity for RNA.[128] Following up this discovery, Wang *et al.* studied tylophorine (racemic, *S* and *R*), (±)-antofine and (±)-deoxytylophorine, finding that they also possessed anti-TMV activity. With the goal of improving solubility and stability, a series of tylophorine salt derivatives were prepared.[129] These salinized analogs, besides being more soluble and stable, had improved *in vitro* and *in vivo* anti-TMV activity, surpassing that of commercial Ningnanmycin.

1.4.5 Summary of biological activity

The prodigious effects of the phenanthropiperidines on living systems are indisputable, but they have yet to be harnessed to treat disease in the clinic. Within the past decade, a there has been a concerted effort to validate their therapeutic potential in both cancer and immune/ inflammatory-related diseases. Although the literature is replete with studies on the phenanthropiperidines, the data extracted from different assays, cell-lines and animal models have led to a fragmented understanding of the mechanism by which these alkaloids modulate

immune responses and inhibit the growth of cancer cells. Nevertheless, protein biosynthesis inhibition and modulation of key transcription-factor activity are among the best validated mechanisms of action. This is not to say, however, that there is a single molecular target. Increasing evidence suggests that the phenanthropiperidines perturb multiple macromolecules. For instance, some of the most well-studied members of this class have affinity for the 40S ribosomal subunit, DNA and RNA. Therefore, the identification of specific targets may not be sufficient to explain the extent of their pharmacology.

1.5 Obstacles to clinical success

While many phenanthropiperidines exhibit promising activity *in vitro*, this activity has not translated well into animal models. The NCI has conducted multiple *in vivo* studies with the salient members in this class: tylophorine, tylocrebrine and tylophorinine. These alkaloids provide up to 150% life-extension in the most responsive tumor model, L1210 leukemia. Unfortunately, other tumor models such as adenocarcinoma 755 and Sarcoma 180 were much less responsive. The basis for this *in vitro*/*in vivo* discrepancy is undoubtedly multifactorial and is just beginning to be understood.

Cheng and coworkers noticed that despite comparable activities *in vitro*, tylophorine and DCB-3503 behaved differently in animal studies.[58] Notably, previous assessment in the NCI hollow fiber assay scored DCB-3503 higher than tylophorine (26 vs. 4). Compounds that score above 20 are generally considered for further animal studies.[130] It was posited that this difference was linked to drug delivery or stability. Both compounds were subsequently

tested in a HepG2 xenograph murine model using multiple dose regimens. Again, DCB-3503 had superior antitumor activity compared with tylophorine.[58] This idiosyncrasy could result from differing pharmacokinetic profiles, but no extensive PK studies have been reported. Indeed, PK data would be invaluable to understanding why such potent compounds fail to perform *in vivo*.

In addition to the aforementioned toxicity of cryptopleurine,[16] the therapeutic window is another important consideration in this discussion. Some toxicological data can be gathered from the NCI database that reports the mortality in each model system. From this and other *in vivo* studies it seems that an effective dose can be reached without causing overt toxic effects. Tylophorine has been studied most extensively with respect to its toxicity. One study reported that an oral administration of tylophorine (1.25-2.5 mg/kg/day) over 15 days produced no toxic effects in rats, whereas an oral dose of 35 mg/kg was lethal in 50% of the animals.[131] In another study, rats and hamsters receiving seven oral doses of 5 mg/kg result had a 50 and 80% mortality rate, respectively.[124] Contrasting with these reports, a dose as high as 500 mg/kg of (*R*)-tylophorine was found to be non-toxic in rats.[117]

In addition to acute toxicity, another impediment to the therapeutic potential of these compounds is their neurological effects. It was observed that at high doses, rodent models experienced CNS depression (ptosis, sedation, decreased motor activity and staggered gait).[117] This is noteworthy because of the CNS effects—namely, ataxia and disorientation—experienced by subjects in tylocrebrine's clinical trials.[2] In light of tylophorine's similar physicochemical properties, it is clear why this is such a concern. In a recent review, Hitchcock and Pennington show that the degree of passive diffusion across the blood-brain

barrier (BBB) correlates with a molecule's polar surface area (PSA), number of H-bond donors (HBD), cLogP, cLogD and molecular weight.[132] Calculating these properties for tylophorine and tylocrebrine reveals that each value falls well within the suggested parameters for CNS drugs on all accounts (Table 1–9). Of course, if the aim is to reduce CNS-mediated side effects the alkaloids should be endowed with properties less conducive to BBB permeation.

Table 1–9. CNS drugs and tylocrebrine's physicochemical properties.

property	top 25 CNS drugs mean values	suggested limits	tylocrebrine
PSA (Å^2)	47	< 90	40
HBD	0.8	< 3	0
cLogP	2.8	2-5	4.3
MW	293	< 500	394

PSA = polar surface area, HBD = hydrogen-bond donors, MW = molecular weight.

Another concern which is intimately related to physicochemical properties is low solubility. The high lipophilicity of these molecules is a likely contributor. Fortunately, mitigating BBB permeation by incorporating polar functional groups will probably improve solubility as well. The planarity of the phenanthrene system is probably another culprit. In a recent review, Loverling *et al.* show that increasing sp^3 character in drug candidates correlates with improved solubility and hence its clinical success.[133] Whether this strategy can be successfully employed for phenanthropiperidines is still to be realized. If these alkaloids exert their effects through intercalation, relying on sheer planarity, improving

solubility by increasing saturation may ultimately be counterproductive. Although these impediments to clinical success seem daunting, there are still many "tricks of the trade" that have yet to be explored.

1.6 Synthesis of phenanthropiperidine alkaloids

The accessibility of bioactive molecules largely determines the feasibility of drug development. Without an adequate supply, even the most active medicinal agents are rendered useless. Currently, supply is not a limitation for *preclinical* investigations of the phenanthropiperidines. Compared with many natural products, these alkaloids are structurally simple, and reliable synthetic routes have—for the most part—replaced isolation methods. Spurred by unique structural features and biological properties, organic and medicinal chemists have endeavored to provide a sustainable source of these alkaloids and to give access to novel synthetic analogs with improved therapeutic potential. Indeed, these routes have greatly facilitated lead optimization. With this in mind, the obstacles to clinical success seem less daunting.

Synthetic approaches to the phenanthropiperidines have matured since the first efforts. Advancements in transition metal catalysis and heterocycle synthesis have been crucial to this enterprise. There is no shortage of total syntheses for many of the well-known members of this class. Owing to their long history and archetypal structures, tylophorine and cryptopleurine boast over twenty distinct routes. Antofine is another popular target due to its extremely potent cytotoxicity. The number of synthetic undertakings that have been

successfully used to prepare these alkaloids far exceeds the scope of this work, so, we will focus only on key sequences within the total syntheses that have led to the construction of the phenanthrene system and indolizidine/quinolizidine scaffolds. Reactions used to prepare parts of these systems (*i.e.* naphthyl, pyrrolidines, piperidines, *etc*.) or reactions that elaborate these two substructures will receive minimal attention. Conceivably, improved reaction sequences could be devised by piecing together parts of others.

1.6.1 First synthetic efforts towards phenanthropiperidines

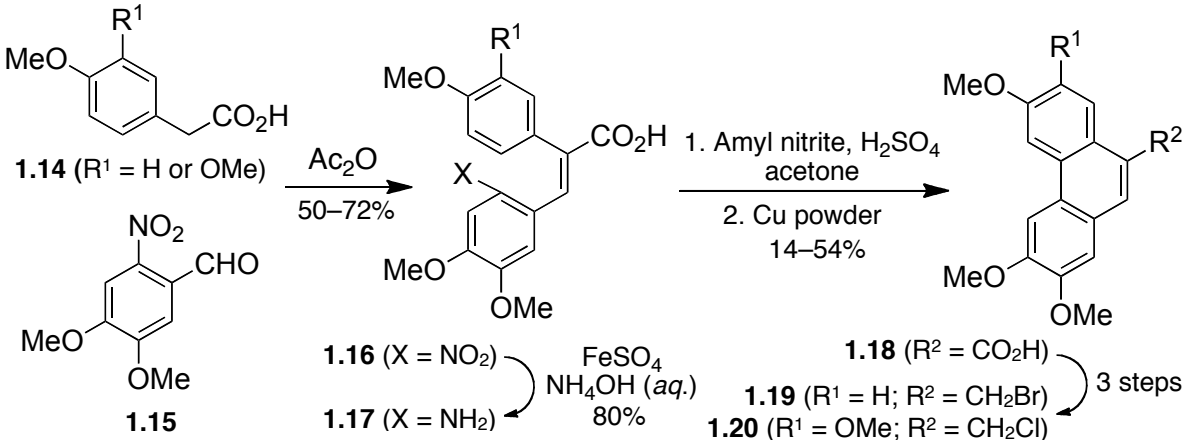

Scheme 1–2. Original method to prepare phenanthrene system.

Less than five years after the structural elucidation of crytopleurine, Bradsher and Berger reported its synthesis.[134, 135] Slightly delayed because of structural uncertainties, the synthesis of tylophorine followed closely behind.[13] With these methods already established, the synthesis of tylocrebrine could be reported simultaneously with isolation giving strong evidence for its proposed chemical structure.[20] All of these synthetic approaches used the same strategy (Schemes 1–3 and 1–4). First, the phenylacetic acid **1.14** was condensed with

nitroveratraldehyde **1.15** (Scheme 1–2). The nitro group was reduced to the amine with ferrous sulfate in preparation for phenanthrene formation (**1.16** → **1.17**). The biaryl coupling was realized using a Pschorr coupling protocol, involving conversion of amine **1.17** into the corresponding diazonium salt. Subsequent treatment with copper mediated a radical decomposition and bond formation to furnish acid **1.18**. The acid was then reduced to an alcohol, and this was displaced by either a bromide or chloride ion. Diverging slightly at this point, cryptopleurine was synthesized via *N*-alkylation of picolinic aldehyde with the phenanthrene **1.19** and cyclized in PPA (Scheme 1–3). The fully oxidized pentacycle **1.21** was then hydrogenated to (±)-cryptopleurine (**1.3**) in the final step. Tylophorine (**1.1**), on the other hand, was prepared through a C-alkylation of pyrrylmagnesium bromide and reduction and then completed using the Bischler-Napieralski protocol from amine **1.22**. The synthesis of (±)-tylocrebrine (**1.4**) was completed in a similar manner.[20]

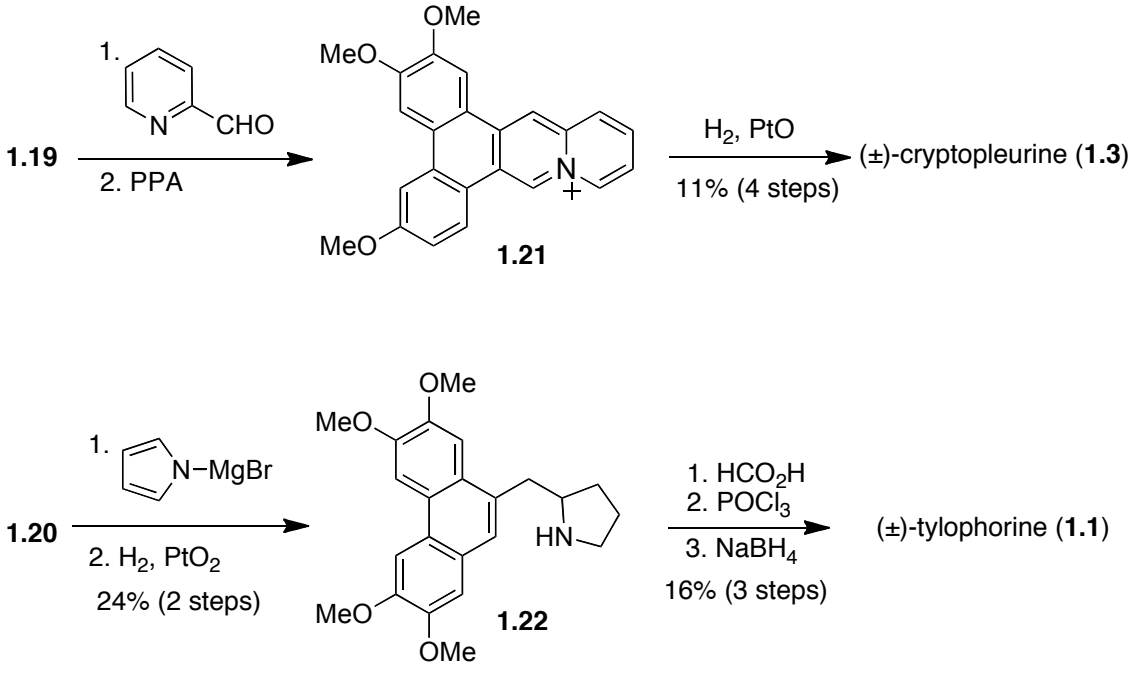

Scheme 1–3. Original syntheses of phenanthropiperidines.

1.6.2 Phenanthrene synthesis

The phenanthrene is a relatively rare component of natural products in comparison to the indolizidine. In most cases, this structure has been constructed using robust biaryl coupling reactions. The point in the syntheses at which the full phenanthrene core is realized varies considerably from route to route. There are several things that should be considered when deciding when to incorporate this moiety. In comparison with the indolizidine amine which often requires protection, the phenanthrene system is remarkably stable and is unperturbed in most reaction conditions. Furthermore, compounds containing a phenanthrene moiety are generally stable crystalline solids and hence simplify purification. On the other hand, these stable crystalline lattices can be poorly soluble making late incorporation advantageous.

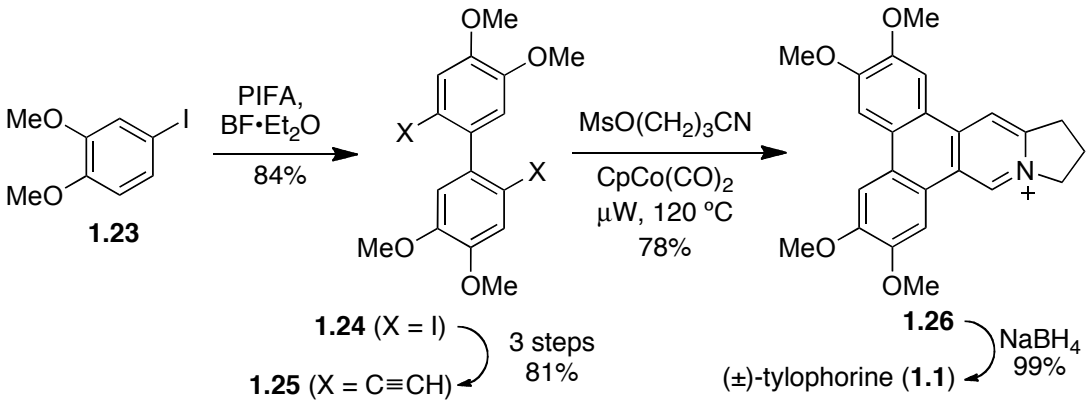

Scheme 1–4. Phenanthrene synthesis via dimerization.

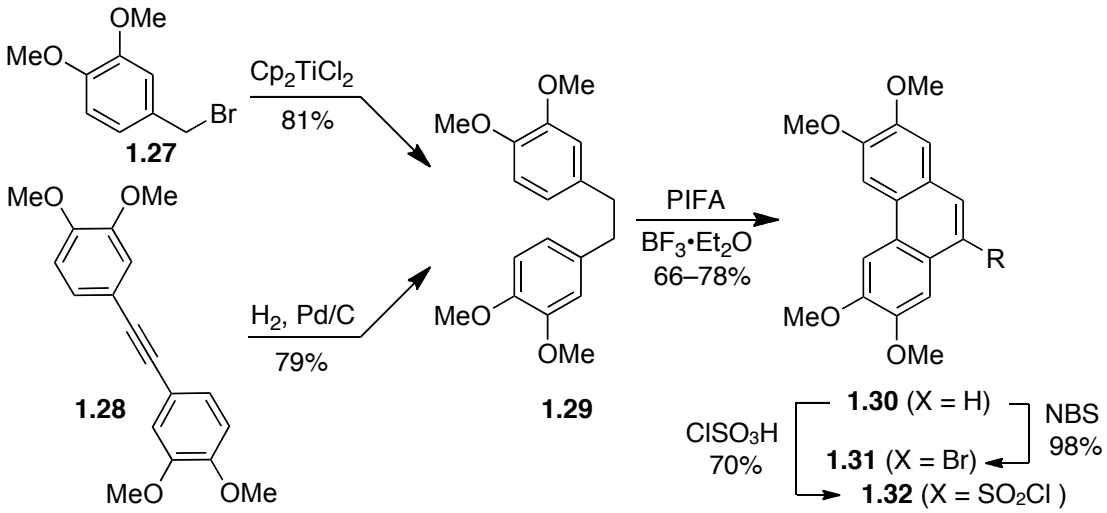

Scheme 1–5. Phenanthrene synthesis via dimerization.

The substitution pattern on the phenanthrene system determines the accessibility of each alkaloid by any given approach. Because of its symmetrical methoxy substituents, tylophorine can be synthesized through dimerization. Deiters and coworkers exploited this symmetry in their synthesis of tylophorine, beginning with a dimerization of 4-iodoveratrole (**1.23**) and subsequent conversion to the diyne **1.25** (Scheme 1–4).[136] This intermediate was desymmetrized using a [2+2+2]-cyclotrimerization with a judiciously chosen nitrile. Upon cycloaddition, the resulting pyridine spontaneously cyclized by displacing the tethered mesylate and furnished dehydrotylophorine (**1.26**), which was reduced to the natural product (**1.1**). In another example, Chelmer and coworkers used a radical-induced dimerization of benzyl bromide **1.27** followed by an oxidative-coupling reaction to prepare symmetrical phenanthrene **1.30** (Scheme 1–5).[137] Alternatively, the benzyl dimer **1.29** can be derived from an alkyne reduction of symmetrical acetylene **1.28** and carried through to phenanthrene **1.30** as before.[138] Further functionalization and desymmetrization were achieved through

bromination with NBS[138] or sulfonylation with chlorosulfonic acid to furnish phenanthrene **1.31** and **1.32**, respectively.[137] Pearson and Walavalkar demonstrated that the oxidative dimerization of homoveratric acid (**1.33**) can be used to prepare the necessary precursor (**1.34**) to (±)-tylophorine (Scheme 1–6).[139]

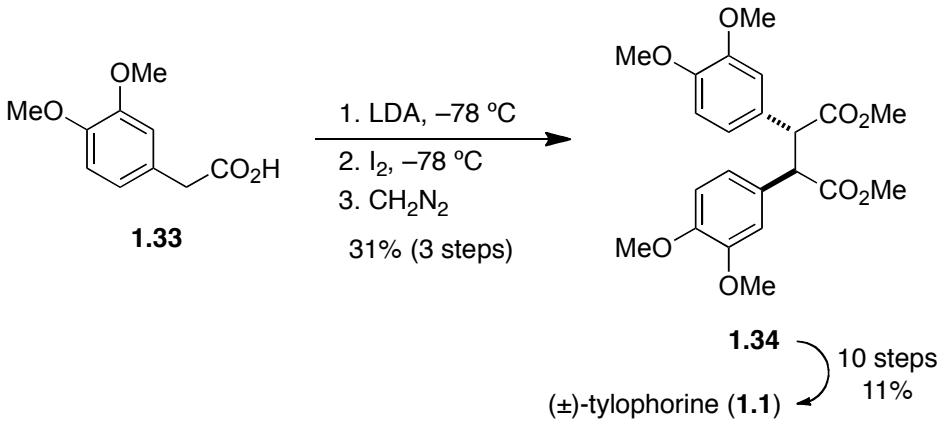

Scheme 1–6. Phenanthrene synthesis via dimerization.

The symmetrical phenanthrene substitution pattern has expedited the latter parts of total syntheses as well. Comins[140, 141] and Padwa[142] have reported the use of Pd-catalyzed bis-arylation reactions to install the requisite aryl groups in septicine, the *seco*-analog of tylophorine (Scheme 1–7).

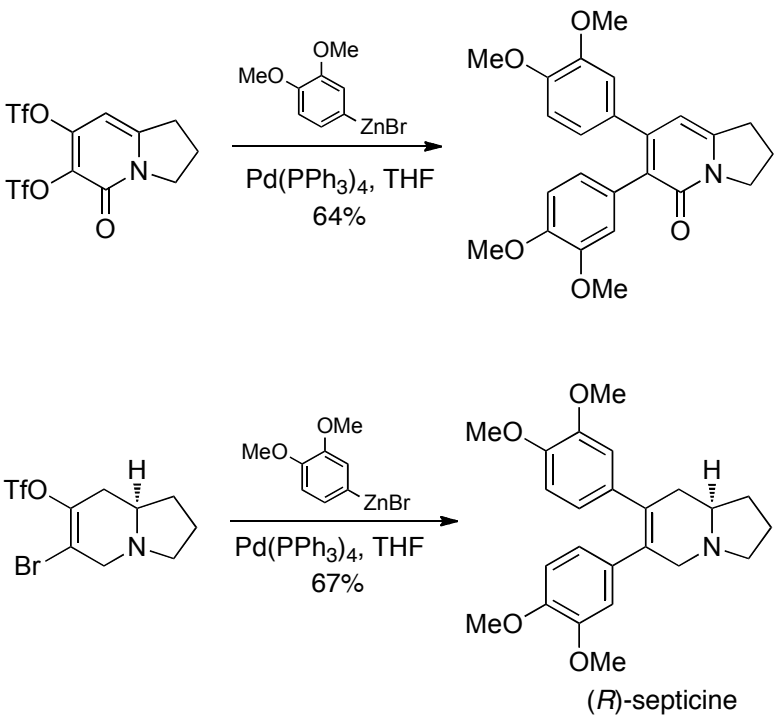

Scheme 1–7. Bisarylation strategy to synthesize phenanthrene precursor.

Despite the advantages of dimerization, desymmetrization can be challenging. The earliest strategies for phenanthrene construction used a different approach. As shown in Schemes 1–3 and 1–4, the first total syntheses of tylophorine and cryptopleurine used aldol reactions and Pschorr couplings to prepare the phenanthrene. Although the Pschorr reaction has been replaced with more efficient biaryl coupling reactions, the aldol method is still widely used[3, 4] because of its simplicity and amenability to scale up.[143] Notably, the tactic permits substituent variability on either the aldehyde or carboxylate arenes allowing the synthesis of unsymmetrical phenanthrene substitution patterns as in cryptopleurine. The stilbene aldol product is typically converted directly into the corresponding phenanthrene using a series of oxidative biaryl coupling protocols. Iron(III), vanadium(V), thallium(III)

and hypervalent iodine reagents have all been successfully used. Thallium works remarkably well for this transformation but is extremely toxic and, hence, is often replaced with less toxic reagents such as iron or PIFA. Photoirradiation can also be used but with poor regioselective control.[144, 145]

This oxidative biaryl coupling approach is synthetically attractive due to its atom economy but regioselectivity is a concern. Free rotation around the aryl-alkene bond is responsible for the formation of regioisomers which can make purification extremely difficult. Fortunately, this problem can be mitigated at low temperatures. Another caveat is that the use of oxidative couplings limits the accessibility of phenanthrenes with C4- or C5-substituents.

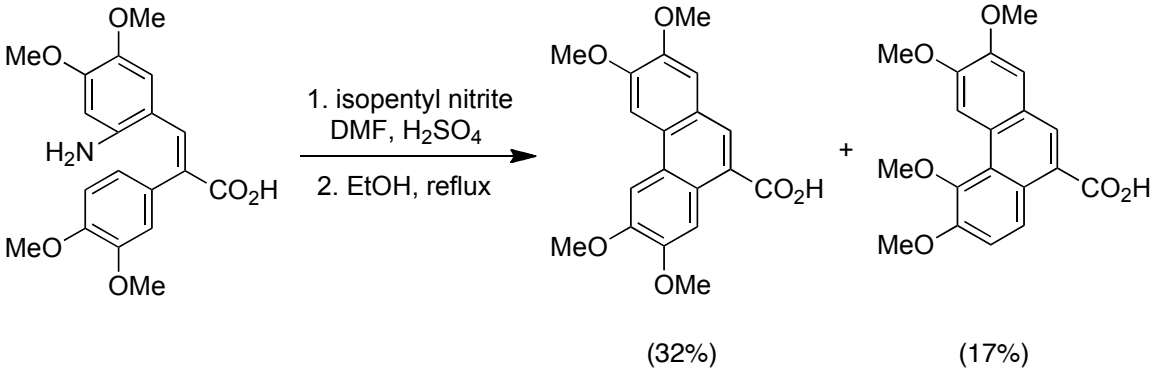

Scheme 1–8. Regioselectivity in synthesis of tylocrebrine.

It is true that tylocrebrine, which bears a C5-methoxy group, was among the first phenanthropiperidines to be synthesized, but this approach relied on the isolation of the minor regioisomer (17% vs. 32% of opposite regioisomer) of an unselective Pschorr coupling

protocol to construct the tetramethoxyphenanthrene system (Scheme 1–8).[146] This synthesis provides less than 1% of racemic tylocrebrine over ten steps and required significant effort to separate it from the other regioisomer (recrystallized three times). There is a clear need to surmount this historic challenge.

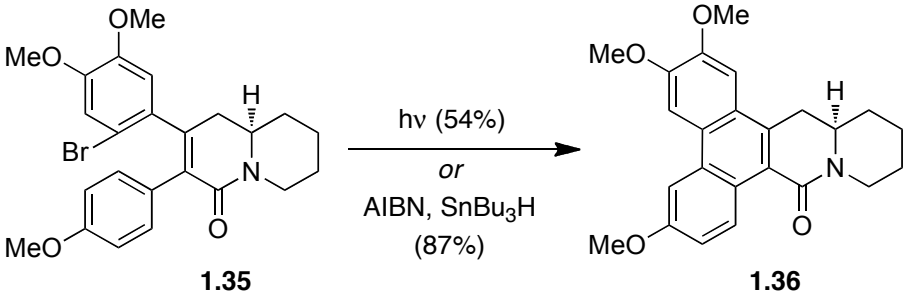

1.35 **1.36**

Scheme 1–9. Halogen-directed biaryl coupling.

Alternative approaches have been used to form the aryl-aryl bond which show promise for the preparation of phenanthrenes with these difficult substitution patterns. For instance, Kibayashi and coworkers prepared seco-analog **1.35** with a strategically placed bromide to direct C–C bond formation (Scheme 1–9).[147, 148] The phenanthrene could then be formed using either light or Bu_3SnH/AIBN to initiate the desired biaryl coupling. Since the position of the bromide determines the position of bond formation—this is analogous to the function of the amine in the Pschorr protocol—a single regioisomer (**1.36**) is obtained. This approach has not been used to synthesize phenanthrenes with C4- or C5-substituents.

It is without question that biaryl coupling strategies have dominated phenanthrene synthesis. Fürstner and Kennedy, however, reported an alternative route to four *Tylophora* alkaloids using a Pt-catalyzed cycloisomerization (Scheme 1–10).[149] This unconventional

approach relied on the assembly of the biaryl system, first via Suzuki cross-coupling. Their judicious use of simple, readily available building blocks (boronic acids and aryl-1,2-dihalides) gives this method the versatility required to access multiple analogs in a divergent manner, a feature that is conducive to lead optimization. Once alkyne **1.37** has been prepared, a Pt(II)-catalyzed cyclization provides phenanthrene **1.38** in up to 97% yield depending on the substrate. Hypothetically, this strategy could give access to the aforementioned phenanthrenes with C4- or C5-substituents, but this has not been reported.

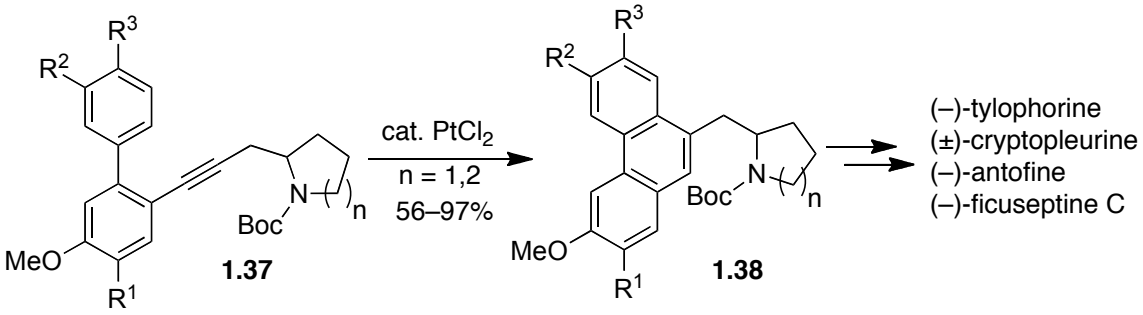

Scheme 1–10. $PtCl_2$-catalyzed phenanthrene formation.

Among the reactions discussed, a single example departs from the conventional strategy of piecing together two oxygenated arenes (Scheme 1–11).[150] In this example the tricyclic nucleus arises from a cascade process with well-placed functionalities. The sequence commences with the coupling of alkyne **1.39** and carbenoid **1.40**. The newly formed chromium carbene complex **1.41** is ideally situated to the γ-ketone oxygen and furnishes diene **1.42**. A strategically placed alkene undergoes a [4+2]-cycloaddition with the pendant furan, and upon ring-opening and dehydration of oxanobernene **1.43**, the desired

dihydrophenanthrene system (**1.44**) is obtained. Using this approach, (±)-antofine could be prepared in 7 steps, but attempts to synthesize (+)-antofine were unsuccessful.

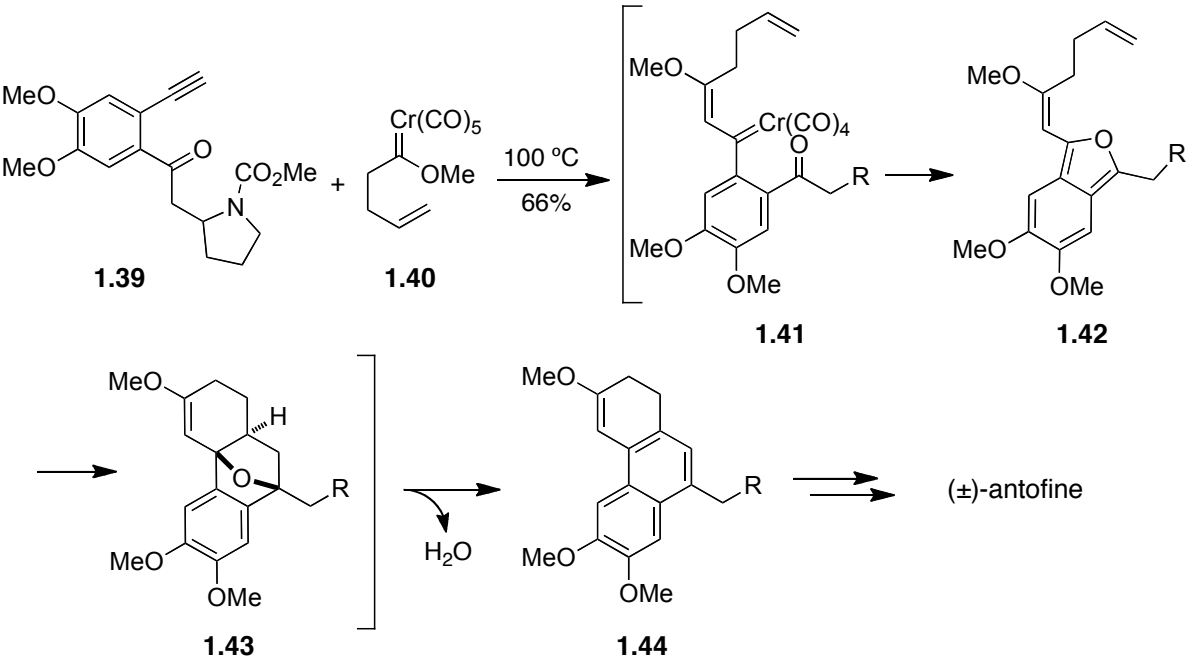

Scheme 1–11. Carbenoid cascade phenanthrene synthesis.

1.6.3. Indolizidine and quinolizidine synthesis

With the many creative and elegant approaches to the phenanthrenes discussed, we will now turn to the aliphatic heterocycle. As before, we will speak generally, emphasizing the diversity of approaches to the indolizidine or quinolizidine nuclei rather than dwelling on the intricacies of each. The strategies will be divided based on the position of the bond that is formed to fully assemble the indolizidine or quinolizidine core. Where possible, the heterocycles will be treated as isolated entities and, accordingly, are numbered as such. Unlike the reactions used in preparing the phenanthrene scaffold, the aliphatic core has been

prepared in a wide variety of ways. The following discussion will be divided based on the location of the bond that is formed in the key step (Fig. 1–11).

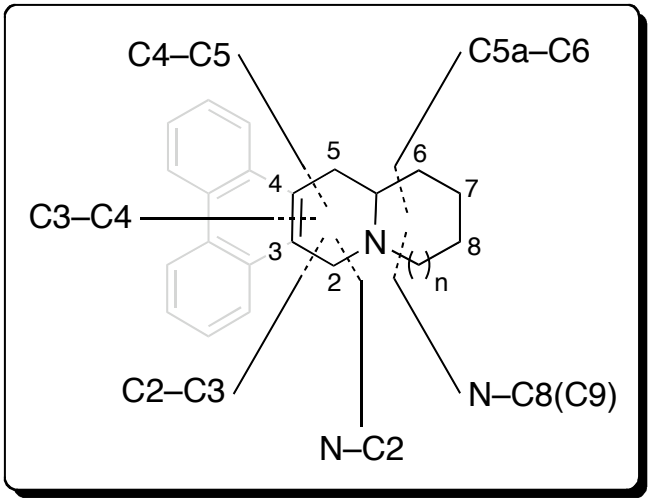

Fig. 1–11. Key-step bond formations.

1.6.3.1 C3–C4 bond forming reactions

The C3–C4 bond is the one point of confluence between the phenanthrene and piperidine structures. These carbons have been successfully conjoined using basic intramolecular aldol condensations.[151-157]

Biocatalytic approaches have successfully condensed cylic imines **1.46** and **1.47** which were enzymatically formed from putrescine and cadaverine *in situ,* with 3-oxopropionic acid **1.45** (Scheme 1–12).[158-160] Alternatively, pyrroline **1.46** can be prepared from 4-aminobutanal diethylacetal and isolated as a stable complex with zinc iodide (not shown).[151, 161] In another example, the *N*-oxides of imines **1.46** and **1.47** have also proven to be viable precursors to

the indolizidine[145, 162] and quinolizidine[144] alkaloids. Iida *et al.* used these nitrones (**1.46** and **1.47**) in a [1,3]-dipolar cycloaddition reaction yielding isoxazolidine **1.52** or its homologue **1.53**. The *N-O* bond was then reduced, providing β-amino alcohol **1.54**. A limitation of these strategies is their lack of stereoselectivity. To address this, Georg and coworkers prepared amine **1.57** in enantiomerically pure from Boc-L-β-homoproline (**1.55**) in three steps.[152, 154]

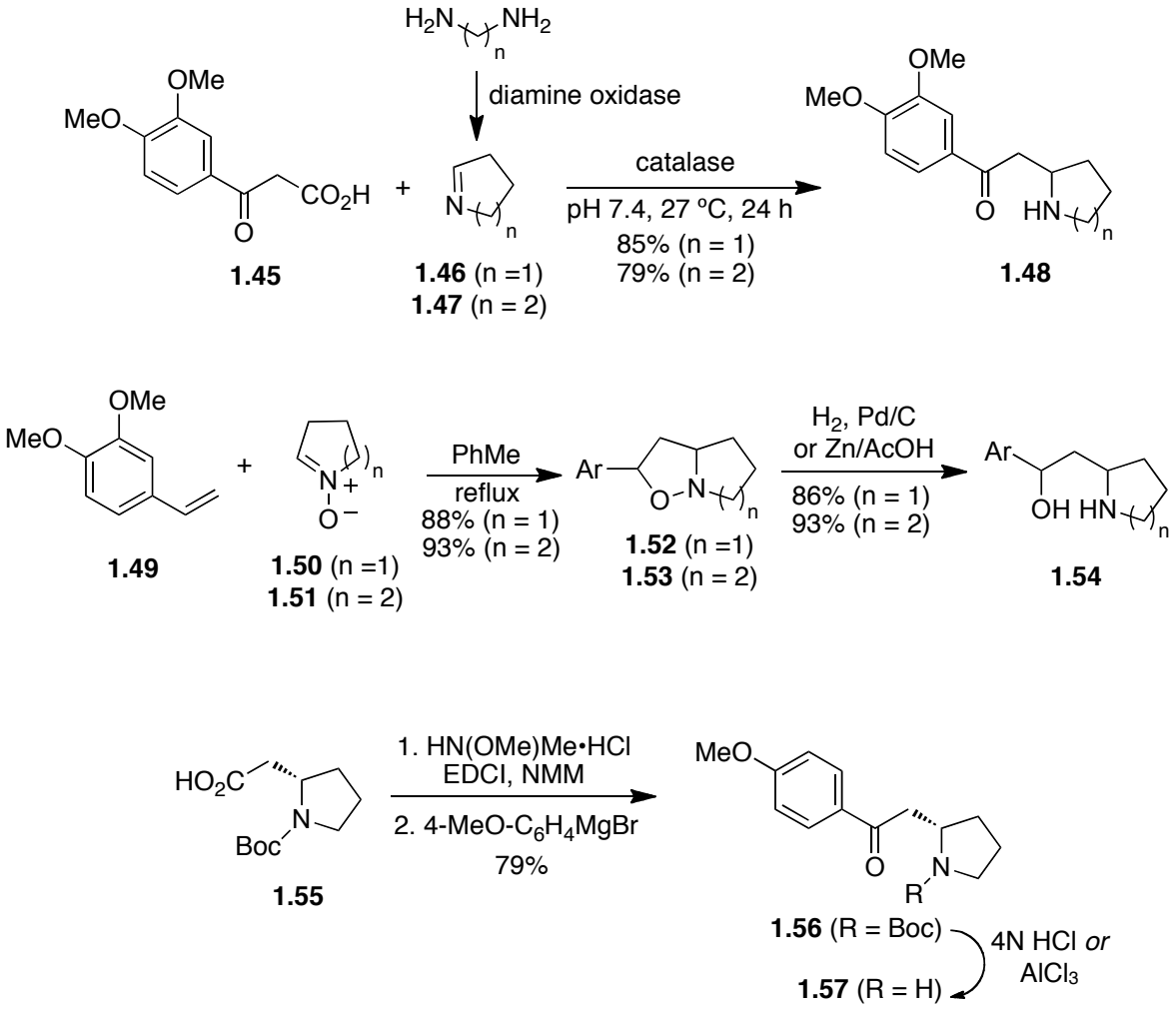

Scheme 1–12. Preparation of aldol precursors.

From amine intermediates **1.48**, **1.54** and **1.57** there have been two general approaches to the access the natural products. The one that most resembles the biosynthetic pathway begins by treating amine **1.48** with a substituted phenylacetaldehyde (Scheme 1–13).[35, 151, 155, 163-167] The enamine condensation product (**1.58**) then reacts further to furnish bisarylated indolizidine **1.59**. Seco-analog **1.60** is prepared upon reduction with $NaBH_4$, situating the intermediate for the final biaryl coupling. This approach is remarkably concise but suffers from low yields (24%). In an alternative approach, amine **1.54** or **1.57** is acylated in preparation for cyclization.[144, 145, 151-153, 162] Diketone **1.61** is then treated with KOH in an alcohol solvent, providing the dehydrated product (**1.62**) in a single step.

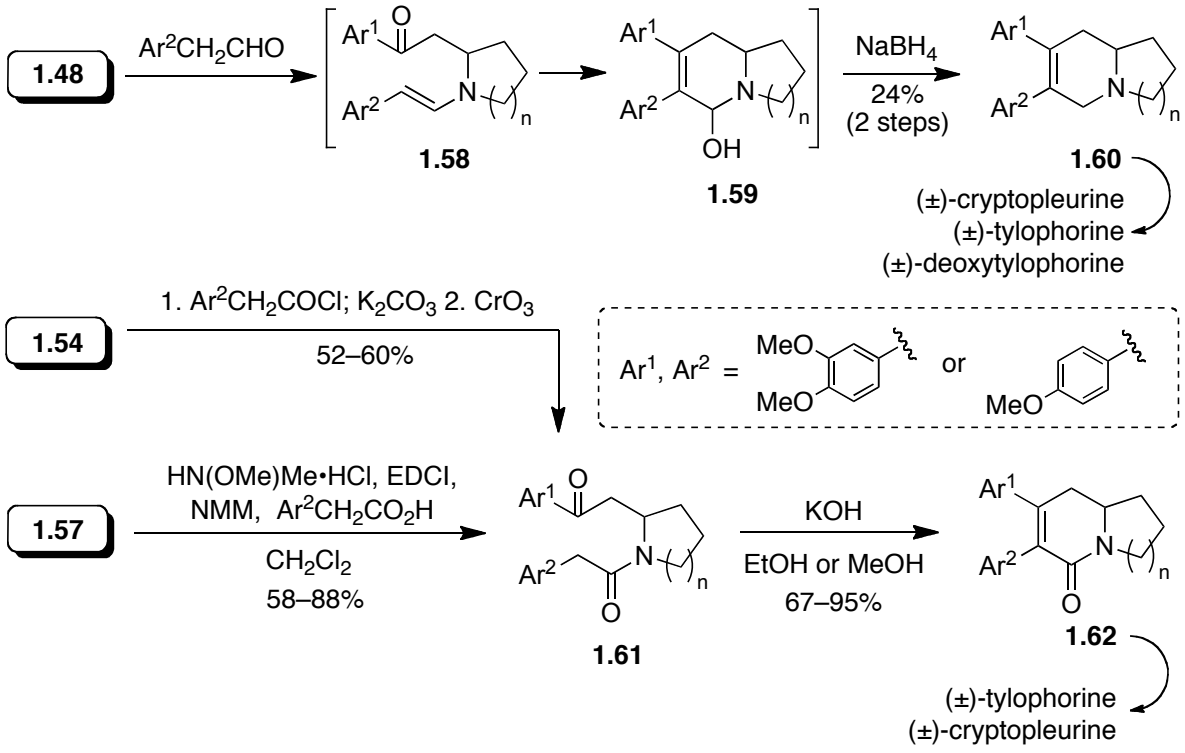

Scheme 1–13. C3–C4 Bond formation via aldol reaction.

A significant limitation was discovered in this approach when the supposedly enantiomerically pure products were found to have undergone partial racemization.[152, 154] Further inquiry into this unexpected result revealed that racemization occurred upon Boc-deprotection (**1.56** → **1.57**) and during the base-promoted aldol condensation (**1.61** → **1.62**).[152] It was proposed that a *retro*-Michael/Michael process was at play that could evidently occur in either acidic or basic conditions (Scheme 1–14). This unfortunate side-reaction has limited the utility of the intramolecular aldol approach.

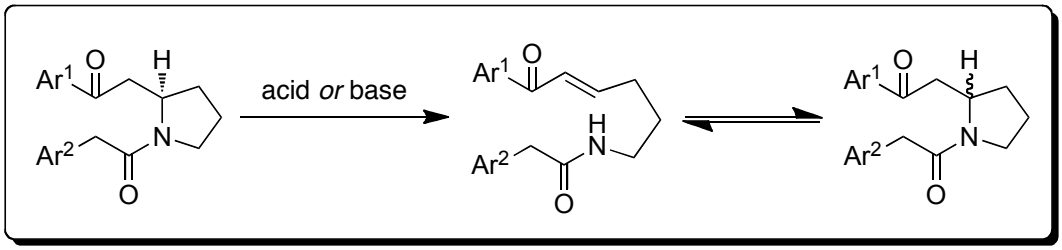

Scheme 1–14. Mechanism of β-racemization in acidic or basic conditions.

Padwa and coworkers developed a unique Rh(II)-catalyzed [1,3]-dipolar cycloaddition for the preparation of highly-substituted 2(1*H*)-pyridones that forms the C2–C3 and C5–C5a bonds of the indolizidine simultaneously (Scheme 1–15).[168] Treatment of pyrrolidinone **1.63** with $Rh(OAc)_2$ generates a cyclic ylide **1.64** *in situ,* which reacts further with substituted alkenes, providing unstable bridged-bicyclic intermediate **1.65** that spontaneously decomposes to form indolizidine **1.66**. This intermediate was then used to complete a formal synthesis of (±)-septicine (see Scheme 1–7).

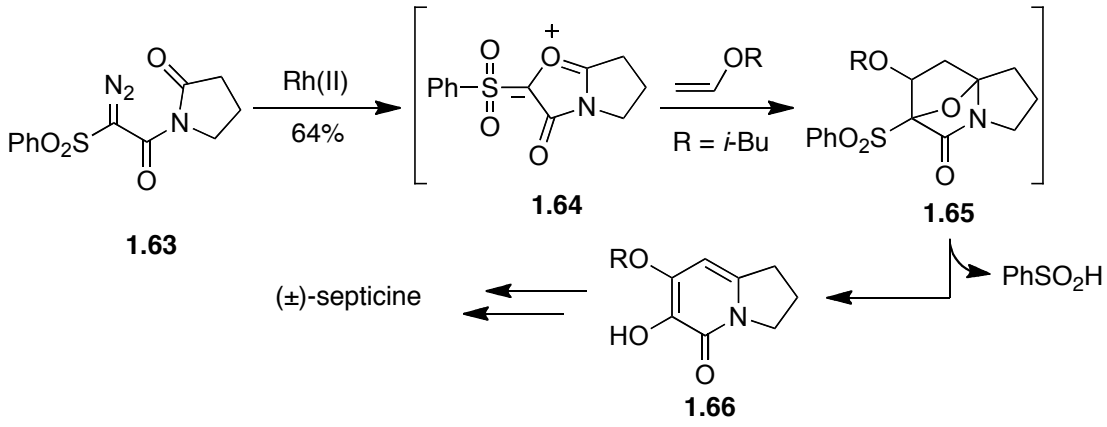

Scheme 1–15. [1,3]-Dipolar cycloaddition cascade to construct the indolizidine core.

1.6.3.2 C2–C3 bond forming reactions

The C2–C3 connection was considered by the first chemists to synthesize these natural products. As already discussed this approach relied on the Bischler-Napieralski isoquinoline synthesis in the penultimate step. This reaction, with a few exceptions,[150] has since been replaced with higher yielding and more direct approaches. Very recently Orito and coworkers reported a Pd-catalyzed aromatic carbonylation reaction, which gave access to a variety of benzolactams (**1.68**, Scheme 1–16).[169] The reactions were generally low yielding unless stoichiometric quantities of palladium were used.

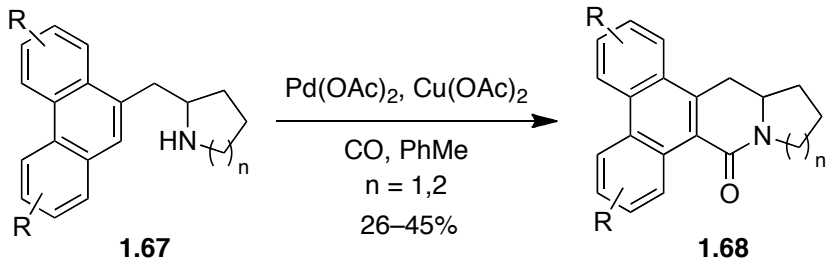

Scheme 1–16. C2–C3 Bond formation via Pd-catalyzed carbonylation.

Reactions of this kind that generate lactams require a subsequent reduction—almost always performed with LAH—to obtain the natural products. A more direct approach, however, has managed to circumvent this final reduction step. This approach, which is now in common usage, relies on the Pictet-Spengler reaction for C2–C3 bond-formation.[63, 137, 143, 149, 170, 62, 171-173] Generally speaking, an amine (**1.69**) is treated with formaldehyde under acidic conditions to form an electrophilic iminium species (**1.70**), which reacts further in a 6-*endo*-trig fashion to afford the phenanthropiperidine **1.71** (Scheme 1–17). Since acidic conditions are used, amines protected with acid-labile protecting groups (*e.g.* Boc) undergo deprotection *in situ*.[62, 149]

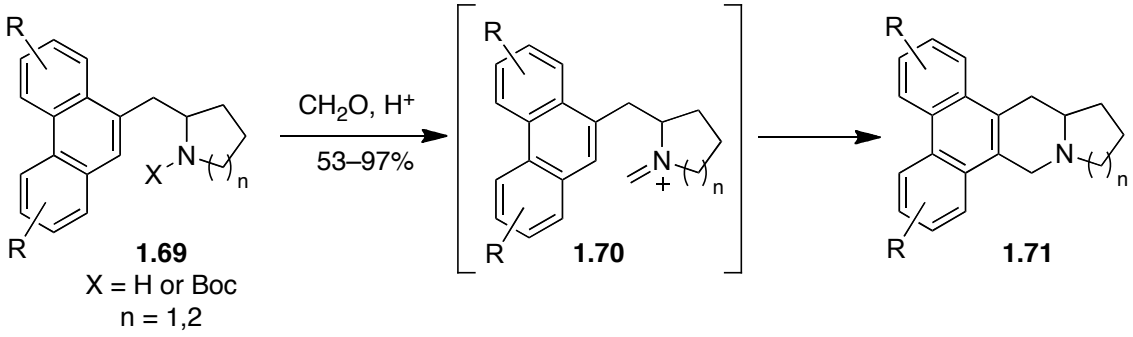

Scheme 1–17. Pictet-Spengler approach to conjoin the C2–C3 bond.

The intramolecular Diels-Alder reaction is another way to construct the C2–C3 bond. Like the Pictet-Spengler approach, this strategy exploits a reactive imine (**1.74** and **1.75**, Scheme 1–18). Weinreb and coworkers were the first to employ this strategy. The imine dienophile was generated by thermal decomposition of methylol acetate **1.72**, which underwent a [4+2]-cycloaddition to form quinolizidine scaffold **1.76**.[174, 175] The foregoing protocol could also be used to prepare the indolizidine counterparts. In an example that is

more reminiscent of the Pictet-Spengler approach, Grieco and Parker generated imine **1.75** upon treatment of phenanthrene **1.73** with formaldehyde.[176] After heating the reaction for 10 h at 180 ºC, (±)-cryptopleurine was isolated in excellent yield without the need to reduce an amide.

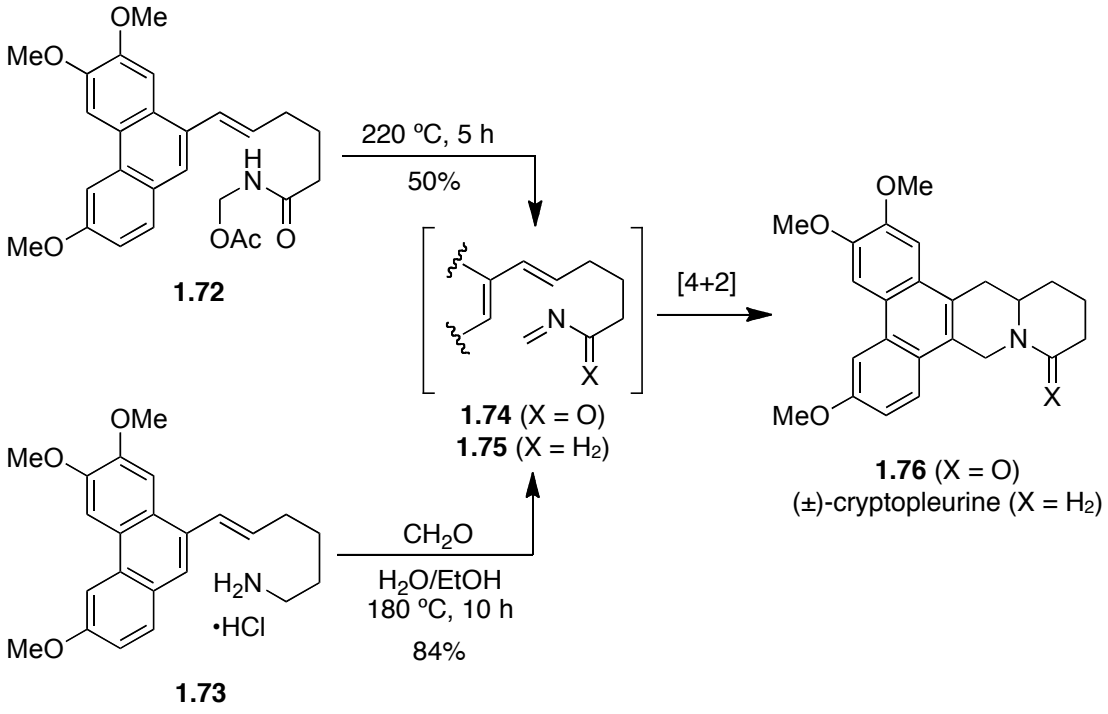

Scheme 1–18. Diels-Alder reaction to prepare quinolizidine.

Pearson and Walavalkar have used an intramolecular [1,3]-dipolar cycloaddition reaction to assemble the indolizidine core (Scheme 1–19).[139] This reaction is initiated by an azide-alkene cycloaddition of phenanthrene **1.77** to form a triazoline intermediate **1.78**, which upon fragmentation reveals a reactive imine (**1.79**). The pendant electrophile then alkylates the imine nitrogen to complete the double cyclization. In the final step, reduction of iminium

1.80 with $NaBH_4$ provides (±)-tylophorine. Kim *et al.* have recently adopted a similar strategy in the synthesis of (±)-antofine and (±)-cryptopleurine from azide **1.81**.[170]

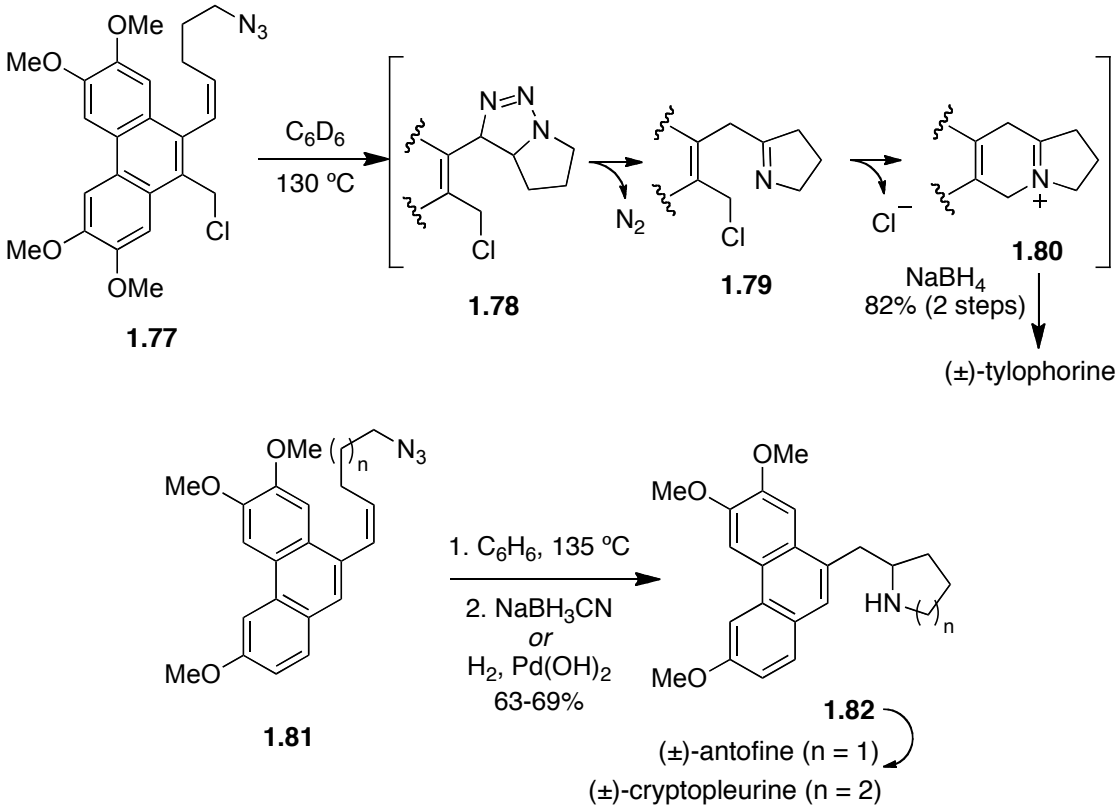

Scheme 1–19. [1,3]-Dipolar cycloadditions to prepare indolizidine.

1.6.3.3 C4–C5 bond forming reactions

The intramolecular Diels-Alder approach is an efficient way to impart complexity in a single reaction. In the aforementioned cycloadditions, however, stereochemical complexity was not addressed. One tactic that has been used to confront the challenge of asymmetric synthesis involves the use of chiral auxiliaries. With previous success in preparing (±)-tylophorine via Diels-Alder chemistry,[177] Ihara *et al.* next investigated an enantioselective

route.[178] This approach relies on the synthesis of stilbene amide **1.83** featuring a tethered (*E)*-unsaturated ester (Scheme 1–20). Using chiral auxiliaries **A** or **B**, the desired indolizidine (**1.85**) could be prepared upon treatment with TBSOTf and TEA. This reaction was deemed an "intramolecular double Michael addition", but a formal Diels-Alder mechanism has not been ruled out. Although a 4:1 mixture of C3-epimers was obtained, both benzylic stereocenters were destroyed upon oxidation to the phenanthrene system with $Tl(CF_3CO_2)_3$, and in a few steps, the first asymmetric synthesis of (*R*)-tylophorine was completed.

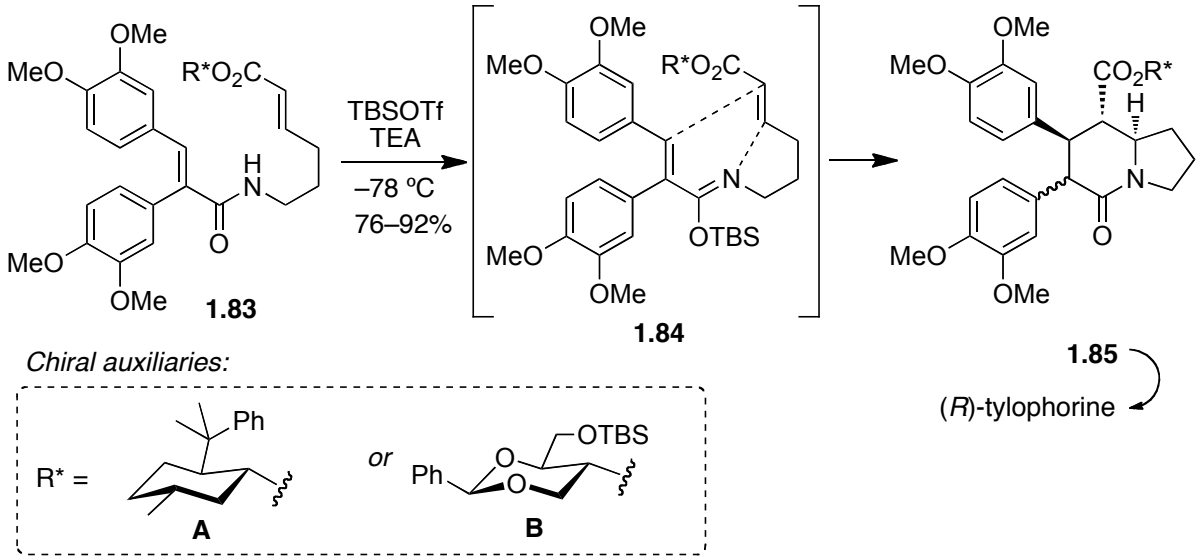

Scheme 1–20. Diels-Alder strategy to prepare indolizidine.

Recently, Chemler and coworkers developed a novel Cu(II)-catalyzed enantioselective carboamination reaction that gives rapid access to sulfam (**1.86**, Scheme 1–21).[137] Upon elimination of sulfur dioxide and Pictet-Spengler reaction, tylophorine could be prepared with an 81% enantiomeric excess. A Pd-catalyzed intramolecular variant of this strategy was

recently reported by Herr and coworkers.[138] In this example, phenanthryl bromide **1.31** undergoes oxidative insertion resulting in coordination of the carbamate and pendant alkene. Nucleophilic attack onto the Pd-activated olefin provides pyrrolidine **1.88** and subsequent reductive elimination conjoins the pyrrolidine to the phenanthrene system affording precursor **1.89**. This convergent approach was used to construct (±)-tylophorine in only six total steps and with a 35% overall yield.

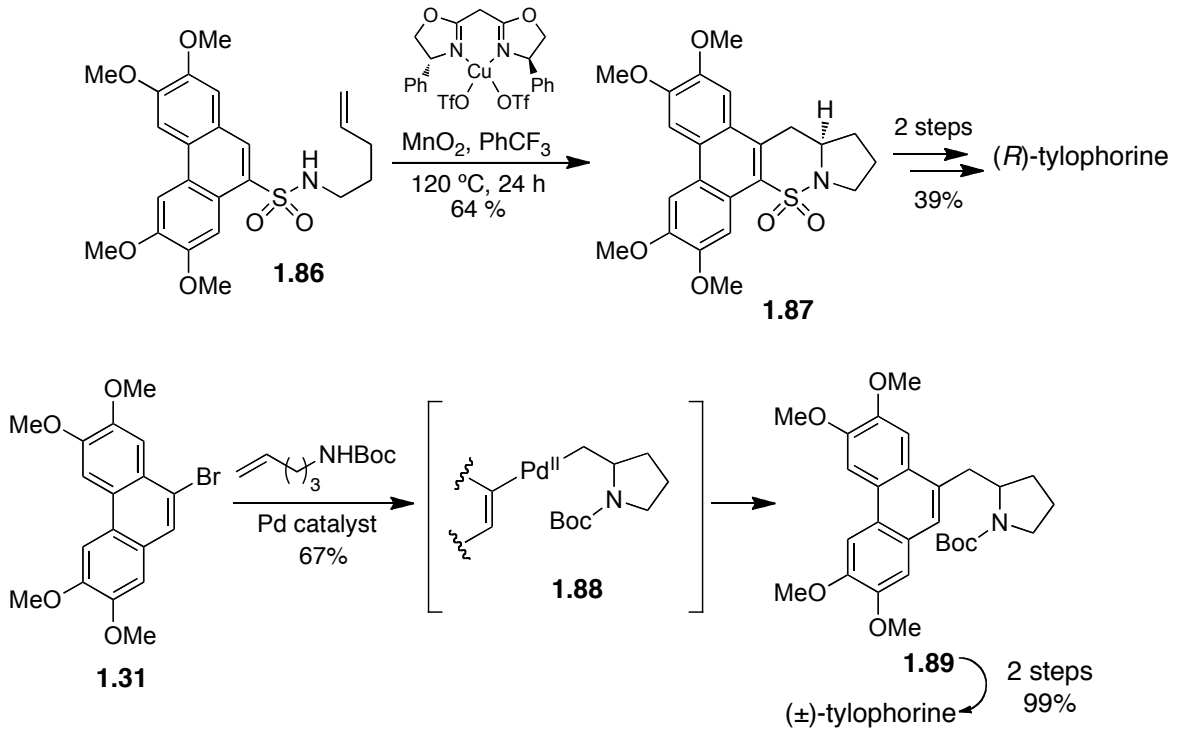

Scheme 1–21. Transition metal-catalyzed C4-C5 construction.

Successful methods to link the C4- and C5-carbons date back to the earliest phenanthropiperidine total syntheses—the first total synthesis of crytopleurine, for instance.[134, 135] This transformation is a Friedel-Crafts–type acylation. The first examples of this strategy treated the amino acid with polyphosphoric acid.[123, 146] By modern standards this

reaction provides the product in relatively poor yields (22–35%). When the acid chloride was used instead the yields greatly improved but were highly dependent on the Lewis acid used.[15] Using $SnCl_4$, for example, allowed the desired product to be isolated in near quantitative yields, whereas $AlCl_3$ gave lower yields and caused partial demethylation of the aromatic ethers. The former strategy (*i.e.* $SnCl_4$) has been reported by several other groups with similar results.[60, 179]

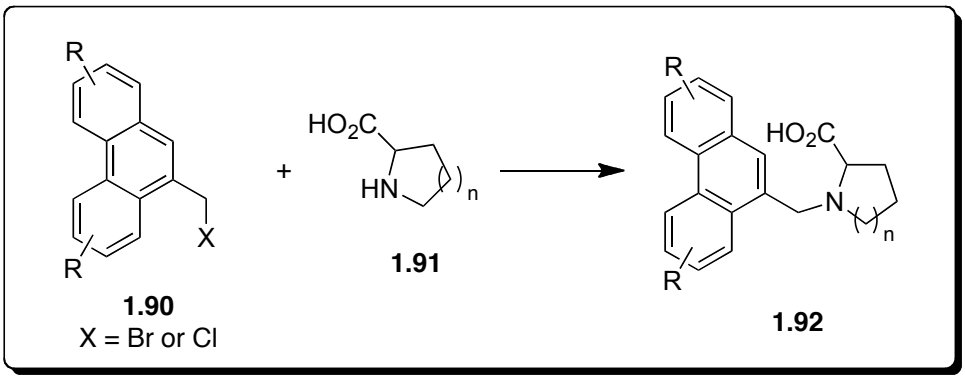

Scheme 1–22. General method to prepare Friedel-Crafts starting material.

The preparation of the Friedel-Crafts starting materials has made this approach quite practical (Scheme 1–22). Akin to the first synthesis of cryptopleurine, simple displacement of the halide of phenanthrene **1.90** with an amino acid (**1.91**) gives rise to the requisite cyclization substrate (**1.92**). Thus, the stereochemistry can arise from the chiral pool using amino acids such proline or pipecolic acid. The stereochemical integrity during the Friedel-Crafts reaction is an obvious concern considering the well-known susceptibility of α-amino acid chlorides to racemization.[180] Although the final natural products are reported to be optically active, the broad range of reported optical rotation values for the isolates makes it

impossible to deduce the enantiomeric purity within a reasonable margin of error. Analytical chiral resolution will be necessary to settle this.

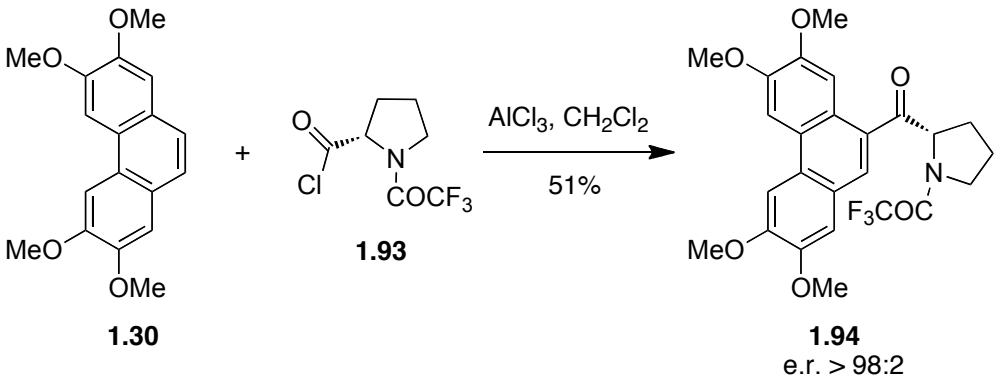

Scheme 1–23. Friedel-Crafts acylation without racemization.

It is worth noting that an *intermolecular* Friedel-Crafts strategy has also been used that did not result in stereochemical damage (Scheme 1–23). Nordlander and Njoroge used *N*-trifluoroacetylprolyl chloride (**1.93**) in the presence of $AlCl_3$ to acylate symmetrical phananthrene **1.30**.[173] Using a lanthanoid chiral shift reagent the enantiomeric purity of the product **1.94** was determined by NMR and found to be greater than 98%.

1.6.3.4 N–C2 bond forming reactions

One particular total synthesis effort demonstrates striking ingenuity in constructing the N–C2 bond. Iwao and coworkers reported a directed *ortho*-metallation strategy in the synthesis of (±)-cryptopleurine and (±)-antofine (Scheme 1–24).[181, 182] The appropriate diethylamide was lithiated with *s*-BuLi to provide intermediate **1.95** and quenched with an

aromatic aldehyde. The oxygen of the newly formed alcohol was then translocated upon lactone formation and C-O bond reduction with Zn-Cu. With all the carbons in place, acid **1.97** was converted to the (±)-antofine and acid **1.98** into (±)-cryptopleurine. The penultimate step is the key reaction in this final sequence which forms the N–C2 bond through an acylation of the heterocyclic amine.

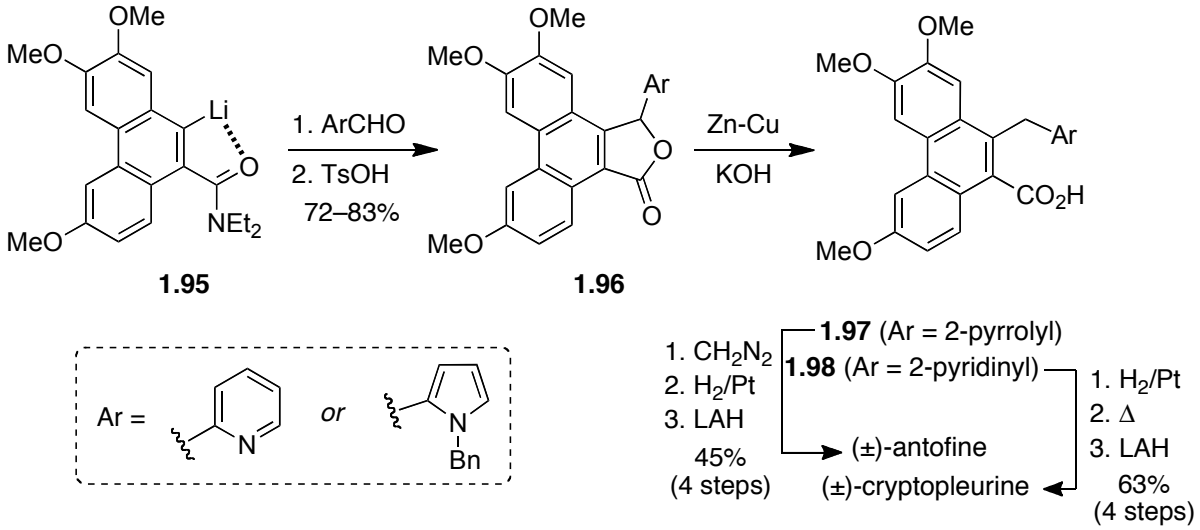

Scheme 1–24. Lactamization strategy to form indolizidine and quinolizidine.

1.6.3.5 N–C8(C9) bond forming reactions

The piperidine heterocycle (ring D) fused to the phenanthrene is completely conserved within all of these alkaloids whereas the distal heterocycle (ring E) adds a new element of structural diversity. The wealth of reliable C–N bond-forming reactions makes this disconnection an obvious choice. Indolizidine formation via pyridine alkylation has been one approach to realize this bond formation.[183] Using this approach, an inverse electron-

demand cycloaddition using styrenes **1.99** and **1.100** furnished pyran **1.101** which could be converted to the pyridine (**1.102**) upon treatment with hydroxylamine (Scheme 1–25). Further elaboration provided the tethered primary alcohol which was displaced upon treatment with mesyl chloride. Treatment with $NaBH_4$ reduced the resultant pyridinium species to the desired indolizidine **1.103**. This strategy was applied to indolizidine and quinolizidine formation and was used to prepare, (±)-tylophorine, (±)-antofine and (±)-cryptopleurine.

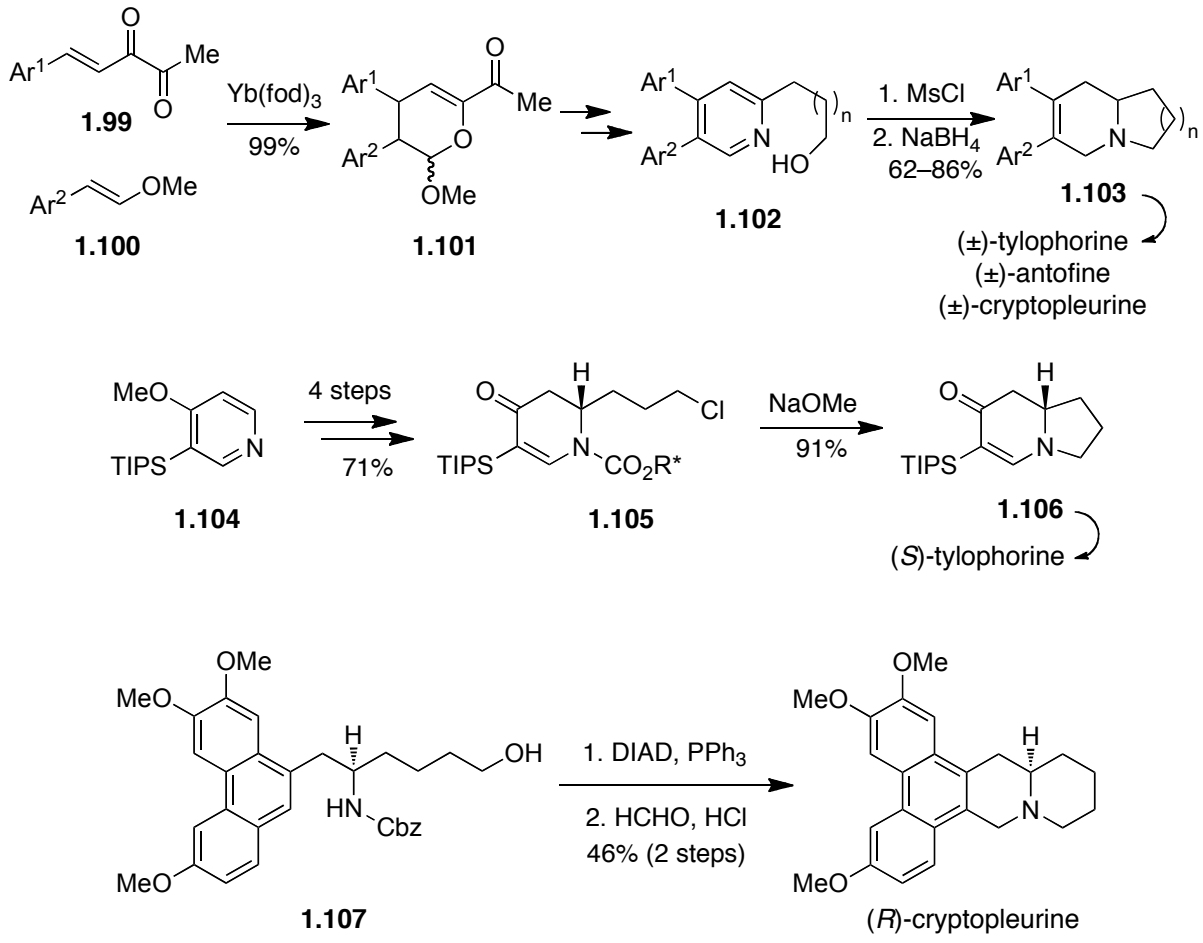

Scheme 1–25. N-Alkylation to construct ring E.

Achieving similar ends in an asymmetric fashion, Comins *et al.* prepared enaminone **1.105** from pyridine **1.104** enantioselectively using *N*-acylpyridinium chemistry.[141] Upon deprotection of the carbamate chiral auxiliary the resultant amine spontaneously cyclized. The enaminone intermediate **1.106** was then used to prepare (*S*)-tylophorine. Similarly, an intramolecular Mitsunobu reaction of Cbz-aminoalcohol **1.107** was employed in the synthesis of (*R*)-cryptopleurine by Kim and coworkers.[184]

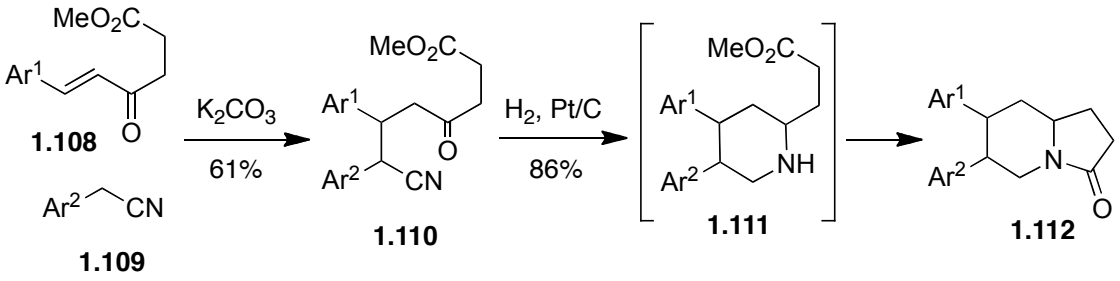

Scheme 1–26. Hydrogenation cascade reaction to form ring E.

Cascade reactions have a strong reputation for being able to rapidly assemble complex molecules. To construct the indolizidine in tylophorine, Leipa *et al.* developed a cascade process using hydrogenation conditions (Scheme 1–26).[185] The starting material was easily prepared *via* Michael-addition of cyanide **1.109** into unsaturated ketone **1.108**. Under reductive conditions, cyanide **1.110** was first reduced to primary amine (not shown), which triggered a tandem condensation/reduction/acylation sequence, providing an excellent yield (86%) of bicyclic product **1.112**.

Preparing heterocycles can often be facilitated through ring expansion reactions and this too has been aptly used in the synthesis of the indolizidine core. Yerxa and coworkers reported an unconventional route to septicine starting from squarate **1.113** (Scheme 1–27).[186]

The necessary aryl groups were installed sequentially in a 5-step sequence yielding cylcohexadienone **1.117**. Desymmetrization takes place upon addition of *N*-lithiopyrrole into a single carbonyl of diketone **1.114** and trapping the alkoxide with TMS-Cl yields pyrrole **1.115**. Upon heating in *p*-xylene, pyrrole **1.115** is thought to undergo an electrocyclization ring-opening to generate an electrophilic ketene **1.116** that intramolecularly acylates the pyrrole system. Reduction of the resultant seco-analog **1.117** yields (±)-septicine.

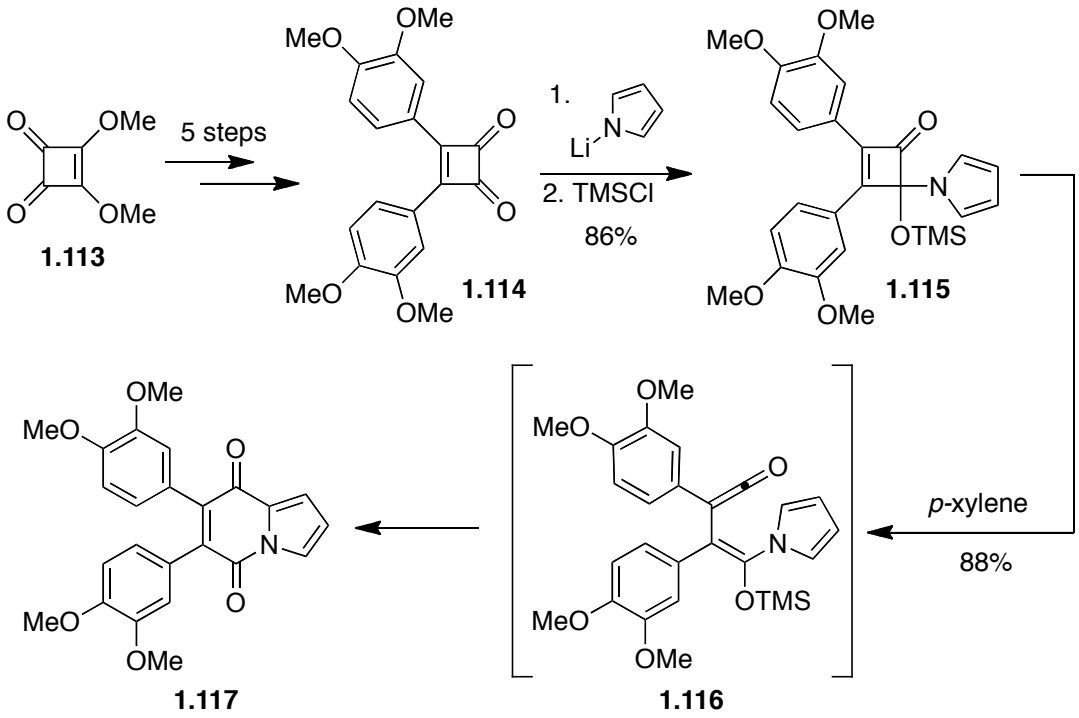

Scheme 1–27. Ring expansion strategy to form ring D.

1.6.3.6 C5a–C6 bond forming reactions

Only one report of a C5a–C6 bond formation reaction exists to construct the indolizidine and quinolizidine system exists. In this example, Chuang *et al.* formed the indolizidine and

quinolizidine nucleus by way of a radical cyclization reaction (Scheme 1–28).[56, 68] Alkyl iodides **1.118** (n = 1 and 2) were treated with AIBN as a radical initiator to yield the desired indolizidine and quinolizidine intermediates **1.119**. This reaction provides the immediate precursors to the phenanthropiperidine alkaloids.

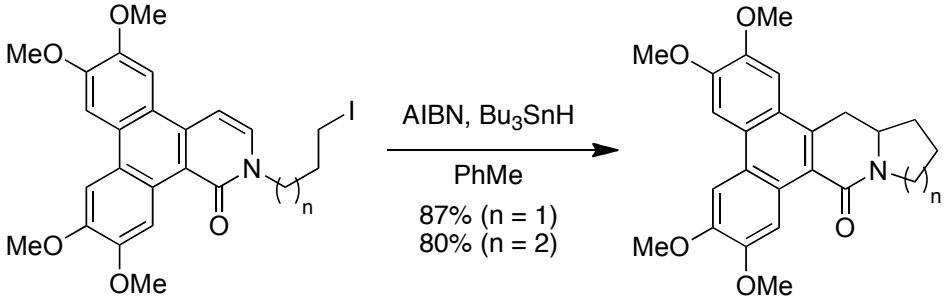

1.118 **1.119**

Scheme 1–28. Radical cyclization to form the C5a–C6 bond.

1.6.3.7 Angular OH or Me groups

The rare 13α-methylphenanthroindolizidines, such as the hypoestestatins, are attractive targets because of their unique structures, low abundance and therapeutic potential.[26-28] The methyl group at the ring juncture, however, presents a formidable challenge for synthetic chemists. A singular report discloses a possible route to these alkaloids.[187] Phenanthryl bromide **1.120** was treated with azobis-cyclohexanecarbonitrile (ACN) triggering a 6-*endo*/5-*endo* radical cascade cyclization yielding amide **1.121** (Scheme 1–29). To prepare hypoestestatin 1, the amide was reduced with LAH. The NMR spectra, however, did not match with that of the isolated alkaloid. The reason for this discrepancy remains unclear.

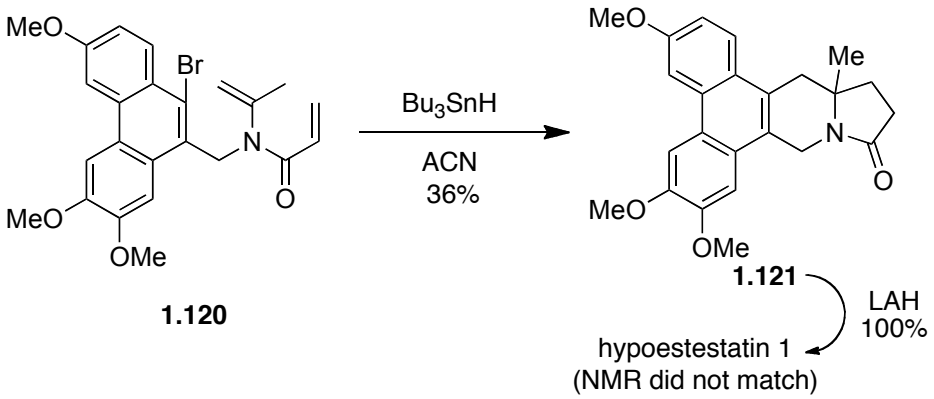

Scheme 1–29. Synthesis of hypoestestatin 1 via cascade radical cyclization.

Phenanthroindolizidines bearing 13α-hydroxy groups are also uncommon but considerably more challenging to synthesize.[29, 188] The labile aminal functionality and susceptibility to oxidation have most likely hampered synthetic efforts. Interest in the biological activity of these alkaloids is still of great interest considering the extraordinary anti-proliferative activity of tyloindicine F and G.

1.6.4 Closing remarks

The synthetic interest in the phenanthropiperidine alkaloids has given rise to a plethora of novel reactions that accentuates the artistic nature of organic chemistry. We have attempted to present these strategies in a new light, focusing on key transformations rather than on complete reaction sequences. More specifically, we opted to address reactions that result in the consummation of predefined substructures (*i.e.* the phenanthrene or fused heterocycle core) and by doing so have, unfortunately, excluded some creative methods used to construct their components. Nevertheless, we hope this review will contribute to the development of

improved reaction sequences to address limitations in yield, stereoselectivity and economy, and to encourage the preparation of novel structures with improved therapeutic utility.

1.7 Summary

This review featured a class of alkaloids, the phenanthropiperidines, which have long been known for their medicinal properties but have yet to be refined into a clinically useful drug. These alkaloids show remarkably potent anti-proliferative and anti-inflammatory/ immune activity, providing impetus for their development as therapeutic agents. Their mechanism of action likely involves multiple targets. Evidence suggests that inhibition of protein synthesis through the 40S ribosomal subunit may play a role in their anti-proliferative effects. Moreover, the best-studied phenanthropiperidines perturb NF-κB–mediated transcription and other major signal transduction pathways. There is also evidence that these planar alkaloids intercalate DNA and RNA. Whatever the cause, the upshot is cytostasis and cell differentiation—not death—that leads to long lasting suppression of cell growth. Despite this positive outlook there is still need for refinement. In regard to cancer, there is a marked difference between activity in cell cultures and activity in animal models. Presumably, the alkaloid's poor PK properties, acute toxicity and low solubility are contributing to this. There is also uncertainty about neurological side effects that could arise as they did in tylocrebrine's clinical trials. The design of new analogs, therefore, should proceed with the goal of addressing these obstacles.

To serve this end, modern synthetic routes have given ready access to the alkaloids and their unnatural congeners, providing a better understanding of SARs and a foundation for designing analogs with improved pharmaceutical and pharmacokinetic profiles. These are formidable challenges, but there is not one here that medicinal chemists have not overcome in the past for already approved drugs. It is hoped that this review will stimulate and guide future investigations into this remarkable class of molecules.

CHAPTER 2

SYNTHESIS OF SIX- AND SEVEN-MEMBERED CYCLIC ENAMINONES: OPTIMIZATION, SCOPE AND MECHANISTIC STUDIES

2.1 Introduction

The foregoing chapter described a number of obstacles that have thwarted efforts to develop a phenanthropiperidine drug. Challenges of both the biological and chemical nature have emerged and undoubtedly exacerbated one another. In particular, a dearth of novel structures within this class—whether because of synthetic limitations or a failure of synthetic chemists to apply established routes to new targets—has made iterative lead optimization burdensome and left SAR studies in a rather inchoate state. New methodologies that enable the synthesis of well-designed libraries and that diverge from the structurally homogenous collection of already-known phenanthropiperidines would prove a boon to the effort to remedy these alkaloid's undesirable properties and improve upon desirable ones. Joining this effort, we have developed a cyclization reaction for the synthesis of enantiomerically pure cyclic enaminones and have set precedent for their use in the synthesis of these alkaloids. This chapter will discuss our investigations into the mechanism and scope of this reaction.

2.2 Background

Enaminones or vinylogous amides (Fig. 2–1) are highly versatile functional groups. As their name suggests they are composed of an alkene, an amine and a ketone. Their reactivity, however, is orthogonal to each of these functional groups in isolation. Remove one of these functional groups and the molecule adopts a completely different nature. For instance, enamines, which lack the carbonyl, are typically prone to hydrolysis or oxidation,[189] whereas enaminones are quite stable and easily isolated. Conversely, enaminones are not as stable as the conventional amide. This, however, makes them more tractable and versatile synthetic intermediates.

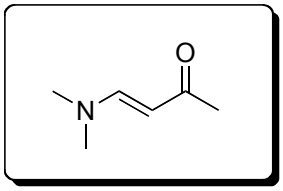

Fig. 2–1. Generic structure of the enaminone.

In addition to their distinct reactivity profile, enaminones have also attracted attention in pharmaceutical development, particularly as anti-convulsants and P-gp modulators.[190-194] Moreover, their stability and favorable physicochemical properties are exemplified by their use as orally active medicinal agents.[193] A combination of the above factors and our interest in anti-cancer natural products encouraged us to develop a synthetic route to previously inaccessible or laboriously synthesized enaminone scaffolds.

Cyclic enaminones, particularly 6-membered enaminones (2,3-dihydro-4-pyridones), are extraordinarily versatile intermediates for the synthesis of piperidine-containing target molecules. Furthermore, this heterocycle exists in numerous drugs and drug candidates as an indispensable binding element. The piperidine moiety is also prevalent in structural classes of numerous bioactive natural products.[195-199] Considering the ubiquity of biologically active piperidine-containing compounds, practical methodologies for the synthesis of these structures, especially those bearing stereogenic centers, are of great value.

The synthetic utility of the enaminone is clear when considering the reactivity of each component (amine, enamine, enone, and alkene) in isolation. The coalescence of these four functional groups in the typical enaminone endows it with four nucleophilic and two electrophilic sites. As depicted in Fig. 2–2, exploiting the unique reactivity of each position on the 6-membered, cyclic enaminone has made possible a plethora of chemoselective transformations (*i.e*. *N*-functionalization,[200, 201] *O*-functionalization,[202-204] C3,[205-208] C4 [1,2-addition],[209-211] C5[212-214] and C6[conjugate addition] functionalization[215-220] and [2+2] cylization,[221] *etc*.).

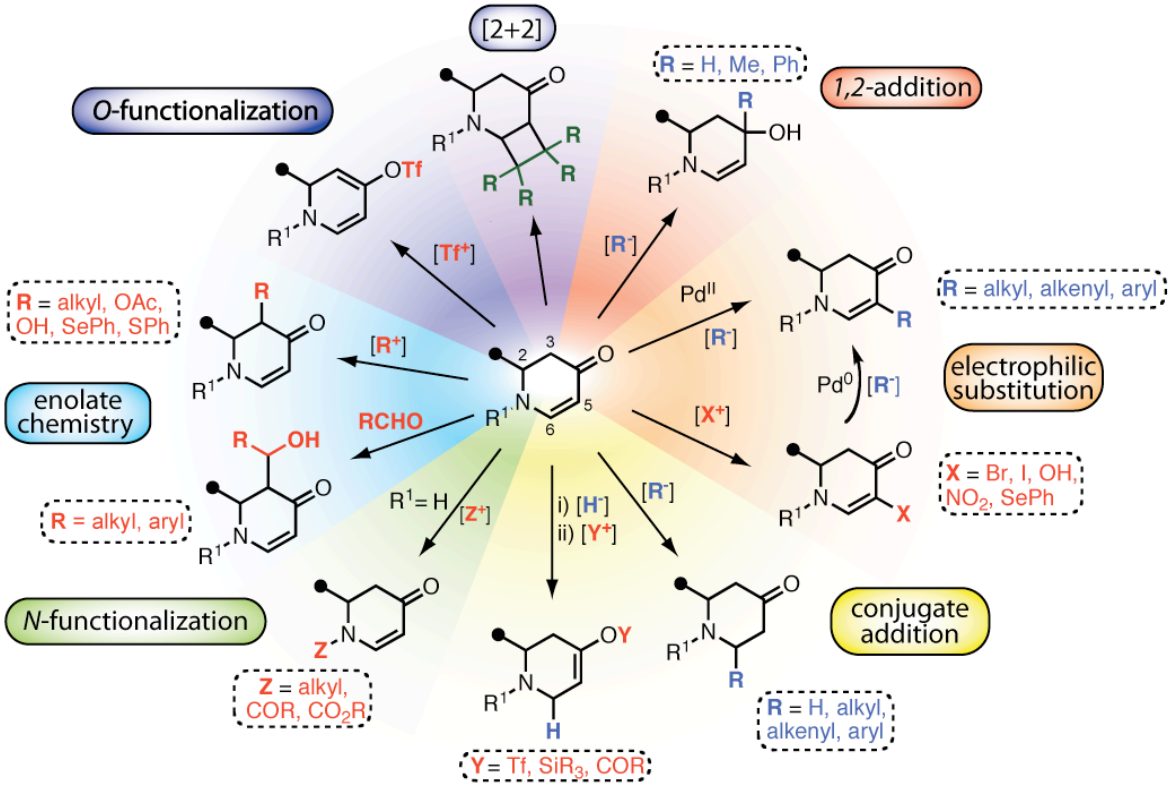

Fig. 2–2. Select synthetic transformations of the 6-membered cyclic enaminone.

Many approaches have been developed to construct the 6-membered enaminone core yet only a few are capable of affording non-racemic products (Scheme 2–1). Comins and co-workers have set precedent for the asymmetric synthesis of enaminones employing chiral *N*-acylpyridinium intermediates.[222] This method has proven to be enormously effective in providing advanced intermediates in the synthesis of numerous natural products.[140, 141, 223-229] More recent efforts have expanded the scope of this chemistry by using an assortment of chiral auxiliaries.[203, 220, 230-236] Another approach, which predates Comins' method, is the asymmetric hetero-Diels–Alder reaction of imines with Danishefsky's diene.[237-249] In this reaction, the imputed chirality can be derived from various chiral auxiliaries appended to the imine[203, 204, 237-242] or through the use of chiral catalysts.[243-249] A noteworthy corollary of this

classic [4+2] approach has recently been reported by the Rovis group in which alkynes and alkenylisocyanates undergo [2+2+2]-cycloaddition in the presence of a chiral rhodium catalyst.[250-254] Although currently limited to the synthesis of the indolizidine enaminones, this method provides rapid access to these bicyclic molecules with impressive enantioselectivity. Despite the success of these asymmetric approaches, innate limitations, such as ring-size and substituent constraints, warranted an exploration of new avenues for the construction of this useful scaffold.

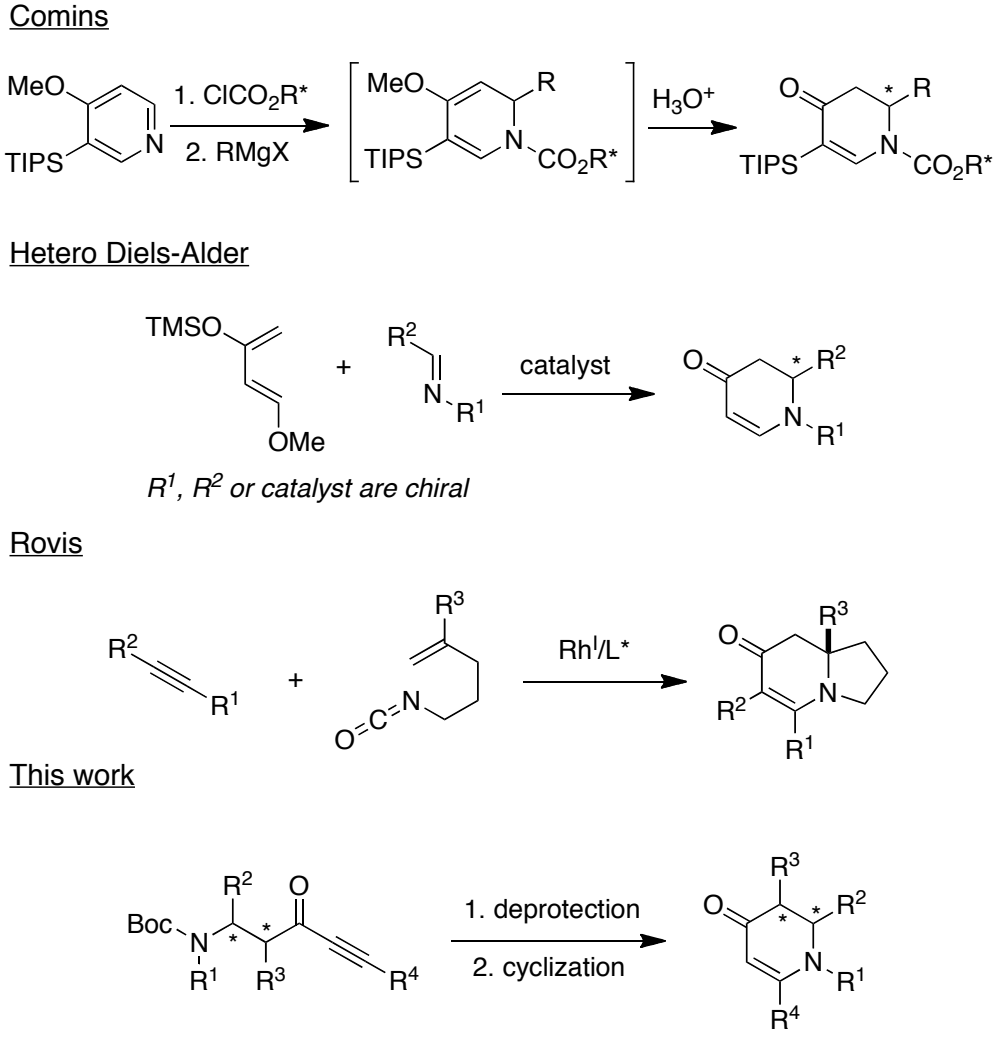

Scheme 2–1. General approaches to access non-racemic 6-membered enaminones.

In pursuit of this goal, a novel ring-forming reaction of amino acid-derived ynones to yield cyclic enaminones has been developed.[255] Our route accesses the target molecules in high enantiomeric purity by utilizing the chiral pool strategy to take advantage of the chirality of readily available starting materials. A notable feature of this methodology is its ability to generate previously unavailable or circuitously-constructed substrates, namely, bicylic enaminones, 2,5-disubstituted enaminones, and enaminones with α- and β-stereocenters. This concise and operationally facile pathway gives ready access to novel 6- and 7-membered enaminones.

2.3 Reaction development

2.3.1 Strategy and considerations for enaminone methodology

As previously said, methods for the construction of non-racemic dihydropyridones (*i.e.* 6-membered cyclic enaminones) are scarce and the existing few, although highly contributive to this area, have left many structurally simple enaminones out of reach. Thus, we envisioned a complementary route to these molecules using the chiral pool strategy (Scheme 2–2). An amine tethered to an ynone could potentially serve as the requisite precursor to our desired scaffold through an intramolecular Michael reaction. The amino-ynone substrates could conceivably be obtained from β-amino acid precursors. This approach was attractive to us not only because it could furnish pyridones with four distinct appendages and two stereogenic centers, but also because it uses easily accessible chiral starting materials. The

strategic use of β-amino acids and their immediate precursors entrusts the chiral pool and well-established asymmetric chemistry[256-263] to provide the desired diversity and complexity of the final products.

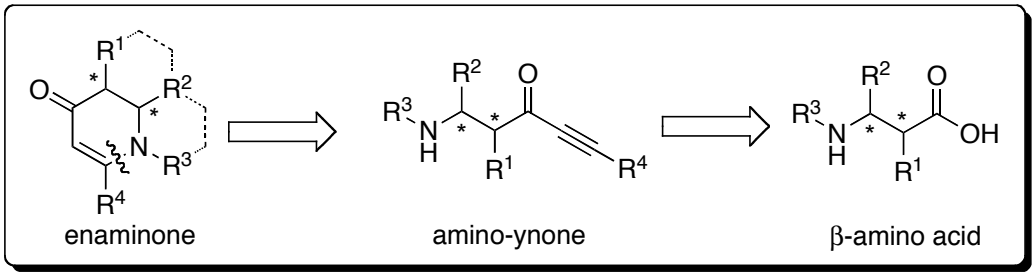

Scheme. 2–2. Retrosynthetic analysis of enaminone construction.[361]

Despite the numerous examples of intermolecular 1,4-additions of amines to ynones, precedent for an intramolecular reaction as proposed is rare. From the outset, we questioned if suitable amine/ynone orbital overlap could be achieved and were concerned about adverse modes of addition that would yield undesired products.

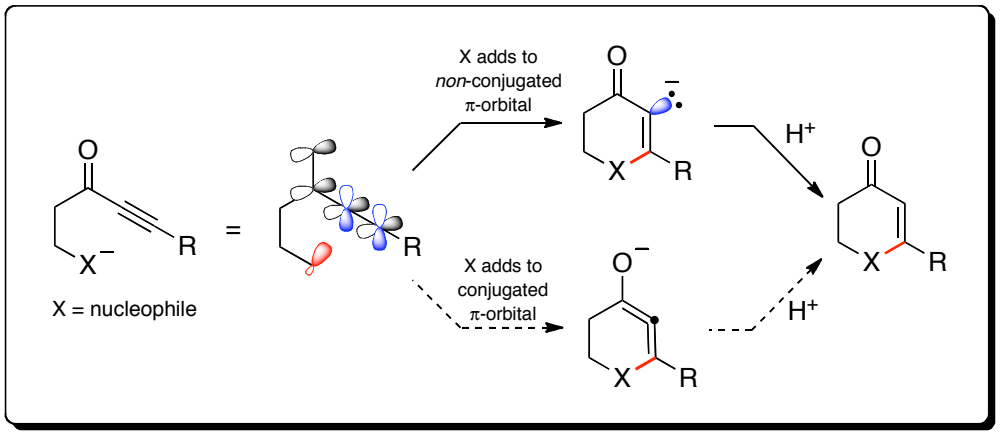

Fig. 2–3. Possible modes of addition for 6-*endo*-dig cyclization.[361]

Taking Baldwin's rules for ring closing reactions into account,[264] there are several alternative pathways for this reaction that needed to be considered. Although the proposed 6-*endo*-dig mode of cyclization appeared to be favored, there remained some uncertainty about our system's propensity towards the (also favored) 5-*exo*-dig pathway. We expanded our literature search to reactions of other first-row periodic elements that could undergo 6-*endo*-dig ring-closures. The few successful examples that we found relied on either metals or π-acids to activate the alkyne for nitrogen addition.[265-273] Deslongchamps and co-workers, however, reported the intramolecular 1,4-addition of β-ketoester nucleophiles into ynones.[274] A new, stereoelectronically-controlled pathway was proposed for this cyclization where, instead of an ordinary addition into the conjugated π-system, the nucleophile adds to the orthogonal π-orbitals to generate a vinylic anion, thereby, circumventing the formation of a highly strained, allenic enolate (Fig. 2–3). This mode of addition was predicted to be applicable for cyclizations of rings smaller than eight atoms[275] and, hence, would be relevant for our system.

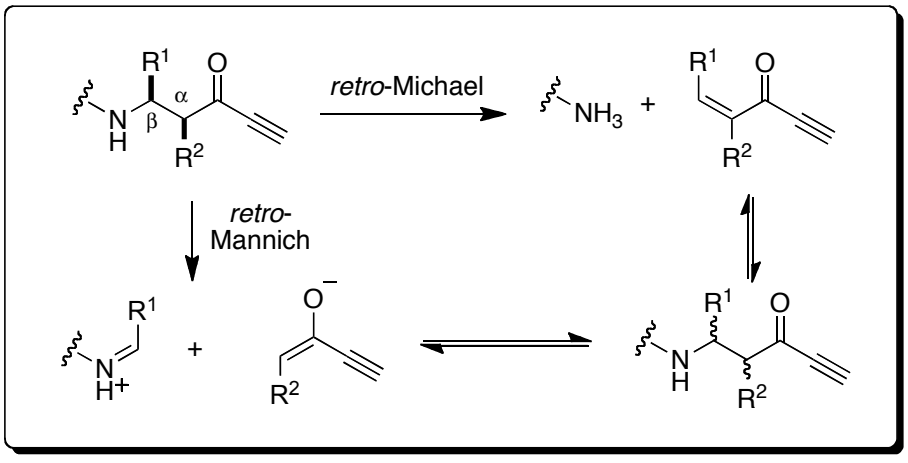

Fig. 2–4. Potential modes of α- and β-racemization/epimerization.[361]

Besides the questions about the mode of addition, concerns arose about racemization and epimerization of the pre-established stereocenters also had to be investigated. Enolization processes leading to loss of α-chiral centers are commonplace and would need to be avoided. We also considered the likelihood of β-amino ketone intermediates to undergo *retro*-Michael/ *retro*-Mannich-type processes (Fig. 2–4).[276-278] If this occurred, both the α- and β-stereocenters would be at risk. Worse yet, substrate decomposition could occur if the *retro*-Michael and Mannich processes were not reversible. With these potential hurdles in mind we ventured to construct the requisite ynone starting materials.

2.3.2 Synthesis of Weinreb amide and ynone intermediates

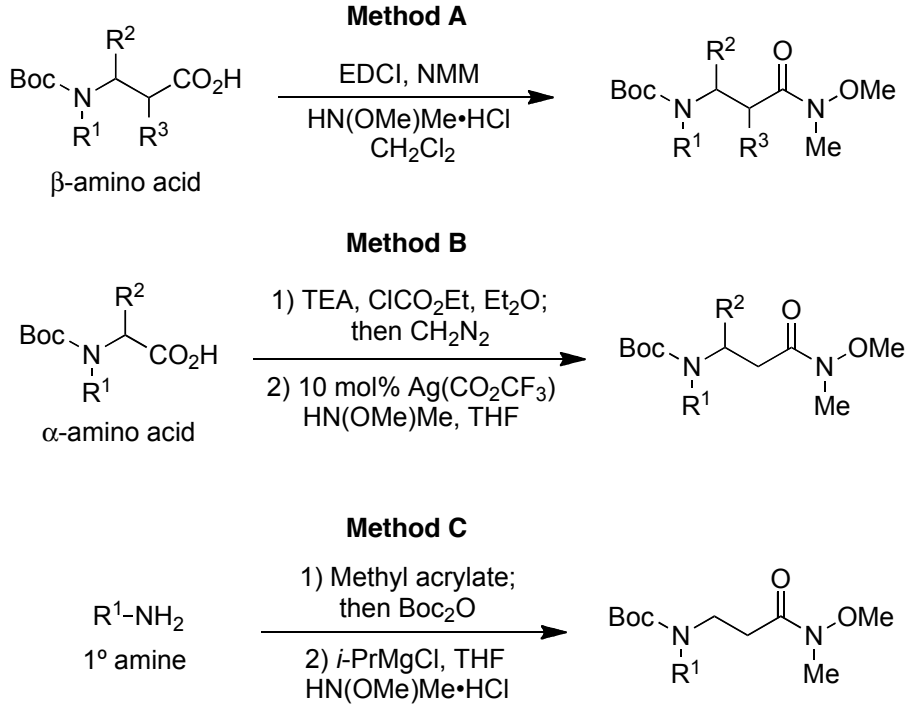

Scheme 2–3. Methods for preparing Weinreb amides **2.1**–**2.13**.

Three routes were devised to obtain β-amino Weinreb amides, the immediate precursors of the desired ynone starting materials. In the cases where the Boc-β-amino acid was commercially available, an EDCI coupling with *N,O*-dimethylhydroxylammonium chloride in the presence of *N*-methylmorpholine (NMM) furnished the corresponding amide in a single step (Method A, Scheme 2–3). Alternatively, Boc-α-amino acids were converted to diazoketones which, in the presence of catalytic silver(I) trifluoroacetate, collapsed to the corresponding ketene. The ketene intermediate was trapped *in situ* with *N,O*-dimethylhydroxylamine providing the desired Weinreb amides (Method B). Unsubstituted Weinreb amides were synthesized through a one-pot Michael-addition/Boc-protection sequence to afford Boc-β-aminomethylesters (Method C). Treatment of the methylesters with *N,O*-dimethylhydroxylammonium chloride and isopropylmagnesium chloride (*i*-PrMgCl) afforded the desired amides.[279] In the event that the Boc-protected amines required *N*-alkylation, this was accomplished subsequent to amide formation using sodium hydride and an appropriate alkyl halide. In the final step, the desired ynones were obtained from the Weinreb amides through the addition of excess (5 equiv) alkynylmagnesium reagents (Scheme 2–4). These simple steps could be conducted on multi-gram scale with minimal diminution of yield.

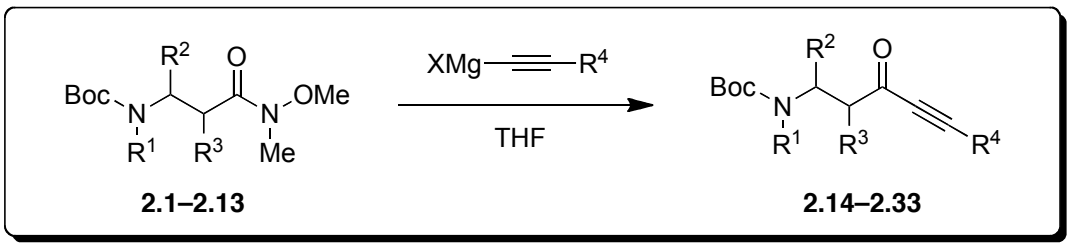

Scheme 2–4. Method used for preparing ynones from Weinreb amides.

Table 2–1. Preparation of ynones from Weinreb amides.

entry	Weinreb amide		ynone		R	method[a]	overall yield[b]
1	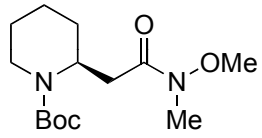	**2.1**	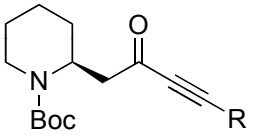	**2.14**	H	B	60
2				**2.15**	Me	B	62
3				**2.16**	Ph	B	60
4	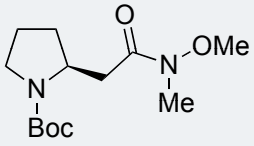	**2.2**	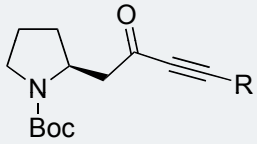	**2.17**	H	A, B	95, 68
5				**2.18**	Me	A, B	93, 66
6				**2.19**	Ph	A, B	92, 66
7	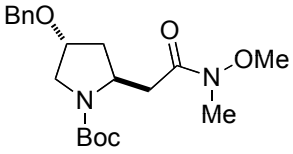	**2.3**	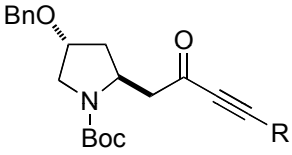	**2.20**	H	B	65
8				**2.21**	Me	B	64
9				**2.22**	Ph	B	60
10	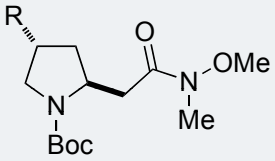	**2.4**	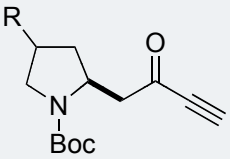	**2.23**	α-OH	B	52
11		**2.5**		**2.24**	β-OH	B[c]	45
12	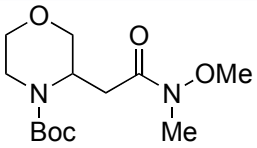	**2.6**	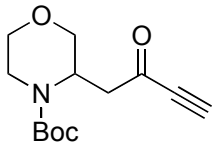	**2.25**		A	94
13	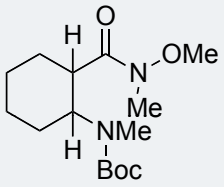	**2.7**	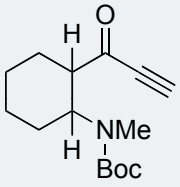	**2.26**	*cis*	A	87
14		**2.8**		**2.27**	*trans*	A	87
15	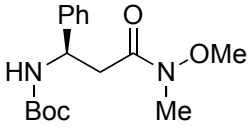	**2.9**	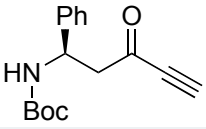	**2.28**		A	75
16	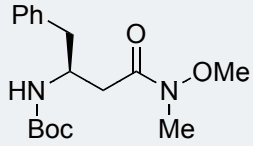	**2.10**	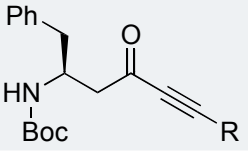	**2.29**	H	B	30
17				**2.30**	Me	B	39
19	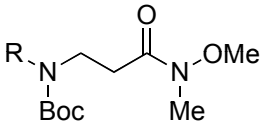	**2.11**	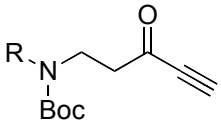	**2.31**	H	A	85
20		**2.12**		**2.32**	$PhCH_2$	C	67
21		**2.13**		**2.33**	Ph	C	46

[a] See Scheme 2–3. [b] Isolated multi-step yield from commercially available starting materials. [c] Stereocenter was inverted from Weinreb amide precursor using the Mitsunobu reaction.

Due to our interest in indolizidine and quinolizidine natural products, we chose to synthesize ynones **2.14**–**2.19** as potential precursors to these important heterocycles (entries 1–6, Table 2–1). The isolated stereogenic center on the pyrrolidine ring of ynones **2.20**–**2.24** was to be used to facilitate detection of the β-epimerization (entries 7–11). Likewise, cyclohexyl systems **2.26** and **2.27** would allow α-epimerization to be detected (entries 13 and 14). Finally, acyclic ynones **2.28**–**2.33** were synthesized to obtain monocyclic enaminones (entries 15–21). Although the enaminones to be generated from ynones **2.31**–**2.33** will be relatively unembellished, we were attracted to these targets because of a surprising lack of general routes to obtain them in spite of their simplicity.

2.3.3 Optimization of enaminone formation

Seminal optimization studies for this reaction were conducted by B. J. Turunen who envisioned a protocol in which the Boc-protecting group would be removed to liberate a nucleophilic amine that would, in turn, react with the tethered ynone moiety. Turunen found success in a two-step deprotection/cyclization protocol to provide enaminone **2.34** (Table 2–2).[255] The use of 4N HCl (entries 4–7, Table 2–2) or TMS-I (entry 8) consistently gave higher yields than when TFA was used to deprotect (entries 1–3), regardless of the cyclization method. We were initially perplexed by this result. The putative ammonium salt intermediates of each method would only differ with respect to their counter ions (Cl^-, I^- or $CF_3CO_2^-$). Upon closer scrutiny it became clear that HCl and TMS-I were acting bi-functionally. In addition to deprotecting the Boc-group, these reagents also prompted

conjugate additions of their halides (Scheme 2–5). Isolation of the deprotected intermediates revealed that, prior to cyclization, the ynone moiety had been converted by HCl and TMS-I to a mixture of vinyl halide **I** and dihaloketone **II**. Trifluoroacetic acid (TFA), however, left the ynone intact (**III**). The addition of chloride or iodide into the ynone prior to cyclization was evidently favoring ring-closure.

Table 2–2. Optimization of deprotection and cyclization.[255]

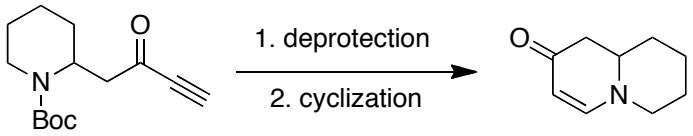

2.14 **2.34**

entry	1. deprotection	2. cyclization	time[a]	yield[b]
1	TFA, CH_2Cl_2	CH_2Cl_2, $NaHCO_3$[c]	na[d]	30
2	TFA, CH_2Cl_2	CH_2Cl_2, K_2CO_3	20 h	0
3	TFA, CH_2Cl_2	THF, K_2CO_3	20 h	0
4	TFA, CH_2Cl_2	CH_2Cl_2, H_2O, K_2CO_3	5 h	38
5	4N HCl/dioxane	CH_2Cl_2, K_2CO_3	20 h	0
6	4N HCl/dioxane	THF, K_2CO_3	20 h	0
7	4N HCl/dioxane	CH_2Cl_2, H_2O, K_2CO_3	1 h	74
8	4N HCl/dioxane	THF, H_2O, K_2CO_3	1 h	75
9	4N HCl/dioxane	MeOH, K_2CO_3	15 min	87
10	TMS-I, CH_2Cl_2	MeOH, K_2CO_3	30 min	95

[a] Reaction time of cyclization step. [b] Isolated yield. [c] Sat. aqueous $NaHCO_3$. [d] Reaction proceeded in a separatory funnel upon work-up.

Another important observation that was made during Turunen's studies was the apparent dependency of the cyclization on water or MeOH.[255] Regardless of the deprotection method, the enaminone would not form in THF or CH_2Cl_2 (entries 2, 3, 5 and 6, Table 2–2) unless water was used as a co-solvent (entries 4, 7 and 8). Although these wet solvents were

proficient in affecting cyclization, MeOH proved to be the best solvent and was chosen to further explore this reaction (entries 9 and 10). With these optimized conditions we proceeded to establish the scope of this reaction.

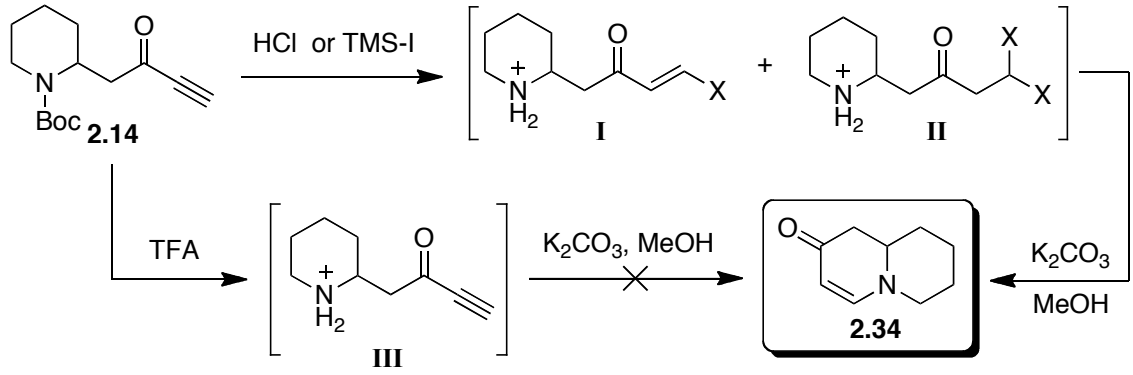

Scheme 2–5. Fate of ynone upon Boc-deprotection.

2.3.4 Mitigating stereochemical damage during enaminone formation

Shortly after we embarked on our study of reaction scope we encountered a formidable challenge. As we had feared, ynones bearing α- or β-stereocenters, when subjected to our one-pot procedure, yielded mixtures of diastereomers or partial racemates. We suspected enolization or β-amino elimination processes were at hand; if not overcome, this would negate the principal advantage of the chiral pool approach. Although both acid- and base-induced epimerizations of this type are possible, we initially focused our attention on the acidic deprotection conditions. Since the most profound stereochemical damage was observed in proline-derived enaminones, hydroxylated ynone **2.23** was employed as our model system to assess the extent of β-epimerization under an array of deprotection conditions (Table 2–3).

Table 2–3. Boc-deprotection and β-epimerization.[361]

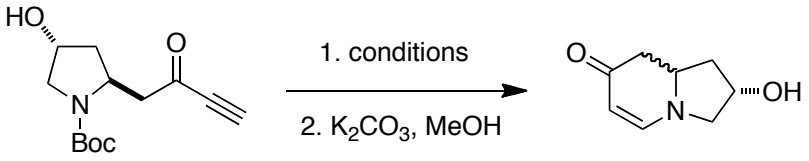

2.23 **2.35**

entry	conditions	yield %[a] (d.r.)[b]
1	4N HCl, dioxane	77 (85:15)
2	TFA (neat)	31 (67:33)
3	TFA/CH_2Cl_2 (1:1)	18 (88:12)
4	1N HCl, ether	36 (67:33)
5	1. TBSOTf, 2,5-lutidine, CH_2Cl_2 2. TBAF	0
6	TESOTf, 2,6-lutidine, CH_2Cl_2	21 (83:17)
7	CAN, MeCN, reflux	0
8	TMS-I (3 equiv), CH_2Cl_2, 0 ºC	99 (75:25)
9	TMS-I (1 equiv), CH_2Cl_2, –78 to 0 ºC; TMS-I (2 equiv)	60 (94:6)
10	HCO_2H, rt	0
11	NaI (3 equiv), HCO_2H, rt	93 (> 95:5)

[a] Isolated yield. [b] ^1H NMR integration.

The previously optimized deprotection conditions had epimerized 15% of the isolated product (entry 1, Table 2–3). In neat and dilute TFA, the yields and diastereomeric ratios of enaminone **2.35** showed no improvement (entries 2 and 3). Slow addition of HCl in ether until all the starting material was consumed also failed to give satisfactory results (entry 4). Positing an acid-induced mode of racemization we attempted to suppress the stereochemical deterioration using basic and neutral conditions (entries 5–7). These too were ineffective. When TMS-I was used to induce Boc-deprotection we observed a marked reduction of epimerization and improvement in yields (entries 8 and 9). It should be noted that ynones have been shown to react with TMS-I at –78 ºC to form β-iodo–allenolates that, upon

warming to 0 ºC, tautomerizes to afford a Danishefsky-type diene (Scheme 2–6).[280] Although this would not directly compromise the integrity of the β-stereocenter, substrates bearing α-stereocenters would be affected.

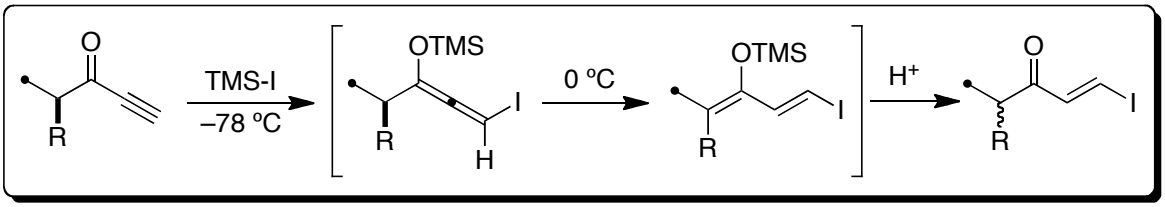

Scheme 2–6. Mechanism of α-epimerization with TMS-I.

To test this, we subjected enolizable substrate **2.26** to the same conditions, and observed that epimerization was even more profound than when using HCl (Scheme 2–7). In addition to the detrimental stereochemical effects of TMS-I, the necessity of rigorously dried solvents, glassware, and cryogenic temperatures provoked a search for a new, simple protocol that would tolerate epimerizable substrates.

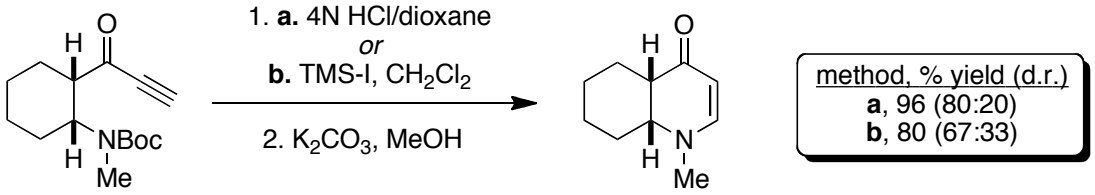

2.26 **2.36**

Scheme 2–7. Epimerization of α-stereocenter using HCl and TMS-I.

With a wealth of known Boc-deprotection protocols to explore, we were attracted to the use of formic acid to avert epimerization.[281] The simple technique of this method was attractive considering it could accomplish the desired deprotection at ambient temperature and in open-air. Furthermore, we hoped that this relatively weak acid would lessen epimerization. Applying these conditions to ynone **2.23**, the Boc-group could be easily removed, yet upon treatment with base, we did not observe any enaminone formation (entry 10, Table 2–3). As shown in earlier experiments, the success of this reaction is not only contingent on the removal of the Boc-group, but also on ynone "activation" with halides (Scheme 2–2). To this end, NaI was added as a nucleophilic halide source and the reaction was repeated (entry 11, Table 2–3). To our delight, the desired enaminone was formed in excellent yield (92%) and without any detectable epimerization. Conceivably, the remote hydroxy group could resist epimerization by directing the re-addition of the eliminated amine to the most favored *anti*-substituted product. We were encouraged to find that, in the absence of diasteromeric control, enaminones could be obtained in high enantiopurity (Scheme 2–8). When ynone **2.17** was subjected to these deprotection conditions a crystalline solid formed in the reaction media and was determined by X-ray analysis to be the desired deprotected, vinyl iodide intermediate (**2.38**, Fig. 2–5). Upon treatment of this salt with base, enaminone **2.37** was formed in less than 2 minutes. More importantly, the product was obtained with an enantiomeric ratio of 98.5**:**1.5 showing that this protocol had effectively mitigated β-epimerization.

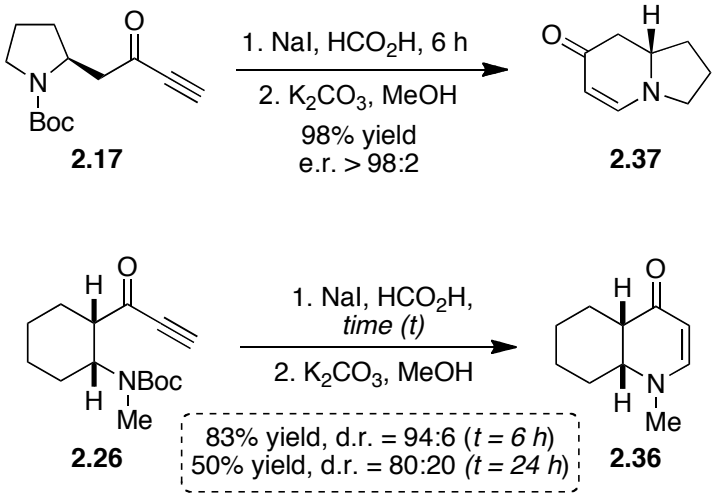

Scheme 2–8. Racemization of α- and β-stereocenters using mild deprotection conditions.

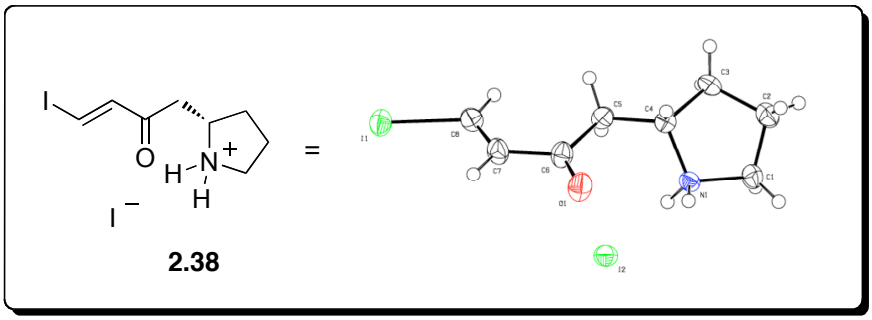

Fig. 2–5. X-ray crystal structure of vinyl iodide **2.38**.

We next investigated these new conditions on enolizable ynone **2.26** as a model for α-epimerization (Scheme 2–8). The new conditions yielded the desired product (**2.36**) with a d.r. of 94:6. This was a considerable improvement over the previous method where the d.r. was 80:20. Interestingly, we also saw a time-dependent increase of epimerization indicating that the acid step was indeed responsible, at least in part, for α-epimerization. Enolate formation during the basic step could also potentiate epimerization and was investigated further.

Vinyl iodides **A**, **B**, and **C** were chosen as model substrates to examine enolization (Scheme 2–9). These substrates were subjected to the cyclization conditions using deuterated methanol (CD_3OD) as a solvent and the extent of α-deuteration was determined. Deuterium incorporation at the α-position is indicative of enolate formation revealing another potential source of epimerization. When intermediate **A** was treated with methanol-d_4 and K_2CO_3, enaminone **2.37** was immediately formed and no deuteration was observed. Once formed, this enaminone was resistant to deuterium incorporation for up to 24 h (*i.e.* to form enaminone **2.37**-d_2). With the intent of slowing the cyclization we used substituted vinyl iodides **B** and **C**. For these cases, the cyclized products **2.39**-d_5 and **2.40**-d_2 were obtained with complete α-deuteration. Furthermore, as observed before, enaminones **2.39** and **2.40**, which were formed in non-deuterated solvent, did not undergo α-deuteration under the prescribed conditions.

The point has already been made that enaminones are reluctant to undergo deuteration in the presence of K_2CO_3; however, an anomaly was noted when investigating enaminone **2.39** (Scheme 2–10). This substrate underwent selective and complete γ-deuteration to provide enaminone **2.39**-d_3 in 2 hours. Although it is out of the scope of this work, this finding reveals another handle on this versatile scaffold for chemoselective modification.[282, 283]

The collective data from the deuterium exchange reactions hinted at another liability in our approach. We feared that the extent of α-deuteration might be diagnostic of pre-cyclized intermediates that would undergo β-amino elimination. Thus, ynones **2.20**, **2.21** and **2.22** were subjected to the two-step procedure (Scheme 2–11). Terminal ynone **2.20** cyclized with no observable epimerization whereas the methyl and phenyl substituted ynones (**2.21** and **2.22**) were obtained as diastereomeric mixtures.

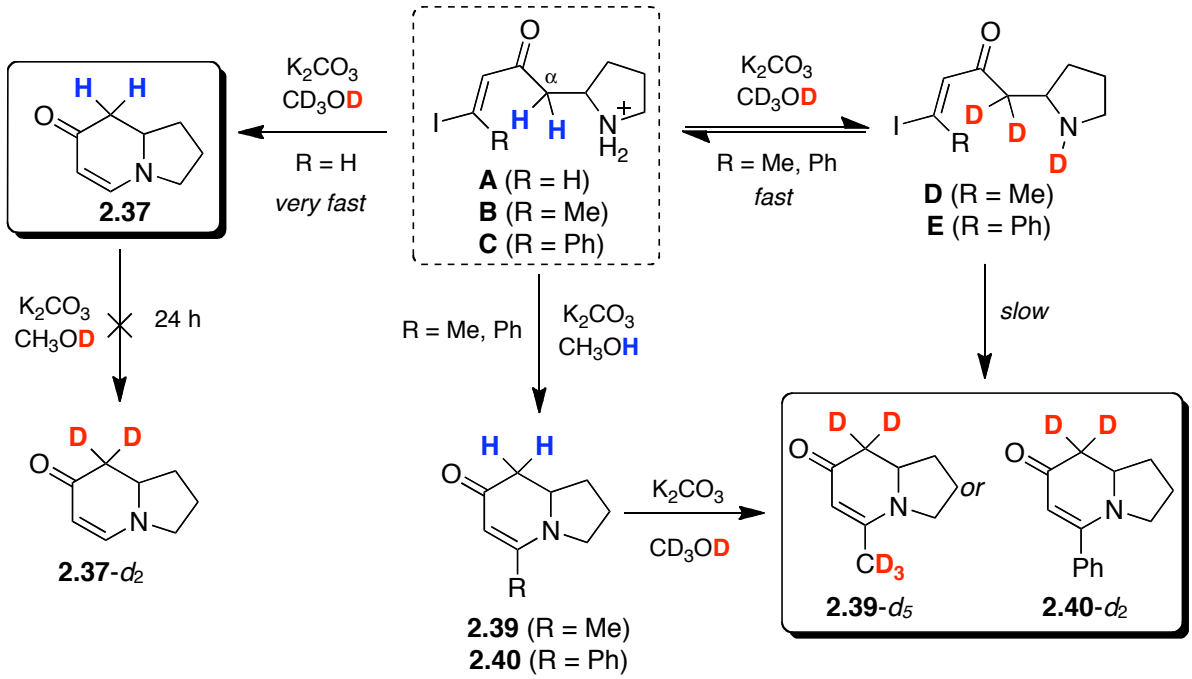

Scheme 2–9. Deuterium exchange during cyclization.

In retrospect, these findings are not surprising. The principles of vinylogy would indeed predict an attenuated acidity of the enaminone α-position in relation to that of its ketone progenitor. Thus, α-epimerization or β-amino elimination is precluded by rapid formation of the vinylogous amide. When the rate of cyclization is retarded with sterically encumbered alkynes there is a significant increase in epimerization, thus showing the vulnerability of the enaminone precursors in basic media. Despite the use of mild deprotection conditions, these new findings suggest that base-induced epimerization is predominant when cyclization is slow.

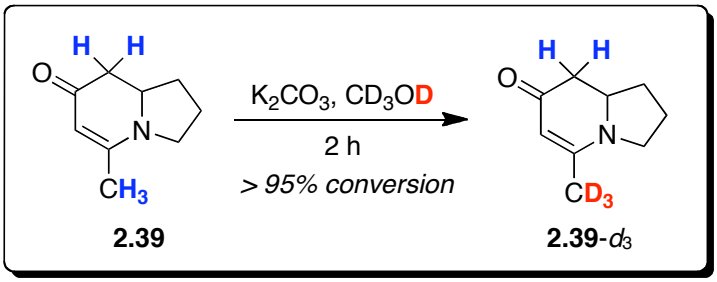

Scheme 2–10. Methyl deuteration of enaminone **2.39**.

Suspicions immediately arose concerning the putative role of the acid in β-amino elimination. Perhaps the discrepancies in the stereochemical outcome of each deprotection condition were attributable to the dissimilar haloketone intermediates and their particular reactivities under basic conditions. For instance, a conspicuous difference exists when considering the halides (Cl *vs*. I). Furthermore, double chloride addition into the ynone occurs in the presence of HCl whereas the diiodo congener is not formed in formic acid and NaI (Scheme 2–5). We were cognizant that these dissimilarities, rather than the strength of the acid used for deprotection, could dictate the extent of epimerization by governing the rate of cyclization. Fortunately, this could be directly investigated.

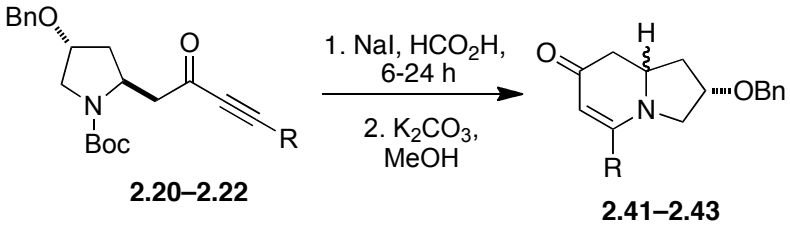

R	yield	d.r.
H (**2.41**)	92%	> 95:5
Me (**2.42**)	94%	2.1:1
Ph (**2.43**)	88%	1.5:1

Scheme 2–11. Epimerization of β-stereocenters on terminal and internal ynones.

Experimental evidence suggests that the primary cause of β-epimerization for *terminal* ynones is the strongly acidic HCl conditions. When ynone **2.20** was subjected to 4N HCl the resultant ammonium salts (**2.44** and **2.45**) were each generated as 2:1 diastereomeric mixtures (Scheme 2–12). From this we conclude that the acid is directly responsible for inducing amino-elimination. As such, this process can be mitigated when using a weaker acid such as HCO_2H. It is important to note that the use of HCO_2H and NaI does not assuage the stereochemical damage in cases where cyclization is slow (*i.e.* substituted ynones). Thus, this mild protocol is most appropriate for terminal ynones. With these insights we next investigated the reaction scope to validate the utility and generality of this protocol.

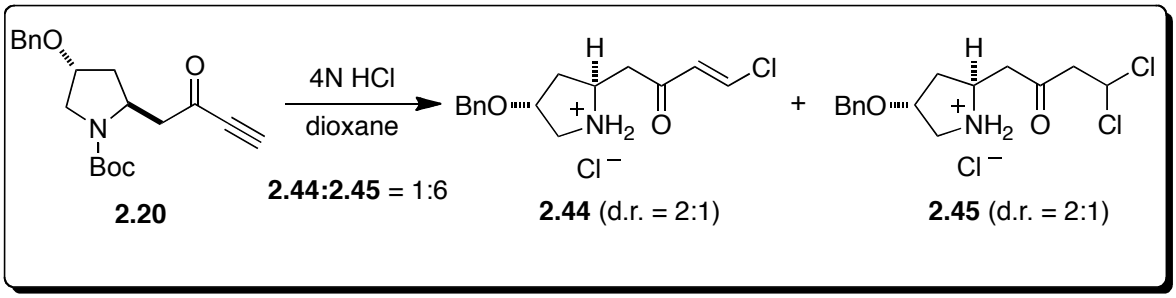

Scheme 2–12. Epimerization during deprotection with HCl.

2.3 Reaction scope

2.3.1 Six-membered enaminones

As can be seen in Table 2–4, a diverse collection of enaminones can be constructed using these developed methods. From this data set we intended to establish a basis for choosing appropriate deprotection conditions. Bicyclic enaminones are formed efficiently, providing a

facile route to quinolizidine (entries 1–3) and indolizidine (entries 4–11) scaffolds. Synthesis of morpholino-enaminone **2.49** was also feasible (entry 12). Pyrrolidine substrates were particularly susceptible to stereochemical damage; however, this could be mitigated in terminal ynone substrates by using a HCO_2H and NaI during the deprotection step. Although the reason for this sensitivity has not been directly assessed, we believe this is due, in part, to the alleviation of pyrrolidine ring-strain. Not surprisingly, *anti*-substitued pyrrolidines were less prone to epimerization than their *syn*-counterparts (entries 10 and 11), evidencing thermodynamic control of the *retro*-Michael/Michael process. Installation of aliphatic and aromatic substituents adjacent to the ring-fused nitrogen was also accomplished by employing terminally substituted ynones (entries 5, 6, 8 and 9). As expected, cyclization was relatively slow (15 min to 3 h) in these substrates, but all proceeded in excellent yields. In these cases, however, the HCO_2H-based deprotection method was ineffective at preventing β-epimerization.

Enolizable stereocenters were also a potential liability considering our protocol featured both an acidic and a basic step. As shown before, the use of HCl and TMS-I were destructive when attempting to establish the *cis*-fused enaminone **2.36**. We were pleased to find that α-epimerization could also be suppressed in this case under the milder conditions with HCO_2H and NaI (entry 13). It should be noted that since the *trans*-substituted product is expected to be more stable, epimerization is likely to be thermodynamically preferred. With this in mind, it was expected that *trans*-fused enaminone **2.50** was more resistant to epimerization in both deprotection conditions and could be acquired in high diasteromeric purity (entry 14).

We next investigated the synthesis of monocyclic enaminones. These compounds would seemingly be more difficult to form, as they have no conformational constraints facilitating

Table 2–4. Substrate scope for the preparation of six-membered enaminones.

entry	enaminone		R	method[a]	yield[b]	e.r.[c] or d.r.[d]
1	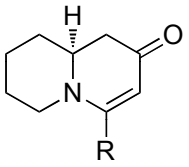	**2.34**	H	A B	87 90	97:3 > 98:2
2		**2.46**	Me	A B	87 80	73:27 73:27
3		**2.47**	Ph	A B	91 85	58:42 69:31
4	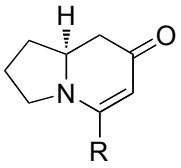	**2.37**	H	A B	89 96	70:30 98:2
5		**2.39**	Me	A	87	–
6		**2.40**	Ph	A	89	–
7	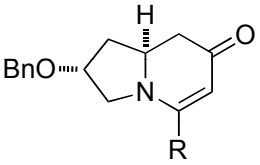	**2.41**	H	A B	94 92	67:33 >95:5
8		**2.42**	Me	A B	87 94	63:37 68:32
9		**2.43**	Ph	A B	85 88	63:37 60:40
10	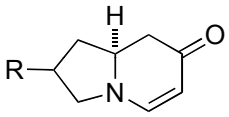	**2.35**	α-OH	A B C	77 93 94	85:15 > 95:5 96:4
11		**2.48**	β-OH	A B C	60 95 70	60:40 92:8 86:14
12	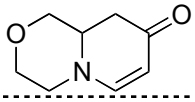	**2.49**		A B	80 95	– –
13	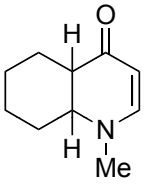	**2.36**	*cis*	A B C	96 83 80	80:20 94:6 67:33
14		**2.50**	*trans*	A B	99 82	> 95:5 > 95:5
15	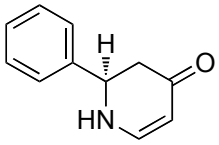	**2.51**		A B	50 50	> 99:1 > 99:1
17	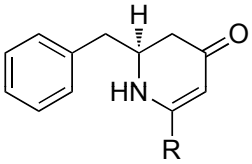	**2.52**	H	A	92	> 95:5
18		**2.53**	Me	A	96	> 95:5
20	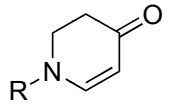	**2.54**	H	A B	70 92	– –
21		**2.55**	$PhCH_2$	A B	50 86	– –
22		**2.56**	Ph	A B	50 70	– –

[a] Method A: a) 4N HCl/dioxane, 15 min. b) K_2CO_3, MeOH; Method B: a) NaI (3 equiv), formic acid, 6-24 h. b) K_2CO_3, MeOH; Method C: a) TMS-I, CH_2Cl_2, –78 to 0 ºC. b) K_2CO_3, MeOH. [b] Isolated yield. [c] Chiral HPLC. [d] ^1H NMR integration.

ring-closure. In this regard, acyclic β-aminoynones were found to be viable substrates (entries 15–22). Even sterically encumbered, internal ynones undergo cyclization to form monocyclic products (entry 18). In cases where the extruded amine is not tethered to the ynone, as in bicylic substrates (entries 1–12), the *retro*-Michael process leads to degradation instead of epimerization. Hence, it was observed that several monocyclic products were obtained in lower yields than their bicyclic analogs were.

The observation that a subtle ring expansion had profound effects on the extent of β-racemization (entry 1 vs. 4) led us to attempt the construction of phenylglycine-derived enaminone **2.51** (entry 15). We envisioned that this substrate would be particularly susceptible to β-amino elimination. Expecting to see a distinct improvement in yield when formic acid was used instead of HCl, we were surprised that both deprotection methods were equally suited for this sensitive substrate. By conducting this reaction in an NMR tube and carefully monitoring its progression, it became apparent that degradation (*i.e.* β-amino elimination) occurred upon the addition of methanolic K_2CO_3 and not during deprotection. The complete retention of stereochemistry suggests that this process was irreversible in contrast to cases where the extruded amine remains tethered to the resultant Michael acceptor (entries 1–12). From these results we suggest alternative methods be used to access enaminones of this type. Fortunately, this is well within the scope of both the Comins' *N*-acylpyridinium[230-236] and the hetero Diels-Alder approach.[237-249]

In addition to introducing steric bulk, attenuating the nucleophilicity of the amine would seemingly impede an efficient ring-closure. The synthesis of enaminone **2.56** demonstrates that despite the use of a significantly less reactive anilino nitrogen, cyclization still occurs (entry 22), albeit in lower yields.

2.3.2 Seven- and five-membered enaminones

With these favorable results for constructing 6-membered enaminones, we next explored the feasibility of constructing 5- and 7-membered rings. This method lacks the strict confines of ring size for the alternative routes to cyclic enaminones. Our initial attempts to cyclize α-amino ynones to form 5-membered enaminones were unsuccessful. This is consistent with our hypothesis that this reaction proceeds through an *endo*-trig mode of cyclization (5-*endo*-trig is disfavored). The synthesis of 5-membered enaminones remains a limitation of this methodology.

Previously reported methods for the construction of cyclic enaminones have not been amenable to the synthesis of 7-membered rings either. Furthermore, to our knowledge, there is no general method for their construction. Without any alteration of our protocol, γ-amino ynones **2.57**–**2.2.60** rendered four novel 7-membered enaminones (entries 1–4, Table 2–5). Notably, pyrrolo[1,2-*a*]azepine **2.61** bears resemblance to the core and distinguishing feature of the well-studied *Stemona* alkaloids.[284, 285] This unique molecule and its piperidino congener **2.62** were both attainable in good yields (entries 1 and 2). Spirocyclic enaminone **2.63** and baclofen-derived enaminone **2.64** were also readily obtained via our deprotection/ cyclization protocol (entries 3 and 4). Although all of these enaminones were constructed in racemic form—hence, their stereochemical liabilities were not investigated—we have no reason to believe that they are susceptible to the stereochemical deterioration seen in β-amino ynones.

Table 2–5. Seven-membered enaminone preparation.

entry	ynone[a]		enaminone		method[b]	yield[c]
1	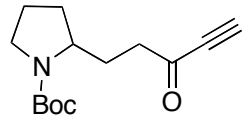	**2.57**	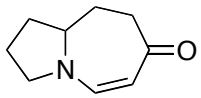	**2.61**	A B	60 64
2	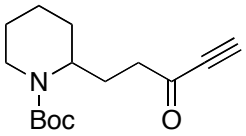	**2.58**	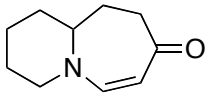	**2.62**	A B	64 63
3	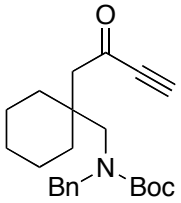	**2.59**	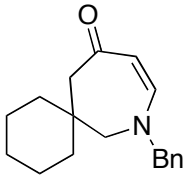	**2.63**	A B	81 84
4	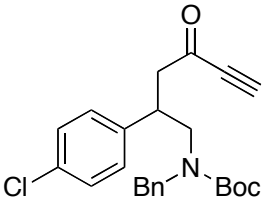	**2.60**	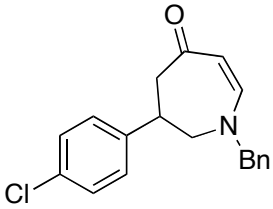	**2.64**	A B	66 65

[a] See Chapter 6 for the synthesis of ynones **2.57**-**2.60**. [b] Method A: a) 4N HCl/dioxane, 15 min. b) K_2CO_3, MeOH; Method B: a) NaI (3 equiv), formic acid, 6-24 h. b) K_2CO_3, MeOH; [c] Isolated yield.

2.3.3 Summary of reaction scope

In summary, we have developed two complementary protocols for synthesizing 6- and 7-membered enaminones. The first method, using HCl, is rapid and able to activate and deprotect internal and terminal ynones in under 15 minutes. It is best suited for substrates without α-stereocenters or those that are not sensitive to acid-induced β-amino elimination. The second method, using formic acid and NaI, although requiring longer reaction times (6-24 h), is ideal for terminal ynones with sensitive α- and β-stereocenters. Both procedures

are operationally facile and can be carried out in a single vessel. Furthermore, these experimentally simple and environmentally benign conditions are conducive to production of multi-gram quantities of these enaminone scaffolds.[286]

2.4 Mechanistic insights

During early optimization studies, Turunen stumbled across two notable features of this reaction during optimization that lay the groundwork for our mechanistic studies. Firstly, when the deprotection reaction did not result in vinyl halide intermediate, the yields were significantly lower. Second, the desired enaminone could was not formed unless water or MeOH were used during the cyclization step.

By isolating the pre-cyclized intermediates **A** and **B** (Fig. 2–6) and verifying a complete consumption of the ynone moiety, the first stipulation (*i.e.* the need for a halide source while deprotecting the Boc-group) became clear. In sufficiently acidic conditions, halides add into the ynone group forming a vinyl halide that readily undergoes ring-closure to form the desired enaminone. When the ynone remains intact, cyclization is not efficient and intermolecular processes (*i.e.* polymerization) predominate. Therefore, pre-activation is required for a successful reaction.

The discovery that the ynone group was transformed in the presence of halogenic acids demanded a reevaluation of our originally proposed 6-*endo*-dig mechanism. With direct evidence for the formation of halides **A** and **B**, a direct 1,4-addition 6-*endo*-trig cyclization/ halide elimination would be one plausible mechanism (Fig. 2–6, Pathway A). We were initially impressed, however, by the strong solvent dependence of this reaction.[255] When the

reaction was carried out in bulky alcoholic (*s*-BuOH or *i*-PrOH) or non-nucleophilic solvents (CH_2Cl_2 or THF) the reaction was significantly impaired. On the other hand, the use of water or MeOH was highly beneficial and independent of the mode of deprotection. In the first disclosure of this reaction, a mechanism was proposed in which an oxygen nucleophile directly involved in bond-making and bond-breaking.[255] Therein, it was suggested that an addition of MeOH into vinyl chloride **C** occurred. Then, upon extrusion of the chloride ion the resultant oxonium intermediate **E** could undergo ring-closure in a 6-*exo*-trig fashion (Pathway B, Fig. 2–6).

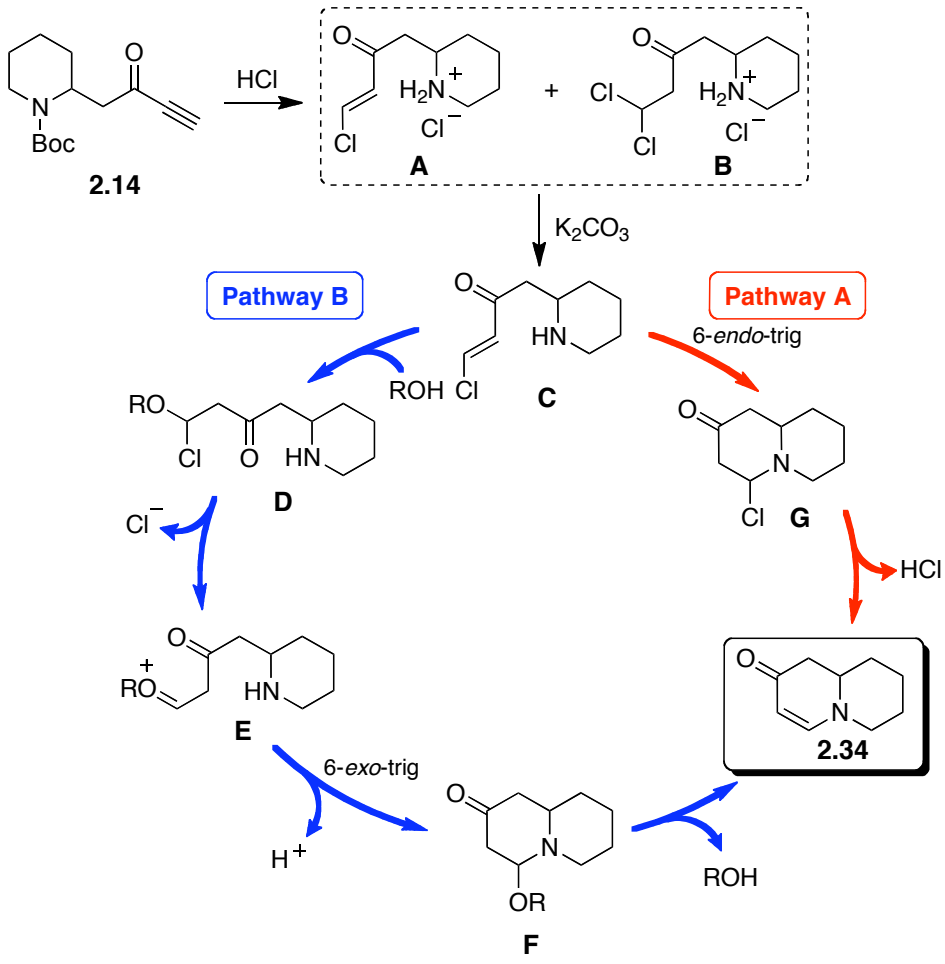

Fig. 2–6. Two potential mechanistic pathways of cyclization.

In an attempt to gain mechanistic insight through detecting transient intermediates, Turunen dissolved the mixture of **A** and **B** in methanol-d_4 and monitored the reaction mixture via ^{1}H NMR after adding a solution of K_2CO_3 dropwise. Dichloride **B** was first converted into vinyl chloride **A** and subsequent additions led to the formation of enaminone **2.34** with no other detectible intermediates. When vinyl iodide analog of **A**, generated from NaI and formic acid, was subjected to these same conditions the product was also formed with no detectable intermediates.

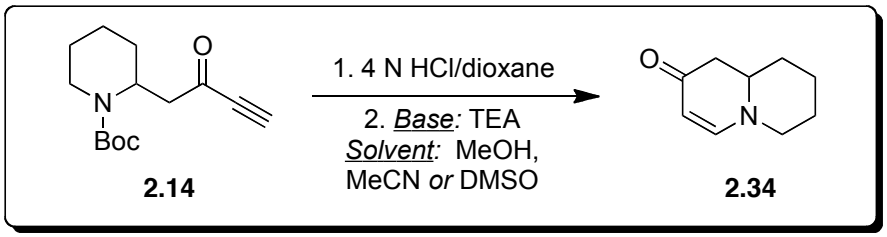

Scheme 2–13. Probing cyclization mechanism through model reactions.

Although Pathway B provided a plausible explanation for the aforementioned solvent effects, dissimilarities in the solubilizing powers of each solvent would still need to be ascertained. Impaired yields would be expected if the protonated amine intermediates (**A** and **B**) or the base (K_2CO_3) were poorly soluble. Whether or not a nucleophilic solvent was necessary, however, was difficult to directly assess due the insolubility of the reaction constituents in most organic solvents. To answer this question, we explored alternative organic bases that we expected would allow the reaction to be carried out in non-nucleophilic solvents. Our first success demonstrated that triethylamine (TEA) could be used instead of K_2CO_3 (Scheme 2–13). As hoped, this base was not only compatible with MeOH but could be used with non-nucleophilic solvents, such as MeCN and DMSO, resulting in the

formation of enaminone **2.34**. Since these solvents are hygroscopic, adventitious water could potentially facilitate the cyclization in a catalytic manner. To rule out this possibility, we constructed ynone **2.65** to determine the fate of the electrophile in the absence of a tethered nitrogen nucleophile (Scheme 2–14). Following treatment with 4N HCl, which formed a 1:6 mixture of ketones **2.66** and **2.67**, the residue was dissolved in MeCN and TEA was added. The NMR spectrum revealed vinyl chloride **2.66** as the sole product. Moreover, upon addition of excess D_2O, vinyl chloride **2.66** remained intact. Clearly, trace amounts of water were not facilitating the cyclization when the reaction was carried out in MeCN.

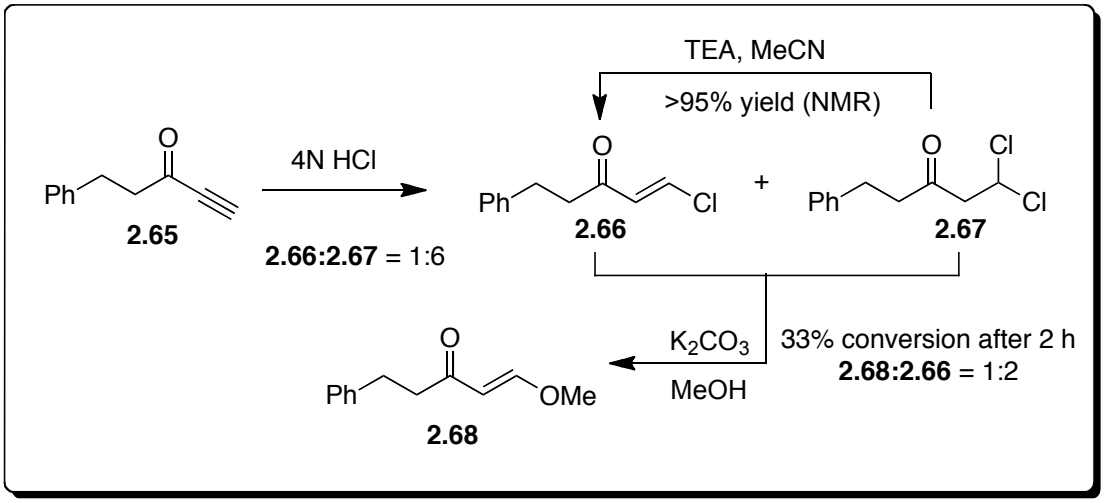

Scheme 2–14. Reactivity of ynone in the absence of an amine.

Delving further we examined the reactivity of intermediates **2.66** and **2.67** in the presence of methanolic K_2CO_3. If MeOH facilitated the cyclization through a conjugate addition it would be expected that the isolated vinyl halide **2.66** would be consumed more rapidly than the vinyl chloride **A** (Fig. 2–6) could form the enaminone. In other words, if the rate of amino cyclization is faster than the rate of addition of MeOH, the former process would

obviate the latter. To test this, a mixture of intermediates **2.66** and **2.67** were reacted in MeOH and K_2CO_3 (Scheme 2–14). After 2 hours the composition of the crude reaction mixture consisted of a 1:2 mixture of vinyl ether **2.68** and unreacted vinyl chloride **2.66** (33% conversion). Thus, the addition of MeOH to the vinyl chloride is much slower than the cyclization process which occurs in less than 5 minutes. From this data, it is reasonable to suggest that the addition of MeOH into a vinyl chloride should not be invoked in the reaction mechanism. Thus, we suggest that these results are strong evidence for a direct 6-*endo*-trig mode of cyclization (Pathway A, Fig. 2–6).

2.5 Summary

We have developed a practical route to non-racemic 6- and 7-membered enaminones starting from amino acids, providing a complementary approach to preexisting methods. Using this approach, asymmetry can be derived from the rich supply of commercially available amino acids. Moreover, access is gained to enaminones that are substituted at four positions, two of which are stereogenic centers.

The key reaction and final step in this sequence is a novel one-flask deprotection/ cyclization reaction of Boc-aminoynones. Two methods were developed to achieve the Boc-deprotection that are suitable for different substrates. The use of 4N HCl in dioxane is most fitting for internal ynones or those without sensitivity to acid-mediated side-reactions. Alternatively, for those substrates that have enolizable stereocenters or are susceptible to acid-promoted β-amino elimination (*i.e*. *retro*-Michael) processes, NaI and formic acid are well-suited. The latter conditions provide a mild alternative and work best for terminal

ynones. Both protocols are economic and operationally facile, having no need for dry solvents/reagents and can be conducted at room temperature. Furthermore, both methods can be carried out on multi-gram scale with comparable yields.

The substrate scope of this reaction was also assessed. It appears that this reaction is general for the construction of 6- and 7-membered enaminones. When the deprotection conditions are judiciously chosen, monocyclic and bicyclic heterocycles can be obtained from amino-ynones in high enantiomeric or diastereomeric purity. Many of the heterocyclic scaffolds reported here, though structurally simple, are unprecedented in the literature.

The mechanism of the final cyclization sequence has also been investigated. The success of this reaction relies on the conversion of the ynone moiety into a vinyl halide species and trapping of the protected amine as an ammonium salt following Boc-degredation. This pre-activation, allows for an efficient intramolecular 1,4-addition once the free amine is released upon the addition of base. Thus, this reaction is thought to proceed through a 6-*endo*-trig ring-closing process. We believe that the asymmetric scaffolds constructed herein will be of great synthetic value for library development and complex molecule synthesis. Specifically, the synthesis of the phenanthropiperidines will be expedited by this direct route. This will be demonstrated in the following chapters.

CHAPTER 3

PALLADIUM(II)-CATALYZED CROSS-COUPLING OF CYCLIC ENAMINONES AND ORGANOTRIFLUOROBORATES

3.1 Introduction

To expand our method for constructing enantiomerically pure enaminones, we began to investigate practical methods for elaborating this scaffold. Our goal was to install aryl groups at the C3-position, which we envisioned to be an essential transformation *en route* to the phenanthrene system of the phenanthropiperidine alkaloids. Importantly, this approach, if successful, would be applicable to a broad range of useful 3-arylpiperidine scaffolds besides the phenanthropiperidines. Indeed, many compounds which feature this scaffold are known to have high affinity for an array of validated targets (Fig. 3–1).[198, 287]

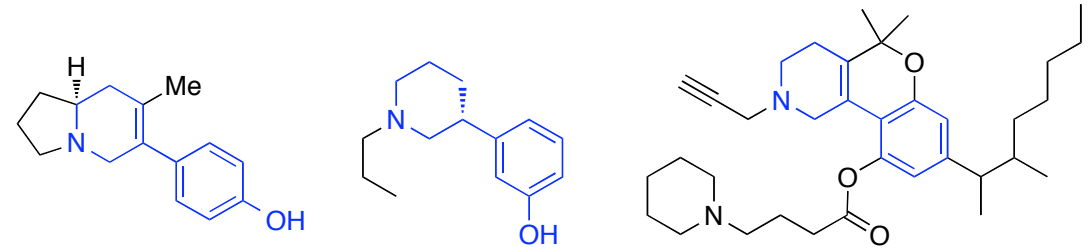

(*S*)-ipalbidine
non-addictive analgesic

(*R*)-preclamol
D2 agonist

Nabitan
anti-emetic/analgesic
(CB agonist)

Fig. 3–1. Examples of 3-aryl piperidine medicinal agents.

Palladium-catalyzed carbon-carbon (C–C) bond formation has been widely used in organic synthesis for arylation reactions, and, therefore, it was an obvious choice for this transformation. Arylation of the C3-position has been accomplished via a two-step sequence involving halogenation and subsequent coupling using a Pd(0)-catalyst, but we realized a more direct arylation protocol that allowed us to avoid preactivation of the enaminone was possible. Herein, we describe our efforts to circumvent the halogenation by taking advantage of the inherent nucleophilicity of the enaminone, which led us to the discovery of a Pd(II)-catalyzed C–H arylation reaction using trifluoroborates.

3.2 Background to Pd-catalyzed cross-coupling

Palladium-catalyzed cross-coupling reactions have emerged as an incredibly versatile method for constructing C–C and carbon-heteroatom (C–X) bonds. Applications of cross-coupling in complex natural product syntheses and commercial scale production have demonstrated the utility of this methodology (Fig. 3–2).[288, 289] Materials as far reaching as electron conductive polymers and liquid crystals have relied on cross-couplings for their preparation.[289] Moreover, the routes to numerous drugs, including Eniluracil, Losartan and Rofecoxib, have these coupling reactions as key steps.[288]

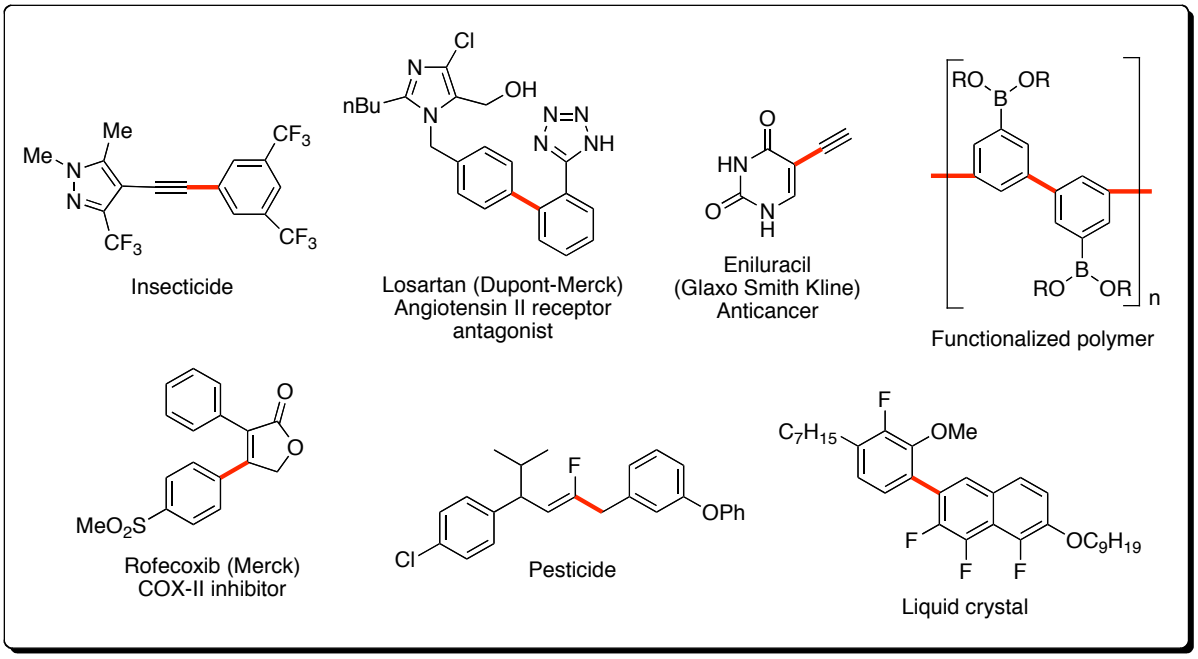

Highlighted bonds were formed using a Pd-catalyzed coupling reaction.

Fig. 3–2. Applications of Pd chemistry.

Following the initial reports of cross-coupling reactions by Kumada and Curriu in the 1970s, the number of publications related to this field have grown dramatically.[289] The versatility of these methodologies can be attributed to the tremendous amount of work done to expand the scope of palladium catalysts and coupling partners. The mechanism of the reaction has received much attention and, although the details may be uncertain, is thought to proceed through three general steps (Fig. 3–3):

1. Oxidative addition of an organic electrophile (R–X) into Pd(0)
2. Transmetallation between Pd(II) and an organometallic nucleophile (MR')
3. Reductive elimination to regenerate Pd(0) and form the C–C σ-bond

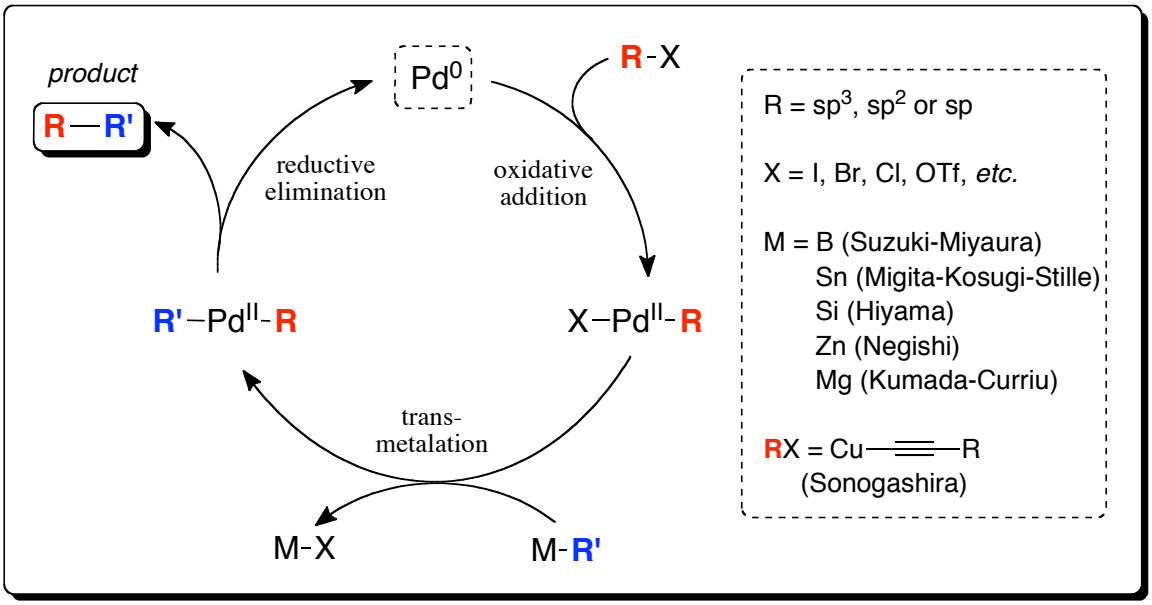

Fig. 3–3. Postulated general cross-coupling catalytic cycle.

Cross-coupling reactions that share this mechanism have been categorized based on the nature of the organometallic nucleophile (M–R'). Among these are the Suzuki-Miyaura (boron-mediated), Migita-Kosugi-Stille (Sn-mediated), Hiyama (Si-mediated), Negishi (Zn-mediated), Kumada (Mg-mediated) and Sonogashira (Cu-mediated) reactions. Each of the organometallic species involved in these reactions exhibit unique reactivity and chemoselectivity profiles allowing reactions to proceed in a broad range of environments—pH and temperature, for example. The Heck-Mizokori reaction is mechanistically distinct from the other cross-coupling reactions and proceeds via carbometallation and subsequent β-hydride elimination, thus, avoiding transmetallation (Scheme 3–4).

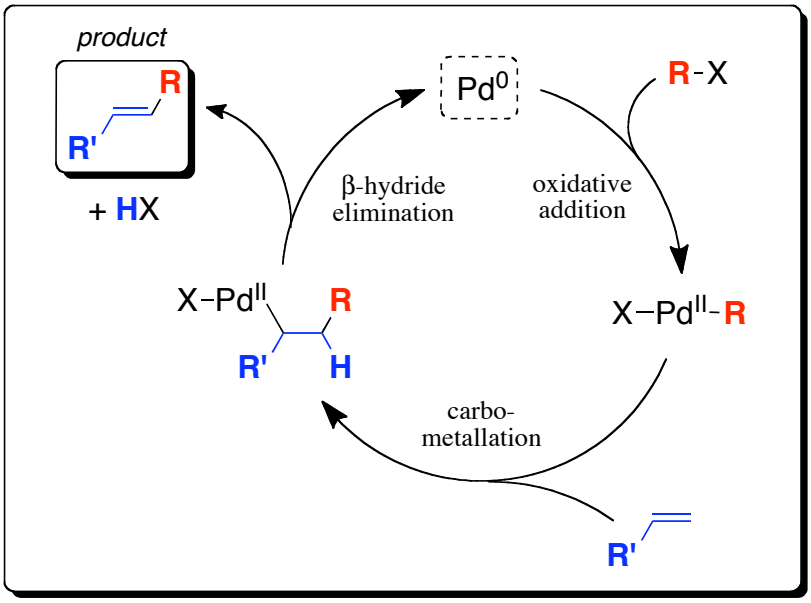

Fig. 3–4. Postulated Heck-Mizokori catalytic cycle.

In the past decade, advancements in Pd-catalyzed cross-coupling have focused on expanding the substrate scope of these traditional methods and developing mechanistically distinct coupling reactions. Through the fine-tuning of ligands, coupling partners, transition metals and additive mixtures, some of the typical constraints seen in cross-coupling reactions have been surmounted. The use of well-chosen catalysts and substrates has even allowed the carbon-hydrogen (C–H) bond to substitute as a reactive electrophile or nucleophile in C–C and C–X bond formations.

3.3 Synthetic strategy

With such extensive precedent for C–C bond formation using palladium, we laid out our plans to elaborate the enaminone scaffolds discussed in Chapter 2. The Suzuki-Miyaura reaction, which uses organoboron reagents, was chosen to install the aryl moiety based on its

well-known versatility. Boronic acids and esters, the most commonly used coupling partners in this reaction, are significantly more stable than their Mg, Zn or Cu counterparts, yet they are sufficiently reactive under mild conditions. Furthermore, these reagents are non-toxic—a limitation for organostannanes—and hundreds, if not thousands, are commercially available—a practical bonus not shared with organosilanes. The latter advantage was particularly attractive because of our desire to access phenanthrene substituents other than the overly-exploited hydroxy or alkoxy groups.

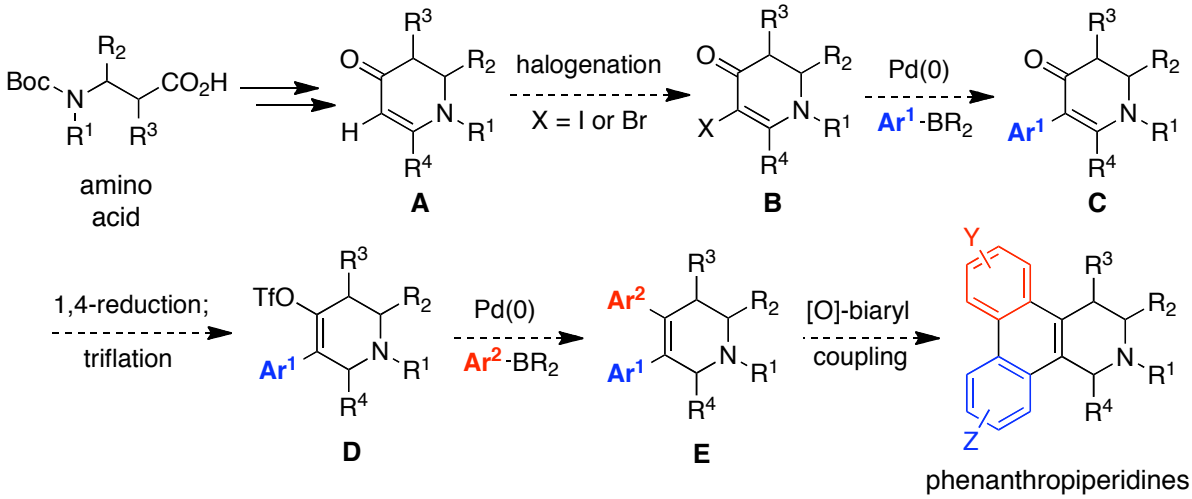

Scheme 3–1. Synthetic strategy for preparation of phenanthropiperidines.

To prepare the natural products, we planned to pre-activate the amino acid-derived enaminone (**A**) for the Suzuki protocol via halogenation (Scheme 3–1). This would allow a subsequent installation of the arene (Ar^1) using an appropriately substituted arylboronic acid (**B**→**C**). The final three steps of the synthesis could be completed in a manner that is not completely foreign to the synthesis of these natural products.[140, 141] From aryl enaminone **C**, the northern arene (Ar^2) could be installed using another cross-coupling reaction, only this

time pre-activation would generate a triflate (**D**), which we envisioned happening through a 1,4-reduction and enolate trapping. Triflate **D** could then react in a cross-coupling reaction to provide seco-analog **E**. Following the second arylation, the sequence could be completed with an oxidative biaryl coupling reaction furnishing the desired phenanthropiperidine.

The proposed sequence has some distinct advantages over previous syntheses. First, the phenanthropiperidines are constructed from three simple building blocks—an amino acid and two boronic acids—that constitute the three extremities of the natural product. These building blocks could be easily interchanged with others from a massive collection of commercially available precursors, giving access to novel permutations of the natural products. As a corollary of this, since the piperidine system (ring D) is derived from amino acids, many of which are available in enantiomerically pure form, asymmetric syntheses will be less daunting. Finally, using various amino acids, unnatural ring E analogs could be prepared and used to probe SARs in this largely unexplored position.

3.4 Activation and classical Suzuki approach

In Chapter 2, the reactivity of the enaminone was discussed. From this it is clear why the C3-position is particularly susceptible to electrophilic halogenation. The nitrogen's nonbonding electrons are conjugated with the π-system explaining this position's enhanced nucleophilicity. Furthermore, the α, β-unsaturated ketone amplifies the selectivity of this transformation by deactivating the C2-position. Indeed, halogenation of α, β-unsaturated ketones without appended heteroatoms occurs almost exclusively at the α-position.

Using enaminone **2.37** as a model substrate, we explored this promising mode of pre-activation. Treatment of the bicyclic system with iodine in the presence of DMAP furnished iodoenaminone **3.1** in near quantitive yield (Scheme 3–2). Bromination was also possible using Br_2 and TEA, but given that C–I bonds are more susceptible to oxidative insertion than are C–Br bonds, iodoenaminone **3.1** was used for the cross-coupling.

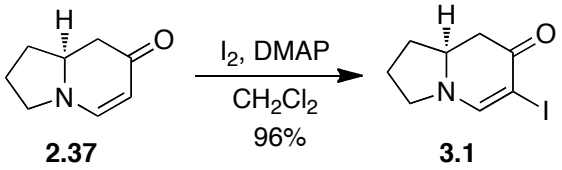

2.37 **3.1**

Scheme 3–2. Iodination of enaminone in preparation for Suzuki reaction.

Previous work in our laboratory had demonstrated that the Suzuki-Miyaura reaction is one possible method for installing the C3-aryl moiety.[213] Under optimized conditions using $Pd(PPh_3)_4$ as a catalyst, the coupling proceeds in 14 h at 100 ºC (entry 1, Table 3–1). Although microwave irradiation could be used to remedy the long reaction times without reduction (or increase) in yield, this demanded a further increase in temperature (entry 2). Observing a considerable amount of degradation under both conditions, we thought it would be profitable to pursue mild alternatives. The necessity of such high temperatures and long reaction times in spite of our use of an iodide electrophile—the most reactive of the halides—is explicable. Oxidative insertion, which is typically the rate-determining step of the Suzuki-Miyaura reaction, proceeds best when the organic electrophile (halide or pseudohalide) is electron-deficient. Since the iodide is located at the most electron-rich position of the vinylogous amide, palladium insertion is less favored. Thus, the nucleophilic

character of C3 is a two-edged sword; it accommodates pre-activation but hinders cross-coupling.

Table 3–1. Suzuki cross-coupling conditions of iodoenaminone.

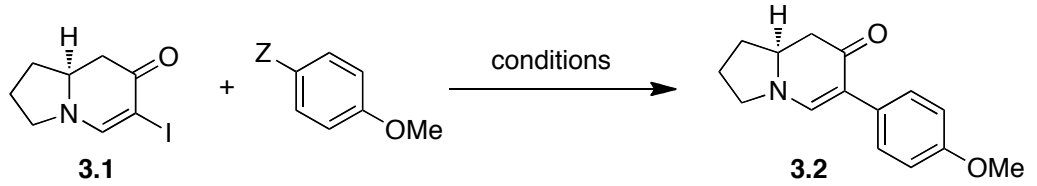

entry	Z	conditions	time	yield (%)[a]
1[b]	-$B(OH)_2$	$Pd(PPh_3)_4$, $Ba(OH)_2$, dioxane/H_2O, 100 ºC	14 h	70
2[b]	-$B(OH)_2$	$Pd(PPh_3)_4$, $Ba(OH)_2$, dioxane/H_2O, 150 ºC, μW	15 min	70
3[c]	-BF_3K	$Pd(OAc)_2$, S-Phos, K_2CO_3, MeOH, 50 ºC	5 h	65

[a] Isolated yield. [b] Reaction conditions: iodoenaminone (0.1 M), $Pd(PPh_3)_4$ (20 mol%), boronic acid (1.7 equiv), $Ba(OH)_2$ (2.0 equiv). [c] Conditions: iodoenaminone (0.07 M), $Pd(OAc)_2$ (1.0 mol%), S-Phos (2.0 mol%), trifluoroborate (1.4 equiv), K_2CO_3 (3.0 equiv).

Besides increasing the reaction temperature, oxidative insertion may also be promoted through the use of Pd-catalysts with higher reductive potentials. This can be achieved through the use of electron-rich ligands. In this regard, we attempted to compensate for the enaminone's low reactivity by using the highly-nucleophilic S-Phos ligand.[290] We chose to use conditions which had been successful in the coupling of aryl chlorides—generally unreactive substrates.[291] Using the prescribed organotrifluoroborate coupling partner, we were pleased to discover this reaction proceeded at 50 ºC in 5 h (entry 3). Unfortunately, the yield was not improved over the previous conditions despite using lower temperatures. Moreover, attempts at improving the yield through additive modifications were unsuccessful. Although the best conditions would probably suffice for our purposes, a reconsideration of the enaminone's innate nucleophilicity led us to pursue a more direct approach through C–H

functionalization. A word about this nascent field will explain our rational for using enaminones as C–H donors.

3.5 C–H Functionalization

The direct conversion of C–H to C–C bonds is one of the final frontiers of organic synthesis. Recent developments in this field have allowed concise and economical routes to valuable materials and synthetic intermediates.[292-296] The use of stoichiometric transition metal complexes to carry out C–H bond functionalization is well-precedented. However, it was not until the early 1990s that catalytic systems were first reported. Ruthenium-, rhodium- and iridium-based catalyst systems are prevalent in scientific literature for activation of C–H bonds—that is, processes that involve *oxidative insertion* into a C–H bond. Palladium, on the other hand, has proven to be quite effective for processes involving electrophilic palladation and ultimately C–H *functionalization*.

Despite early examples of C–H functionalization, this field remains largely unexplored due to four major challenges.[297] First, the typical C–H bond, sometimes referred to as the "un-functional group",[298] is relatively unreactive. Secondly, over-functionalization (chemoselectivity) is often a favorable side-reaction. Third, the ubiquity of C–H bonds has made regioselectivity a significant challenge as organic molecules typically contain many C–H motifs that are difficult to differentiate. Finally, the functionalization of sp^3 carbons allows for the prospect, and hence the challenge, of generating stereogenic centers with high stereoselectivity.

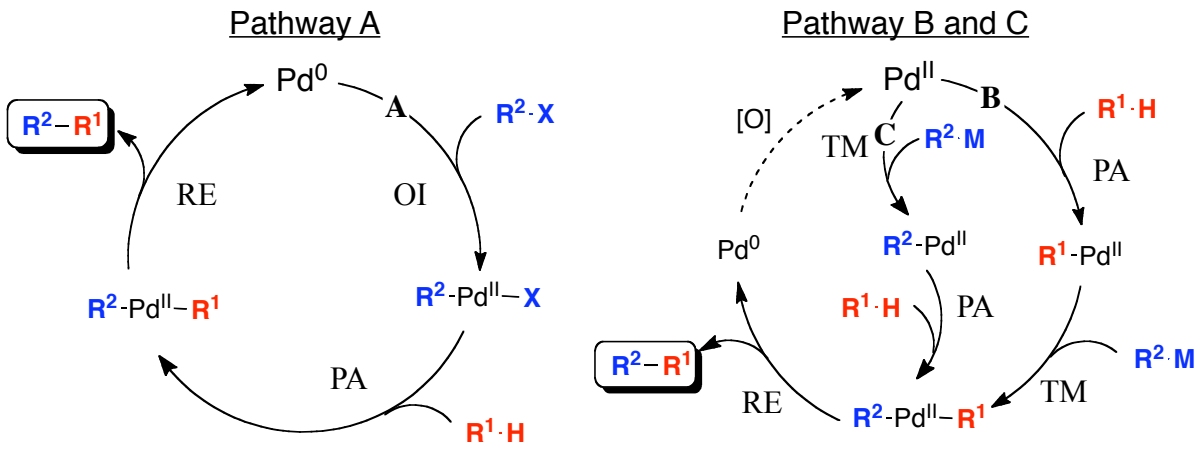

(OI = oxidative insertion; PA = palladation; RE = reductive elimination; TM = transmetallation)

Fig. 3–5. Plausible mechanisms for Pd-catalyzed C–H functionalization reactions.

From a mechanistic standpoint, the essential feature of Pd-catalyzed C–H functionalization reactions is the generation of a C–Pd bond from a C–H bond. Once this occurs, the fate of the palladium complex parallels that of the classical Pd-catalyzed cross-coupling reactions, and the desired C–C bond is ultimately formed upon reductive elimination (Fig. 3–5) or β-hydride elimination (not shown). The point in the catalytic cycle at which the coupling partner is introduced varies and is dependent on the substrate's reactivity towards the Pd-catalyst. Coupling partners, such as aryl halides, will undergo oxidative insertion in the presence of Pd(0) prior to palladation of the C–H donor (Fig. 3–5, Pathway A). Alternatively, if an organic nucleophile, such as a boronic acid, is used, transmetallation may occur before (Pathway B) or after (Pathway C) palladation. A key distinction between these catalytic cycles is that Pathway A begins with a Pd(0)-catalyst whereas Pathways B and C begin with a Pd(II)-catalyst. The significance of this lies in the fact that Pd(0) is generated upon reductive elimination—the final step for all pathways—allowing catalytic turnover for only one (Pathway A). Unless an oxidant is present for

processes initiated with Pd(II)-mediated palladation or transmetallation (Pathway B and C), the catalytic cycle will not be reiterated. Fortunately, this can be accommodated for by adding an external oxidant which oxidizes Pd(0) into the active Pd(II)-catalyst.

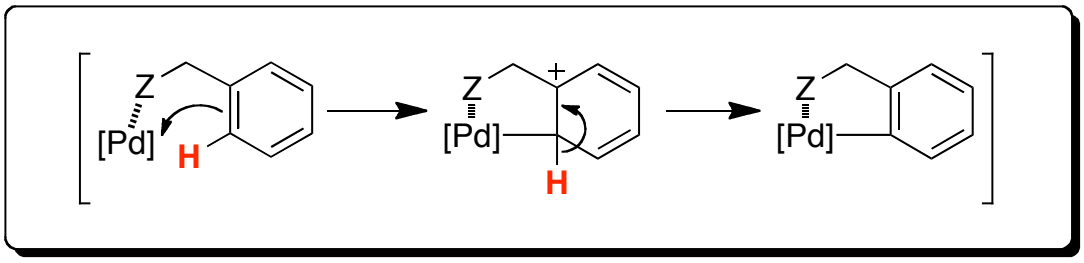

Fig. 3–6. Directing group-assisted C–H palladation via electrophilic substitution.

Their are two main strategies that have been used to selectively functionalize C–H bonds in Pd-catalyzed cross-couplings. The first strategy is to exploit Lewis basic directing groups to guide palladation. By taking advantage of chelating functionalities, such as acetamides, carboxylates and pyridines, the electrophilic catalyst is guided into close proximity of the C–H bond. There are several plausible mechanisms that can be proposed for palladation, but the exact pathway is highly dependent on the substrate, catalyst, solvent and other additives.[299] The most common and relevant for our purposes is electrophilic substitution (Fig. 3–6). In this process, the electrophilic Pd(II)-complex, which is coordinated to the directing group, reacts with the π-electrons from an appropriately situated olefin resulting in a cationic intermediate. The positive charge is then quenched upon loss of a proton which marks the cleavage of the key C–H bond. When the olefin is embedded within an aromatic system, besides quenching the positive charge, the C–H bond scission is also driven by rearomatization. Once palladation has occurred the palladacycle can be intercepted with a

variety of coupling partners. This is better demonstrated using case studies. Pathway A (Scheme 3–3) is illustrated well in a reaction reported by Daugulis and Zaitsev.[300] Here, aryl iodides are coupled with anilides in excellent yields. In this reaction the σ-bonded aryl-Pd(II) complex that is formed from oxidative insertion of the active Pd(0)-catalyst into the C–I bond is directed by the acetamide group for palladation. Product formation results from a reductive elimination of the resultant palladacycle. In this example, the *ortho* methyl group prevents this process from recurring on the opposite side.

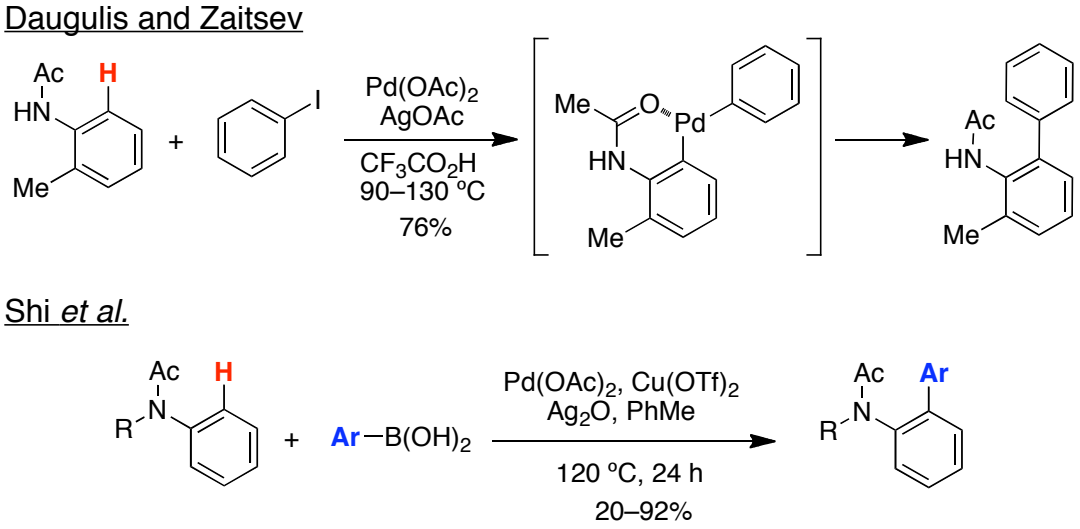

Scheme 3–3. Directed Pd-catalyzed C–H functionalization reactions.

Pathway B is exemplified in a reaction reported by Shi *et al.*, in which, like before, acetamides are used as directing groups (Scheme 3–3).[301] Unlike before, since the catalytic cycle begins with Pd(II), this reaction required the use of $Cu(OTf)_2$ and Ag_2O as oxidants to regenerate the active Pd(II) species necessary for palladation.

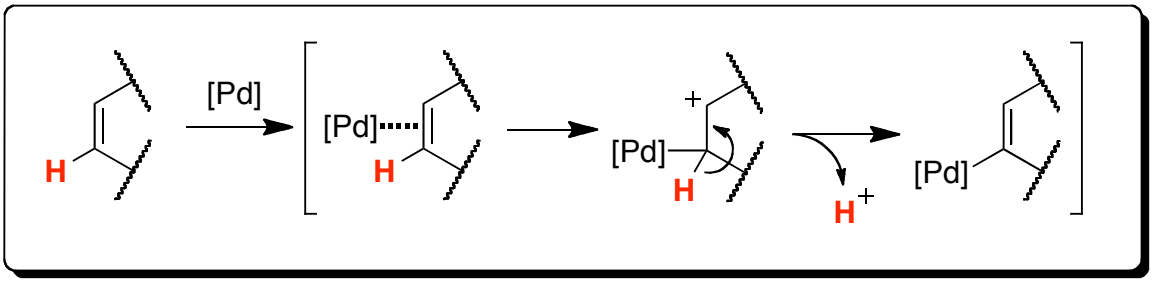

Fig. 3–7. Reactivity-assisted C–H palladation.

The second strategy for attaining C–H selectivity is to use the innate reactivity, particularly π-nucleophilicity, of that carbon.[302] If the C–H bond in question is acidic, basic conditions can be used to assist cleavage.[299] There are many substrates, however, that are not acidic and still exhibit sufficient reactivity towards electrophilic palladation. Electron-rich aromatic systems such as phenols, indoles and pyrroles are the commonly used in this type of cross-coupling.[299, 302, 303] Although a directing group is not present, association of the Pd-catalyst and substrate is assisted by the π-nucleophilicity of the active double bond. The mechanism is essentially identical to the previously described directing group-assisted palladation. Following η^2-coordination of the catalyst, substrate palladation occurs to furnish a stabilized cation which is subsequently quenched upon deprotonation (Fig. 3–7). As before, the cleavage of the C–H bond is driven by rearomatization.

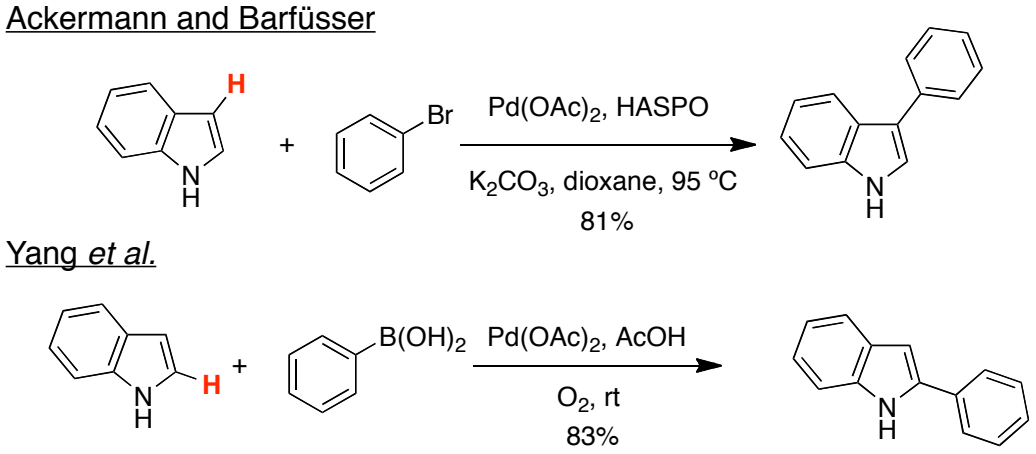

Scheme 3–4. Direct C2- and C3-arylation of indoles.

This approach has been applied in numerous settings.[299, 302, 303] Ackermann and Barfüsser have used this strategy in a direct C3-coupling of indoles and aryl bromides (Scheme 3–4). In contrast, Yang *et al*. reported a C2-selective cross-coupling of indole C–H donors and boronic acids.[304] These two examples represent Pathway A and C (Fig. 3–5), respectively. However, it should not be concluded from this that the regioselectivity of indole arylation is determined by these particular mechanistic pathways. Both C2- and C3-arylations of indoles have been reported for Pd-mediated C–H functionalization reactions.[305] Sames and coworkers give compelling evidence that the regioselectivity of this reaction is dependent on the ease of Pd-migration for specific reaction intermediates (Fig. 3–8).[306] It was proposed that palladation occurs exclusively at the C3-position generating an iminium which can rearrange to stabilize the Pd–C bond through the adjoining nitrogen. The rate of migration, which is influenced by the size of N-substituent and Pd-ligands, determines the regioselectivity of the reaction. In other words, rearomatization precludes Pd-migration and secures the position of C–C bond formation.

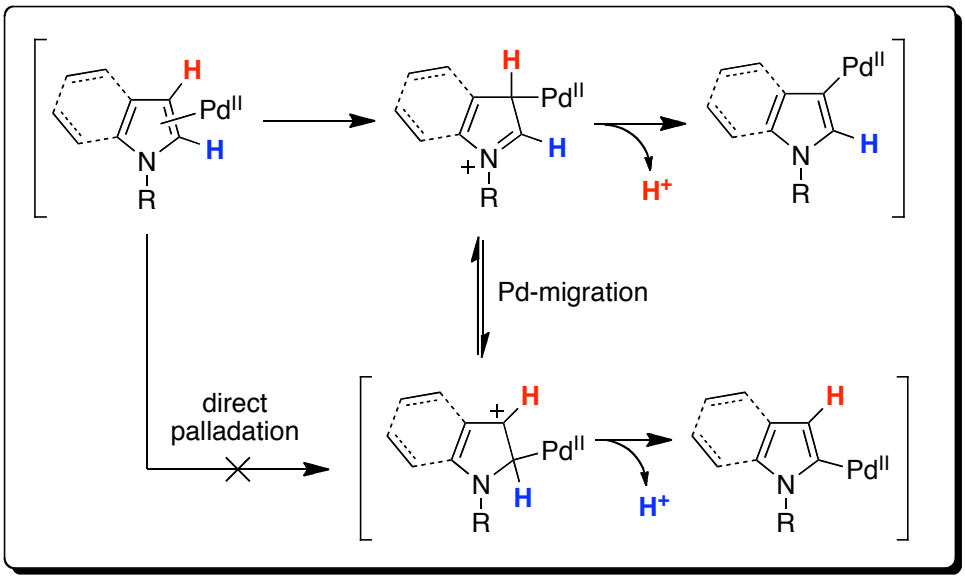

Fig. 3–8. C3/C2 Pd-migration of palladated indoles.

The latter of these two strategies (*i.e.* taking advantage of π-nucleophilicity) inspired us to investigate enaminones in Pd-catalyzed C–H functionalization reactions. Like indoles and pyrroles, the enaminone is endowed with an enamine system which is exceptionally nucleophilic. The major difference between the two substrates is that the enamine in enaminones are embedded within an aromatic systems; hence, C–H bond cleavage would not be driven by rearomatization. Instead, deprotonation would be favored by the acidity of the C3-proton which is flanked by two electron-withdrawing functionalities: a ketone and the transient iminium group (Fig. 3–9). Given the switchable regioselectivity in indole systems, we considered the possibility of a similar C3/C2 palladium migration in the enaminone. We reasoned that this would not be likely based on the instability of the resultant carbocation

(being adjacent to a ketone) and the rate of the highly-favored deprotonation that would compete with the migration.

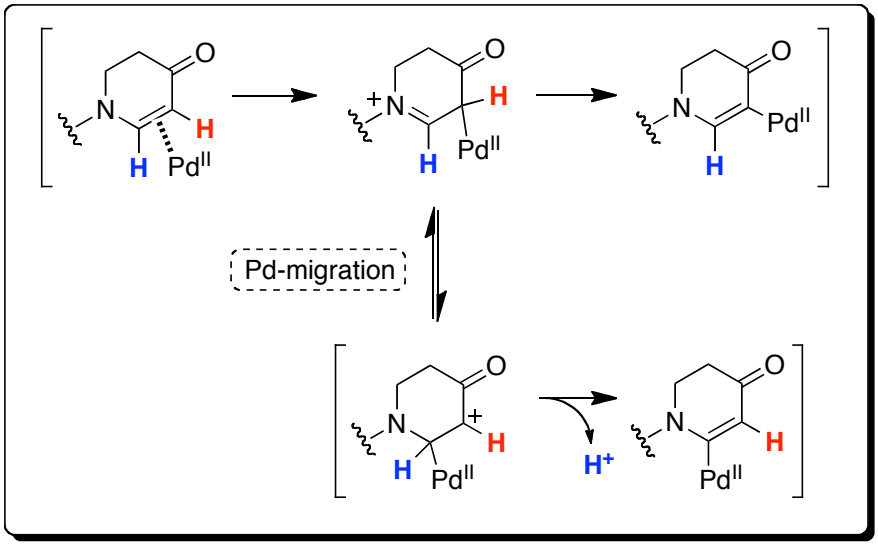

Fig. 3–9. C3/C2 palladium migration of palladated enaminones.

The success of this approach would ultimately depend on the innate nucleophilic character of the enaminone to give access to the same putative transition-metal species as in the two-step process, only in a catalytic and one-step fashion. If this key intermediate was generated *in situ*, it could presumably be intercepted with a suitable coupling partner. Thus, this strategy uses what was once a liability, namely the nucelophilicity of the enaminone, as an asset, allowing us to circumvent pre-activation of the enaminone.

3.6 Reaction optimization

3.6.1 Reoxidant screen

Our first goal was to establish the feasibility of this reaction. The first conditions we investigated were inspired by a Pd(II)-catalyzed alkenylation reaction reported by Garg, Caspi and Stoltz.[307] Since our aim was to install arenes instead of olefins like the Stoltz group, we needed a suitable aryl coupling partner. One concern was that the use of an acidic cosolvent, thought to promote palladation by increasing the electrophilicity of the Pd(II) center,[308] would limit the potential of basic or nucleophile-promoted organometallic coupling partners (*i.e.* organozinc reagents, boronates, silanes…*etc*). With previous success using organotrifluoroborates—Molander *et al.* have found to these to be robust equivalents of organoboronic acids[309]—we chose to employ these for our investigations.

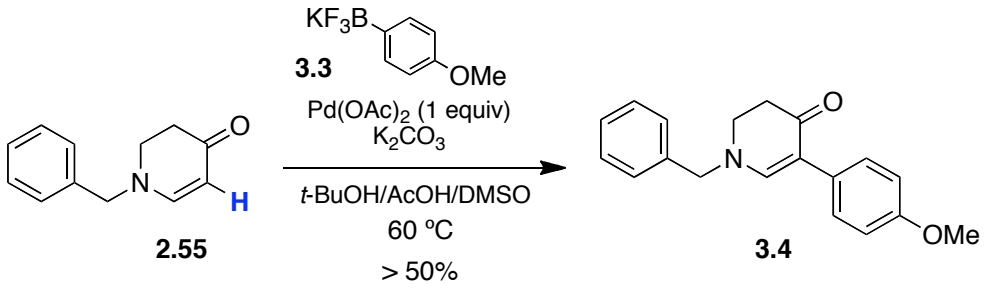

Scheme 3–5. Direct C–H arylation of model enaminone using stoichiometric Pd.

Initial attempts to couple enaminone **2.55** and trifluoroborate **3.3** using stoichiometric $Pd(OAc)_2$ were surprisingly successful (Scheme 3–5). With good reason to move forward we next pursued conditions allowing catalytic quantities of palladium. Assuming that this

reaction would proceed through either Pathway B or C (Fig. 3–5), we investigated reoxidants to achieve catalytic turnover. Copper reagents have had longstanding use as palladium oxidants, and so we investigated several Cu(II) reagents for such a purpose (entries 1–3, Table 3–2). Each copper reoxidant proved to be effective in driving the reaction to completion using catalytic quantities of $Pd(OAc)_2$. Over two equivalents of each reagent were used since palladium undergoes a two-electron oxidation ($Pd^0 \rightarrow Pd^{II}$) and copper, a single-electron reduction ($Cu^{II} \rightarrow Cu^{I}$).

Table 3–2. Screen of reoxidants.

entry[a]	oxidant (equiv)	yield (%)[b]
1	$CuCl_2$ (3.0)	66
2	$Cu(OTFA)_2$ (3.0)	82
3	$Cu(OAc)_2$ (3.0)	82
4	$Cu(OAc)_2$ (1.0) / O_2 (1 atm)	40
5	BQ (1.0)	14
6	duroquinone (1.0)	75

[a] Reaction conditions unless otherwise specified: enaminone **2.55** (0.1 M), trifluoroborate **3.3** (2-3 equiv), $Pd(OAc)_2$ (0.3 equiv), oxidant, K_2CO_3 (3 equiv) at 60 °C. [b] Isolated yield of enaminone **3.4**.

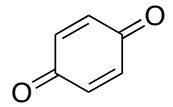

benzoquinone (BQ)

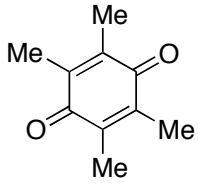

duroquinone

One strategy that has been used to avoid using such high amounts of copper is to carryout the reaction in an oxygen atmosphere. Copper reagents such as $Cu(OAc)_2$ are known to undergo aerobic oxidation more readily their palladium counterparts and have been exploited in reactions requiring palladium oxidation. In fact, the aerobic oxidation of CuCl to $CuCl_2$ is among the fastest inorganic reactions—a boon for the development of industrial-scale Wacker processes.[310] Thus, catalytic quantities of the copper reoxidant can be used, because

the active Cu(II) species is regenerated when it reacts with oxygen. Applying this strategy, the reaction was conducted in the presence of oxygen and substoichiometric quantities of $Cu(OAc)_2$ (entry 4). Unfortunately, the reaction yield was significantly lower than when 3 equivalents of copper were used.

Benzoquinone (BQ) is another widely used palladium oxidant[302] but was deleterious in this reaction (entry 5). Unlike when catalytic amounts of $Cu(OAc)_2$ was used, this reaction did not simply stop progressing, rather, the starting material was shunted to an undesired byproduct (BQ-adduct **C**). Under the supposition that enaminone palladation precedes transmetallation, this unexpected product could conceivably arise from enaminone-Pd(II) complex **A** following the carbometallation and β-hydride elimination of BQ (Scheme 3–6).

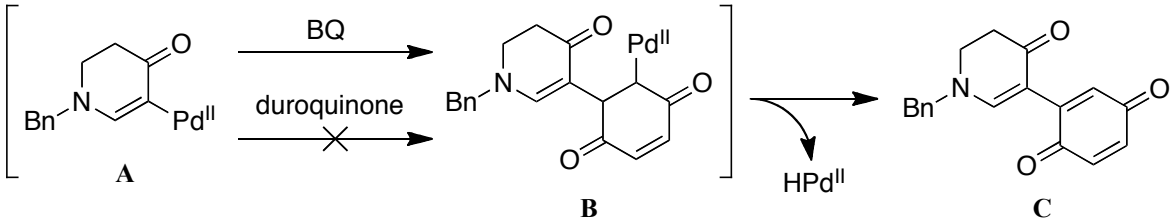

Scheme 3–6. Mechanism for formation of BQ-adduct.

To prevent this side-reaction, we used duroquinone (entry 6)—a BQ analog with four methyl groups blocking the equivalent reactive positions. This reoxidant provided significantly higher yields than BQ but was not as effective as $Cu(OAc)_2$ or $Cu(OTFA)_2$. Although $Cu(OAc)_2$ and $Cu(OTFA)_2$ were comparable as reoxidants, we chose to proceed with the more economic of the two: $Cu(OAc)_2$.

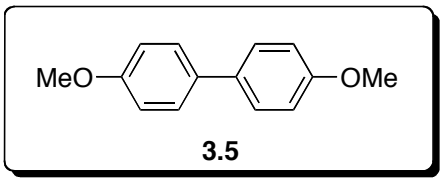

Fig. 3–10. Homocoupling product of trifluoroborate **3.3**.

A greater concern about the fate of the reoxidant arose when we discovered a significant amount of biphenyl **3.5** was being generated (Fig 3–10). This was accounted for by considering the potential for homocoupling within our proposed mechanistic model (Fig. 3–11). The catalytic cycle deserves further attention at this point.

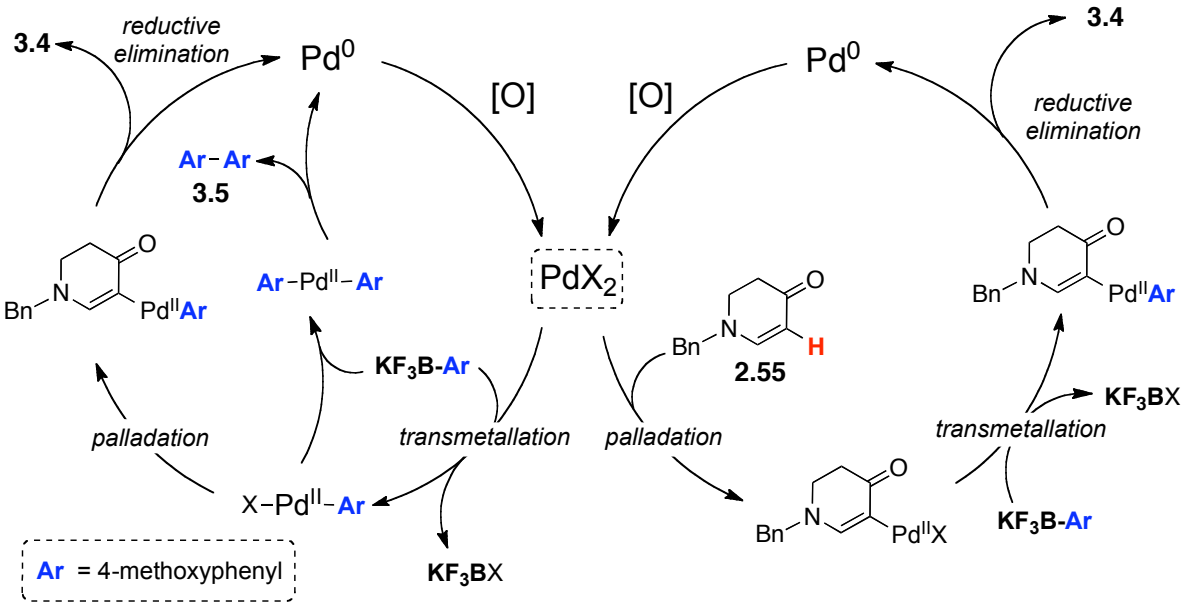

Fig. 3–11. Proposed catalytic cycle for direct-arylation of enaminones.

The mechanism for the palladation of enaminones presumably resembles that of indoles.[296] It is likely initiated by an electrophilic attack of palladium on the enaminone as already

discussed. In the presence of an appropriate organometallic substrate, transmetallation and reductive elimination would provide the desired coupled product. Alternatively, transmetallation could precede enaminone palladation providing an intermediate that would either undergo palladation or another transmetallation. If the latter occurs, reductive elimination would yield homocoupled byproduct **3.5**. The upshot of this side-reaction is that both the reoxidant and aryl coupling partner are irreversibly consumed without contributing to product formation. By isolating significant amounts of the homocoupled product, we realized that this process was competing with enaminone palladation and that, if not abated in the future, excess reagents—as we have been using—would continue to be necessary to drive the reaction to completion. With that in mind, keeping the amounts of reoxidant and coupling partner constant, we sought out conditions that would improve yields and would not leave unreacted starting material.

3.6.2 Palladium-catalyst screen

First investigating palladium sources, we confirmed that palladium was indeed necessary and that the reaction was not mediated by the copper reagent or trace impurities therein (entry 1, Table 3–3). $Pd(OAc)_2$ (entry 2) was found to be superior to $PdCl_2$ and $Pd(CF_3CO_2)_2$ (entries 3 and 4). It should be noted here that the use of 0.3 equivalents of the catalyst was most effective for complete conversion in this reaction. Considering the limited stability of our enaminone substrate, the higher Pd(II)-catalyst loading allowed us to avoid long reaction times and high temperatures which were otherwise required to drive the reaction to completion. Another reason for using high-catalyst loading was because of an apparent

inhibition of the Pd-catalyst. This was confirmed by experiments showing that spiking the reaction mixture with additional palladium, but not with other reagents, could drive arrested reactions to completion.

Table 3–3. Screen of palladium catalysts.

entry[a]	Pd catalyst	yield (%)[b]
1	None	0
2	$Pd(OAc)_2$	82
3	$PdCl_2$	61
4	$Pd(CF_3CO_2)_2$	60

[a] Reaction conditions unless otherwise specified: enaminone **2.55** (0.1 M), trifluoroborate **3.3** (2-3 equiv), Pd source (0.3 equiv), $Cu(OAc)_2$ (3 equiv), K_2CO_3 (3.0 equiv) at 60 °C. [b] Isolated yield of enaminone **3.4**.

3.6.3 Solvent screen

Although a number of solvents were also investigated, we found that the original solvent mixture gave the best results (Table 3–4, entry 1). Each of the three components were important in this reaction; any one of them in isolation significantly reduced yields (entries 2–5). The presence of DMSO was beneficial and may help to solubilize or stabilize the palladium or copper complexes, but the exact role is unknown (entry 2). The use of AcOH as a solvent enhanced the rate of the reaction and drove it to completion, but the enaminone underwent substantial degradation when it was used as the sole solvent, and less than 10% of the product was isolated (entry 3). The role of the *t*-BuOH is not entirely clear either; however, we were aware that non-tertiary alcohols were prone to Pd-mediated oxidation

which would result in a rapid depletion of the reoxidant.[311] Nevertheless, *t*-BuOH was not an effective solvent when used by itself. Realizing that the reaction was extremely slow in the absence of AcOH, we attempted to increase the rate of reaction by raising the reaction temperature. Using several higher-boiling solvents (entries 5–7), we carried out the reaction under acid-free conditions and found that product formation was severely impaired.

Table 3–4. Screen of solvents.

entry[a]	solvent	temperature (ºC)	yield (%)[b]
1	*t*-BuOH/AcOH/DMSO	60	82
2	*t*-BuOH/AcOH	60	< 50
3	AcOH	50	< 10
4	*t*-BuOH	50	< 10
5	DMSO	100	3
6	DMF	100	6
7	PhMe	120	10

[a] Reaction conditions unless otherwise specified: enaminone **2.55** (0.1 M), trifluoroborate **3.3** (2-3 equiv), $Pd(OAc)_2$ (0.3 equiv), $Cu(OAc)_2$ (3.0 equiv), K_2CO_3 (3 equiv) at 60 °C. [b] Isolated yield of enaminone **3.4**.

3.6.4 Additive screen

Our final effort to improve the yield of this reaction was to investigate the role of additives (Table 3–5). Throughout our optimization studies we had chosen to use K_2CO_3, but we were still uncertain of its necessity. It soon became clear that K_2CO_3 was important simply by observing that its absence decreased the reaction yield by almost 20% (entry 2). It is extremely difficult to decipher the role of inorganic additives in complex mixtures, but we posit that the beneficial effects of K_2CO_3 were distinct from its basic properties. This

conclusion was borne out of the realization that K_2CO_3 would decompose in the presence of AcOH, which is in large excess, to generate KOAc, CO_2 and H_2O. Indeed, upon the addition of the solvent mixture to the solid reagents, we observed bubbling as evidence of CO_2 production. We reasoned from this that the reaction was aided by acetate or potassium ions or both. With this in mind, we replaced K_2CO_3 with KOAc and found a slight improvement (entry 4). On the other hand, when NaOAc was used instead of K_2CO_3, we observed a marked reduction in yield (entry 3). One possible explanation of this is simply that the potassium salt is more soluble than its sodium congener. However the additives work, potassium salts are evidently beneficial.

Table 3–5. Screen of additives.

entry[a]	additive A (equiv)	additive B (equiv)	temperature (ºC)	yield (%)[b]
1	K_2CO_3 (3.0)	–	60	82
2	None	–	60	63[c]
3	NaOAc (3.0)	–	60	54
4	KOAc (3.0)	–	60	87
5	CF_3CO_2K (0.2)	–	30	54
6	CF_3CO_2K (1.0)	–	60	49
7	CF_3CO_2K (3.0)	–	60	70
8	CF_3CO_2Ag (3.0)	–	60	41
9	K_2CO_3 (1.0)	CF_3CO_2K (1.0)	50	69
10	K_2CO_3 (2.0)	CF_3CO_2K (1.0)	50	77
11	K_2CO_3 (3.0)	CF_3CO_2K (0.5)	50	70
12	K_2CO_3 (1.0)	CF_3CO_2K (0.2)	50	71
13	K_2CO_3 (2.0)	–	60	93

[a] Reaction conditions unless otherwise specified: enaminone **2.55** (0.1 M), trifluoroborate **3.3** (2-3 equiv), $Pd(OAc)_2$ (0.3 equiv), $Cu(OAc)_2$ (3.0 equiv), additives A and B (0.2-3 equiv) at 30-60 °C. [b] Isolated yield of enaminone **3.4**.

As stated before, we observed that acids enhanced the rate of reaction. This phenomenon reflects the dependence of this reaction on an electrophilic palladation process. The acid presumably enhances the electrophilicity of the palladium complex by assisting anionic ligand dissociation.[308] Another way to enhance the electrophilicity of the Pd-complex is to use ligands that are stable anions, also assisting ligand dissociation. Thus, we investigated the effect of trifluoroacetate salts on the rate and yield of reaction (entries 5–8). Given the apparent benefit of potassium salts, we used potassium trifluoroacetate (CF_3CO_2K). Although the yield was not improved, the reaction time was decreased from 8 to 2 h. Quantities as low as 0.2 equivalents conferred complete conversion in less than 3 h at 30 ºC (entry 5). Silver(I) trifluoroacetate (CF_3CO_2Ag) did not improve yields at all (entry 8). The lower yields are attributed to the production of multiple side-products since all of the starting material had reacted, but the side-products could be identified. Attempting to maintain the short reaction times but mitigate the side-reactions, we used K_2CO_3 in conjunction with CF_3CO_2K (entries 9–12). Even though the reaction times were improved, the yields did not match those in the absence of CF_3CO_2K. Settling on K_2CO_3 as the only additive to be used, we took one last measure to improve the reaction, relying on the notion that lowering the concentration of the trifluoroborate at any given moment would suppress homocoupling. To do this, the coupling partner was added incrementally over the reaction time. Seeing that this provided the highest yields yet (entry 13), we used these conditions to probe the scope of this reaction by using a diverse set of enaminones and coupling partners.

3.7 Scope of trifluoroborates

With optimized conditions in hand, we first explored coupling partners with a variety of electronic and steric properties. Electron-rich trifluoroborates underwent rapid (2-6 h) and high-yielding cross-coupling. On the other hand, electron-deficient and sterically-encumbered trifluoroborates (entries 3 and 4, Table 3–6,) required longer reaction times (24 h) and proceeded in relatively low yields. This trend should not be taken too strictly given several unpredictable results we obtained. For instance, it was unexpected that the 2-naphthyl (entry 9) and 3-hydroxyl (entry 11) systems reacted with such high yields. Interestingly, the 3-hydroxyphenyl boronic acid was poorly tolerated in our former Pd(0)-catalyzed approach, which demonstrates that this reaction is not merely a shorter method to arylate enaminones, but that it has a unique and complimentary scope as well.[213]

Although electronic considerations are not acutely predictive, the generalization that electron-rich, unhindered trifluoroborates react more rapidly and in higher yields than their electron-poor or hindered counterparts is completely consistent with our findings and sheds new light on the reaction's mechanism. Both electron-deficient and sterically-hindered coupling partners are less prone to transmetallation. That these properties are sufficient to alter the rate of reaction suggests that transmetallation is—at least in certain circumstances—the rate-determining step. This conclusion does not dismiss the importance of palladation but introduces a competing process that must be considered.

Table 3–6. Successfully coupled aryltrifluoroborates.

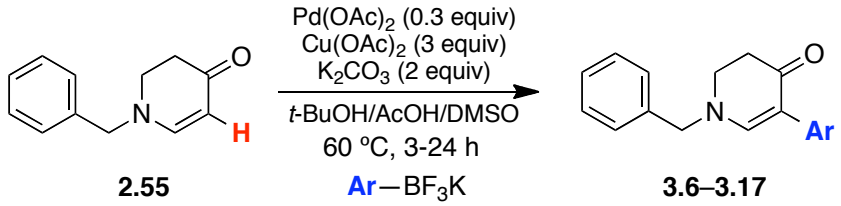

2.55 **3.6–3.17**

entry[a]	Ar (product)		yield (%)[b]	entry[a]	Ar (product)		yield (%)[b]
1	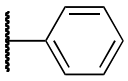	**3.6**	72	7	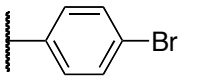	**3.12**	73
2	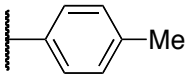	**3.7**	86	8	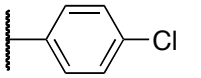	**3.13**	71
3	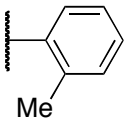	**3.8**	40	9	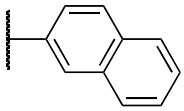	**3.14**	96
4	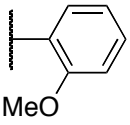	**3.9**	27	10	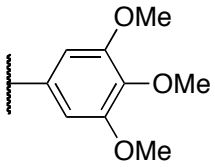	**3.15**	83
5	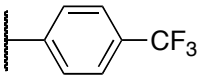	**3.10**	44	11	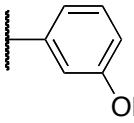	**3.16**	97
6	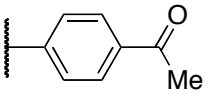	**3.11**	42	12	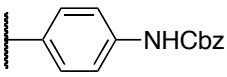	**3.17**	80

[a] Reaction conditions: enaminone **2.55** (0.1 M), R-BF_3K (2-3 equiv), $Pd(OAc)_2$ (0.3 equiv), $Cu(OAc)_2$ (3 equiv), K_2CO_3 (2 equiv) in *t*-BuOH/AcOH/DMSO (20:5:1) at 60 °C. [b] Isolated yield.

Besides giving valuable information about sterics and electronics, this sample set provides a cursory look into functional group compatibility. The phenol moiety is clearly stable under these conditions (entry 11) and the protected aniline group is also well-tolerated (entry 12). More significantly, the scope of this chemistry extends to aryl halides (entry 7 and 8) which react exclusively at the carbon-boron bond. The stability of these

functionalities (*i.e.* sp^2 halides) under the prescribed conditions reveal the complementarity of this protocol with the classical Suzuki-Miyaura reaction. As discussed already, the classic Suzuki-Miyaura protocol is initiated by a Pd(0)-mediated oxidative insertion process of the organohalide substrate. In the presence of Pd(0), aryl halides would normally react, but apparently, Pd(0), which does not contribute to product formation in this reaction, is oxidized before it can react with the carbon-halide bond.

Table 3–7. Aryltrifluoroborates that did not couple.

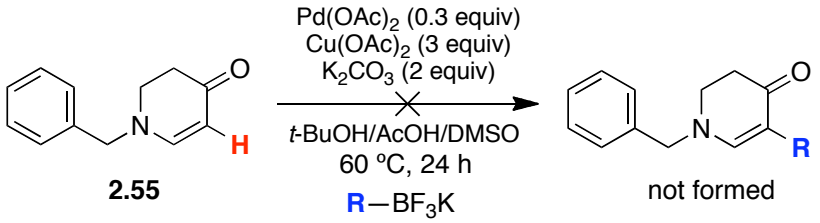

entry[a]	R	entry[a]	R	entry[a]	R
1	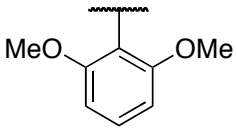	6		10	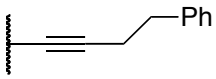
2	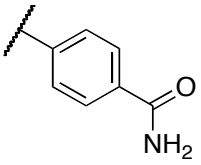	7	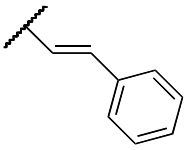	11	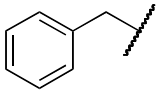
3	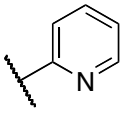	8	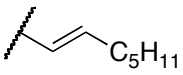	12	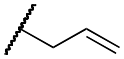
4	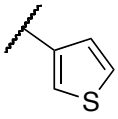	9	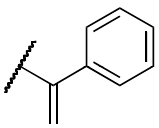	13	
5	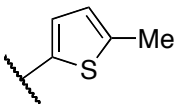			14	

[a] Reaction conditions: enaminone **2.55** (0.1 M), R-BF_3K (2-3 equiv), $Pd(OAc)_2$ (0.3 equiv), $Cu(OAc)_2$ (3 equiv), K_2CO_3 (2 equiv) in *t*-BuOH/AcOH/DMSO (20:5:1) at 60 °C. [b] Isolated yield.

The limitations of this reaction were quite clear when we began to investigate more challenging coupling partners (Table 3–7). Fourteen of these organotrifluoroborates were intractable (*i.e.* no coupled product was observed after 24 h). Knowing that steric congestion can hinder efficient coupling, it was not surprising that 2,6-dimethoxyphenyltrifluoroborate was unable to be coupled (entry 1). Attempts to install the benzamide moiety were also unsuccessful (entry 2). Interestingly, the reaction color change (from blue/green to black) that normally coincides with cross- or homo-coupling was not observed. Although one might suggest that its electron deficiency hampers transmetallation, this does not explain the qualitative difference between equally electron-deficient 4-acetylphenyl group (entry 6, Table 3–6). We postulate instead that the free N-H group is responsible for poisoning the Pd-catalyst. This effect was presumably overridden in the coupling of the N–H-containing anilino group (entry 12, Table 3–6), because the requisite coordinating ability of that nitrogen was sufficiently attenuated by two electron-withdrawing groups: the phenyl and carbamate.

Cross-coupling of pyridine and thiophene systems did not furnish the desired product and the starting material remained unreacted (entries 3–5, Table 3–7). Also, attempts to couple alkenyl and alkynyl trifluoroborates were unsuccessful (entries 6–10). This type of organic nucleophile generally undergoes transmetallation more rapidly than their phenyl congeners, and hence, homocoupling would most likely outcompete palladation of the enaminone. This is consistent with the observation that the reaction mixtures turned black almost instantaneously—indicating a coupling of some kind—but the enaminone starting material was essentially unreacted. In contrast, when using sp^3 coupling partners, the reaction mixture remained its original green/blue color, most likely reflecting the less-favored transmetallation process on alkyl centers (entries 11–14). Again, the starting material was intact after 24 h.

3.8 Scope of enaminones

An initial investigation of enaminone compatibility revealed that monocyclic and bicyclic, unattenuated enaminones were viable substrates in this reaction. Direct arylation of the indolizidine and quinolizidine scaffolds showed the potential of this reaction to be used in the synthesis of the phenanthropiperidine alkaloids (entries 1 and 2, Table 3–8). Interestingly, the reactivity of the two scaffolds were markedly different. Not only did the quinolizidine enaminone give higher yields of product, but it was completely reacted in less than half of the time it took for the indolizidine. One possible explanation of this is that the non-bonding orbital of the lone pair on the nitrogen and olefin p-orbitals are poorly aligned due to the more constrained 5,6-bicyclic system. With less orbital overlap, the contribution of the nitrogen would be less pronounced, resulting in a less nucleophilic enaminone. The ultimate consequence of this is that transmetallation outcompetes palladation and the organoborate and reoxidant are consumed in the production of the homodimer.

With reason to be concerned about epimerization of stereocenters (see Chapter 2) we subjected enaminones **2.36** and **2.50** to our optimized protocol (entries 3 and 4). We were pleased that our mildly-acidic conditions were suitable for these substrates, and they reacted with no observable epimerization.

Table 3–8. Successfully coupled of enaminones.

entry[a]	C–H donor		product		time (h)	yield (%)[b]
1	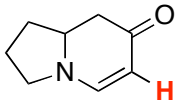	**2.37**	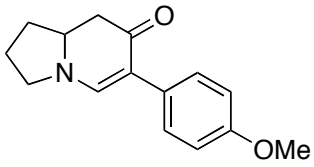	**3.2**	8	70
2	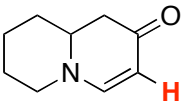	**2.34**	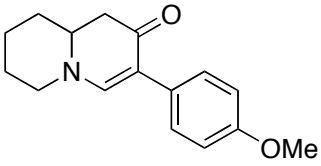	**3.20**	3	98
3	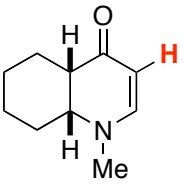	**2.36**	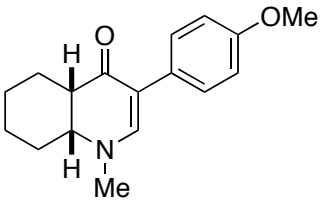	**3.21**	7	86
4	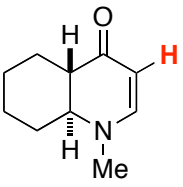	**2.50**	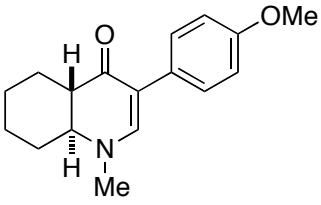	**3.22**	7	77
5	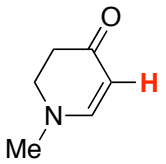	**3.18**	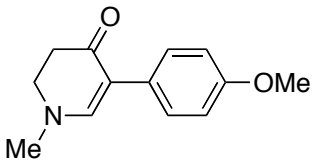	**3.23**	6	80
6	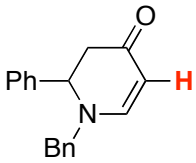	**3.19**	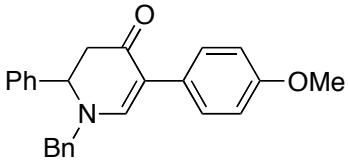	**3.24**	7	79

[a] Reaction conditions: enaminone (0.1 M), trifluoroborate **3.3** (2-3 equiv), $Pd(OAc)_2$ (0.3 equiv), $Cu(OAc)_2$ (3 equiv), K_2CO_3 (2 equiv) in *t*-BuOH/AcOH/DMSO (20:5:1) at 60 °C. [b] Isolated yield. [c]Starting material was recovered. PMP = 4-methoxyphenyl.

Despite the success of this reaction in monocyclic and bicyclic systems there were a several enaminones that did not react (Table 3–9). An *N*-Boc-protected enaminone was found to be unreactive under our optimized conditions, which we suggest is owing to its

decreased nucleophilicity (entry 1, Table 3–9). Likewise, adding another degree of unsaturation to the piperidine system is sufficient to suppress the reaction (entries 2–4). In each of these examples, we postulate that palladation is too slow to compete with homocoupling. Another way to impede enaminone palladation is to incorporate steric encumberance. We found that methyl and phenyl substituents could inhibit cross-coupling in the ordinarily reactive quinolizidine system (entries 5 and 6). Notably, the phenylquinolizidine can be coupled under Pd(0)-catalyzed conditions when pre-activated via C3-iodination,[213] showing again that these two methods are complimentary.

Table 3–9. Enaminones that did not couple.

entry[a]	C–H donor	entry[a]	C–H donor	entry[a]	C–H donor
1	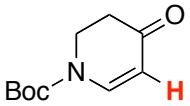	3	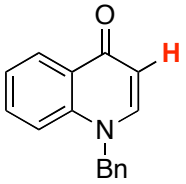	5	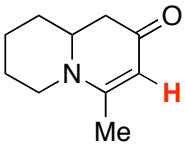
2	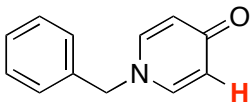	4	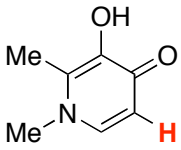	6	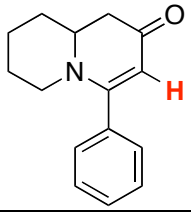

[a] Reaction conditions: enaminone (0.1 M), trifluoroborate **3.3** (2-3 equiv), $Pd(OAc)_2$ (0.3 equiv), $Cu(OAc)_2$ (3 equiv), K_2CO_3 (2 equiv) in *t*-BuOH/AcOH/DMSO (20:5:1) at 60 °C. [b] Isolated yield. [c] Starting material was recovered. PMP = 4-methoxyphenyl.

3.9 Extensions and directions for the future

The success of this reaction seems to rely on a delicate balance between the rates of palladation and transmetallation. This has been a major limitation with respect to both the enaminone and trifluoroborate. The *N*-alkyl substituted enaminones are on the threshold of

reactivity, and when even subtle changes are introduced, such as a methyl group, the desired reaction is overwhelmed by the competing dimerization process. The same effect can result from the use of organotrifluoroborates that are exceedingly prone to transmetallation. On the other hand, alkyl trifluoroborates, which reluctantly transmetallate, fail to react altogether. Such obstacles will be challenging to overcome without approaching the problem from this mechanistic standpoint.

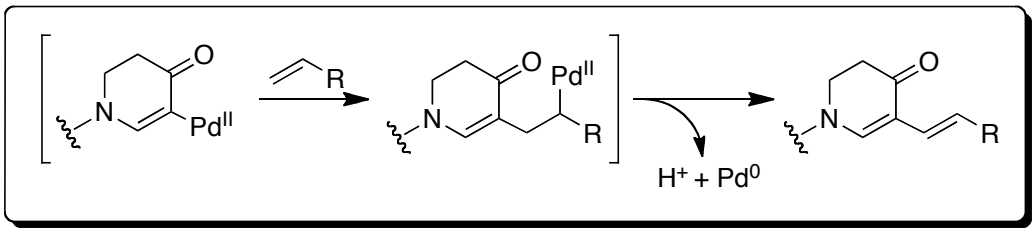

Fig. 3–12. Mechanism of Pd(II)-catalyzed olefination.

One potential solution to this problem is to use coupling partners that are not susceptible to dimerization—those that do not undergo transmetallation, for instance. In this regard, we envisioned a Heck-type modification as an apt extension. Akin to our optimized arylation, this reaction would depend on initial enaminone palladation to generate a σ-bonded Pd-enaminone complex. The subsequent steps would be identical to the classical Heck-Mizokori reaction, involving migratory insertion of an alkene substrate followed by β-hydride elimination (Fig. 3–12). We tested the feasibility of this reaction by replacing our trifluoroborate coupling partner with methylacrylate under our optimized conditions (Scheme 3–7). Even though this olefination was slower than the arylation, we were able to isolate enaminone **3.25** in 62% yield. This is clearly a promising approach to prepare the previously

inaccessible C3-alkenyl enaminones. Furthermore, without the competing transmetallation process, enaminones that are less prone to palladation could be still be used. This has been borne out in subsequent studies by Yiyun Yu in our laboratory.

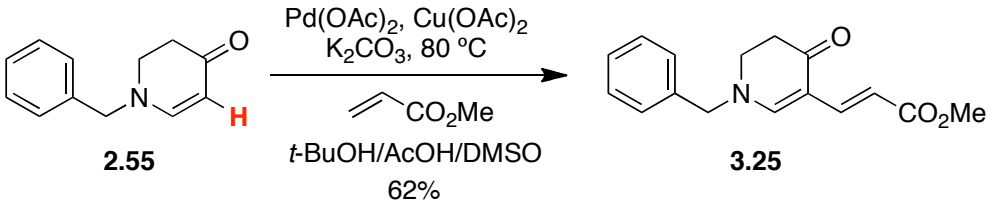

Scheme 3–7. Direct C–H olefination of enaminone.

The Heck-variation of this reaction is a limited solution to the problem, because only alkenes can be used as coupling partners. If this strategy is to be applied to preparing phenanthropiperidines from less reactive enaminones, aryl groups must also be accommodated. There is much precedent from the literature that suggests arylhalides could be used for this purpose.[299] In a strikingly relevant example reported by Pelletier, Larivée and Charette, cyclic enamines were coupled with aryl iodides using a Pd(0)-catalyst (Scheme 3–8).[312] This strategy not only minimizes the likelihood of aryl homocoupling but also eliminates the need for a reoxidant. As such, this approach holds great promise to expand the substrate scope of enaminone C–H functionalization reactions.

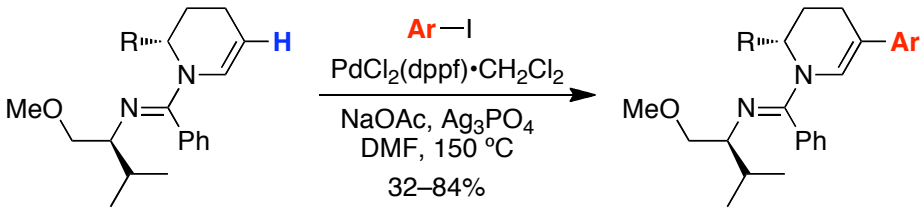

Scheme 3–8. Direct Pd(0)-catalyzed arylation of cyclic enamines by Pelletier *et al*.[312]

3.10 Summary

In summary, this methodology provides a direct route for the construction of 3-arylpiperidine scaffolds, a privileged structure and prevalent motif in many natural products. Although the substrate scope of this reaction is somewhat limited, this work provides a foundation for future efforts to broaden it. This method is a significant advance over the existing two-step method. Also, this reaction is the first example of C–H functionalization on enaminones (a *non-aromatic* enamine system) and contributes to the rapid accretion of viable C–H donors. Most importantly, the ultimate goal of this work—to synthesize 3-arylenaminones as intermediates to phenanthropiperidines—has been met. What remains is the utilization of these structures for phenanthropiperidine synthesis.

CHAPTER 4

SYNTHESIS OF (+)-ANTOFINE AND (+)-IPALBIDINE

4.1 Introduction

The value of synthetic methodologies is often tentative until they validated through practical applications. Hitherto, this work has described the development of two reactions that have been designed to facilitate the preparation of phenanthropiperidine alkaloids, but now we will turn to how these methods can be utilized. In Chapter 2, we discussed the development of a method that gives ready access to a variety of cyclic enaminones (**A**, Scheme 4–1), including indolizidine and quinolizidine scaffolds. In Chapter 3, we showed how these scaffolds could be elaborated through the development of a Pd(II)-catalyzed method that directly functionalizes the C3-position of the enaminone and can be used to install the requisite aryl moiety, which constitutes ring C of the phenanthrene system (**A** → **B**). As intended, the amino acids and aryl coupling partners are interchangeable building blocks providing a means for preparing numerous permutations of the 3-arylpiperidine scaffold. Herein, we demonstrate that that these intermediates can be used as precursors to (+)-antofine (**4.2**), a representative phenanthropiperidine, and (+)-ipalbidine (**4.1**), a structurally-related indolizidine alkaloid (Fig. 4–1).

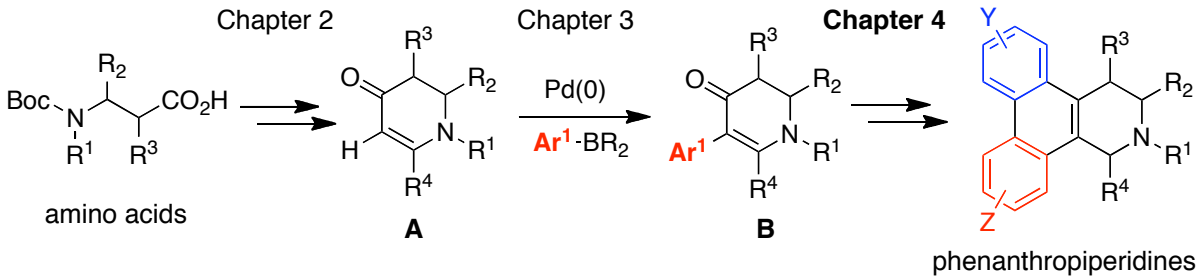

Scheme 4–1. Route to phenanthropiperidines using our developed methods.

These natural products were chosen not only by virtue of their prototypical structure but also for their remarkable biological profiles. (+)-Ipalbidine (**4.1**) is a non-addictive analgesic, an oxygen free-radical scavenger, and has demonstrated inhibitory effects on the respiratory burst of leukocytes.[313-315] (–)-Antofine, on the other hand, exhibits low nanomolar cytotoxic activity (IC_{50}) in drug-sensitive and MDR cancer cell lines alike, already being described in Chapter 1. We chose to prepare the unnatural enantiomer, (+)-antofine (**4.2**), considering that both natural products could be synthesized in a divergent fashion from a late-stage intermediate. Although these natural products have been synthesized before,[142, 158, 316-327, 149, 56, 63, 146, 150, 170-172, 181, 184, 328] our method herein gives access to these molecules in a exceptionally concise and high-yielding manner.

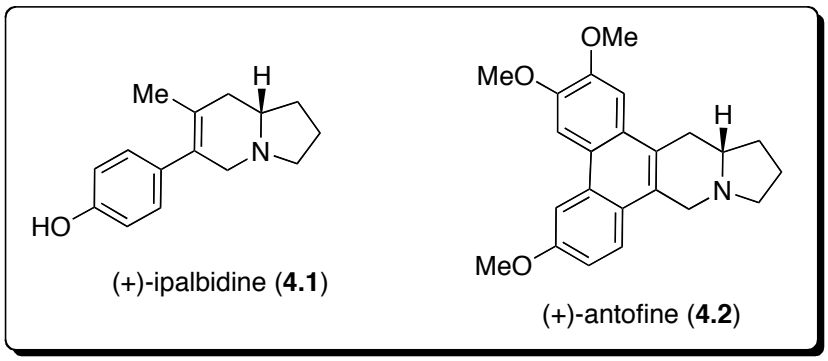

Fig. 4–1. Structures of (+)-ipalbidine and (+)-antofine.

4.2 Total synthesis of (+)-ipalbidine

Despite being addressed at this point in this work, our efforts to synthesize (+)-ipalbidine predate the full development of our ynone cyclization and direct-arylation protocols that have been already described in depth. In fact, it was not until our total synthesis of (+)-ipalbidine was complete that we discovered that the indolizidine stereocenter had partially racemized. The details of this discovery and our work to suppress what was later discovered to be an acid-mediated process was discussed in Chapter 2. Our seminal work on (+)-ipalbidine also involved pre-activating the enaminone prior to installing the C3-aryl moiety, which was greatly improved upon the discovery and development of a direct-arylation method (see Chapter 3). In order to contrast the old with the new routes, the evolution of our synthetic strategy to (+)-ipalbidine will be discussed in detail.

4.2.1 First attempt to synthesize (+)-ipalbidine

Starting with Boc-L-proline, Weinreb amide **2.2** was prepared in three steps (Scheme 4–2). The amino acid was homologated using a standard Arndt-Eistert reaction, first converting the acid into diazoketone **4.3** and then catalyzing the Wolff rearrangement with CF_3CO_2Ag. When using H_2O as a solvent during the rearrangement, Boc-L-β-homoproline (**4.4**) was obtained in 49% yield over two steps along with 26% of unreacted starting material. Though the acid could be converted into the desired Weinreb amide **2.2** using a high-yielding EDCI

coupling, the difficulty of separating the two homologues following the Arndt-Eistert protocol inspired us to look for improvements.

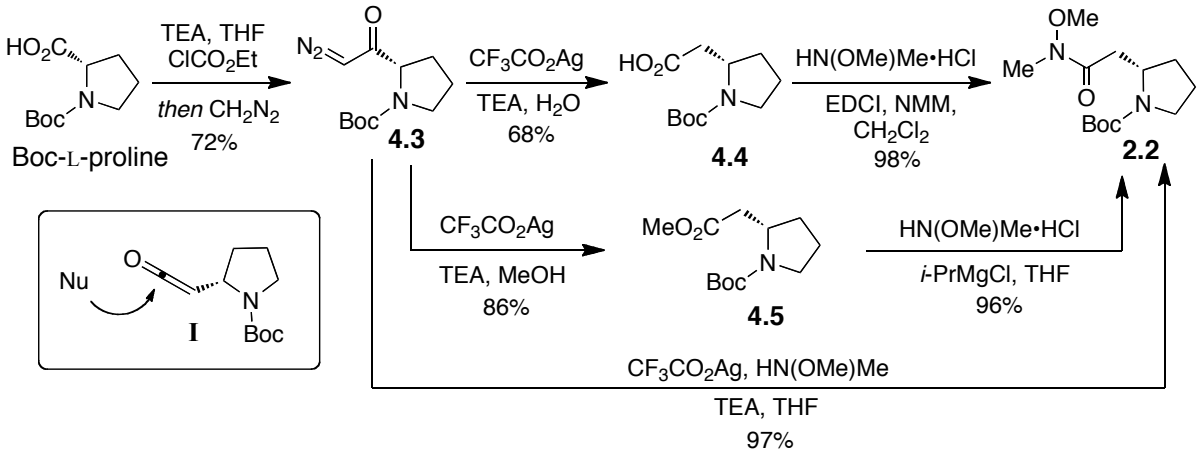

Scheme 4–2. Preparation of Weinreb amide.

Realizing that the acid functional group was contributing to poor chromatographic separation, we switched solvents during the Wolff rearrangement to MeOH in order to obtain a more tractable methyl ester. We were pleased to find that using MeOH was beneficial, not only because it facilitated purification, but also because it improved the yield. Weinreb amide **2.2** could then be prepared from methyl ester **4.5** using an easily scalable protocol reported by Williams *et al*.[279] This approach served us well in the preparation of multi-gram quantities of the Weinreb amide, but our constant search for shorter reaction sequences led us to a even shorter route. It occurred to us that if acids and esters could be prepared from the addition of oxygen nucleophiles into ketene intermediate (**I**, Scheme 4–2), then amides could also be prepared using nitrogen nucleophiles. To test this, we carried out the rearrangement

in a non-nucleophilic solvent (THF) and added freshly distilled *N*,*O*-dimethylhydroxylamine. The reaction was successful, and the product (**2.2**) was isolated in 97%.

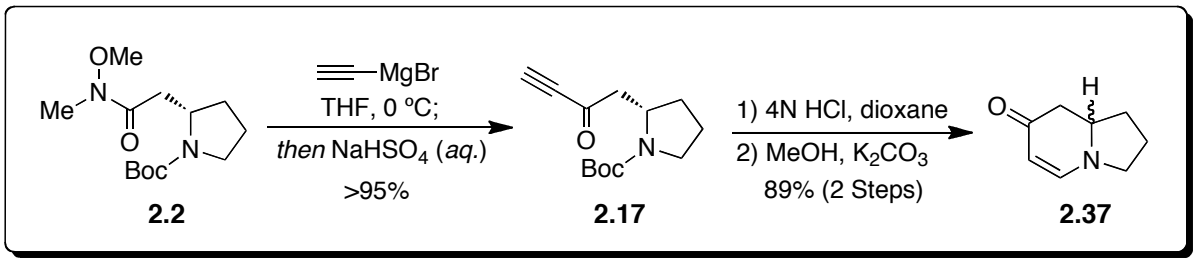

Scheme 4–3. Synthesis of indolizidine enaminone from Weinreb amide.

Next, we prepared ynone **2.17** by adding excess ethynylmagnesium bromide to amide **2.2** at 0 ºC (Scheme 4–3). The outcome of this reaction was highly dependent on the quality of the Grignard reagent and on the work-up method. The reaction was typically quenched with a weak acid, since the Boc-protecting group could decompose in strong acids. The acid also served to sequester the nucleophilic *N*,*O*-dimethylhyrdroxylamine byproduct as an ammonium salt in order to prevent it from adding into the ynone.[329] Hence, when the reaction was deemed complete, aqueous $NaHSO_4$ was added and the reaction stirred for 1 h. This method consistently provided the ynone product in greater than 95% yield.

From ynone **2.17**, enaminone **2.37** was prepared upon stepwise treatment with 4N HCl in dioxane and methanolic K_2CO_3, the details of which were discussed in Chapter 2. At the time, unbeknownst to us, the stereocenter had racemized during the deprotection step. This was not obvious at the time, since the product had a high optical rotation value ($[\alpha]_D = -190$) and no standard to compare it to. Furthermore, despite numerous attempts, we were unable to analytically separate the enantiomers using chiral HPLC.

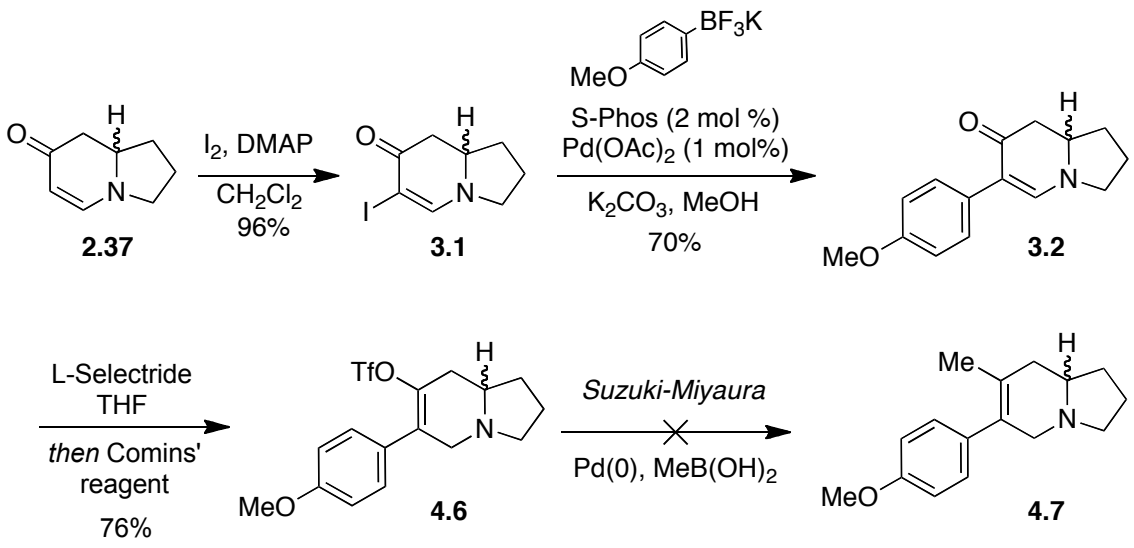

Scheme 4–4. First approach to (+)-ipalbidine.

Unaware of its low enantiomeric purity, we subjected enaminone **2.37** to I_2 in the presence of DMAP, to afford iodoenaminone **3.8** (Scheme 4–4). The *p*-methoxyphenyl group was installed next using a Buchwald modification of the Suzuki-Miyaura reaction (see Chapter 3).[291] To install the methyl substituent in the place of carbonyl group we first investigated a Pd-catalyzed cross-coupling approach. This involved the preparation of triflate **4.6**, which could be achieved using L-Selectride to mediate 1,4-reduction and trapping the resulting enolate with Comins' reagent as an triflate source. We attempted a number of Suzuki-Miyaura protocols to couple the methyl group to the indolizidine scaffold, but they were unsuccessful, providing low yields of difficult-to-purify product.

4.2.2 Second approach to (+)-ipalbidine

Turning to our second approach, enaminone **3.2** was once more reduced in a 1,4-fashion with L-Selectride, only this time, without subsequent treatment with Comins' reagent, and

ketone **4.8** was isolated. Methyl lithium was then added to the ketone to furnish tertiary alcohol **4.9**. Our initial attempts to dehydrate indolizidine **4.7** were unsuccessful. We had initial concerns that multiple olefin isomers would be obtained and be difficult to separate but hypothesized that the desired isomer would be the most stable—being a tetra-substituted olefin and conjugated with the phenyl group—and that the unwanted isomers could be channeled to the desired product under thermodynamic conditions. This rational also inspired us to prepare indolizidine **4.7** from a methenylation reaction of ketone **4.8** with Tebbe reagent and subsequent isomerization; unfortunately, we could not obtain sufficient quantities of indolizidine **4.10**.

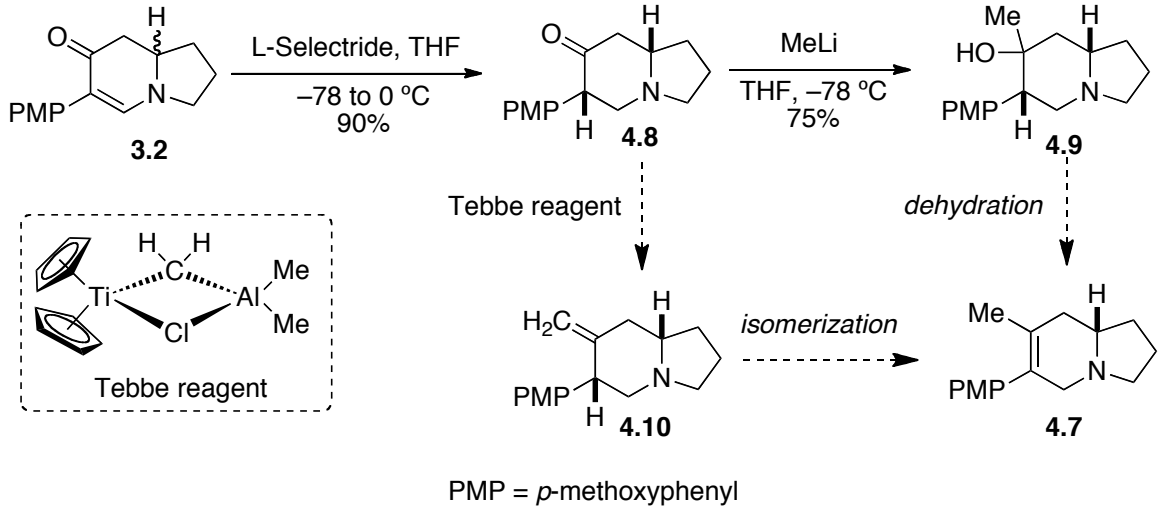

Scheme 4–5. Second approach to prepare (+)-ipalbidine.

Returning to tertiary alcohol **4.9**, we explored several conventional methods to dehydrate alcohols (Table 4–1). From of the methods tried, neat $POCl_3$ and $SOCl_2$ (entries 3 and 6) in pyridine showed promising results with $SOCl_2$ being the best. Observing that this reaction

was complete in less than 30 minutes and that degradation was causing a significant loss in yield, the reaction was: (1) diluted with THF, (2) run at lower temperatures (–30 to –10 ºC) and (3) run with only a slight excess of $SOCl_2$ and pyridine (entries 7 and 8). These modifications dramatically improved the outcome of the reaction, providing 88% of the product. From product **4.7**, we could prepare (+)-ipalbidine (**4.1**) by removing the *O*-methyl group with BBr_3 (Scheme 4–6).

Table 4–1. Optimization of dehydration conditions.

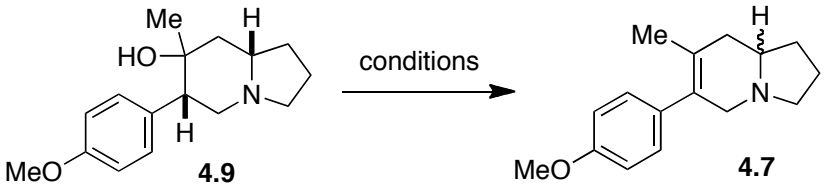

entry	conditions	yield (%)[a]
1	I_2, PPh_3, CH_2Cl_2, 16 h	NR
2	BF_3•OEt_2, CH_2Cl_2, 16 h	NR
3	$POCl_3$, pyridine	30
4	TsOH, AcOH, reflux	NR
5	TsOH, PhMe, reflux	NR
6	$SOCl_2$, pyridine, rt	52
7	$SOCl_2$ (5 equiv), pyridine (5 equiv), THF, –30 ºC to rt	78
8	$SOCl_2$ (2.5 equiv), pyridine (5 equiv), THF, –30 to –10 ºC	88

NR = no reaction (*i.e.* starting material was recovered). [a] Isolated yield.

It was at this point that we realized that the natural product was not enantiomerically pure. The optical rotation was significantly lower than reported values. Fortunately, ipalbidine's enantiomers were easily resolved using chiral HPLC, which showed that we had obtained the natural product with an e.r of 70:30. As already discussed, the root cause of

racemization was a *retro*-Michael/Michael process that had occurred during the acidic deprotection step of the ynone cyclization reaction. This was remedied by using HCO_2H, a much weaker acid, to deprotect the Boc-group, and NaI to activate the ynone prior to cyclization. These conditions virtually eliminated the racemization and the enaminone could be prepared in a high enantiomeric purity. Several other modifications of this third approach, which improve the yields and shorten the entire sequence, deserve further attention.

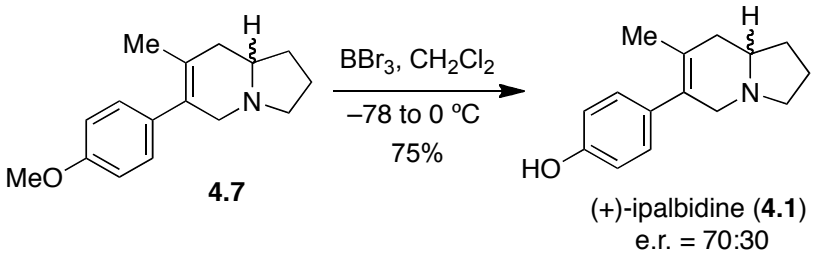

Scheme 4–6. Final reaction to prepare (+)-ipalbidine.

4.2.3 Third approach to (+)-ipalbidine

A third approach to synthesize (+)-ipalbidine was devised to enhance the enaniomeric purity of the final product and also to take advantage of recently developed methods to improve the reaction sequence as a whole (Scheme 4–7). After resynthesizing enaminone **2.37** with our mild cyclization conditions, we used our just-developed Pd(II)-chemistry to bypass the iodination reaction and prepared the intermediate **3.2** in a single step. We were also able to abridge the final sequence by reverting back to triflate intermediate **4.6**. Previously, we had had little success installing the methyl group with the Suzuki-Miyaura protocol using this triflate. This was, presumably, due to the steric demand of the a tetra-substituted olefin. To compensate for this, the Negishi reaction, which has an outstanding

reputation in alkyl cross-couplings, was used instead. The methyl zincate was prepared immediately beforehand from methylmagnesium bromide and $ZnBr_2$ (not shown). This reagent was added to triflate **4.6** and $Pd(PPh_3)_4$, and in 4 h at 60 ºC the product was isolated in 91% yield. (+)-Ipalbidine (**4.1**) was once again completed upon removal of the *O*-methyl group, and the enantiomeric ratio was identical to the enaminone it was derived from (e.r. = 98:2).

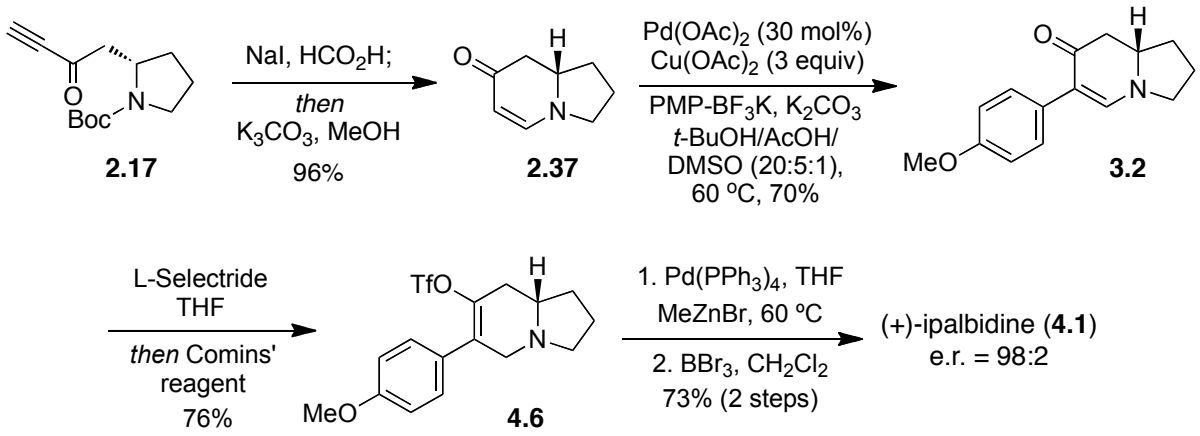

Scheme 4–7. Racemization-free approach to (+)-ipalbidine.

4.3 Total synthesis of (+)-antofine

Our featured route was employed to synthesize (+)-antofine (**4.2**) as well (Scheme 4–8). Fortuitously, this phenanthropiperidine, which is among the most potent in its class, can be accessed from the same triflate intermediate (**4.6**) used to prepare (+)-ipalbidine. With previous success using the Negishi protocol, we attempted to install the necessary aryl group using the same method. The zinc reagent was prepared from a lithium-halogen exchange reaction of 4-bromoveratrole and *t*-BuLi and a subsequent quench with $ZnBr_2$. The aryl

zincate was then coupled with triflate **4.6** using the same conditions as before to furnish seco-antofine in 96% yield. Finally, a PIFA-mediated biaryl coupling yielded (+)-antofine (**4.2**), which exhibited optical activity that matched those reported in the literature.[149, 171, 184, 326]

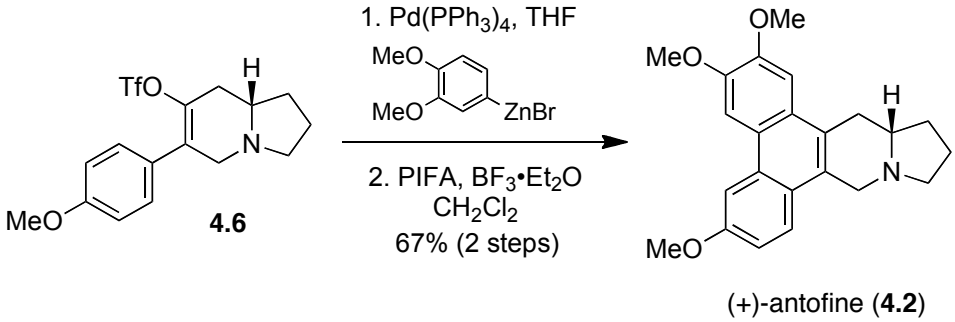

Scheme 4–8. Synthesis of (+)-antofine from triflate **4.6**.

4.4 Summary

Aided by our new approach to arylated cyclic enaminones, the syntheses of (+)-ipalbidine (**4.1**) and (+)-antofine (**4.2**) can be accomplished in a remarkably concise fashion. Moreover, both of the natural product's were obtained in high yield and enantiomeric purity. By these total syntheses, the utility of two methodologies are exemplified. Specifically, we have shown that cyclic enaminones can be efficiently prepared from the chiral pool and directly functionalized to provide versatile intermediates that can be applied to the synthesis of complex molecules which, in this case, are of medicinal interest.

These syntheses can be considered a proof-of-concept. Although they have been validated in a sense, their design was intended to facilitate the production of a library of phenanthropiperidines, not just one. Nevertheless, the two methods, which were developed along the way to these natural products, are a contribution to the rapidly growing arsenal of

organic reactions. The sheer simplicity of the cyclic enaminone and the prevalence of the piperidine and 3-arylpiperidine systems suggest that these reactions will be broadly applicable. Our purposes herein are more focused and, therefore, we will now turn to the preparation of phenanthropiperidine analogs.

CHAPTER 5

SYNTHESIS AN BIOLOGICAL EVALUATION OF (*R*)-TYLOCREBRINE AND RELATED ANALOGS

5.1 Introduction

The phenanthropiperidines are being intensely pursued as drug leads, primarily for the treatment of cancer but also for inflammatory conditions, such as arthritis. Although select members of this class are exhibit promising therapeutic potential, there is concern that they may also possess undesired neurological activity. This concern arises from the failed clinical trial of tylocrebrine (**1.4**), the only member of this class to be tested in humans. Considering the highly-conserved structural features across this class, there is reason to speculate that other phenanthropiperidines are also neurologically active. The molecular basis for tylocrebrine's side-effects has not been investigated, nor has the neurological effects of other phenanthropiperidine drug leads. Hence, in order to guide our design of phenanthropiperidine analogs, we have begun to study the CNS activity of tylocrebrine and its related analogs. Herein, we report the synthesis and initial biological studies of tylocrebrine and some closely related analogs to better understand the neurological liabilities of these alkaloids.

5.2 Possible mechanisms for neurological effects

The complete absence of neurological data for the phenanthropiperdines, besides a brief reference to tylocrebrine's clinical trial,[2] makes our search extraordinarily difficult. Suffness reported that the patients who were administered the alkaloid experienced "disorientation and ataxia" (ataxia being a motor-neurological condition defined as the loss of coordination).[2] Unfortunately, no other data is available. Presumably, more detailed descriptions, such as dosage, mode of administration and alkaloid source, were recorded at the time of the clinical trials, but this data could not be obtained even after correspondence with the NCI. Without this data, we simply concluded that tylocrebrine—in some manner—affects motor centers in the CNS. Although this does not lead us to a molecular target, it does provide a direction for our investigations.

Since little is known of the nature of tylocrebrine's neurological effects or, for that matter, of its pharmacology in general, one cannot rule out the possibility that these two effects are inseparable (*i.e.* the mechanism of tylocrebrine's anti-proliferative effects is the same as that of its neurological effects). For this scenario, it would be necessary to characterize the peripheral and central effects in order to assess the feasibility of designing safer phenanthropiperidines. If both peripheral and central effects were equally severe, this would bring the therapeutic potential of these alkaloids into question. On the other hand, if the side-effects were primarily induced by CNS interactions, a promising strategy would be to prevent BBB permeation. Nothing suggests, however, that these alkaloids are exerting their CNS and anti-cancer effects through the same target(s).

In the event that the CNS and anti-cancer mechanisms can be differentiated, different strategies could be used. The most obvious one would involve the design of analogs that have greater selectivity for their therapeutic target. The challenge of this approach lies in the difficulty of assessing CNS interactions with adequate throughput. Identifying the specific target(s) responsible for the neurological effects would be highly valuable to this enterprise by providing a means to test synthetic leads *in vitro*. One advantage of this approach is that it is would not be necessary to identify the therapeutic target given that anti-proliferative cell-based assays are relatively high-throughput already. If the therapeutic target and off-target cannot be differentiated based on binding affinities or functional activity, they can perhaps be differentiated based on location. In other words, if the target(s) responsible for the side-effects is localized within the CNS or is only implicated therein, designing analogs that do not cross the BBB could address this.

This latter approach, however, comes with a caveat: namely, that tumors bounded by the BBB will be unaffected. Although this limitation is common to many anti-cancer agents and would not be reason to discontinue development, it is one that, if possible, should be avoided. The treatment of cancers within the CNS is immensely challenging, primarily because of the difficulty of designing active agents that reach tumors within the BBB.[330] With tylocrebrine, however, the challenge is on another front. Tylocrebrine is extremely potent and evidently reaches the CNS already. Thus, the remaining obstacle is to impart neurological selectivity in order to tune-out unwanted side-effects. Although this may also be difficult to achieve, it has yet to be attempted.

Designing phenanthropiperidines that do not cross the BBB is more straightforward than designing analogs that do not interact with specific targets. As described in Chapter 1, CNS

exposure has been linked to specific physicochemical parameters that can be adjusted to help or hinder BBB-permeation.[132] These parameters are essentially descriptors of lipophilicity (*i.e*. cLogP, polar surface area, H-bond donors and cLogD). When these properties are taken into account, it not surprising that tylocrebrine, which is highly lipophilic, passes through the BBB. In this regard, this approach should be directed towards increasing the polarity (or hydrophilicity) of the phenanthropiperidines in a manner that does not affect their activity. Incidentally, imparting the physicochemical properties that hinder BBB-permeation will also improve the water solubility, which is another advantage of this approach (concerns about the limited solubility of these alkaloids are discussed in Chapter 1). From what is already known about the SAR of this class, several positions on the phenanthropiperidine scaffold are promising for introducing polar functional groups (Fig. 5–1). The C3-, C6- and C14-positions, for instance, are relatively insensitive to derivatization and could be used to install polarizing groups. Furthermore, ring E (C11–13) is virtually unexplored and may also provide additional points of functionalization.

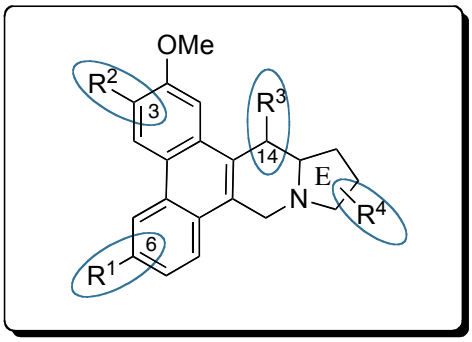

Fig. 5–1. Promising sites for derivatization.

The design of non-BBB–penetrating analogs has the luxury being possible without a precise mechanistic understanding of the neurological effects. A more challenging strategy, however, is to design analogs which are neurologically inert yet retain the anti-proliferative effects of the parent alkaloids. We have chosen to pursue this route for the potential it has to treat tumors of the CNS. In order to determine the viability of this approach, we set out to elucidate the mechanism for tylocrebrine's side-effects to assure that they can be separated from its anti-proliferative effects. Before this search commenced, the alkaloid would need to be obtained. It is crucial that tylocrebrine—not other phenanthropiperidines—be studied since it is the only alkaloid with demonstrated neurological effects in humans. Thus, attaining sufficient quantities of tylocrebrine was our first goal.

5.3 Synthesis of tylocrebrine and analogs

To date, the only synthetic strategy that has been used to prepare tylocrebrine relies on the isolation of the minor regioisomer (17%) of an unselective Pschorr coupling protocol, which furnishes the tetramethoxyphenanthrene system (Scheme 1–8). This synthesis provides less than 1% of racemic tylocrebrine over ten steps.[146] Thus, we envisioned the development of a new synthetic route to provide a sustainable source of tylocrebrine and, importantly, to provide it in enantiomerically pure form.

In Chapter 4, the synthesis of (+)-antofine was described in which we successfully employed our newly developed methodologies. In relation to previous phenanthropiperidine syntheses (see Chapter 1), our approach was unique except for the final step (*i.e.* the oxidative biaryl coupling). Although the biaryl coupling method is atom economic and

presumably versatile with respect to the aryl substituents, the accessibility of certain phenthrene regioisomers is limited. Free rotation around the aryl-alkene bond makes possible the formation of multiple regioisomers. In our synthesis of antofine, for example, there was a possibility of forming two regioisomers (Scheme 5–1). The major product (**IV**) of these reactions is predictable when considering the steric interactions that arise from rotation of the arene (**I** ⇋ **II**). Hence, the oxidative biaryl coupling approach limits the accessibility of phenanthrenes with C4- or C5-substituents, because bulky substituents in these positions introduce a significant amount of strain. Indeed, the 1,4-strain energy between the C4- and C5-hydrogens in *unsubstituted* phenanthrene amounts to 5–6 kJ/mol.[331, 332]

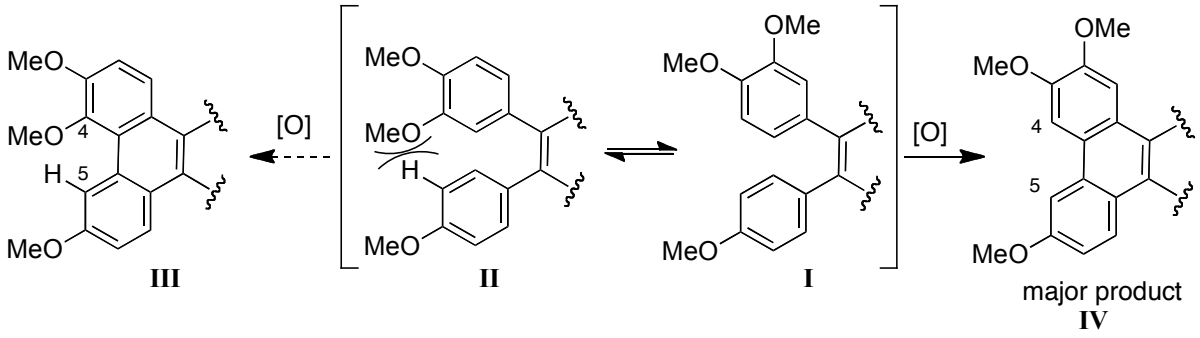

Scheme 5–1. Regioisomer formation in biaryl coupling reaction.

This synthetic limitation explains the absence of strategies to prepare tylocrebrine (**1.4**), which bears a C5-methoxy group, despite it being one of the most well-studied members in this class. Considering the shortcomings of the biaryl coupling approach and inaccessibility of certain phenanthrene substitution patterns, it is surprising that these obstacles are largely unconquered. Because our biological studies were dependent on the availability of

tylocrebrine, we had to devise a new strategy allowing construction of C5-substituted phenanthrenes.

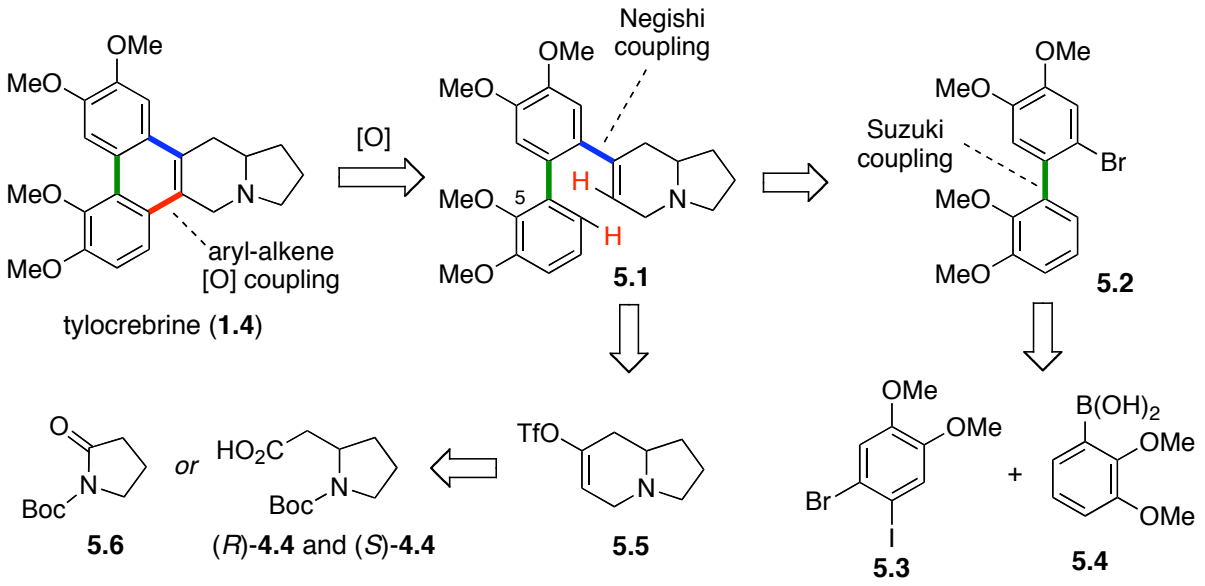

Scheme 5–2. Retrosynthetic analysis of tylocrebrine.

Our synthetic plan involved three sequential C–C bond forming steps (Scheme 5–2). The key step would be the final ring-closure proceeding through an aryl-alkene oxidative coupling. Unlike, the standard biaryl-coupling approach, this disconnection imposes regioselective control by exploiting the once-problematic methoxy substituent to block coupling at the C5-position. The requisite precusor **5.1**, in turn, could be derived from a Negishi reaction of a organozincate prepared from biphenyl bromide **5.2** and triflate **5.5**. The biaryl bond (shown in green) could be prepared from a halogen-selective Suzuki reaction from a commercially available boronic acid **5.4** and reported veratrole derivative **5.3**.[149] Using our method to prepare 6-membered enaminones, the indolizidine core can be prepared from Boc-L-β-homproline. Alternatively, to access the racemic indolizidine core we

envisioned starting with *N*-Boc-pyrrolidinone (**5.6**). Once the enaminone functionality was realized, the indolizidine enaminone could be converted into triflate **5.5** in preparation for the Negishi protocol.

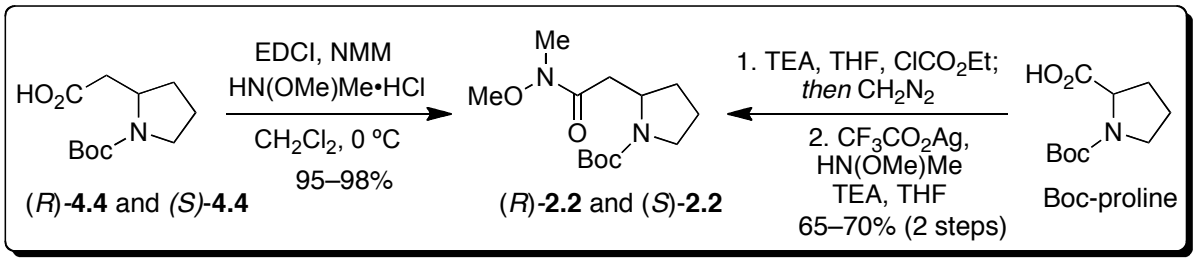

Scheme 5–3. Synthesis of (*R*) and (*S*)-Weinreb amide.

First looking to the indolizidine fragment, we began our synthesis with Boc-D-β-homoproline and Boc-L-β-homoproline, which were to be carried through in parallel (Scheme 5–3). Although each enantiomer of amide **2.2** could be formed directly using an EDCI coupling, the two-step homologation procedure (discussed in Chapter 4) was used as an economic alternative (Boc-D-β-homoproline > $300/g). Nevertheless, the use of large quantities of diazomethane during homologation is still a drawback.

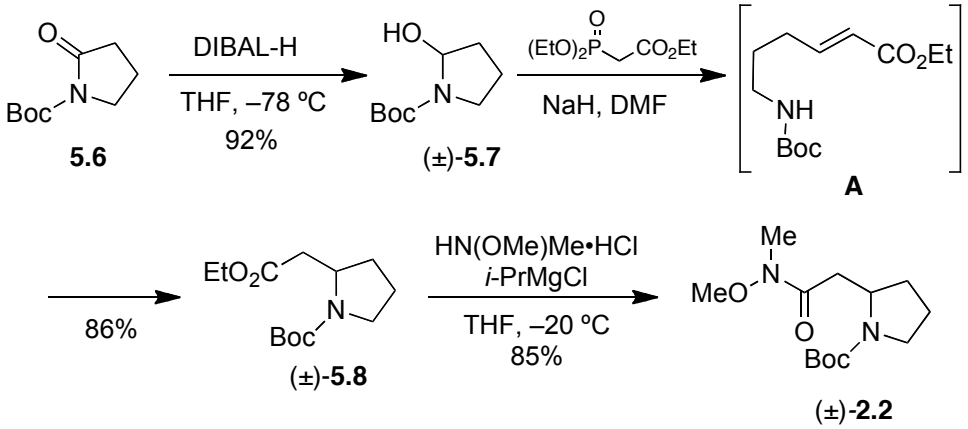

Scheme 5–4. Synthesis of racemic Weinreb amide **2.2**.

Considering the amenability of this synthesis to diversification, and thereby library development, we thought that the synthesis of racemic precursors would also be of value, particularly if they could be obtained in large quantities. Thus, an alternative approach was devised for the synthesis of racemic Weinreb amide **2.2** (Scheme 5–4). In this approach, Boc-pyrrolidinone (**5.6**) was reduced to hemiaminal **5.7** with DIBAL-H and then subjected to Horner-Wadsworth-Emmons conditions in which the putative ring-opened intermediate **A** spontaneously cyclized to provide the β-proline derivative **5.8**. Racemic amide **2.2** could then be directly obtained from ester **5.8** using conditions reported by Williams *et al*.[279] Although this sequence includes a greater number of steps compared with the enantiospecific synthesis, the payoff is the ease and cost of scale-up. Moreover, it avoids the use of large quantities of hazardous diazomethane which would otherwise be necessary to prepare multi-gram quantities of the desired intermediates.

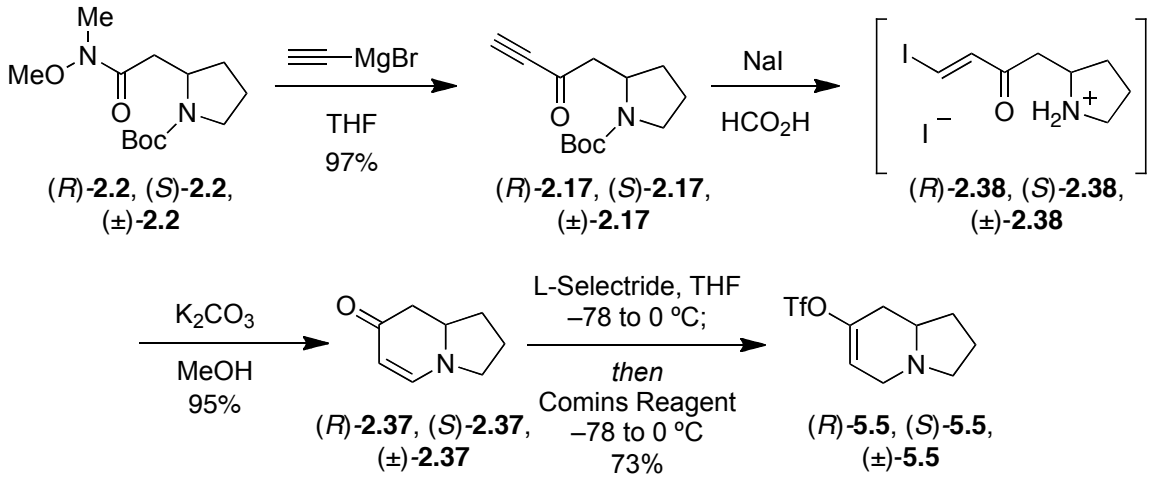

Scheme 5–5. Synthesis of indolizidine triflate **5.5**.

Constructing the indolizidine fragment was our next goal. Grignard addition of ethynylmagnesium bromide to Weinreb amide **2.2** provided the desired ynone **2.17** in excellent yield (Scheme 5–5). Indolizidine formation could be achieved using our one-pot deprotection/cyclization strategy. Either 4N HCl in dioxane or NaI in HCO_2H can be used for Boc-deprotection. Although the yields of the latter conditions (NaI/HCO_2H) were generally higher, work-up following the cyclization was easier when using the HCl-deprotection method. It should be recalled, however, that the use of 4N HCl promotes *retro*-Michael/Michael-type racemization of the β-stereocenter and could not be used for constructing non-racemic indolizidine **2.37**. With the indolizidine core assembled, the triflate moiety was installed using a 1,4-reduction and enolate trapping with Comins' reagent, providing triflate **5.5**.

Table 5–1. Synthesis of biaryl fragment.

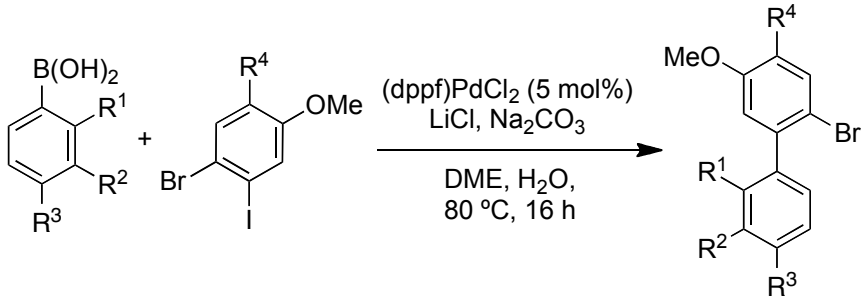

entry	R^1	R^2	R^3	R^4	product	yield (%)
1	OMe	OMe	H	OMe	**5.2**	72
2	H	OMe	OMe	OMe	**5.9**	67
3	OMe	H	H	OMe	**5.10**	77
4	H	OMe	H	OMe	**5.11**	68
5	H	H	OMe	OMe	**5.12**	70
6	H	OMe	OMe	H	**5.13**	70

We next turned to the synthesis of the biaryl fragment. Fürstner and Kennedy have previously reported a straightforward route to biarylbromides that were used for the synthesis of several phenanthropiperidine alkaloids.[149] Although biarenes with *ortho* substituents previously had not been synthesized, the reported conditions showed no impartiality to our hindered boronic acid **5.4** (entry 1, Table 5–1). Notably, this stage of the synthesis is poised for diversification considering the collection of boronic acids available for purchase. Although our primary focus remained on the synthesis of tylocrebrine (**1.4**), we also synthesized biaryl bromides **5.9**–**5.13** which bear the substitution pattern of several other prominent members of this class—tylophorine, antofine and deoxypergularinine (entries 2, 4 and 6)—and two unnatural isomers that have never been synthesized before (entries 3 and 5). Our intent was not only to demonstrate the feasibility of diversification at this point in the synthesis, but, also, to explore the scope of this chemistry and its application for the

construction of C5-unsubstituted analogs—these could potentially form regioisomers in the final aryl-alkene coupling reaction.

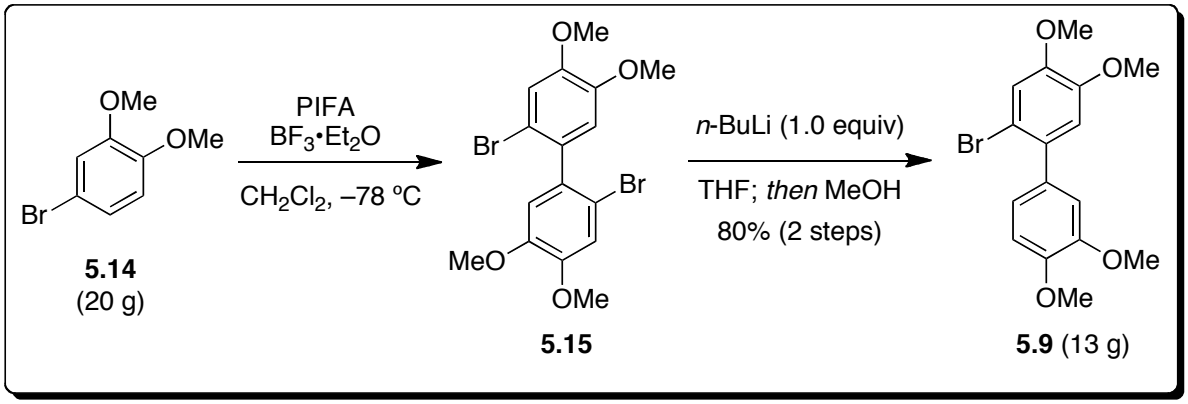

Scheme 5–6. Scalable approach to biaryl bromide **5.9**.

An important consideration for us was the ease of scale-up and cost efficiency. Admittedly, we did not labor over reaction optimization for the Suzuki protocol, in which we had encountered an number of drawbacks (*e.g.* challenges in work-up and purification) when preparing multi-gram quantities of product, but realized that a scalable, Pd-free approach to biarylbromide **5.9** was possible (Scheme 5–6). This could be achieved through a PIFA-mediated dimerization of 4-bromoveratrole (**5.14**). The resultant dibromide **5.15** was desymmetrized upon treatment with one equivalent of *n*-BuLi and a subsequent MeOH quench. Both steps could be carried out in 20 g batches and, conveniently, without the use of column chromatography providing 13 g of product (80% yield over two steps).

Having had previous success with Negishi cross-couplings of sterically-encumbered triflates, we employed analogous conditions to install the biaryl moiety using the appropriate coupling partner. The zincate **5.16** was prepared from biaryl bromide **5.2** via sequential treatment with *t*-BuLi and $ZnBr_2$. The exact conditions as used before were first employed

for the cross-coupling. Using this protocol, the reaction was complete in 30 min. Because this reaction was so rapid, we reduced the reaction temperature from 60 ºC to room temperature and decreased the catalyst loading to 2 mol%. We were pleased to find that this cross-coupling proceeded in under an hour to provide near quantitative yields of the desired indolizidine **5.1** (Scheme 5–7).

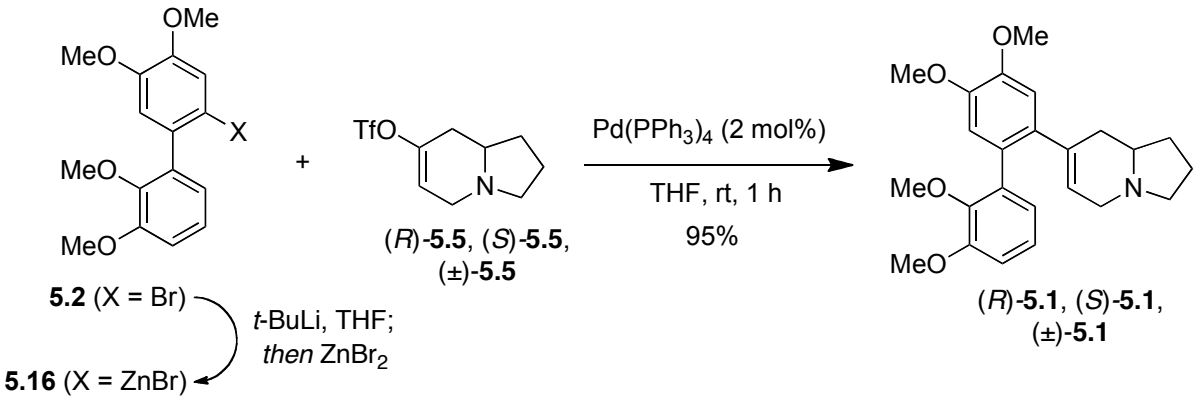

Scheme 5–7. Coupling of indolizidine and biaryl fragments.

Having all the desired carbons in place we could now explore conditions for an oxidative aryl-alkene coupling. To our knowledge there has only been only one report of such a reaction which used $(p\text{-}BrC_6H_4)_3N{\bullet}SbCl_6$.[333] Concerned by this lack of precedent, we undertook a systematic investigation using tylocrebrine precursor **5.1** as a model stubstrate, and reagents that have found success in the related biaryl coupling reaction (Table 5–2). In our first attempt, $(p\text{-}BrC_6H_4)_3N{\bullet}SbCl_6$ left the starting material unperturbed (entry 1). Slightly more success was found under photochemical conditions (entry 2) or when using PIFA (entry 3 and 4); however, substantial amounts of degradation were also observed. We were pleased to find that $FeCl_3$ (entry 5) could induce the desired oxidative coupling with greatly improved yields. The greatest success was found with the use of VOF_3 (entry 7),

which gave the desired product in 62% yield. With the success of this reaction, this method was applied to the both enantiomers of indolizidine **5.1**, marking the first asymmetric synthesis of (*R*)- and (*S*)-tylocrebrine. The natural products were synthesized in 7 linear steps and in up to 39% overall yield from Boc-D-β-homoproline.

Table 5–2. Oxidative aryl-alkene coupling optimization.

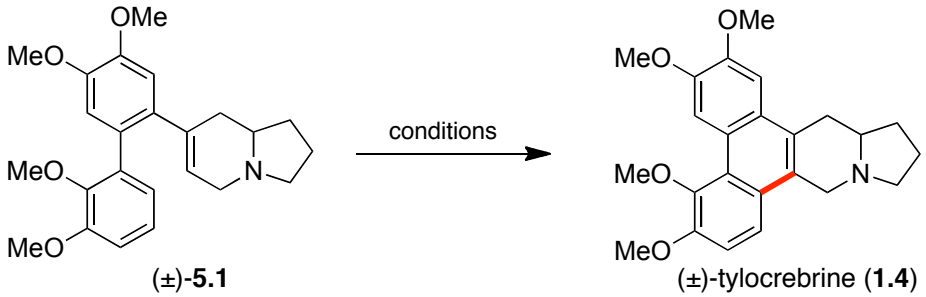

entry	conditions	yield (%)[a]
1	(p-$BrC_6H_4)_3N$•$SbCl_6$ (1.0 equiv), 2,6-lutidine (0.2 equiv), CH_2Cl_2, rt	0[b]
2	I_2 (1.0 equiv), PhMe, hν	7
3	PIFA (2.0 equiv), CH_2Cl_2:TFA (2:1), 0 ºC to rt	10
4	PIFA (2.0 equiv), BF_3•Et_2O, CH_2Cl_2, –40 ºC	11
5	$FeCl_3$ (6.0 equiv), $MeNO_2$, CH_2Cl_2, rt	44
6	$VOCl_3$ (1.1 equiv), CH_2Cl_2, rt	decomp.
7	VOF_3 (4.0 equiv), CH_2Cl_2, EtOAc, TFA, TFAA, –78 to –15 ºC, 4 h	70 (62)[c]

[a] NMR yield using $MeSiPh_3$ as an internal standard. [b] Recovered starting material. [c] Isolated yield.

In hopes that this methodology would be applicable to more than tyocrebrine, we also attempted the synthesis of various analogs with varying methoxy substitution patterns. Each of the biaryl bromide analogs (**5.9**–**5.13**) were coupled with racemic triflate **5.5** using the modified Negishi protocol that was used to prepared indolizidine **5.1** (Table 5–3). The yields

of these reactions were comparable and, except for compound **5.20**, the indolizidine products were isolated in 95% yield or greater. The lower yield for compound **5.20** is probably not an accurate reflection of reactivity but more likely resulted from an experimental oversight. Having obtained these phenanthropiperidine precursors, we next turned to the final oxidative coupling.

We were initially concerned that when the C5-methoxy group was not present (R^1 = H, Table 5–3), this would introduce the possibility of producing multiple regioisomeric products. Fortunately, these reactions proceeded in excellent yields, providing phenanthropiperidines **5.23**–**5.26** with no observable regioisomer formation. Notably, the reaction yields were significantly higher without the C5-methoxy group (R^1 = H) than with it (R^1 = OMe), showing that the C5-substituent is not essential and may even retard the progression of this reaction. Indeed, the oxidative coupling of indolizidines **5.18**–**5.21** were complete in 1 h—compared with 4 h for tylocrebrine precursor **5.1**—and did not require warming above –78 ºC. Conversely, coupling of indolizidine **5.17** was slow and accompanied by numerous side-reactions that left less than 30% of the isolable product. Notwithstanding the poor yields of this reaction, all of the products were isolated in sufficient quantities to begin an investigation of tylocrebrine's neurological target. Each analog was prepared in only racemic form, whereas racemic, (*R*)- and (*S*)-tylocrebrine were synthesized. This route is an improvement over previous routes, being shorter, higher yielding and allowing the synthesis of both enantiomers and previously inaccessible phenanthrene substitution patterns.

Table 5–3. Final two steps to prepare (±)-tylocrebrine and its analogs.

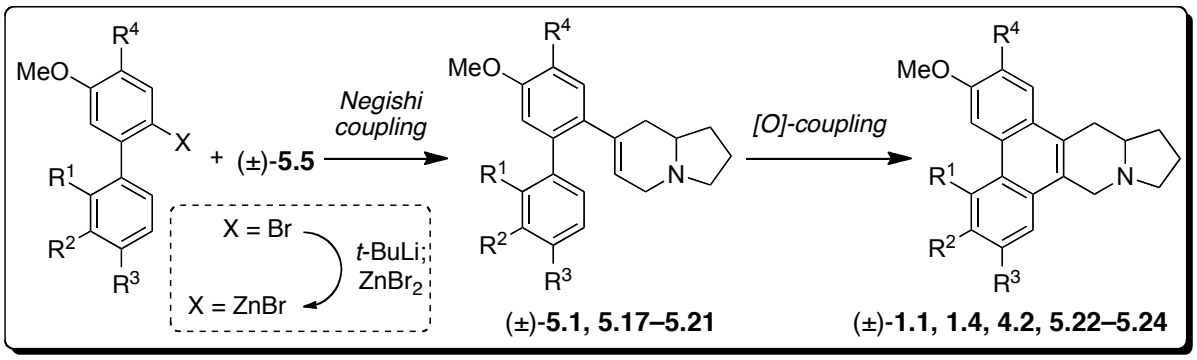

R1	R2	R3	R4	Negishi yield (%)[a]	Negishi product	[O]-Coupling yield (%)[a]	[O]-Coupling product	overall yield (%)[b]
OMe	OMe	H	OMe	95	(±)-**5.1**	62[c]	(±)-**1.4**	**27**
OMe	H	H	OMe	97	(±)-**5.17**	28[c]	(±)-**5.22**	**12**
H	OMe	H	OMe	95	(±)-**5.18**	70	(±)-**4.2**	**30**
H	H	OMe	OMe	98	(±)-**5.19**	85	(±)-**5.23**	**37**
H	OMe	OMe	OMe	70	(±)-**5.20**	68	(±)-**1.1**	**22**
H	OMe	OMe	H	98	(±)-**5.21**	89	(±)-**5.24**	**39**

Conditions: Negishi coupling, $Pd(PPh_3)_4$ (2 mol%), THF, rt, 1 h; [O]-coupling, VOF_3, TFA, TFAA, CH_2Cl_2, EtOAc, –78 ºC. [a] Isolated yield. [b] Yield over 8 steps from *N*-Boc-pyrrolidinone [c] Required warming to 0 ºC.

5.4 Biological studies of tylocrebrine and related analogs

5.4.1 Cancer

With six phenanthropiperidine analogs in hand, including tylocrebrine, we began our investigation of their neurological activity in search of "CNS-safe" analogs. The first task was to assess the anti-cancer properties of each compound so that we could eventually determine if the therapeutic effect could be separated from the undesired effects. We chose three human tumor cell lines for our initial studies: MCF-7, COLO-205 and NCI/ADR-RES.

Using the alamarBlue® assay to measure cell proliferation, each analog assessed in the select tumor cell lines. As expected, most of the analogs exhibited potent growth inhibition in each cell line. Unfortunately, exact GI_{50} values could not be obtained for several analogs since lowest concentration used resulted in almost complete growth inhibition. For these analogs we have indicated that their GI_{50} is less than the lowest concentration used (*i.e.* 3.1 nM). Although this data does not lend itself to ranking each compound in order of its activity, it does give valuable qualitative data from which new SARs can be gleaned.

Table 5–4. Cytotoxicity of phenanthroindolizidines.

		IC_{50} (nM)[b]		
	compound[a]	COLO-205	MCF-7	NCI/ADR-RES
	Taxol	1.8	1.9	NA
(*S*)-**1.4**	(*S*)-tylocrebrine	8.8	105	207
(±)-**1.4**	(±)-tylocrebrine	< 3.1	< 3.1	< 3.1
(±)-**5.22**	(±)-6-desmethoxytylocrebrine	< 3.1	< 3.1	< 3.1
(±)-**4.2**	(±)-antofine	< 3.1	< 3.1	< 3.1
(±)-**5.23**	(±)-6-desmethoxytylophorine	265	533	1340
(±)-**1.1**	(±)-tylophorine	< 3.1	< 3.1	< 3.1
(±)-**5.24**	(±)-deoxypergularinine	8.5	5.8	196

[a] Each phenanthropiperidine is in racemic form unless otherwise specified. [b] Determined using alamarBlue® assay; COLO-205 = human colorectal adenocarcinoma; MCF-7 = human breast carcinoma; NCI-ADR-RES = drug-resistant human ovarian adenocarcinoma; NA = Not active at the highest concentration tested (293 nM).

We have found that tylocrebrine's racemate exhibited anti-tumor activity which exceeded that of the (*S*)-enantiomer alone (Table 5–4). Furthermore, of tylocrebrine's analogs, only one was significantly less cytotoxic than taxol in COLO-205 or MCF-7 cell lines whereas, unlike taxol, each alkaloid retained activity in NCI/ADR-RES, a multi-drug resistant cancer cell line. 6-Desmethoxytylophorine (**5.23**), an unnatural analog, was much less active than

tylocrebrine (**1.4**), confirming the importance of the C6-methoxy group, which is present in all of the most active phenanthropiperidines. Corroborating earlier studies, this data shows that removal of either the C2-, C5- or C7-methoxy groups is not detrimental. This information will indeed be valuable for designing novel anti-cancer agents.

5.4.2 Neurological side-effects hypothesis

We next began our investigations into the cause of the adverse neurological effects observed in tylocrebrine's original clinical trial. The absence of clinical data forced us to search for clues elsewhere. The symptoms alluded to by Suffness[2]—who seems to have acquired his data from a primary source—indicate that, at some level, tylocrebrine interferes with normal voluntary movement. Thus, we chose to explore two potential mechanisms for tylocrebrine's side-effects based on its structural similarity to bioactive molecules known to influence motor function in the CNS: 1-methyl-4-phenyl-1,2,3,6-tetrahydropyridine (MPTP) and dopamine (DA).

5.4.2.1 MPTP-like toxicity

In the 1980s, Langston (in collaboration with the NIH) chanced upon a neurotoxin that induced parkinsonism. This substance, later identified as MPTP, affected illicit drug users that had self-injected contaminated batches of MPPP, a synthetic opioid.[334] The neurotoxin was found to have remarkable selectivity for the substantia nigra and DA neurons, thus, mimicking the pathophysiology of Parkinson's disease. Research over the following decades

has shown that MPTP undergoes a fatal sequence of events that leads to DA neuronal cell death (Fig. 5–2). Being highly lipophilic, MPTP passively diffuses across the BBB to enter the CNS. Within glial cells it is oxidized by monoamine oxidase-B (MAO-B) to the active toxin, 1-methyl-4-phenylpyridinium (MPP+, Fig. 5–3)—this makes MPTP, strictly speaking, a protoxin. Following this oxidation, MPP+ is actively transported into DA neurons at the nerve terminal via the dopamine transporter (DAT); hence, the selectivity for dopaminergic neurons. Within the neuron, the active toxin (MPP+) effectively shuts down cellular metabolism in the mitochondria by inhibiting Complex I (NADH dehydrogenase) of the electron transport chain, ultimately resulting in cell death.

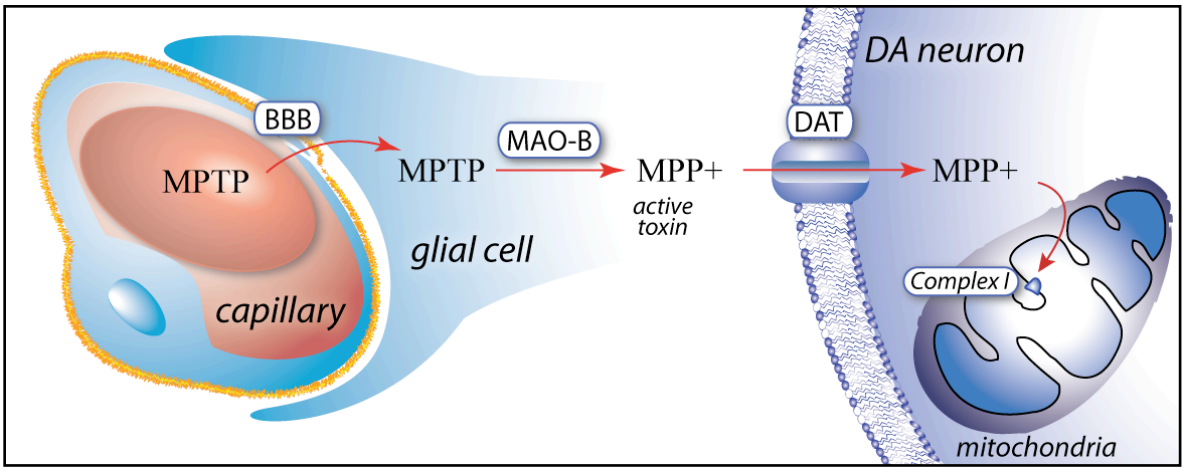

Fig. 5–2. Mechanism for MPTP-induced toxicity.

The basis for investigating tylocrebrine's similarity to MPTP arose from several commonalities. Firstly, the structure of MPTP (Fig. 5–3) is embedded within tylocrebrine. Second, tylocrebrine readily undergoes oxidation to form MPP+-like dehydrotylocrebrine (Fig. 5–3). Phenanthropiperidines are prone to aerobic oxidation while in solution. The exact mechanism of the oxidation is unknown, but the end product is presumably the dubious

pyridinium salt. This raises the question as to the integrity of the phenanthropiperidines in living systems and as to if the side-effects are due to this metabolite rather than the parent compound. Indeed, if oxidation is facile in aerobic conditions, this process may also be implicated in physiological conditions.

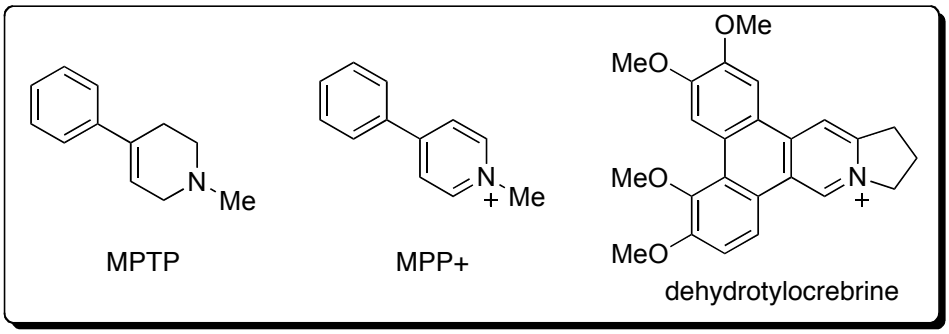

Fig. 5–3. Structure of MPTP, MPP+ and dehydrotylocrebrine.

Another concern is enzymatic oxidation. Having structural similarities to monoamine neurotransmitters and to MPTP, phenanthropiperidines could potentially undergo MAO-mediated oxidation. To explore this hypothesis further, each analog was tested in the MAO Amplex® Red assay (Graph 5–1). This assay measures H_2O_2 (a byproduct of MAO oxidation) production as an indicator of MAO activity. Using *p*-tyramine as a standard, MAO-A and MAO-B activities were measured in the presence of the phenanthropiperidines and MPTP. As expected, MPTP was shown to be a substrate for MAO-B and, to a much lesser extent, MAO-A. Conversely, at concentrations up to 100 μM, none of our analogs increased MAO-A or MAO-B activity, showing that oxidation via this mechanism is unlikely. This does not, however, rule out oxidation by other metabolic enzymes or non-enzymatic oxidation.

Graph 5–1. Phenanthropiperidines as a substrate for MAO-A and MAO-B.

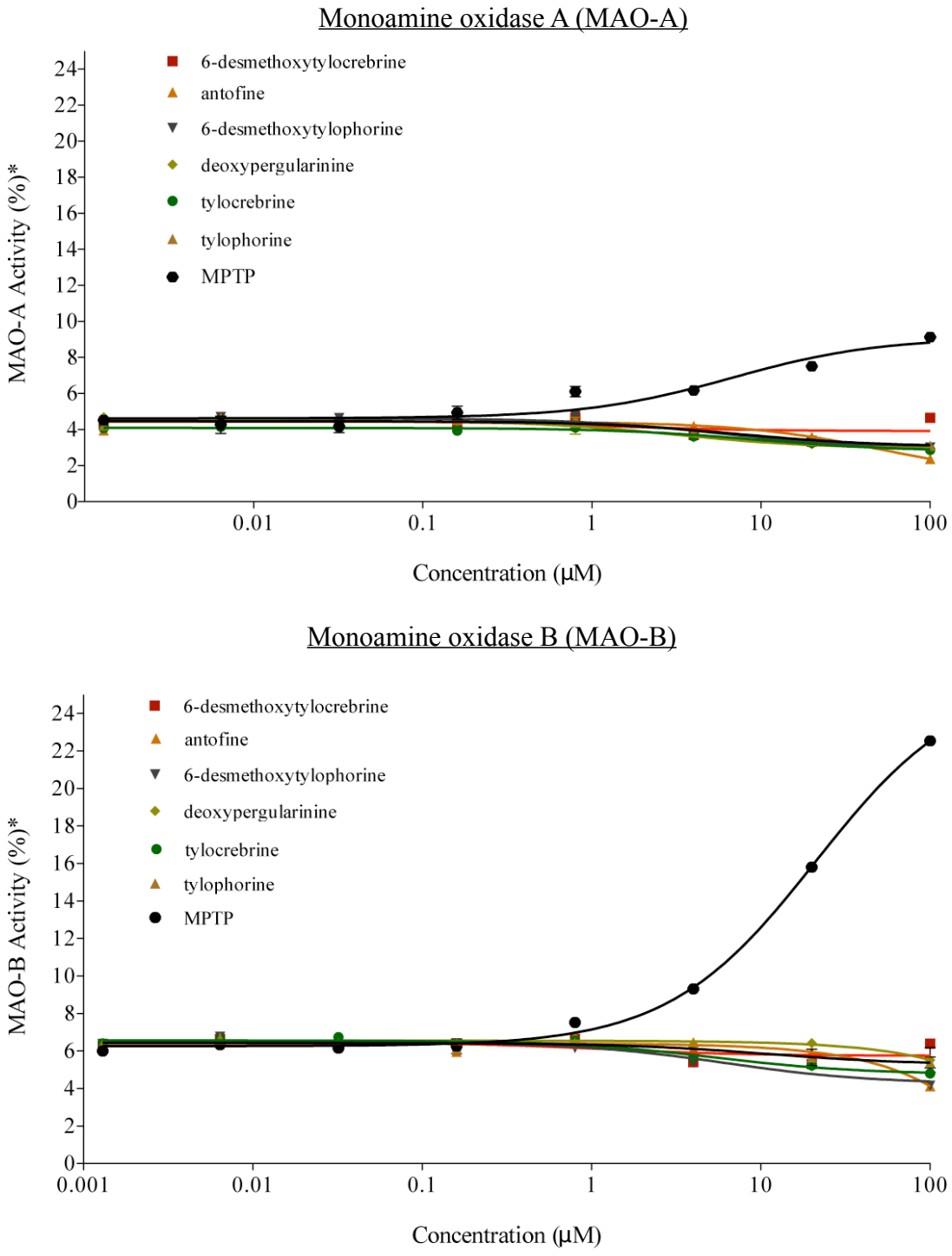

* Percent activity of the MAO enzyme where the activity induced by *p*-tyramine (a known substrate) is set at 100%.

In another effort to identify similarities between tylocrebrine and MPTP, we determined if any phenanthropiperidine analogs were subject to active transport by three major neurotransmitter transporters found in the CNS: DAT, NET and SERT. Even if tylocrebrine's mechanism was different from MPTP, identifying an active transporter would give valuable insight into the region of influence that could aid a physiological explanation when juxtaposed with the tylocrebrine's side-effects. We also tested dehydrotylocrebrine in this assay, which was prepared from tylocrebrine (**1.4**), to see if this potential metabolite might exert CNS effects. The affinity of each analog for the transporters was determined at a single concentration (10 μM) in a radioligand displacement assay. It was clear from this assay that none of the phenanthropiperidines tested exhibited marked affinity for the transporters (Table 5–5).

Table 5–5. Phenanthropiperidine affinity for monoamine transporters.

		% radioligand displacement @ 10 μM[b]		
entry	compound[a]	DAT	NET	SERT
1	6-desmethoxytylocrebrine	10	31	4.9
2	6-desmethoxytylophorine	39.7	8	32
3	antofine	26.0	25.7	0
4	deoxypergularinine	25.1	20.4	4.7
5	tylocrebrine	30.3	30.1	0
6	tylophorine	1.6	18.5	8.2
7	dehydrotylocrebrine	19.2	41.2	0

[a] Each phenanthropiperidine is in racemic form unless otherwise specified. [b] Determined at the NIHM-PDSP. DAT = dopamine transporter, NET = norepinephrine transporter, SERT = serotonin transporter.

Further testing is required to unambiguously define tylocrebrine's (or dehydrotylocrebrine's) role in the electron transport chain before it can be dismissed as an MPTP-like neurotoxin. Nevertheless, compelling evidence, here and elsewhere, gives reason to conclude tylocrebrine is unique in this respect. Firstly, MPTP is activated via oxidation by MAO-B for which tylocrebrine is not a substrate. Second, MPTP's active metabolite, MPP+, exploits DAT to reach its cellular target, whereas, dehydrotylocrebrine is not accommodated by this transporter. Thus, if tylocrebrine or an active metabolite exerts its effect in the neurons of the substantia nigra, which is yet to be demonstrated, it does so through a different pathway.

Another distinction can be made on the basis of MPTP's and tyocrebrine's physiological effects. Administration of MPTP incurs the characteristic parkinsonian rigidity, bradykinesia, tremor and postural instability. These symptoms, as with Parkinson's disease, result from a damaged substantia nigra which is, among other things, responsible for fine motor control. Strictly speaking, this differs from the ataxia which is allegedly caused by tylocrebrine. Ataxia is defined as the loss of coordination and results from dysfunctional sensory or cerebellar systems. Since ataxia is symptomatically and pathologically distinct from parkinsonism, tylocrebrine's and MPTP's motor effects are probably unrelated.

Could the known causes of ataxia shed light on the neurological effects associated with the administration of tylocrebrine? Yes, but uncertainty still remains. Their is no evidence to suggest that tylocrebrine's side-effects are not simply a manifestation of non-specific interactions across the CNS and periphery. Indeed, among its numerous CNS effects, ethanol can induce ataxia.[335] Unfortunately, without the original clinical data, nothing is known about

how the ataxic symptoms present, and therefore, we cannot assume that tylocrebrine's effects are localized or specific.

5.4.2.2 Dopaminergic and other CNS receptors

Another concern we had was that tylocrebrine was interfering with neurotransmission by mimicking biogenic amines. This arose out of the realization that tylocrebrine was endowed with the pharmacophore of DA and bore a resemblance to known DA receptor ligands such as dihydrexidine (DHX) and dinoxyline (Fig. 5–4). DA's pivotal role in the CNS led us to explore the dopaminergic system as the culpable source of tylocrebrine's neurological side-effects. The dopaminergic system is intimately connected to motor control, cognition, emotion, motivation and many other functions.[336] Furthermore, abnormalities of the dopaminergic system can have devastating consequences which are manifested, for instance, in Parkinson's disease, schizophrenia, bipolar disorder and drug addiction. Thus, if tylocrebrine is found to modulate the dopaminergic system, there is good reason to attenuate these interactions during lead optimization.

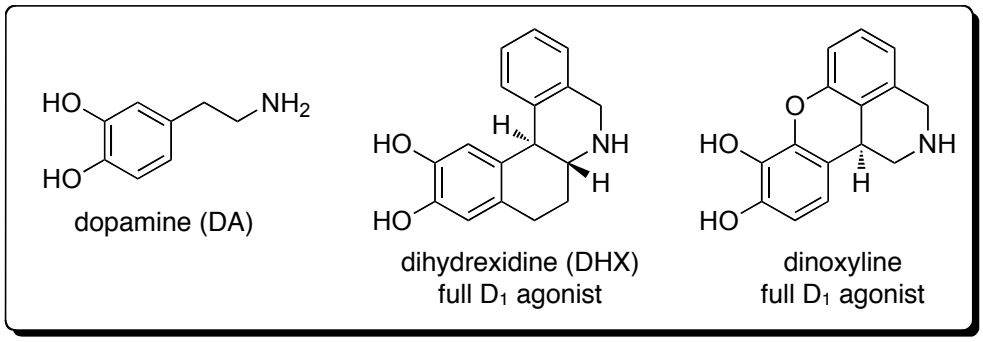

Fig. 5–4. Structurally related molecules of interest.

It was not simply the dopaminergic effects, however, that concerned us. There is appreciable overlap between the ligands of DA receptors and other biogenic amine receptors (*e.g.* adrenergic and serotonergic) in the CNS.[337] Thus, tylocrebrine could possibly exert more extensive effects than those limited to the dopaminergic system. For this reason, we selected a broad panel of CNS targets to investigate rather than focus on a specific receptor.

Our collection of phenanthropiperidines was submitted to the National Institutes of Mental Health-Psychoactive Drug Screening Program (NIHM-PDSP) for a comprehensive CNS-target screen (Table 5–6). A primary screen identified compounds which had significant binding (defined as greater than 50% displacement of a radioligand) to receptors at 10 μM. For those "hits", the K_D was determined in a secondary assay.

The results from the primary screen confirmed our suspicions about tylocrebrine having DA receptor affinity. Five of the six phenanthropiperidine analogs (excluding dehydrotylocrebrine) bound to the D_1 subtype with moderate selectivity. The uniform activity at D_1 of each tylocrebrine analog could be indicative of a more universal liability for these natural products. These analogs also showed moderate affinity at the D_5 receptor and, to a much lesser extent, the D_2, D_3 and D_4 subtypes. This selectivity profile is typical for D_1 agonists and antagonists. The D_5 receptor, having a high degree of structural homology with D_1, is often targeted by D_1 ligands. The D_2, D_3 and D_4 receptors, on the other hand, all belong to the D_2-like family and, therefore, achieving selectivity between these three receptors is more difficult than between them and D_1-like subtypes. The D_1 selectivity exhibited by tylocrebrine is notable, because this receptor is the most highly expressed subtype within the dopaminergic system and widely dispersed in the mammalian forebrain.[336] Modulating this receptor alone could have wide-ranging physiological ramifications.

Table 5–6. Comprehensive CNS target primary screen from NIHM-PDSP.

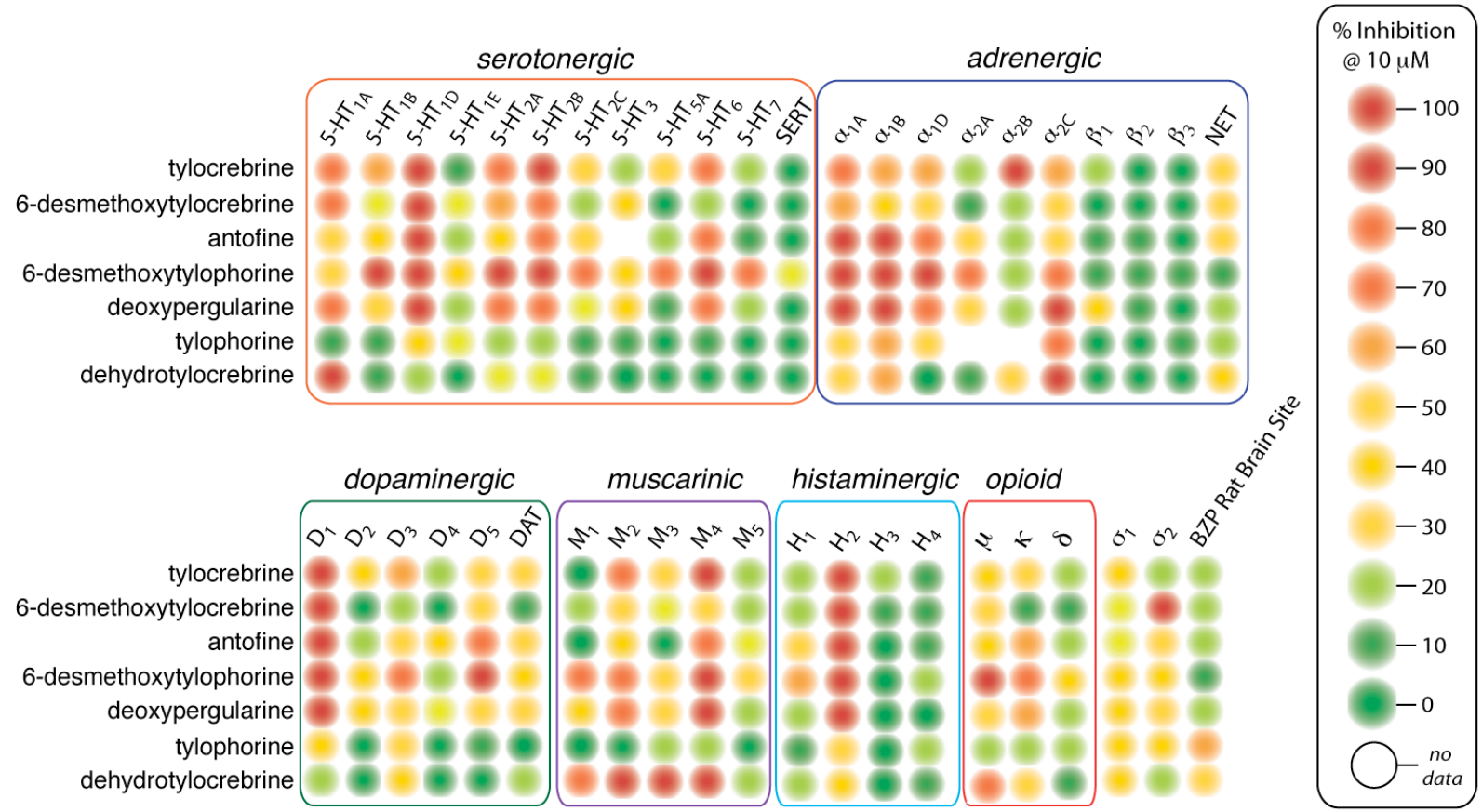

Table 5–7. Affinity for phenanthropiperidine for biogenic amine receptors.

	K_D (nM)[b]							
compound[a]	D_1	D_2	D_3	D_4	D_5	5-HT_{1D}	α_{1A}	H2
6-desmethoxytylocrebrine	219	NA	NA	NA	–	1098	2790	885
6-desmethoxytylophorine	89	NA	5078	NA	749	737	105	222
antofine	181	NA	5849	NA	1695	1553	1092	1724
deoxypergularinine	587	NA	7384	NA	5004	2596	1195	2010
tylocrebrine	448	NA	NA	NA	3644	3123	1784	537
tylophorine	2617	NA	NA	NA	–	NA	NA	9846

[a] Each phenanthropiperidine is in racemic form unless otherwise specified. [b] Determined at the NIHM-PDSP. NA = not active (K_D is greater than 10 μM).

To better characterize the alkaloids affinity for each receptor, the K_D values for each "hit" in the primary screen were determined (Table 5–7). This, however, did not settle the matter. If tylocrebrine had displayed high affinity for the D_1 receptor, this would have forged a promising link to its adverse effects, whereas, if it had weak affinity, it would give good reason to pursue another hypothesis. In reality, tylocrebrine had moderate affinity for the D_1 receptor with a K_D of 448 nM, raising new questions about its nature of activity and the details of its clinical trial. To aid interpretation of this result the dosages used in the tylocrebrine's clinical trials would be extremely valuable. Considering that racemic tylocrebrine was used in these experiments, the affinity of each enantiomer should also be determined before pursuing this route any further. Moreover, the functional effect of binding should be characterized. Although this binding information is useful, a physiological connection cannot be made until a functional assay elucidates tylocrebrine's efficacy upon

the receptor in question (*i.e.* whether tylocrebrine is an agonist, antagonist, partial agonist, *etc.*).

The secondary assay also provided some useful information about how structure influences receptor binding. 6-Desmethoxytylophorine had the highest affinity for the D_1 subtype out of all the phenanthropiperidines tested (K_D = 89 nM). This compound's phenanthrene substitution pattern, which renders it much less active in anti-proliferation assays, will therefore be avoided in analog development. Tylophorine, on the other hand, has the least affinity for the D_1 receptor and also exceptional anti-cancer activity. If D_1-interaction is ever linked to adverse side-effects in the phenanthropiperidines, this information provides a potential strategy to minimize them.

Besides showing notable affinity for the D_1 receptor, tylocrebrine and most of the analogs tested also bind to several subtypes within each class (*e.g.* serotonergic, muscarinic, histaminergic, *etc.*). Particularly, the 5-HT_{1D}, α_{1A} and H_2 receptors were targeted by each analog albeit to a lesser extent than the D_1 receptor. Tylocrebrine had comparable binding to the H_2 receptor and D_1 receptor. The primary functions of the H_2 receptor are in the regulation of gastric acid secretion, smooth and cardiac muscle relaxation and in the immune response.[338] There is little to suggest, however, that H_2 ligands could affect the neurological responses induced by tylocrebrine. Likewise, the α_{1A} receptors has not been directly linked to motor coordination, but its expression in the ventral and dorsal motor area of rat spinal cord suggests that it may regulate movement in some fashion,[339] as does its α_{1B} counterpart.[340] Tylocrebrine's relatively low affinity for this receptor and the 5-HT_{1D} receptor, which also has no known connection to motor functions, renders these implausible targets. Although

these results redirect our search for the mechanism of tylocrebrine's side-effects, they presage other neurological effects that could potentially hamper lead development.

The primary and secondary assays give further confirmation that 6-desmethoxytylophorine and closely related structures could indiscriminately modulate neurotransmission through the biogenic amine receptors. Conversely, tylophorine, which has weak binding to every target that was tested, may be a good lead to base next generation analogs on. It is surprising, however, that this subtle modification—the presence or absence of a single methoxy group—confers such a drastically different CNS receptor profile.

Another possible explanation for this anomaly is that tylophorine gives a false negative result by virtue of its insolubility. Indeed, in the process of making DMSO solutions of each alkaloid it was quite apparent that tylophorine was the least soluble. Furthermore, it is significant that tylophorine's decomposition point (284–285 ºC) is more than 50 ºC above that of the other alkaloids (ranging from 203–230 ºC). Although the decomposition temperature of a chemical entity is not correlated with solubility, as is the melting point,[133] this data demonstrates that the physicochemical properties of tylophorine are significantly different from the other alkaloids, and this difference—rather than actual receptor binding—may be the basis for its anomalous behavior in the PDSP-CNS target screen.

Table 5–8. Tylocrebrine's and dehydrotylocrebrine's affinity for muscarinic receptors.

	K_D (nM)[b]				
compound[a]	M1	M2	M3	M4	M5
tylocrebrine	2664	4602	NA	3176	NA
dehydrotylocrebrine	186	156	339	169	1561

[a] Each phenanthropiperidine is in racemic form unless otherwise specified. [b] Determined at the NIHM-PDSP. NA = not active (K_D is greater than 10 μM).

It is also worthy to note that dehydrotylocrebrine exhibits a unique binding profile. Rather than targeting the monoamine receptors, this derivative of tylocrebrine has considerable affinity for the muscarinic receptors (Table 5–6 and 5–8). This could be a concern if dehydrotylocrebrine is generated *in vivo*. Muscarinic receptors, like dopaminergic systems, are expressed throughout the CNS and PNS, and they are associated with cognition, learning, and memory as well as proper functioning of the heart, gastrointestinal tract, lung bronchioles and urinary bladder.[341, 342] Moreover, these GPCRs are the target of numerous toxins, including its eponymous mushroom toxin muscarine.[343] However, the muscarinic system functions primarily, if not exclusively, in the autonomic nervous system and has not been linked to voluntary motor control or coordination. Therefore, dehydrotylocrebrine's affinity for these receptors does not explain tylocrebrine's side-effects, but, as before, discloses potential off-target interactions that could limit the success of phenanthropiperidine-based therapeutics. If oxidation does occur *in vivo*, preventing it through appropriately designed analogs would be presumably curtail the muscarinic effects.

5.5 Summary

Tylocrebrine's early failure in clinical trials, despite precluding characterization of its efficacy, established a liability for this class of alkaloids and their use as chemotherapeutic agents. Until now, the neurological effects that derailed the clinical trials have not been investigated, despite recent interest in the medicinal properties of the phenanthropiperidines. The lack of practical syntheses for tylocrebrine was a major impediment to these studies. We

addressed this by designing a new synthetic approach that accounted for the challenging phenanthrene substitution pattern. Our method provided a simple and high-yielding route to tylocrebrine and provided sufficient quantities to assist characterization of its inimical CNS effects. This route was also used to synthesize a small library of tylocrebrine analogs—some were known natural products, others were unnatural analogs—to aid SAR studies.

Herein, we reported preliminary work to understand the CNS effects of tylocrebrine by exploring two hypothetical links between its structure and the nature of its side-effects. Firstly, we investigated the similarities of tylocrebrine to the known neurotoxin MPTP and found that there is unlikely overlap between their biological effects. Second, we investigated tylocrebrine's and its analogs' similarity to key biogenic amines in the NIHM-PDSP comprehensive CNS target screen. The screen has uncovered several pitfalls that could be encountered in the development of a phenanthropiperidine drug, especially one that is designed to treat tumors within the CNS. It also uncovered risk factors that contribute to the off-target interactions that will guide lead optimization studies. The mechanism of tylocrebrine-induced ataxia and disorientation is still not understood, making it difficult, without an experimental model, to design "CNS-safe" analogs at this time. One strategy that is feasible, however, involves the preparation of phenanthropiperidines that do not cross the BBB at all. Since this approach does not require a mechanistic understanding of tylocrebrine's neurological effects, it warrants immediate attention.

CHAPTER 6

EXPERIMENTAL DATA

6.1 Materials and methods

Unless otherwise specified, all starting materials, reagents and solvents are commercially available and were used without further purification. Flash column chromatography was carried out on silica gel. TLC was conducted on silica gel 250 micron, F_{254} plates. ^{1}H NMR spectra were recorded on a 400 MHz NMR instrument. Chemical shifts are reported in ppm with TMS or $CHCl_3$ as an internal standard (TMS: 0.00 ppm, $CHCl_3$: 7.26 ppm). Data are reported as follows: chemical shift, multiplicity (s = singlet, d = doublet, t = triplet, q = quartet, b = broad, m = multiplet), integration and coupling constants (Hz). ^{13}C NMR spectra were recorded on a 100 MHz NMR spectrometer with complete proton decoupling. Chemical shifts are reported in ppm with the solvent as internal standard ($CHCl_3$: 77.2 ppm). IR of solids were obtained by dissolving the sample in $CHCl_3$ and letting the solvent evaporate on a KBr plate. High-resolution mass spectrometry was performed by the University of Minnesota Mass Spectrometry Facility.

6.2 Chapter 2

6.3.1 Preparation of Weinreb amides:

Method A: Weinreb amide preparation from β-amino acids.

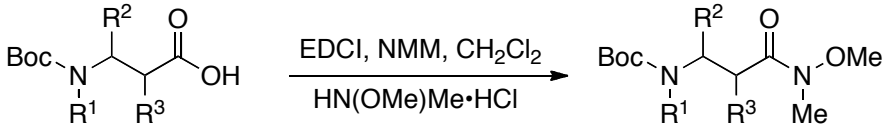

The β-amino acid (4.0 mmol, 1.0 equiv) was dissolved in anhydrous CH_2Cl_2 (100 mL) under an argon atmosphere and cooled to –15 °C. To this solution was added *N*,*O*-dimethylhydroxylamine•HCl (4.4 mmol, 1.1 equiv) and *N*-methylmorpholine (4.4 mmol, 1.1 equiv) followed by EDCI (4.2 mmol, 1.1 equiv). The reaction mixture was then allowed to come to room temperature. After 2 h the reaction was again cooled to 0 °C and quenched by the addition of an ice cold 10% HCl solution (25 mL) and allowed to stir at this temperature for 5 min. The reaction was diluted with water (50 mL) and extracted with CH_2Cl_2 (x3). The combined organic layers were washed with saturated $NaHCO_3$ (x1), dried over Na_2SO_4, filtered and concentrated. Purification via SiO_2 flash chromatography using EtOAc and hexanes as the eluent afforded pure Weinreb amides.

Method B: Weinreb amide preparation from α-amino acids.

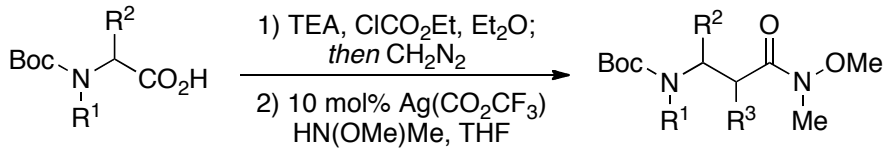

Warning: Large amounts of diazomethane were used for this transformation. Proper care should be taken when handling this highly explosive reagent. All glassware used was free of cracks, scratches or ground-glass joints and a blast shield was used. The *N*-Boc-amino acid (50.0 mmol, 1.00 equiv) was taken into THF (100 mL) with stirring and cooled to 0 ºC with an ice bath. The reaction solution was treated with TEA (7.66 mL, 55.0 mmol, 1.10 equiv) and allowed to react for 15 min to fully deprotonate the carboxylic acid. With the addition of ethyl chloroformate (5.23 mL, 55.0 mmol, 1.10 equiv), a thick white precipitate formed. Stirring was continued for 15 min then stopped. In a separate flask, an ice-cold ethereal solution of diazomethane was prepared and, without stirring, was carefully decanted into the freshly prepared anhydride reaction flask using a glass funnel. The reaction solution was lightly stirred for 4 seconds then stirring was stopped. The mixture was allowed to warm to room temperature and react overnight. Any additional diazomethane was carefully quenched with 0.5 N acetic acid (100 mL). The drop-wise addition of saturated sodium bicarbonate regulated the solution back to a basic pH 8-9 with gentle stirring. The organic and aqueous layers were separated. The organic phase was washed twice each with saturated sodium bicarbonate and brine then dried over sodium sulfate. The solvent was evaporated under reduced pressure and placed under high vacuum overnight. The diazoketone was taken into THF (250 mL) and cooled to 0 ºC. Foil was used to cover the reaction flask so as to exclude light from the reaction solution. To this was added freshly distilled *N,O*-dimethylhydroxylamine (9.16 g, 150 mmol, 3.00 equiv).[344] In a separate foil covered flask, silver trifluoroacetate (1.10 g, 5.00 mmol, 0.10 equiv) was dissolved in TEA (130 mL). This solution was added to the diazoketone mixture over 30 min. The reaction temperature was allowed to slowly warm to room temperature and the solution was stirred overnight. To the

reaction mixture was added activated charcoal (~2 g) and the reaction mixture was stirred for 5 min and filtered. The filtrate was concentrated and the residue redissolved in EtOAc. To this was added activated charcoal (~2 g) and the process repeated. When the filtrate had been concentrated a second time the residue was purified via SiO_2 flash chromatography using a mixture of EtOAc and hexane as eluent affording the pure Weinreb amide.

Method C: Procedure for Weinreb amide preparation from amines.

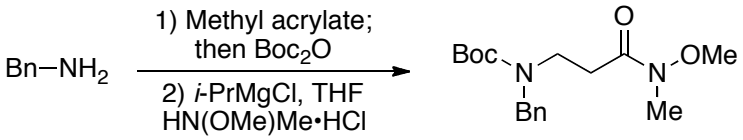

A round-bottomed flask was charged with benzylamine (8.00 mL, 73.1 mmol, 3.00 equiv) and cooled to –40 ºC. Methyl acrylate (2.20 mL, 86.1 mmol, 1.00 equiv) was added dropwise over 5 min and the reaction was stirred at this temperature (–40 ºC) for 24 h. Excess benzylamine was distilled off of under reduced pressure. The remaining residue was dissolved in MeOH (50 mL) and di-*tert*-butyldicarbonate (6.40 g, 29.2 mmol, 1.20 equiv) was added slowly. The reaction mixture was stirred for another 30 min and the solvent was removed *in vacuo*. The concentrated reaction mixture was redissolved in CH_2Cl_2 (300 mL) and washed with cold 10% HCl (100 mL x 2) and brine (100 mL x 2). The organic layer was dried with $MgSO_4$, concentrated and purified via SiO_2 flash chromatography (25% EtOAc in hexanes) to afford 6.62 g (88%) of the methyl ester as a clear viscous oil. This oil was converted to the corresponding Weinreb amide using the procedure reported by Williams *et al*.[279] The crude product was purified via SiO_2 flash chromatography (40% EtOAc in

hexanes) to give 6.29 g (86%) of the Weinreb amide as a clear viscous oil. See below for spectral data.

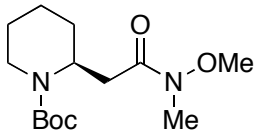

2.1

(*S*)-*tert*-Butyl 2-(2-(Methoxy(methyl)amino)-2-oxoethyl)piperidine-1-carboxylate (2.1). The title compound was obtained as a colorless oil using Method B (64% over 2 steps). Spectral data of the title compound was identical to that reported in the literature.[255]

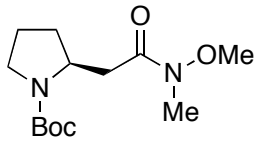

2.2

(*S*)-*tert*-Butyl 2-(2-(Methoxy(methyl)amino)-2-oxoethyl)pyrrolidine-1-carboxylate (2.2). The title compound could be obtained as a colorless oil using either Method A (98%) or Method B (70% over 2 steps). Spectral data of the title compound was identical to that reported in the literature.[152]

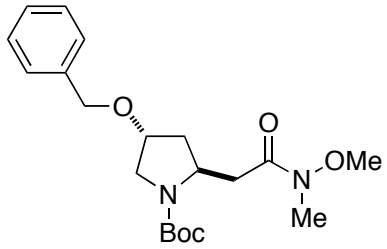

2.3

(2*S,4*R**)-*tert*-Butyl 4-(Benzyloxy)-2-(2-(methoxy(methyl)amino)-2-oxoethyl)-pyrrolidine-1-carboxylate (2.3).** The title compound was obtained as a white solid from Boc-*O*-benzyl-hydroxyproline using Method B (72% over 2 steps): mp 69.5-70.3 °C; ^{1}H NMR (400 MHz, $CDCl_3$) δ (1:1 mixture of rotamers) 1.46 (s, 18H), 1.95-2.03 (bm, 2H), 2.30-2.38 (bm, 2H), 2.44-2.54 (bm, 2H), 3.03-3.16 (m, 2H), 3.16 (s, 6H), 3.41-3.56 (m, 3H), 3.67 (s, 6H), 3.67-3.75 (m, 1H), 4.09-4.14 (bm, 2H), 4.27-4.34 (bm, 2H), 4.46-4.54 (m, 4H), 7.26-7.35 (m, 10H); ^{13}C NMR (100 MHz, $CDCl_3$) δ 28.5, 32.0, 36.4, 36.9, 37.4, 38.1, 51.1, 51.9, 52.9, 61.2, 70.8, 75.7, 76.4, 79.3, 79.7, 127.6, 127.6, 128.4, 138.1, 154.5, 172.1, 172.4; IR (neat) 2974, 1693, 1665, 1397, 1160, 1118 cm^{-1}; HRMS (ESI^{+}) *m/e* calc'd for $[M+H]^{+}$ $C_{20}H_{31}N_2O_5$: 379.2233, found 379.2222.

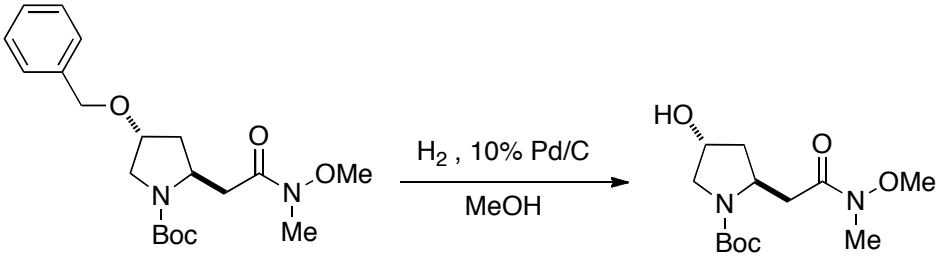

2.3 **2.4**

(2*S,4*R**)-*tert*-Butyl 4-Hydroxy-2-(2-(methoxy(methyl)amino)-2-oxoethyl) pyrrolidine-1-carboxylate (2.4)**. The title compound was obtained as a colorless oil (98%) using the hydrogenation procedure reported by Epperson *et al*.[345] Spectral data of for this compound was identical to that reported in the literature.[152]

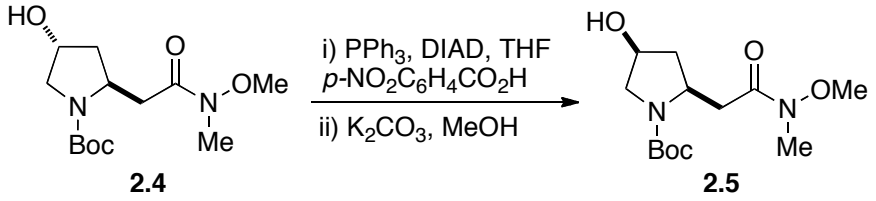

2.4 **2.5**

(2*S,4*S**)-*tert*-Butyl 4-Hydroxy-2-(2-(methoxy(methyl)amino)-2-oxoethyl) pyrrolidine-1-carboxylate (2.5).** The title compound was obtained from a Mitsunobu reaction of compound **2.4**. Weinreb amine **2.4** (90 mg, 0.32 mmol, 1.0 equiv) was dissolved in THF (10.0 mL) under an argon atmosphere and cooled to 0 °C. Triphenylphosine (164 mg, 0.62 mmol, 2.0 equiv) and *p*-nitrobenzoic acid (104 mg, 0.62 mmol, 2.0 equiv) were than added sequentially. DIAD (126 mg, 0.62 mmol, 2.0 equiv) was then added slowly and the reaction was allowed to come to room temperature. The reaction was monitored via TLC (100% EtOAc) and judged complete in less than an hour. The reaction mixture was poured into a saturated $NaHCO_3$ solution and extracted thrice with EtOAc. The combined organic layers were dried over Na_2SO_4, filtered and concentrated. This crude material was purified via flash chromatography (1 EtOAc/1 hexanes) to provide 134 mg (98%) of a colorless oil: ^{1}H NMR (400 MHz, $CDCl_3$, 50 °C) δ 1.48 (s, 9H), 2.25 (d, J = 14.6 Hz, 1H), 2.43-2.51 (m, 1H), 2.75-2.80 (m, 1H), 3.17 (s, 4H), 3.64 (s, 4H), 3.81-3.86 (m, 1H), 4.40-4.50 (bs, 1H), 5.54-5.57 (m, 1H), 8.21-8.29 (m, 4H); ^{13}C NMR (125 MHz, $CDCl_3$, 50 °C) δ 22.3, 28.9,

36.7, 37.5, 52.9, 53.9, 61.6, 75.4, 80.4, 123.9, 131.1, 135.8, 151.2, 154.3, 164.4, 173.3; This *p*-nitrobenzoyl ester (0.12 g, 0.26 mmol) was dissolved in MeOH (10 mL) and K_2CO_3 (*excess*) added. After 5 min the reaction was judged complete by TLC (100% EtOAc) and the reaction solvent was removed under reduced pressure. This residue was then dissolved in a 1:1 CH_2Cl_2 and water mixture and extracted with CH_2Cl_2 (x3). The combined organic layers were dried over Na_2SO_4, filtered and concentrated. This crude material was purified via flash chromatography (100% EtOAc) to provide 60 mg (91%) of the desired product: ^{1}H NMR (400 MHz, $CDCl_3$, 50 °C) δ 1.44 (s, 9H), 1.92 (d, *J* = 14 Hz, 1H), 2.20-2.31 (m, 1H), 2.89-3.11 (m, 3H), 3.15 (s, 3H), 3.38 (d, *J* = 12 Hz, 1H), 3.55 (bs, 1H), 3.68 (s, 3H), 4.22 (bs, 1H), 4.39 (bs, 1H); ^{13}C NMR (100 MHz, $CDCl_3$, 50 °C) δ 28.9, 32.5, 37.4, 39.8, 54.0, 55.7, 61.5, 70,7, 79.8, 154.7; IR (neat) 3439, 2974, 2935, 1680, 1400, 1172 cm^{-1}; HRMS (ES+) *m/e* calc'd for $[M+H]^+$ $C_{13}H_{25}N_2O_5$: 289.1763, found 289.1752.

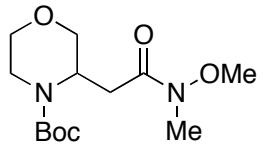

2.6

***tert*-Butyl 3-(2-(Methoxy(methyl)amino)-2-oxoethyl)morpholine-4-carboxylate (2.6).** The title compound was obtained from *N*-Boc-3-morpholineacetic acid using Method A as a white solid (99%) after flash chromatography (80% EtOAc/hexanes): mp 71.9-72.7 °C; ^{1}H NMR (400 MHz, $CDCl_3$) δ 1.46 (s, 9H), 2.54-2.64 (bm, 1H), 2.97-3.17 (bm, 2H), 3.17 (s, 3H), 3.45 (dt, *J* = 5.8, 2.8 Hz, 1H), 3.58 (dd, *J* = 11.7, 2.2 Hz, 1H), 3.71 (s, 3H), 3.71-3.88 (m, 3H), 4.41-4.46 (bm, 1H); ^{13}C NMR (100 MHz, $CDCl_3$) δ 28.4, 31.1, 32.1, 39.2, 48.5,

61.3, 66.8, 69.1, 80.1, 154.5, 171.9; IR (neat) 2975, 1696, 1663, 1408, 1171, 1106 cm^{-1}; HRMS (ESI+) *m/e* calc'd for $[M+H]^+$ $C_{13}H_{25}N_2O_5$: 289.1763, found 289.1770.

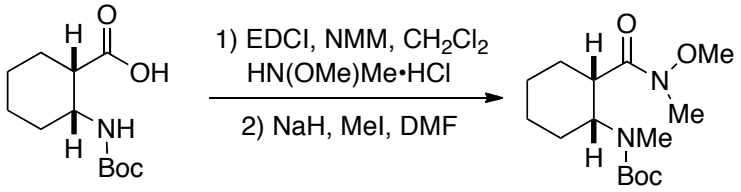

2.7

***tert*-Butyl (*cis*)-2-(Methoxy(methyl)carbamoyl)cyclohexyl(methyl)carbamate** (**2.7**). The title compound was obtained from *N*-Boc-*cis*-2-aminocyclohexanecarboxylic acid using Method A and a subsequent methylation. The Weinreb amide intermediate (following Method A) was isolated as a colorless oil (95%) after purification via flash chromatography (25% EtOAc/hexanes): ^{1}H NMR (400 MHz, $CDCl_3$, 50 °C) δ 1.16-1.40 (m, 2H), 1.38 (s, 9H), 1.48-1.64 (m, 4H), 1.78-1.88 (m, 1H), 2.05-2.12 (m, 1H), 3.10 (bs, 1H), 3.12 (s, 3H), 3.65 (s, 3H), 3.85 (bs, 1H), 4.98 (bs, 1H); ^{13}C NMR (100 MHz, $CDCl_3$, 50 °C) δ 23.1. 2, 25.9, 28.7, 30.1, 32.7, 41.4, 48.9, 61.6, 79.2, 155.8, 175.2; IR (neat) 3439, 2930, 2860, 1700, 1500, 1168 cm^{-1}; HRMS (ES+) *m/e* calc'd for $[M+H]^+$ $C_{14}H_{27}N_2O_4$: 287.1971, found 287.1971. *Methylation Procedure:* The Weinreb amide (160 mg, 0.56 mmol, 1.0 equiv) and MeI (170 μL, 2.8 mmol, 5.0 equiv) were dissolved in anhydrous DMF (15 mL) under an argon atmosphere and cooled to 0 °C. To this solution was added 60% NaH (45 mg, 1.1 mmol, 2.0 equiv) in one portion and the reaction was allowed to come to room temperature. It was found crucial to use high quality NaH for this reaction to proceed. After 8 h the reaction was judged complete by TLC (50% EtOAc/hexanes). The reaction was quenched by

the addition of water and placed in a separatory funnel. This solution was diluted with water and extracted with EtOAc (x3). The combined organic layers were back extracted with water (x2) to remove any residual DMF then dried over Na_2SO_4, filtered and concentrated. This crude material was purified via flash chromatography (25% EtOAc/hexanes) to provide 162 mg (92%) of the title compound as a colorless oil: ^{1}H NMR (400 MHz, $CDCl_3$, 50 °C) δ 1.32-1.52 (m, 3H), 1.45 (s, 9H), 1.55-1.66 (m, 1H), 1.78-1.97 (m, 3H), 2.35-2.44 (m,1H), 2.72 (s, 3H), 3.13 (s, 3H), 3.42 (bs, 1H), 3.55 (s, 3H), 4.06 (bs, 1H); ^{13}C NMR (100 MHz, $CDCl_3$, rotameric) δ 20.9, 25.7, 26.0, 28.4, 28.5, 29.1, 29.6, 32.2, 36.4, 37.1, 55.9, 56.9, 61.3, 79.1, 155.9; IR (neat) 3400, 1643, 1145 cm^{-1}; HRMS (ES+) *m/e* calc'd for [M+H]+ $C_{15}H_{29}N_2O_4$: 301.2127, found 301.2116.

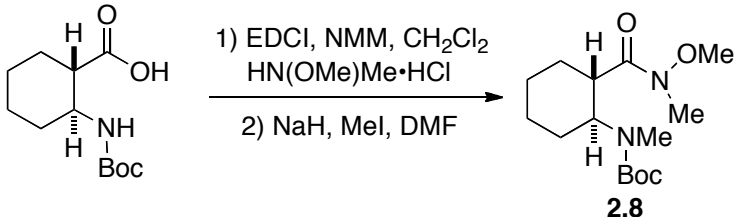

2.8

***tert*-Butyl (*trans*)-2-(Methoxy(methyl)carbamoyl)cyclohexyl(methyl)carbamate (2.8).** The title compound was obtained from *N*-Boc-*trans*-2-aminocyclohexanecarboxylic acid using Method A and a subsequent methylation. The Weinreb amide intermediate (following Method A) was isolated as a colorless oil (96%) after purification via flash chromatography (25% EtOAc/hexanes): ^{1}H NMR (400 MHz, $CDCl_3$, 50 °C) δ 1.16-1.58 (m, 4H) 1.38 (s, 9H), 1.65-1.82 (bm, 3H), 1.98-2.07 (m, 1H), 2.90 (bs, 1H), 3.15 (s, 3H), 3.42-3.53 (m, 1H), 3.68 (s, 3H), 4.67 (bs, 1H); ^{13}C NMR (100 MHz, $CDCl_3$) δ 25. 2, 25.4, 28.7, 29.4, 32.8, 44.9,

52.6, 61.8, 79.2, 155.4, 175.9; IR (neat) 3303, 2977, 2953, 2856, 1767, 1639, 1178 cm-1; HRMS (ES+) *m/e* calc'd for $[M+H]^+$ $C_{14}H_{27}N_2O_4$: 287.1971, found 287.1968. *Methylation Procedure:* The Weinreb amide (70 mg, 0.25 mmol, 1.0 equiv) and MeI (80 μL, 1.3 mmol, 5.0 equiv) were dissolved in anhydrous DMF (20 mL) under an argon atmosphere and cooled to 0 °C. To this solution was added 60% NaH (20 mg, 0.49 mmol, 2.0 equiv) in one portion and the reaction was allowed to come to room temperature. It was found crucial to use high quality NaH for this reaction to proceed. After 8 h the reaction was judged complete by TLC (50% EtOAc/hexanes). The reaction was quenched by the addition of water and placed in a separatory funnel. This solution was diluted with water and extracted with EtOAc (x3). The combined organic layers were back extracted with water (x2) to remove any residual DMF then dried over Na_2SO_4, filtered and concentrated. This crude material was purified via flash chromatography (25% EtOAc/hexanes) to provide 73 mg (99%) of the title compound as a colorless oil: ^{1}H NMR (400 MHz, $CDCl_3$, 50 °C) δ 1.15-1.58 (m, 3H), 1.43 (s, 9H), 1.65-1.89 (bm, 6H), 2.79 (s, 3H), 3.14 (s, 3H), 3.42-3.53 (bs, 1H), 3.69 (s, 3H); ^{13}C NMR (100 MHz, $CDCl_3$, rotameric) δ 25.0, 25.1, 25.5, 25.6, 28.0, 28.5, 29.2, 29.9, 30.0, 32.3, 42.6, 61.5, 78.8, 79.5, 154.9, 155.8, 175.1, 175.7; IR (neat) 2957, 1680, 1360 cm^{-1}; HRMS (ES+) *m/e* calc'd for $[M+H]^+$ $C_{15}H_{29}N_2O_4$: 301.2127, found 301.2110.

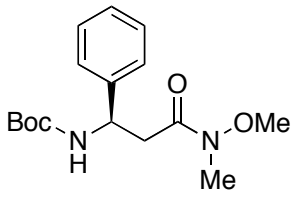

2.9

(*R*)-*tert*-Butyl 3-(Methoxy(methyl)amino)-3-oxo-1-phenylpropylcarbamate (2.9). The title compound was obtained using Method A as a colorless oil (99%) after flash chromatography (70% EtOAc/hexanes): ^{1}H NMR (400 MHz, $CDCl_3$) δ 1.41 (s, 9H), 2.83 (dd, *J* = 15.2, 4.3 Hz, 1H), 3.03-3.10 (m, 1H), 3.10 (s, 3H), 3.50 (s, 3H), 5.11 (bs, 1H), 6.14 (bs, 1H), 7.20-7.26 (m, 1H), 7.29-7.33 (m, 4H); ^{13}C NMR (100 MHz, $CDCl_3$) δ 28.4, 31.9, 37.8, 51.3, 61.2, 79.3, 126.1, 127.1, 128.5, 142.1, 155.2, 171.8; IR (neat) 2977, 1712, 1655, 1496, 1366, 1170 cm^{-1}; HRMS (ESI+) *m/e* calc'd for $[M+H]^+$ $C_{16}H_{25}N_2O_4$: 309.1814, found 309.1800; $[\alpha]_D^{22} = -12.0$ (*c* 1.00, $CHCl_3$).

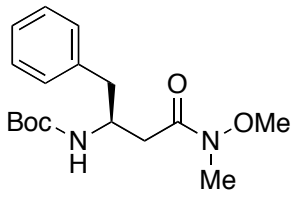

2.10

(*S*)-*tert*-Butyl 4-(Methoxy(methyl)amino)-4-oxo-1-phenylbutan-2-ylcarbamate (2.10). The crude material from Method B was purified via flash chromatography (25% EtOAc/ hexanes) to provide the desired product as a colorless oil (54% 2 steps): ^{1}H NMR (400 MHz, $CDCl_3$, 50 °C) δ 1.38 (s, 9H), 2.50-2.62 (bm, 2H), 2.80-2.87 (m, 1H), 2.96-3.02 (m, 1H), 3.13 (s, 3H), 3.49 (s, 3H), 4.14 (bs, 1H), 5.52 (bs, 1H), 7.16-7.30 (m, 5H); ^{13}C NMR (100

MHz, $CDCl_3$, 50 °C) δ 28.8, 32.3, 34.8, 40.7, 49.3, 61.4, 79.3, 126.8, 128.8, 129.7, 138.9, 155.7, 173.0; IR (neat) 3342, 2975, 2934, 1713, 1660, 1496, 1171 cm^{-1}; HRMS (ES^+) *m/e* calc'd for $[M+H]^+$ $C_{17}H_{27}N_2O_4$: 323.1971, found 323.1943; $[\alpha]_D^{22} = -21$ (*c* 0.75, $CHCl_3$).

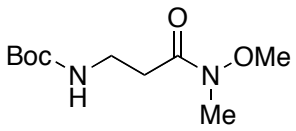

2.11

***tert*-Butyl 3-(Methoxy(methyl)amino)-3-oxopropylcarbamate (2.11).** The title compound was obtained according to Method A as a colorless oil (95%) after flash chromatography (85% EtOAc/hexanes): ^1H NMR (400 MHz, $CDCl_3$) δ (1:1 mixture of rotamers) 1.43 (s, 9H), 2.63-2.67 (bm, 2H), 3.19 (s, 3H), 3.42 (td, *J* = 5.8, 5.8 Hz, 2H), 3.68 (s, 3H), 5.31 (bm, 1H); ^{13}C NMR (100 MHz, $CDCl_3$) δ28.3, 28.3, 31.9, 32.2, 35.7, 61.1, 61.2, 78.9, 155.9, 173.1; IR (neat) 3349, 2976, 1713, 1660, 1520, 1173 cm^{-1}; HRMS (ESI+) *m/e* calc'd for $[M+H]^+$ $C_{10}H_{21}N_2O_4$: 233.1501, found 233.1501.

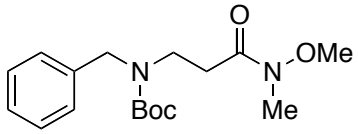

2.12

***tert*-Butyl Benzyl(3-(methoxy(methyl)amino)-3-oxopropyl)carbamate (2.12).** The title compound was obtained using Method C as a colorless oil (76% 2 steps) after flash

chromatography (70% EtOAc/hexanes): ^{1}H NMR (400 MHz, $CDCl_3$) δ (1:1 mixture of rotamers) 1.44 (s, 9H), 1.50 (s, 9H), 2.58-2.63 (bm, 2H), 2.67-2,72 (bm, 2H), 3.15 (s, 6H), 3.43-3.48 (bm, 2H), 3.51-3.55 (bm, 2H), 3.63 (bs, 6H), 4.48 (s, 4H), 7.22-7.35 (m, 10H); ^{13}C NMR (100 MHz, $CDCl_3$) δ 28.4, 31.2, 32.1, 42.8, 43.1, 50.6, 51.6, 61.2, 61.3, 79.8, 127.2, 127.3, 127.8, 128.4, 138.4, 138.8, 155.5, 155.8, 172.5, 172.9; IR (neat) 2974, 1693, 1664, 1413, 1366, 1167 cm^{-1}; HRMS (ESI+) *m/e* calc'd for $[M+H]^+$ $C_{17}H_{27}N_2O_4$: 323.1971, found 323.1957.

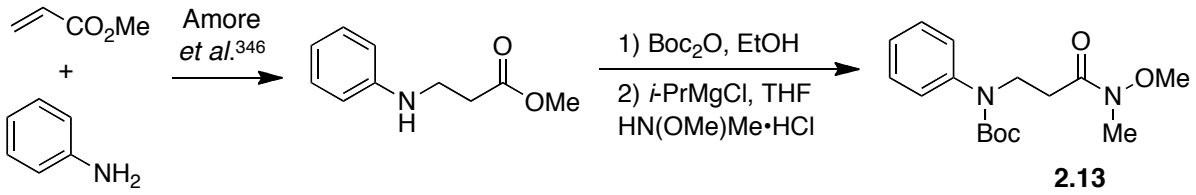

2.13

***tert*-Butyl 3-(Methoxy(methyl)amino)-3-oxopropyl(phenyl)carbamate (2.13).** The methyl ester precursor was synthesized from aniline (5.0 mL, 53 mmol, 1.0 equiv) and methyl acrylate (4.7 mL, 53 mmol, 1.0 equiv) as reported by Amore *et al*.[346] The crude product was redissolved in ethanol (100 mL) and di-*tert*-butyldicarbonate (12.6 g, 57.8 mmol, 1.10 equiv) was added slowly. The reaction mixure was stirred for 24 h and the solvent was removed *in vacuo*. The concentrated reaction mixture was redissolved in CH_2Cl_2 (300 mL) and washed with cold 10% HCl (100 mL x 2) and brine (100 mL x 2). The organic layer was dried with $MgSO_4$, concentrated and purified via SiO_2 flash chromatography (25-50% EtOAc in

hexanes) to afford 8.71g (57% for 2 steps) of the methyl ester as a clear viscous oil. This oil was converted to the corresponding Weinreb amide using the procedure reported by Williams *et al*.[279] The crude product was purified via SiO_2 flash chromatography (40% EtOAc in hexanes) to afford 7.89 g (82%) of the Weinreb amide as a clear viscous oil: ^{1}H NMR (400 MHz, $CDCl_3$) δ 1.43 (s, 9H), 2.73 (t, *J* = 7.5, 2H), 3.12 (s, 3H), 3.65 (s, 3H), 3.96 (t, *J* = 7.5 Hz, 2H), 7.22-7.17 (m, 3H), 7.34-7.31 (m, 2H); ^{13}C NMR (100 MHz, $CDCl_3$) δ28.3, 31.1, 32.0, 46.3, 61.3, 80.3, 126.1, 127.0, 128.7, 142.3, 154.5, 172.4; IR (neat) 2976, 1698, 1664, 1456, 1391, 1168 cm^{-1}; HRMS (ESI+) *m/e* calc'd for $[M+H]^+$ $C_{16}H_{25}N_2O_4$: 309.1814, found 309.1821.

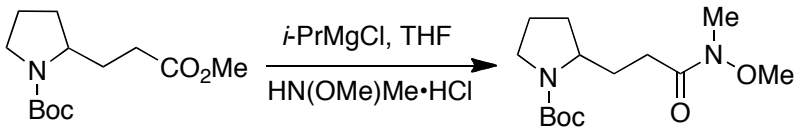

***tert*-Butyl 2-(3-(Methoxy(methyl)amino)-3-oxopropyl)pyrrolidine-1-carboxylate.** The methyl ester precursor to the title compound was prepared in 4 steps (88%) from the precedent of Poon *et al*.[347] The title compound was obtained as a colorless oil using step 2 of Method C: ^{1}H NMR (400 MHz, $CDCl_3$) δ (1:1 mixture of rotamers) 1.46 (s, 18H), 1.62-1.76 (m, 4H), 1.79-2.00 (bm, 8H), 2.40-2.49 (bm, 4H), 3.18 (s, 6H), 3.29-3.34 (bm, 3H), 3.40-3.47 (bm, 1H), 3.69 (s, 6H), 3.80-3.91 (bm, 2H); ^{13}C NMR (100 MHz, $CDCl_3$) δ23.0, 23.7, 28.0, 28.5, 29.1, 29.5, 29.7, 30.1, 30.9, 32.2, 46.0, 46.3, 56.7, 56.9, 61.1, 61.2, 78.8

79.2, 154.8, 174.2; IR (neat) 2972, 1692, 1393, 1367, 1172, 1107 cm^{-1}; HRMS (ESI+) *m/e* calc'd for $[M+H]^+$ $C_{16}H_{25}N_2O_4$: 287.1971, found 287.1982.

\

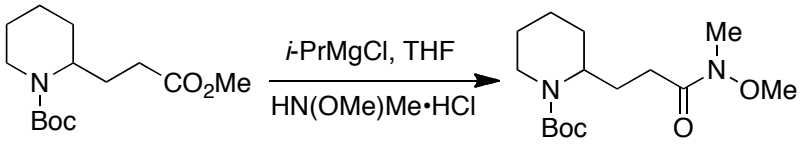

***tert*-Butyl 2-(3-(Methoxy(methyl)amino)-3-oxopropyl)piperidine-1-carboxylate.** The methyl ester precursor to the title compound was prepared in 4 steps (85%) from the precedent of Poon *et al*.[347] The title compound was obtained as a colorless oil using step 2 of Method C:^{1}H NMR (400 MHz, $CDCl_3$) δ1.33-1.50 (m, 1H), 1.45 (s, 9H), 1.56-1.73 (m, 6H), 2.05-2.15 (m, 1H), 2.31-2.49 (m, 2H), 2.75-2.81 (m, 1H), 3.17 (s, 3H), 3.66 (s, 3H), 3.99 (bs, 1H), 4.27 (bs, 1H); ^{13}C NMR (100 MHz, $CDCl_3$) δ19.1, 24.6, 25.6, 28.5, 28.9, 29.1, 32.2, 38.5, 50.2, 61.1, 79.1, 155.1, 174.4; IR (neat) 2936, 1687, 1417, 1365, 1273, 1162 cm^{-1}; HRMS (ESI+) *m/e* calc'd for $[M+H]^+$ $C_{15}H_{29}N_2O_4$: 301.2127, found 301.2132.

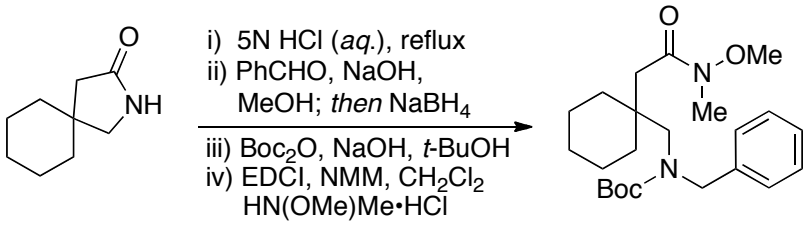

***tert*-Butyl Benzyl ((1 - (2- (methoxy (methyl)amino) 2 - oxoethyl) cyclohexyl) methyl) carbamate.** Spirocyclic lactam (4.0 g, 26 mmol, 1.0 equiv) was dissolved in 5N HCl *aq*. (100 mL). The solution was heated to reflux for 24 h. The solvent was removed *in vacuo* leaving an off-white solid. The solid was redissolved in MeOH (60 mL) and to the solution was added solid NaOH (2.6 g, 65 mmol, 2.5 equiv). When everything had dissolved benzaldehyde (3.7 mL, 37 mmol, 1.4 equiv) was added. After 10 min of stirring, the reaction mixture was cooled to 0 ºC and $NaBH_4$ (1.3 g, 34 mmol, 1.3 equiv) was added and the reaction stirred for 2 h. The solvent was removed under reduced pressure and the residue redissolved in MeOH (50 mL). This was repeated 3 times. The residue was dissolved in *t*-BuOH (60 mL) and di-*tert*-butyldicarbonate (7.4 g, 34 mmol, 1.3 equiv) was added slowly. 10% NaOH was added to the reaction mixture until pH = 12. The reaction was stirred for 5 h keeping the pH at 12 by adding 10% NaOH when appropriate. The reaction was quenched by adding 1N $NaHSO_4$ until the pH reached 2 and EtOAc (150 mL) was added. The product was extracted with EtOAc (3x). The combined organic layers were dried over Na_2SO_4 and purified *via* SiO_2 flash chromatography using 10 % EtOAc in hexanes (1% AcOH) as eluent to afford 5.3 g (56%) of the carboxylic acid as a clear viscous oil. Method A was used to convert the acid into the Weinreb amide. The title compound was obtained as a colorless oil after flash chromatography (25% EtOAc/hexanes): ^{1}H NMR (400 MHz, $CDCl_3$) δ 1.33 (s,

9H), 1.33-1.56 (m, 8H), 1.64-1.71 (m, 2H), 2.51 (s, 2H), 3.15 (s, 3H), 3.39 (bs, 1H), 3.48 (bs, 1H), 3.65 (s, 3H), 4.49 (bs, 2H), 7.18-7.23 (m, 3H), 7.27-7.31 (m, 2H); ^{13}C NMR (100 MHz, $CDCl_3$) δ21.9, 26.0, 28.3, 32.0, 33.9, 35.1, 39.4, 53.3, 54.5, 61.0, 79.4, 126.7, 127.4, 128.3, 139.5, 157.1, 173.4; IR (neat) 2931, 1695, 1454, 1407, 1248, 1165 cm^{-1}; HRMS (ESI+) *m/e* calc'd for $[M+H]^+$ $C_{23}H_{37}N_2O_4$: 405.2753, found 405.2738.

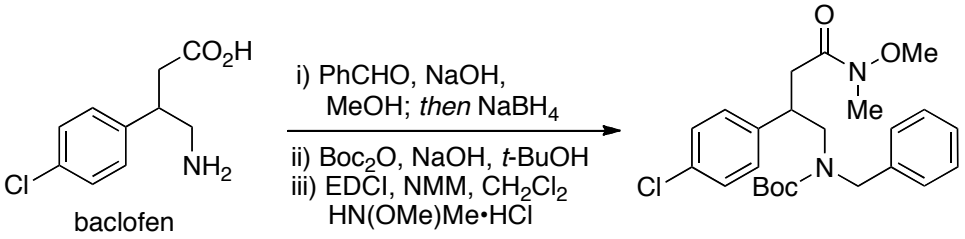

***tert*-Butyl Benzyl(2-(4-chlorophenyl)–4-(methoxy (methyl) amino)-4-oxobutyl) carbamate.** Baclofen (900 mg, 4.2 mmol, 1.0 equiv) was dissolved in MeOH (10 mL) and to the solution was added solid NaOH (190 mg, 4.6 mmol, 1.1 equiv). When everything had dissolved benzaldehyde (0.60 mL, 5.9 mmol, 1.4 equiv) was added. After 10 min of stirring, the reaction mixture was cooled to 0 ºC and $NaBH_4$ (210 mg, 5.5 mmol, 1.3 equiv) was added and the reaction stirred for 2 h. The solvent was removed under reduced pressure and the residue redissolved in MeOH (10 mL). This was repeated three times. The residue was dissolved in *t*-BuOH (10 mL) and di-*tert*-butyldicarbonate (1.2 g, 5.5 mmol, 1.3 equiv) was added slowly. 10% NaOH was added to the reaction mixture until pH = 12. The reaction was stirred for 5 h keeping the pH at 12 by adding 10% NaOH when appropriate. The reaction was quenched by adding 1N $NaHSO_4$ until the pH of the reaction mixture had reached 2. The product was extracted with EtOAc (3x). The combined organic layers were

dried over Na_2SO_4 and purified via SiO_2 flash chromatography using 15 % EtOAc in hexane (1% AcOH) as eluent to afford 1.2 g (69%) of carboxylic acid as a clear viscous oil. Method A was used to convert the acid into the Weinreb amide. The title compound was obtained as a colorless oil after flash chromatography (35% EtOAc/hexanes): ^{1}H NMR (400 MHz, $CDCl_3$) δ (1:1 mixture of rotamers) 1.38 (s, 9H), 1.44 (s, 9H), 2.63-2.84 (m, 4H), 3.08 (s, 6H), 3.25-3.34 (m, 2H), 3.37-3.42 (m, 1H), 3.55-3.66 (m, 3H), 3.59 (s, 6H), 4.13 (d, *J* = 15.6 Hz, 2H), 4.45-4.52 (m, 2H), 7.10-7.31 (m, 18H); ^{13}C NMR (100 MHz, $CDCl_3$) δ 28.3, 32.1, 35.3, 35.5, 39.2, 39.6, 49.7, 50.1, 50.8, 51.5, 61.2, 79.9, 127.2, 127.9, 128.5, 128.6, 129.3, 132.4, 132.4, 138.0, 138.1, 140.8, 155.8, 172.1, 172.4; IR (neat) 2975, 1693, 1416, 1366, 1165, 701 cm^{-1}; HRMS (ESI+) *m/e* calc'd for $[M+H]^+$ $C_{24}H_{32}ClN_2O_4$: 447.2051, found 447.2053.

6.3.2 Preparation of ynones:

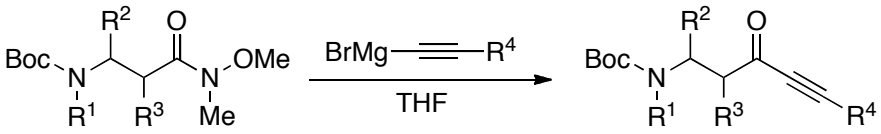

The Weinreb amide (2.52 mmol, 1.00 equiv) was dissolved in anhydrous THF (40 mL) under an argon atmosphere and cooled to 0 °C. To this reaction vessel, was added dropwise, a solution of ethynyl magnesium bromide reagent (12.6 mmol, 5.00 equiv) in THF and allowed to come to room temperature. After the reaction was judged complete by TLC it was quenched by the addition of an ice cold 10% HCl solution (15 mL) and allowed to stir at this temperature for 5 min. The reaction was diluted with water and extracted with EtOAc (x3).

The combined organic layers were washed with saturated $NaHCO_3$ (x1), dried over Na_2SO_4, filtered and concentrated. This crude material was purified via flash chromatography using EtOAc in hexanes as eluent to provide pure *N*-Boc-ynone.

Compounds previously reported in Turunen and Georg.[255]

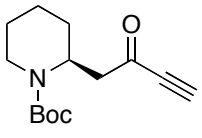

2.14

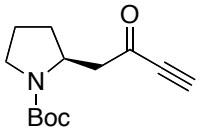

2.17

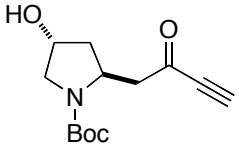

2.23

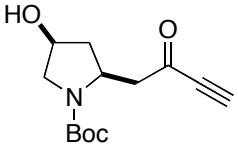

2.24

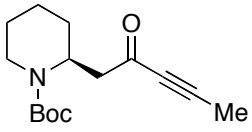

2.15

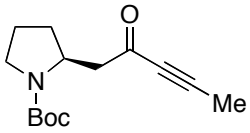

2.18

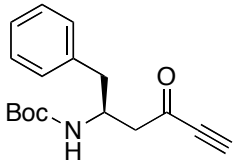

2.29

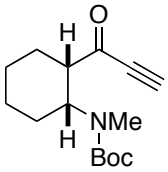

2.26

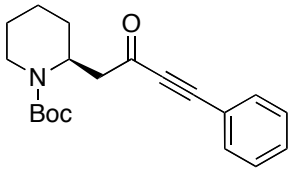

2.16

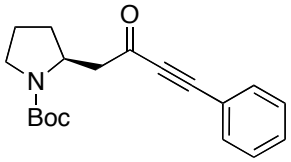

2.19

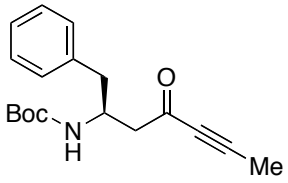

2.30

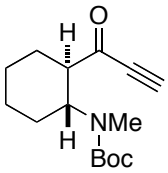

2.27

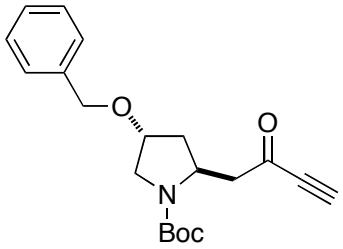

2.20

(2*S,4*R**)-*tert*-Butyl 4-(Benzyloxy)-2-(2-oxobut-3-ynyl)pyrrolidine-1-carboxylate (2.20).** The title compound was obtained as a colorless oil (92%) after flash chromatography (20% EtOAc/hexanes): ^{1}H NMR (400 MHz, $CDCl_3$) δ (1:1 mixture of rotamers) 1.46 (s, 9H), 1.48 (s, 9H), 1.77-1.87 (bm, 2H), 2.35 2.35 (dddd, *J* = 13.3, 7.7, 3.9, 1.0 Hz, 2H), 2.65-2.73 (bm, 2H), 3.16 (bd, *J* = 15.3 Hz, 1H), 3.26 (bd, *J* = 16.9 Hz, 2 H), 3.35-3.42 (m, 3H), 3.56 (bd, *J* = 11.3 Hz, 1H), 3.78 (bd, *J* = 11.6 Hz, 1H), 4.06-4.10 (m, 2H), 4.30-4.38 (bm, 2H), 4.44-4.55 (bm, 2H), 4.50 (bd, *J* = 10.2 Hz, 2H), 7.28-7.36 (m, 10H); ^{13}C NMR (100 MHz, $CDCl_3$) δ 28.5, 36.9, 38.2, 49.7, 50.9, 51.1, 51.9, 52.2, 70.9, 75.6, 76.1, 78.8, 79.1, 79.7, 80.3, 81.5, 127.6, 127.7, 127.7, 128.5, 137.9, 154.4, 154.5, 185.0, 185.3; IR (neat) 2976, 2091, 1685, 1399, 1367, 1162 cm^{-1}; HRMS (ESI+) *m/e* calc'd for $[M+H]^+$ $C_{20}H_{26}NO_4$: 344.1862, found 344.1854.

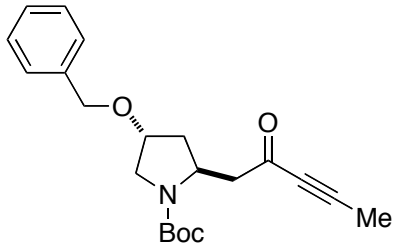

2.21

(2*S*,4R)-*tert*-Butyl 4-(Benzyloxy)-2-(2-oxopent-3-ynyl)pyrrolidine-1-carboxylate (2.21).** The title compound was obtained as a colorless oil (90%) after flash chromatography (20% EtOAc/hexanes): ^{1}H NMR (400 MHz, $CDCl_3$) δ (1:1 mixture of rotamers) 1.46 (s, 9H), 1.48 (s, 9H), 1.80-1.88 (m, 2H), 2.01 (s, 6H), 2.33 (dddd, *J* = 13.5, 7.7, 4.1, 1.5 Hz, 2H), 2.60 (dd, *J* = 15.8, 9.2 Hz, 2H), 3.09 (bd, *J* = 14.7 Hz, 1H), 3.34-3.44 (m, 3H), 3.55 (bd, *J* = 10.4 Hz, 1H), 3.75 (bd, *J* = 11.4 Hz, 1H), 4.09 (p, *J* = 1.2 Hz, 2H), 4.29-4.37 (m, 2H), 4.46-4.54 (m, 4H), 7.26-7.36 (m, 10H); ^{13}C NMR (100 MHz, $CDCl_3$) δ 4.1, 28.5, 36.8, 38.1, 49.6, 50.9, 51.0, 51.9, 52.5, 70.9, 75.7, 76.2, 79.6, 80.0, 80.4, 127.6, 127.7, 127.7, 128.5, 137.9, 154.4, 185.8, 186.0; IR (neat) 2975, 2219, 1694, 1398, 1366, 1166 cm^{-1}; HRMS (ESI+) *m/e* calc'd for $[M+H]^+$ $C_{21}H_{28}NO_4$: 358.2018, found 358.2003.

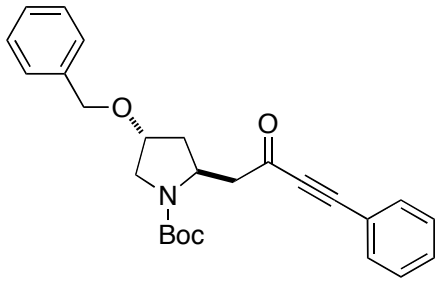

2.22

(2*S,4*R**)-*tert*-Butyl 4-(Benzyloxy)-2-(2-oxo-4-phenylbut-3-ynyl)pyrrolidine-1-carboxylate (2.22).** The title compound was obtained as a yellow oil (85%) after flash chromatography (15% EtOAc/hexanes): ^{1}H NMR (400 MHz, $CDCl_3$) δ (1:1 mixture of rotamers) 1.46 (s, 9H), 1.50 (s, 9H), 1.87-1.94 (bm, 2H), 2.36-2.42 (bm, 2H), 2.75-2.83 (bm, 2H), 3.22 (bd, *J* = 14.5 Hz, 1H), 3.41-3.53 (bm, 3H), 3.58 (bd, *J* = 10.7 Hz, 1H), 3.79 (bd, *J* = 11.2 Hz, 1H), 4.11 (p, *J* = 4.1 Hz, 2H), 4.38-4.44 (bm, 2H), 4.46-4.55 (m, 2H), 4.5 (d, *J* = 10.7 Hz, 2H), 7.27-7.41 (m, 14H), 7.43-7.48 (bm, 2H), 7.57 (d, *J* = 7.12 Hz, 4H); ^{13}C NMR (100 MHz, $CDCl_3$) δ 28.5, 36.9, 38.2, 49.6, 50.9, 51.1, 52.0, 52.6, 70.9, 75.7, 76.2, 79.6, 80.2, 88.0, 91.0, 91.4, 119.7, 119.9, 127.6, 127.7, 127.7, 128.4, 128.6, 128.7, 130.7, 130.9, 133.1, 137.9, 154.5, 185.6, 185.9; IR (neat) 2975, 2203, 1692, 1397, 1366, 1160 cm^{-1}; HRMS (ESI+) *m/e* calc'd for $[M+H]^+$ $C_{26}H_{30}NO_4$: 420.2175, found 420.2157.

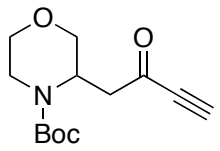

2.25

***tert*-Butyl 3-(2-Oxobut-3-ynyl)morpholine-4-carboxylate (2.25).** The title compound was obtained as a white solid (95%) after flash chromatography (20% EtOAc/hexanes): mp 86.3-86.7 °C ^{1}H NMR (400 MHz, $CDCl_3$) δ 1.46 (s, 9H), 2.87 (dd, *J* = 15.8, 5.4 Hz, 1H), 3.08-3.16 (m, 2H), 3.34 (s, 1H), 3.46 (dt, *J* = 11.8, 2.5 Hz, 1H), 3.59 (dd, *J* = 11.8, 2.8 Hz, 1H), 3.71-3.90 (m, 3H), 4.43-4.52 (bm, 1H); ^{13}C NMR (100 MHz, $CDCl_3$) δ 28.3, 39.0, 44.6,

47.9, 66.8, 69.0, 79.0, 80.7, 81.5, 154.3, 184.7; IR (neat) 2977, 2092, 1685, 1408, 1367, 1170 cm^{-1}; HRMS (ESI+) *m/e* calc'd for $[M+H]^+$ $C_{13}H_{20}NO_4$: 254.1392, found 254.1386.

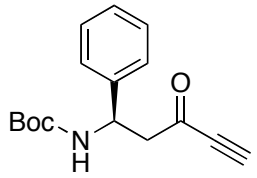

2.28

(*R*)-*tert*-Butyl 3-Oxo-1-phenylpent-4-ynylcarbamate (2.28). The title compound was obtained as a off-white solid (76%) after flash chromatography (20% EtOAc/hexanes): mp 94.1-95.4 ºC; ^{1}H NMR (400 MHz, $CDCl_3$) δ 1.42 (s, 9H), 3.08 (dd, *J* = 16.2, 6.1 Hz, 1H), 3.18-3.24 (bm, 1H), 3.27 (s, 1H), 5.16 (bs, 1H), 5.23 (bs, 1H), 7.25-7.36 (m, 5H); ^{13}C NMR (100 MHz, $CDCl_3$) δ 28.3, 50.9, 51.3, 79.9, 79.9, 81.1, 126.3, 127.7, 128.8, 140.7, 154.9, 184.3; IR (neat) 3270, 2979, 2094, 1687, 1367, 1169 cm^{-1}; HRMS (ESI+) *m/e* calc'd for $[M+H]^+$ $C_{16}H_{20}NO_3$: 274.1443, found 274.1452; $[\alpha]_D^{22} = -20$ (*c* 0.61, $CHCl_3$).

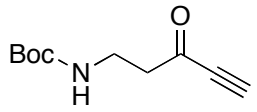

2.31

***tert*-Butyl 3-Oxopent-4-ynylcarbamate (2.31).** The title compound was obtained as a colorless oil (89%) after flash chromatography (25% EtOAc/hexanes): ^{1}H NMR (400 MHz, $CDCl_3$) δ 1.43 (s, 9H), 2.86 (t, *J* = 5.8 Hz, 2H), 3.32 (s, 1H), 3.42 (dt, *J* = 5.96, 5.96 Hz, 2H)

4.97 (bs, 1H); ^{13}C NMR (100 MHz, $CDCl_3$) δ 28.4, 34.9, 45.6, 79.4, 79.5, 81.2, 155.7, 186.1; IR (neat) 3353, 2979, 2093, 1683, 1515, 1172 cm^{-1}; HRMS (ESI+) *m/e* calc'd for $[M+H]^+$ $C_{10}H_{16}NO_3$: 198.1130, found 198.1121.

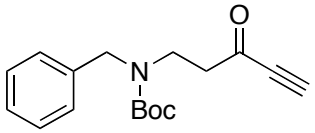

2.32

***tert*-Butyl Benzyl(3-oxopent-4-ynyl)carbamate (2.32).** The title compound was obtained as a colorless oil (89%) after flash chromatography (20% EtOAc/hexanes): ^{1}H NMR (400 MHz, $CDCl_3$) δ (1:1 mixture of rotamers) 1.45 (s, 9H), 1.50 (s, 9H), 2.75-2.80 (bm, 2H), 2.86-2.91 (bm, 2H), 3.24 (s, 2H), 3.45-3.55 (bm, 4H), 4.45 (bs, 4H), 7.21-7.35 (m, 10H); ^{13}C NMR (100 MHz, $CDCl_3$) δ 28.4, 41.5, 41.9, 44.3, 44.6, 50.5, 51.6, 79.1, 80.3, 81.3, 127.2, 127.8, 127.3, 128.6, 138.2, 155.4, 185.3; IR (neat) 2977, 2092, 1684, 1415, 1367, 1165 cm^{-1}; HRMS (ESI+) *m/e* calc'd for $[M+H]^+$ $C_{17}H_{22}NO_3$: 288.1600, found 288.1594.

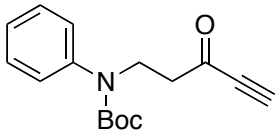

2.33

***tert*-Butyl 3-Oxopent-4-ynyl(phenyl)carbamate (2.33).** The title compound was obtained as a colorless oil (99%) after flash chromatography (15% EtOAc/hexanes): ^{1}H NMR (400

MHz, $CDCl_3$) δ 1.42 (s, 9H), 2.89 (t, *J* = 7.2, 2H), 3.24 (s, 1H), 3.99 (t, *J* = 7.2 Hz, 2H), 7.16-7.23 (m, 3H), 7.32-7.36 (m, 2H); ^{13}C NMR (100 MHz, $CDCl_3$) δ 28.3, 44.3, 45.1, 79.1, 80.7, 81.2, 126.5, 127.2, 128.9, 141.9, 154.4, 185.0; IR (neat) 2978, 2092, 1694, 1393, 1368, 1163 cm^{-1}; HRMS (ESI+) *m/e* calc'd for $[M+H]^+$ $C_{16}H_{20}NO_3$: 274.1443, found 274.1445.

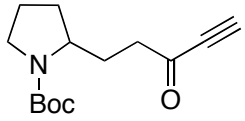

2.57

***tert*-Butyl 2-(3-Oxopent-4-ynyl)pyrrolidine-1-carboxylate (2.57).** The title compound was obtained as a colorless oil (90%) after flash chromatography (20% EtOAc/hexanes): ^1H NMR (400 MHz, $CDCl_3$) δ (1:1 mixture of rotamers) 1.47 (s, 9H), 1.58-1.66 (m, 1H), 1.73-2.01 (m, 5H), 2.59-2.68 (m, 2H), 3.25-3.48 (m, 2H), 3.26 (s, 1H), 3.80-3.91 (m, 1H); ^{13}C NMR (100 MHz, $CDCl_3$) δ 23.0, 23.7, 28.5, 30.2, 30.9, 42.4, 42.6, 46.1, 46.5, 78.6, 79.1, 79.5, 81.4, 154.8, 186.6, 186.9; IR (neat) 2974, 2090, 1686, 1396, 1171, 1112 cm^{-1}; HRMS (ESI+) *m/e* calc'd for $[M+H]^+$ $C_{14}H_{22}NO_3$: 252.1600, found 252.1599.

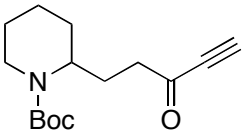

2.58

***tert*-Butyl 2-(3-Oxopent-4-ynyl)piperidine-1-carboxylate (2.58).** The title compound was obtained as a colorless oil (95%) after flash chromatography (20% EtOAc/hexanes): ^{1}H NMR (400 MHz, $CDCl_3$) δ 1.34-1.48 (m, 2H), 1.46 (s, 9H), 1.51-1.75 (m, 5H), 2.06-2.15 (m, 1H), 2,51-2.67 (m, 2H), 2.72 (bdd, *J* = 13.0, 13.0 Hz, 1H), 3.25 (s, 1H), 3.98 (bs, 1H), 4.25 (bs, 1H); ^{13}C NMR (100 MHz, $CDCl_3$) δ 19.0, 23.4, 25.5, 28.4, 29.0, 38.6, 42.3, 49.5, 78.5, 79.5, 81.5, 155.1, 186.6; IR (neat) 2936, 2090, 1683, 1418, 1366, 1162 cm^{-1}; HRMS (ESI+) *m/e* calc'd for $[M+H]^+$ $C_{15}H_{24}NO_3$: 266.1756, found 266.1750.

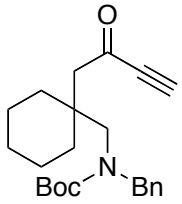

2.59

***tert*-Butyl Benzyl((1-(2-oxobut-3-ynyl)cyclohexyl)methyl)carbamate (2.59).** The title compound was obtained as a colorless oil (93%) after flash chromatography (15% EtOAc/ hexanes): ^{1}H NMR (400 MHz, $CDCl_3$) δ 1.26-1.68 (m, 19H), 2.73 (s, 2H), 3.15 (s, 1H), 3.35 (bs, 2H), 4.47 (bs, 2H), 7.16-7.25 (m, 3H), 7.29-7.32 (m, 2H); ^{13}C NMR (100 MHz, $CDCl_3$) δ 21.7, 25,9, 28.3, 33.9, 40.3, 49.3, 53.2, 54.5, 79.8, 82.8, 126.8, 126.9, 128.4, 139.0, 157.0, 186.5; ^{13}C NMR (100 MHz, $CDCl_3$) δ 21.7, 25.9, 28.3, 33.9, 40.3, 49.3, 53.2, 54.6, 79.8, 80.3, 82.8, 126.8, 126.9, 128.4, 138.9, 157.0, 186.5; IR (neat) 2930, 2090, 1692, 1409, 1248, 1164 cm^{-1}; HRMS (ESI+) *m/e* calc'd for $[M+H]^+$ $C_{23}H_{32}NO_3$: 370.2382, found 370.2385.

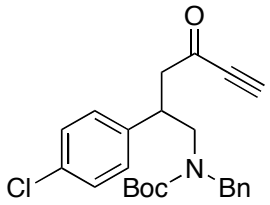

2.60

***tert*-Butyl Benzyl(2-(4-chlorophenyl)-4-oxohex-5-ynyl)carbamate (2.60).** The title compound was obtained as a colorless oil (95%) after flash chromatography (15% EtOAc / hexanes): ^{1}H NMR (400 MHz, $CDCl_3$) δ (1:1 mixture of rotamers) 1.41 (s, 9H), 1.46 (s, 9H), 2.85-3.04 (m, 4H), 3.20 (s, 2H), 3.21 (dd, *J* = 13.9, 7.7 Hz, 2H), 3.32-3.39 (m, 1H), 3.55-3.70 (m, 3H), 4.07 (bs, 1H), 4.11 (bs, 1H), 4.37-4.46 (m, 2H), 7.05-7.18 (m, 8H), 7.23-7.32 (m, 10H); ^{13}C NMR (100 MHz, $CDCl_3$) δ 28.3, 38.9, 39.3, 48.6, 48.9, 50.2, 50.8, 51.6, 79.1, 80.3, 81.3, 127.2, 127.3, 127.8, 128.6, 128.8, 129.1, 132.9, 137.9, 139.5, 155.9; IR (neat) 2976, 2092, 1686, 1413, 1366, 1164 cm^{-1}; HRMS (ESI+) *m/e* calc'd for $[M+Na]^+$ $C_{24}H_{26}NO_3ClNa$: 434.1493, found 434.1479.

6.3.3 Preparation of cyclic enaminones

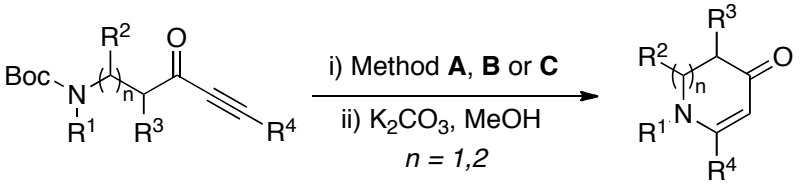

Representative procedures for deprotection:

METHOD A: The ynone (0.50 mmol) was dissolved in a 4N HCl-dioxane solution (1.5 mL) and allowed to react for 15 min. After this time the dioxane and excess HCl were

allowed to evaporate while passing air over the reaction mixture. The remaining solid was placed under vacuum for 15 min and carried on to the cyclization step without further purification.

METHOD B: The ynone (0.50 mmol, 1.0 equiv) was dissolved in 98% formic acid (5.0 mL) under a N_2 atmosphere and NaI (230 mg, 1.5 mmol, 3.0 equiv) was added. *Note*: *For terminal ynones the reaction was left stirring for 6 h. When internal ynones were used the reaction was left for 24 h.* The solvent was removed by passing N_2 over the reaction mixture. The remaining residue was placed under vacuum for 15 min and was carried on to the cyclization step without further purification.

Large Scale Modification: When using greater that 1.0 gram of ynone, the desired deprotected amine can be isolated by pouring the reaction mixture into ether and filtering the precipitate.

METHOD C: The ynone (0.50 mmol, 1.0 equiv) was dissolved in anhydrous CH_2Cl_2 (10 mL) under an argon atmosphere and cooled to –78 °C. A solution of TMS-I (0.50 mmol, 1.0 equiv) in anhydrous CH_2Cl_2 (5 mL) was then added dropwise at this temperature. After 20 min at this temperature the reaction was allowed to warm to 0 °C and additional TMS-I (0.50-2.5 mmol) was added until all starting material was consumed (TLC, 25% EtOAc in hexanes). After 20 min the reaction was judged complete and this mixture was concentrated under reduced pressure and placed under vacuum for 15 min.

Representative procedures for cyclization:

The deprotected intermediates from Methods A, B and C were dissolved in MeOH (50 mL) and excess K_2CO_3 (a minimum of 5.0 equiv) was added. The reactions were stirred for various lengths of time depending on the substrate (For enaminones **2.37**, **2.41**, **2.35**, **2.48**, **2.36** and **2.50** reactions were stirred for 1 h; for enaminones **2.34**, **2.49**, **2.52**, **2.51**, **2.54** and **2.55** reactions were stirred for 3 h; for enaminones **2.46**, **2.47**, **2.39**, **2.40**, **2.42**, **2.43**, **2.53**, **2.56**, **2.61**, **2.62**, **2.63** and **2.64** reactions were stirred for 6 h). At this time CH_2Cl_2 was added, the reaction suction filtered, and the organic solvents concentrated. To the solid residue was added more CH_2Cl_2 and the precipitates were once again filtered away. This residue was purified via flash chromatography to provide pure enaminone.

Large Scale Modification: When the reaction was complete, the MeOH was removed *in vacuo* and the remaining residue redissolved in brine. The product was extracted with CH_2Cl_2 (3x). The combined organic layers were dried over Na_2SO_4 and purified via SiO_2 flash chromatography. *Note: Several of the enaminones (e.g.* ***2.34****,* ***2.37****,* ***2.35***, ***2.48***, *etc.) were water soluble and could not be purified by this method.*

Compounds previously reported by Turunen and Georg.[255]

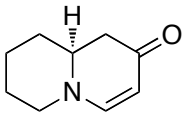

2.34

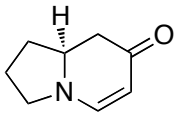

2.37

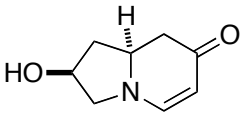

2.35

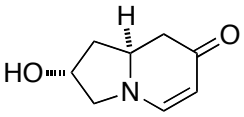

2.48

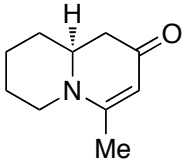

2.46

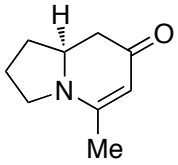

2.39

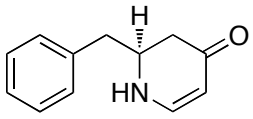

2.52

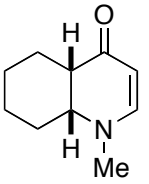

2.36

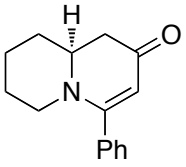

2.47

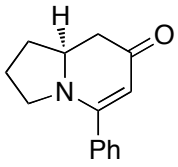

2.40

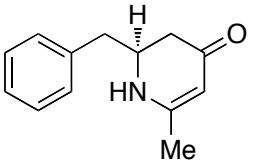

2.53

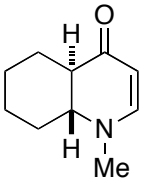

2.50

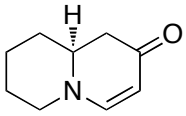

2.34

(*S*)-7,8,9,9a-Tetrahydro-1*H*-quinolizin-2(6*H*)-one (2.34). Spectral data of the title compound was identical to that reported in the literature[255] with the exception of optical rotation: Comparison to the reported value, $[\alpha]_D^{22} = -146$ (*c* 0.885, $CHCl_3$), indicated an ee of 93% and 99% for Method A ($[\alpha]_D^{22} = -135$ (*c* 0.925, $CHCl_3$)) and Method B ($[\alpha]_D^{22} = -145$ (*c* 1.15, $CHCl_3$)), respectively. These enantiomeric ratios were verified via chiral HPLC

using a Baker Chiralcel OJ column. Conditions: *i*-PrOH 2-15% in hexanes, 60 min, 0.5 mL/ min, 30 °C. (–)-Enantiomer: R_t = 40.1 min; (+)-Enantiomer: R_t = 41.6 min. Method A: ee = 94%. Method B: ee = 96%.

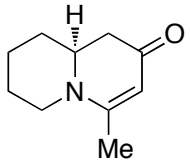

2.46

(*S*)-4-Methyl-7,8,9,9a-tetrahydro-1*H*-quinolizin-2(6*H*)-one (2.46). Spectral data of the title compound was identical to that reported in the literature.[255] The optical rotation, however, has not been previously reported: Enantiomeric ratios were determined via chiral HPLC using a Chiralcel OD column. Conditions: *i*-PrOH 1-25% in hexanes, 60 min, 1.0 mL/min, 30 °C. (–)-Enantiomer: R_t = 36.3 min; (+)-Enantiomer: R_t = 39.6 min. Method A: ee = 44%; Method B: ee = 44%. Method A and B $[\alpha]_D^{22}$ = –95.0 (*c* 0.924, $CHCl_3$).

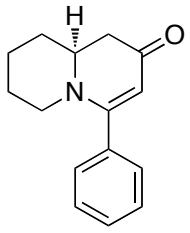

2.47

(*S*)-4-Phenyl-7,8,9,9a-tetrahydro-1*H*-quinolizin-2(6*H*)-one (2.47). Spectral data of the title compound was identical to that reported in the literature.[255] The optical rotation, however, has not been previously reported: Enantiomeric ratios were determined via chiral

HPLC using a Chiralcel AD-H column. Conditions: *i*-PrOH 1-20% in hexanes, 40 min, 1.0 mL/min, 30 °C. (–)-Enantiomer: R_t = 30.4 min; (+)-Enantiomer: R_t = 29.0 min. Method A: ee = 16%; Method B: ee = 38%. Method A $[\alpha]_D^{22}$ = –4.2 (*c* 1.00, $CHCl_3$); Method B $[\alpha]_D^{22}$ = –10.7 (*c* 1.00, $CHCl_3$).

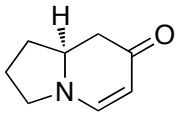

2.37

(*S*)-2,3,8,8a-Tetrahydroindolizin-7(1*H*)-one (2.37). Spectral data of the title compound was identical to that reported in the literature[255] with the exception of optical rotation. Method A: ee = 40%. Method B: ee = 96%; Method A $[\alpha]_D^{22}$ = –180 (*c* 1.00, $CHCl_3$); Method B $[\alpha]_D^{22}$ = –727 (*c* 1.00, $CHCl_3$); Method C $[\alpha]_D^{22}$ = –628 (*c* 1.00, $CHCl_3$). Enantiomeric ratios were determined via chiral HPLC using a Chiralcel OJ column after converting enaminone **2.37** to aryl derivative **3.2**. Conditions for arylenaminone **3.2**: *i*-PrOH 70% in hexanes, 30 min, 1.0 mL/min, 30 °C. (–)-Enantiomer: R_t = 20.9 min; (+)-Enantiomer: R_t = 11.1 min.

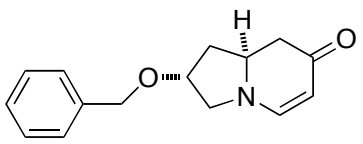

2.41

(2*R, 8a*S**)-2-(Benzyloxy)-2,3,8,8a-tetrahydroindolizin-7(1*H*)-one (2.41).** The title compound was obtained as a colorless oil (*Method A, 94%; Method B, 92%)* after flash chromatography (100% acetone): ^{1}H NMR (400 MHz, $CDCl_3$) δ 1.77 (ddd, *J* = 13.2, 11.2, 4.5 Hz, 1H), 2.35 (dd, *J* = 16.2, 16.2 Hz, 1H), 2.44-2.51 (m, 2H), 3.60 (d, *J* = 11.8 Hz, 1H), 3.70 (dd, *J* = 11.8, 4.9 Hz, 1H), 4.07 (dddd, *J* = 16.4, 10.9, 5.3, 5.3 Hz, 1H), 4.29 (dd, *J* = 4.5, 4.5 Hz, 1H), 4.51 (d, *J* = 11.8 Hz, 1H), 4.56 (d, *J* = 11.8 Hz, 1H), 4.99 (d, *J* = 7.1 Hz, 1H), 7.17 (d, *J* = 7.1 Hz, 1H), 7.29-7.38 (m, 5H); ^{13}C NMR (100 MHz, $CDCl_3$) δ 38.5, 41.4, 55.4, 56.2, 71.0, 77.1, 97.9, 127.6, 128.0, 128.6, 137.5, 149.9, 191.9; IR (neat) 2929, 1631, 1579, 1460, 1306, 1099 cm^{-1}; HRMS (ESI+) *m/e* calc'd for $[M+H]^+$ $C_{15}H_{18}NO_2$: 244.1338, found 244.1332.

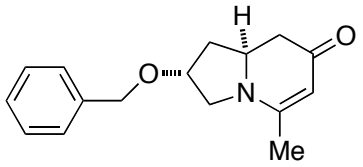

anti-**2.42**

(2*R,8a*S**)-2-(Benzyloxy)-5-methyl-2,3,8,8a-tetrahydroindolizin-7(1*H*)-one (*anti*-2.42).** The title compound was obtained as a colorless oil [*Method A, 87% (d.r. 63:37); Method B, 94% (d.r. 68:32)]* after flash chromatography (1-10% MeOH/EtOH): ^{1}H NMR (400 MHz, $CDCl_3$) δ1.67 (ddd, *J* = 13.3, 11.4, 4.5 Hz, 1H), 1.92 (s, 3H), 2.22 (dd, *J* = 16.1, 16.1 Hz, 1H), 2.36-2.43 (m, 2H), 3.33 (d, *J* = 12.16 Hz, 1H), 3.61 (dd, *J* = 12.2, 4.7 Hz, 1H), 4.00 (dddd, *J* = 16.3, 10.7, 5.0, 5.0 Hz, 1H), 4.22 (dd, *J* = 4.5, 4.5 Hz, 1H), 4.43 (d, *J* = 11.8 Hz, 1H), 4.51 (d, *J* = 11.8 Hz, 1H), 4.89 (s, 1H), 7.22-7.31 (m, 5H); ^{13}C NMR (100 MHz, $CDCl_3$)

δ20.4, 38.3, 41.0, 53.5, 56.8, 71.0, 76.3, 98.5, 127.6, 128.0, 128.6, 137.5, 160.8, 191.3; IR (neat) 2928, 1622, 1550, 1497, 1431, 1093 cm^{-1}; HRMS (ESI+) *m/e* calc'd for $[M+H]^+$ $C_{19}H_{20}NO_2$:, 258.1494, found 258.1491.

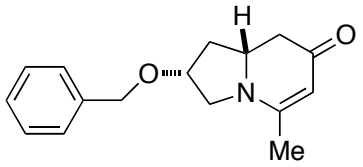

syn-**2.42**

(2*R, 8a*R**)-2-(Benzyloxy)-5-methyl-2,3,8,8a-tetrahydroindolizin-7(1*H*)-one (*syn*-2.42).** This compound is the minor diastereomer of the above reaction. The compound was obtained as a colorless oil after flash chromatography (1-10% MeOH/EtOH): ^1H NMR (400 MHz, $CDCl_3$) δ1.79 (ddd, *J* = 12.5, 10.0, 7.7 Hz, 1H), 1.89 (s, 3H), 2.33 (d, *J* = 16.0 Hz, 1H), 2.39 (d, *J* = 16.0 Hz, 1H), 2.49 (ddd, *J* = 12.7, 6.4, 6.4 Hz, 1H), 3.41 (dd, *J* = 11.2, 5.6 Hz, 1H), 3.60 (dd, *J* = 11.2, 7.0 Hz, 1H), 3.71 (dddd, *J* = 16.4, 10.0, 6.6, 6.6 Hz, 1H), 4.19 (m, 1H), 4.44 (d, *J* = 11.8 Hz, 1H), 4.53 (d, *J* = 11.8 Hz, 1H), 4.87 (s, 1H), 7.23-7.32 (m, 5H); ^{13}C NMR (100 MHz, $CDCl_3$) δ20.4, 38.3, 41.5, 52.3, 57.4, 71.9, 76.0, 98.9, 127.7, 128.1, 128.6, 137.5, 160.7, 191.3; IR (neat) 2870, 1623, 1551, 1496, 1432, 1125 cm^{-1}; HRMS (ESI+) *m/e* calc'd for $[M+H]^+$ $C_{16}H_{20}NO_2$: 258.1494, found 258.1493.

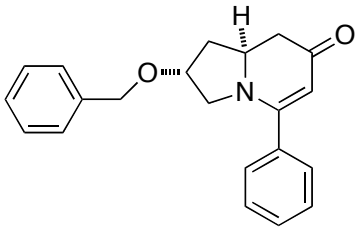

anti-**2.43**

(2*R,8a*S**)-2-(Benzyloxy)-5-phenyl-2,3,8,8a-tetrahydroindolizin-7(1*H*)-one (*anti*-2.43).** The title compound was obtained as a colorless oil [*Method A, 85% (d.r. 63:37); Method B, 88% (d.r. 60:40)]* after flash chromatography (1-10% MeOH/EtOH): ^{1}H NMR (400 MHz, $CDCl_3$) δ 1.80 (ddd, *J* = 13.3, 9.9, 4.7 Hz, 1H), 2.38-2.48 (m, 3H), 3.37 (dd, *J* = 12.3, 4.8 Hz, 1H), 3.52 (d, *J* = 12.3 Hz, 1H), 4.12-4.15 (m, 1H), 4.22 (dddd, *J* = 15.6, 10.3, 5.9, 5.9 Hz, 1H), 4.40 (d, *J* = 11.9 Hz, 1H), 4.48 (d, *J* = 11.9 Hz, 1H), 5.03 (s, 1H), 7.21-7.36 (m, 10H); ^{13}C NMR (100 MHz, $CDCl_3$) δ 38.0, 41.4, 54.5, 57.1, 71.1, 76.2, 100.4, 127.5, 127.6, 127.9, 128.6, 128.6, 129.8, 135.9, 137.6, 162.8, 191.8; IR (neat) 2930, 1627, 1531, 1470, 1241, 701 cm^{-1}; HRMS (ESI+) *m/e* calc'd for $[M+H]^+$ $C_{21}H_{22}NO_2$: 320.1651, found 320.1638.

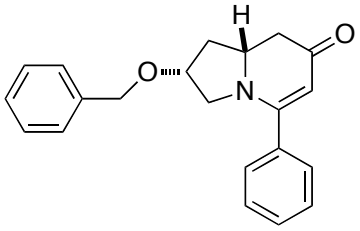

syn-**2.43**

(2*R,8a*R**)-2-(Benzyloxy)-5-phenyl-2,3,8,8a-tetrahydroindolizin-7(1*H*)-one (*syn*-2.43).** This compound is the minor diastereomer of the above reaction. The compound was obtained

as a colorless oil after flash chromatography (1-10% MeOH/EtOH): ^{1}H NMR (400 MHz, $CDCl_3$) δ1.94-2.00 (m, 1H), 2.34 (dd, *J* = 16.1, 4.1 Hz, 1H), 2.43 (ddd, *J* = 13.5, 7.9, 5.6 Hz, 1H), 2.74 (dd, *J* = 16.2, 16.2 Hz, 1H), 3.32 (dd, *J* = 11.8, 3.0 Hz, 1H), 3.53 (dd, *J* = 11.8, 5.2 Hz, 1H), 4.05-4.14 (m, 2H), 4.35 (d, *J* = 11.9 Hz, 1H), 4.43 (d, *J* = 11.8 Hz, 1H), 5.08 (s, 1H), 7.18-7.38 (m, 10H); ^{13}C NMR (100 MHz, $CDCl_3$) δ36.9, 41.8, 54.9, 57.9, 71.3, 77.3, 100.6, 127.5, 127.8, 127.9, 128.5, 128.6, 130.1, 136.0, 137.5, 162.9, 192.4; IR (neat) 2926, 1626, 1529, 1467, 1242, 700 cm^{-1}; HRMS (ESI+) *m/e* calc'd for $[M+H]^+$ $C_{21}H_{22}NO_2$: 320.1651, found 320.1640.

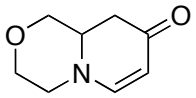

2.49

3,4,9,9a-Tetrahydropyrido[2,1-*c*][1,4]oxazin-8(1*H*)-one (2.49). The title compound was obtained as a white solid (*Method A, 80%; Method B, 95%)* after flash chromatography (100% acetone): mp 58.1-60.2 °C; ^{1}H NMR (400 MHz, $CDCl_3$) δ2.27 (dd, *J* = 16.3, 14.2 Hz, 1H), 2.33 (dd, *J* = 16.5, 6.2 Hz, 1H), 3.21-3.29 (m, 2H), 3.39 (dd, *J* = 10.9, 10.9 Hz, 1H), 3.49-3.57 (m, 1H), 3.65 (ddd, *J* = 11.5, 10.0, 4.6 Hz, 1H), 3.91-3.98 (m, 2H), 5.06 (d, *J* = 7.7 Hz, 1H), 6.89 (d, *J* = 7.7 Hz, 1H); ^{13}C NMR (100 MHz, $CDCl_3$) δ37.9, 50.2, 55.3, 66.5, 70.7, 100.6, 154.1, 191.1; IR (neat) 2854, 1639, 1590, 1445, 1223, 1121 cm^{-1}; HRMS (ESI+) *m/e* calc'd for $[M+H]^+$ $C_8H_{12}NO_2$: 154.0868, found 154.0859.

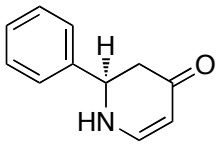

2.51

(*R*)-2-Phenyl-2,3-dihydropyridin-4(1*H*)-one (2.51). The title compound was obtained as a white solid [*Method A, 50% (*e.r. > 99:1*); Method B, 50% (*e.r. > 99:1)] after flash chromatography (90% acetone/hexanes): mp 107.7-110.9 °C; ^{1}H NMR (400 MHz, $CDCl_3$) δ 2.39 (dd, *J* = 16.3, 5.0 Hz, 1H), 2.62 (dd, *J* = 16.3, 14.6 Hz, 1H), 4.68 (dd, *J* = 14.6, 5.0 Hz, 1H), 4.99 (d, *J* = 7.3 Hz, 1H), 5.93 (bs, 1H), 7.25-7.38 (m, 6H); ^{13}C NMR (100 MHz, $CDCl_3$) δ 44.3, 58.2, 99.0, 126.6, 128.4, 128.9, 139.9, 151.8, 192.4; IR (neat) 3234, 3030, 1620, 1571, 1233, 699 cm^{-1}; HRMS (ESI+) *m/e* calc'd for $[M+H]^+$ $C_{11}H_{12}NO$: 174.0919, found 174.0918; $[\alpha]_D^{22} = +233$ (*c* 0.720, $CHCl_3$) [Lit. +332.3 (*c* 2.42, EtOH)].[236] Enantiomeric ratios were determined via chiral HPLC using a Chiralcel OD column. Conditions: *i*-PrOH 1-25% in hexanes, 60 min, 1.0 mL/min, 30 °C. (–)-Enantiomer: R_t = 48.0 min; (+)-Enantiomer: R_t = 45.2 min.

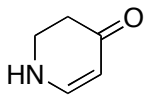

2.54

2,3-Dihydropyridin-4(1*H*)-one (2.54). The title compound was obtained as a colorless oil (*Method A, 70%; Method B, 92%)* after flash chromatography (10% EtOH/EtOAc): ^{1}H NMR (400 MHz, CD_3OD) δ 2.31 (t, *J* = 8.1 Hz, 2H), 3.45 (t, *J* = 8.1 Hz, 2H), 4.82 (d, *J* = 7.0 Hz,

1H), 7.32 (d, *J* = 7.0 Hz, 1H) ^{13}C NMR (100 MHz, CD_3OD) δ 36.1, 41.9, 99.3, 151.8, 192.8; IR (neat) 3041, 1575, 1409, 1351, 1245, 1174 cm^{-1}; HRMS (ESI+) *m/e* calc'd for $[M+Na]^+$ $C_5H_7NO_2Na$: 120.0425, found 120.0423.

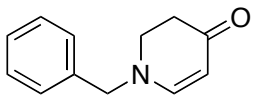

2.55

1-Benzyl-2,3-dihydropyridin-4(1H)-one (2.55). The title compound was obtained as an colorless oil (*Method A, 50%; Method B, 86%)* after flash chromatography (85% EtOAc). Spectral data of the title compound was identical to that reported in the literature.[348]

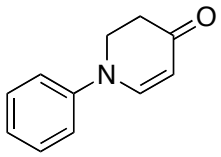

2.56

1-Phenyl-2,3-dihydropyridin-4(1*H*)-one (2.56). The title compound was obtained as an off white solid (*Method A, 50%; Method B, 70%)* after flash chromatography (100% EtOAc): mp 89.0-90.5 °C; ^{1}H NMR (400 MHz, $CDCl_3$) δ 2.67 (t, *J* = 7.6 Hz, 2H), 4.01 (t, *J* = 7.6 Hz, 2H), 5.24 (d, *J* = 7.8 Hz, 1H), 7.09-7.18 (m, 3H), 7.37-7.41 (m, 2H), 7.45 (d, *J* = 7.8 Hz, 1H); ^{13}C NMR (100 MHz, $CDCl_3$) δ 35.9, 47.6, 102.0, 118.2, 124.4, 129.7, 145.1, 149.7, 192.1; IR

(neat) 3057, 1647, 1579, 1495, 1316, 1220 cm^{-1}; HRMS (ESI+) *m/e* calc'd for $[M+H]^+$ $C_{11}H_{12}NO$: 174.0919, found 174.0913.

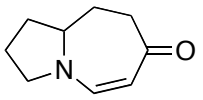

2.61

(*Z*)-2,3,9,9a-Tetrahydro-1*H*-pyrrolo[1,2-*a*]azepin-7(8*H*)-one (2.61). The title compound was obtained as a light yellow solid (*Method A, 60%; Method B, 64%)* after flash chromatography (100% acetone): mp 106.2-114.4 °C; ^1H NMR (400 MHz, $CDCl_3$) δ 1.29-1.39 (m, 1H), 1.58-1.69 (m, 1H), 2.09-2.34 (m, 4H), 3.00-3.09 (m, 1H), 3.12-3.25 (m, 2H), 3.41-3.50 (bm, 1H), 3.93-4.00 (m, 1H), 4.99 (d, *J* = 8.4 Hz, 1H), 9.34 (bd, *J* = 6.8 Hz, 1H); ^{13}C NMR (100 MHz, $CDCl_3$) δ28.0, 29.5, 31.4, 34.2, 43.3, 66.8, 95.7, 166.0, 186.8; IR (neat) 2860, 1623, 1583, 1398, 1190, 802 cm^{-1}; HRMS (ESI+) *m/e* calc'd for $[M+H]^+$ $C_9H_{14}NO$: 152.1075, found 152.1068.

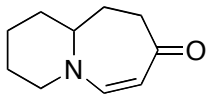

2.62

(*Z*)-1,2,3,4,10,10a-Hexahydropyrido[1,2-*a*]azepin-8(9*H*)-one (2.62). The title compound was obtained as a light yellow solid (*Method A, 64%; Method B, 63%)* after flash chromatography (100% acetone): mp 69.5-70.3 °C ^1H NMR (400 MHz, $CDCl_3$) δ1.16-1.26

(m, 1H), 1.38-1.52 (m, 2H), 1.55-1.65 (m, 1H), 1.74-1.81 (m, 1H), 1.87-1.94 (m, 1H), 1.98 (d, J = 13.3 Hz, 1H), 2.20-2.28 (m, 1H), 2.81-2.90 (m, 2H), 3.13-3.21 (bm, 1H), 3.38-3.46 (m, 1H), 3.72 (d, J = 13.0 Hz, 1H), 5.10 (bd, J = 5.7 Hz, 1H), 9.42 (bs, 1H); ^{13}C NMR (100 MHz, $CDCl_3$) δ23.4, 24.2, 27.8, 28.8, 32.6, 43.7, 62.4, 94.7, 167.6, 187.2; IR (neat) 2940, 1624, 1583, 1394, 1189, 779 cm^{-1}; HRMS (ESI+) *m/e* calc'd for $[M+H]^+$ $C_{10}H_{16}NO$: 166.1232, found 166.1223.

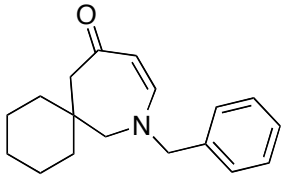

2.63

8-Benzyl-8-azaspiro[5.6]dodec-9-en-11-one (2.63). The title compound was obtained as a yellow oil (*Method A, 81%; Method B, 84%)* after flash chromatography (100% acetone): ^{1}H NMR (400 MHz, $CDCl_3$) δ1.36-1.55 (m, 10H), 2.91 (bs, 2H), 3.22 (s, 2H), 4.38 (s, 2H), 5.27 (d, J = 7.5 Hz, 1H), 7.18 (d, J = 6.8 Hz, 2H), 7.28-7.36 (m, 3H), 9.41 (d, J = 6.6 Hz, 1H); ^{13}C NMR (100 MHz, $CDCl_3$) δ23.1, 25.5, 36.0, 39.5, 42.5, 50.1, 63.1, 95.7, 127.5 (2C), 127.9, 128.9, 135.2, 168.0, 187.5; IR (neat) 2925, 1632, 1591, 1552, 1397, 1188 cm^{-1}; HRMS (ESI +) *m/e* calc'd for $[M+H]^+$ $C_{18}H_{24}NO$: 270.1858, found 270.1852.

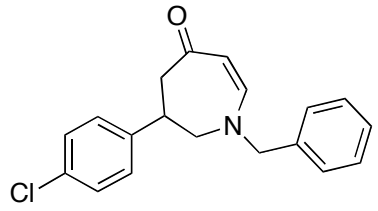

2.64

(*Z*)-1-Benzyl-6-(4-chlorophenyl)-6,7-dihydro-1*H*-azepin-4(5*H*)-one (2.64). The title compound was obtained as a yellow oil (*Method A, 66%; Method B, 65%)* after flash chromatography (100% acetone): ^{1}H NMR (400 MHz, $CDCl_3$) δ 3.13-3.22 (m, 1H), 3.44 (dd, *J* = 10.0, 6.6 Hz, 1H), 3.54-3.66 (m, 2H), 3.80 (dd, *J* = 10.0, 8.0 Hz, 1H), 4.46 (d, *J* = 2.8 Hz, 2H), 5.36 (d, *J* = 7.9 Hz, 1H), 7.11 (d, *J* = 8.4 Hz, 2H), 7.21 (d, *J* = 6.64 Hz, 2H), 7.27-7.37 (m, 5H), 9.46 (bd, *J* = 4.7 Hz, 1H); ^{13}C NMR (100 MHz, $CDCl_3$) δ 38.0, 39.5, 50.2, 59.2, 95.7, 127.6, 128.1, 129.0, 133.1, 134.8, 139.7, 166.9, 187.5; IR (neat) 1625, 1590, 1549, 1398, 1190, 702 cm^{-1}; HRMS (ESI+) *m/e* calc'd for $[M+H]^+$ $C_{19}H_{19}ClNO$: 312.1155, found 312.1155.

6.3.4 Supplementary studies

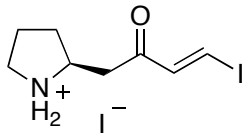

2.38

(*E*)-2-(4-Iodo-2-oxobut-3-enyl)pyrrolidinium Iodide (2.38). Ynone **2.17** (0.50 mmol, 1.0 equiv) was dissolved in 98% formic acid (5.0 mL) under a N_2 atmosphere and NaI (230 mg,

1.5 mmol, 3.0 equiv) was added. After 6 h, Et_2O (200 mL) was slowly added to the reaction mixture allowing a precipitate to form. The precipitate was filtered and washed several times with Et_2O. The filtered precipitate was air dried and used without further purification. To obtain crystals for X-ray analysis, the precipitate was recrystallized from formic acid. See below for X-ray crystal structure report. ^{1}H NMR (400 MHz, CD_3OD) δ 1.59-1.69 (m, 1H), 1.82-1.92 (m, 1H), 1.94-2.04 (m, 1H), 1.12-2.20 (m, 1H), 2.97 (dd, *J* = 18.9, 9.8 Hz, 1H), 3.13-3.24 (m, 3H), 3.76-3.83 (m, 1H), 7.16 (d, *J* = 15.2 Hz, 1H), 8.17 (d, *J* = 15.2 Hz, 1H); ^{13}C NMR (100 MHz, CD_3OD) 24.6, 31.2, 42.6, 46.6, 56.8, 102.8, 145.2, 196.4; ^{1}H NMR (400 MHz, $(CD_3)_2SO$) δ 1.49-1.58 (m, 1H), 1.74-1.95 (m, 2H), 2.04-2.12 (m, 1H), 3.04 (dd, *J* = 18.7 , 9.2 Hz, 1H), 3.04-3.17 (m, 2H), 3.17 (dd, *J* = 18.7, 4.3 Hz, 1H), 3.71-3.78 (m, 1H), 7.21 (d, *J* = 15.3 Hz, 1H), 8.26 (d, *J* = 15.3 Hz, 1H), 8.28 (bs, 1H), 8.85 (bs, 1H); ^{13}C NMR (100 MHz, $(CD_3)_2SO$) δ 23.1, 29.7, 41.4, 45.0, 54.3, 104.7, 143.7, 195.4.

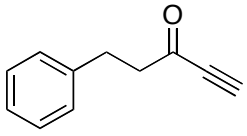

2.65

5-Phenylpent-1-yn-3-one (2.65). The title compound was prepared using Method A for Weinreb amide formation and subsequent Grignard addition as described above. The product was obtained as a colorless oil (86% over 2 steps) after flash chromatography (5% EtOAc/ hexanes): ^{1}H NMR (400 MHz, $CDCl_3$) δ 2.89-2.93 (m, 2H), 2.96-3.00 (m, 2H), 3.22 (s, 1H), 7.17-7.23 (m, 3H), 7.26-7.30 (m, 2H); ^{13}C NMR (100 MHz, $CDCl_3$) δ 29.5, 46.9, 78.9, 81.3,

126.3, 128.3, 128.6, 139.9, 186.2; IR (neat) 3029, 2093, 1683, 1454, 1102, 699 cm^{-1}; HRMS (EI+) *m/e* calc'd for $[M+H]^+$ $C_{11}H_{11}O$: 158.0732, found 158.0722.

EXPERIMENT 1: TERMINAL YNONE CYCLIZATION.

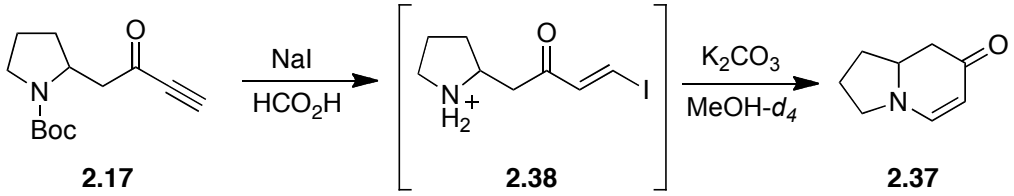

2.17 **2.38** **2.37**

Vinyl iodide **2.38** was prepared according to Method B. Et_2O was added to the reaction mixture prior to HCO_2H evaporation and the precipitate (**2.38**) was collected via filtration. The precipitate was dried in vacuo for 1 h. Vinyl iodide **2.38** (10 mg, 0.025 mmol) was dissolved in CD_3OD (1.0 mL) and added (0.60 mL) to an NMR tube. An initial NMR spectrum was recorded. To the NMR tube was added 0.30 mL of a saturated solution of K_2CO_3 in CD_3OD and the NMR tube was rigorously agitated. Although an NMR spectrum was recorded immediately, enaminone formation was complete prior to spectrum acquisition (~2 min).

EXPERIMENT 1: NMR

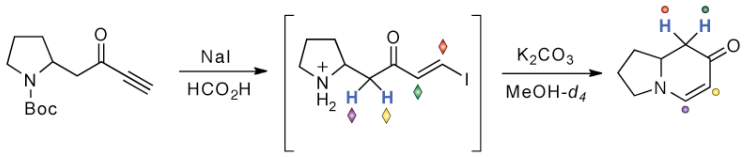

Spectra expansion

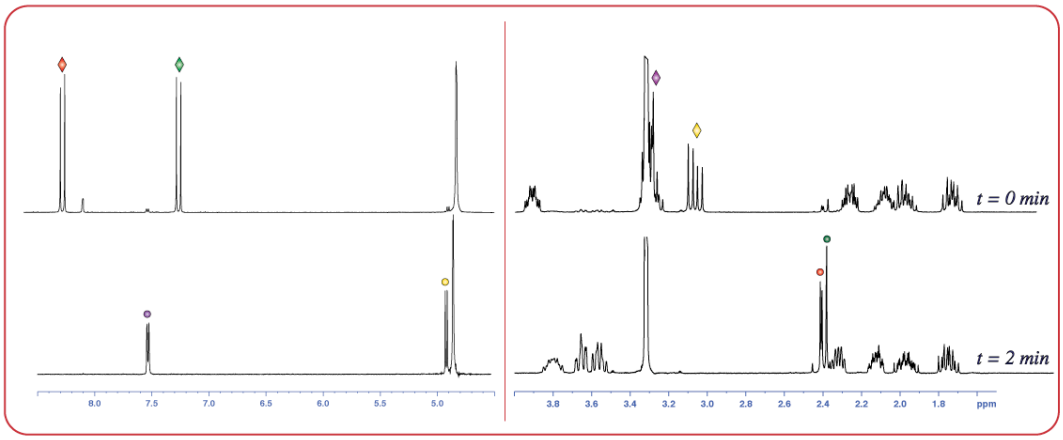

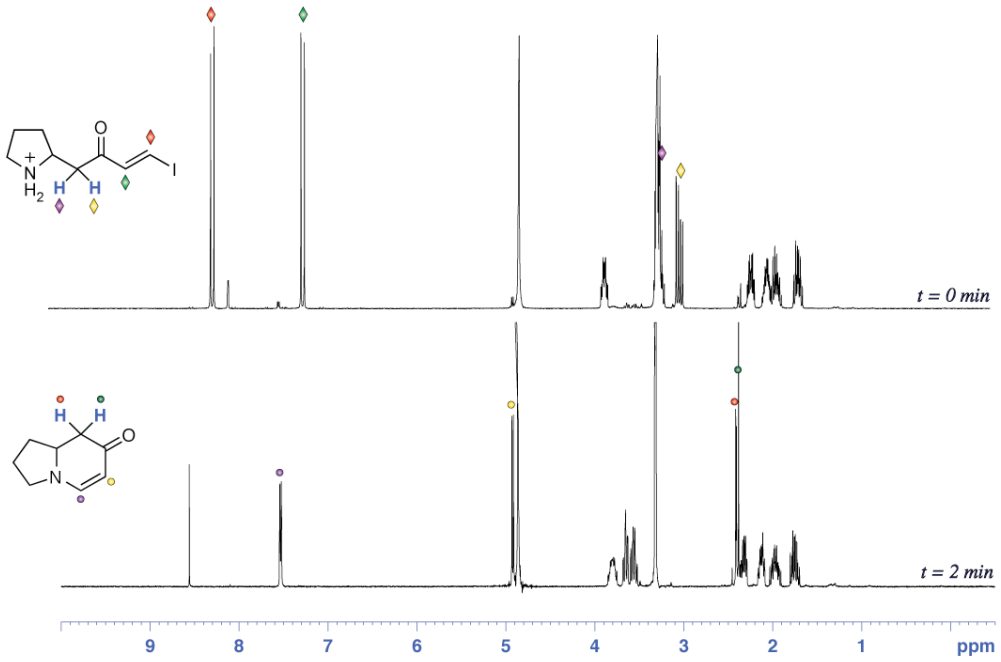

EXPERIMENT 2: METHYLYNONE CYCLIZATION.

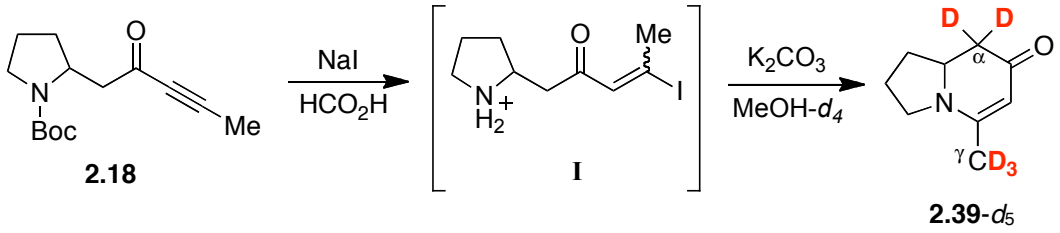

Vinyl iodide **I** was prepared from ynone **2.18** (20 mg, 0.080 mmol) according to Method B. Following evaporation of HCO_2H, the residue containing vinyl iodide **I** was dissolved in CD_3OD (2.0 mL) and added (0.60 mL) to an NMR tube. An initial NMR spectrum was recorded. To the NMR tube was added 0.30 mL of a saturated solution of K_2CO_3 in CD_3OD and the NMR tube was rigorously agitated. NMR spectra were recorded at various time increments from 2.0 min to 22.0 min. Deuteration of the α-position was immediate and complete, whereas γ-deuteration was slow, proceeding almost to completion over 22 min, and subsequent to cyclization.

EXPERIMENT 2: NMR

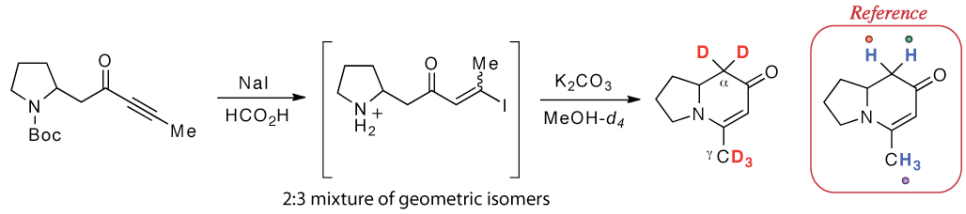

2:3 mixture of geometric isomers

Spectra expansion

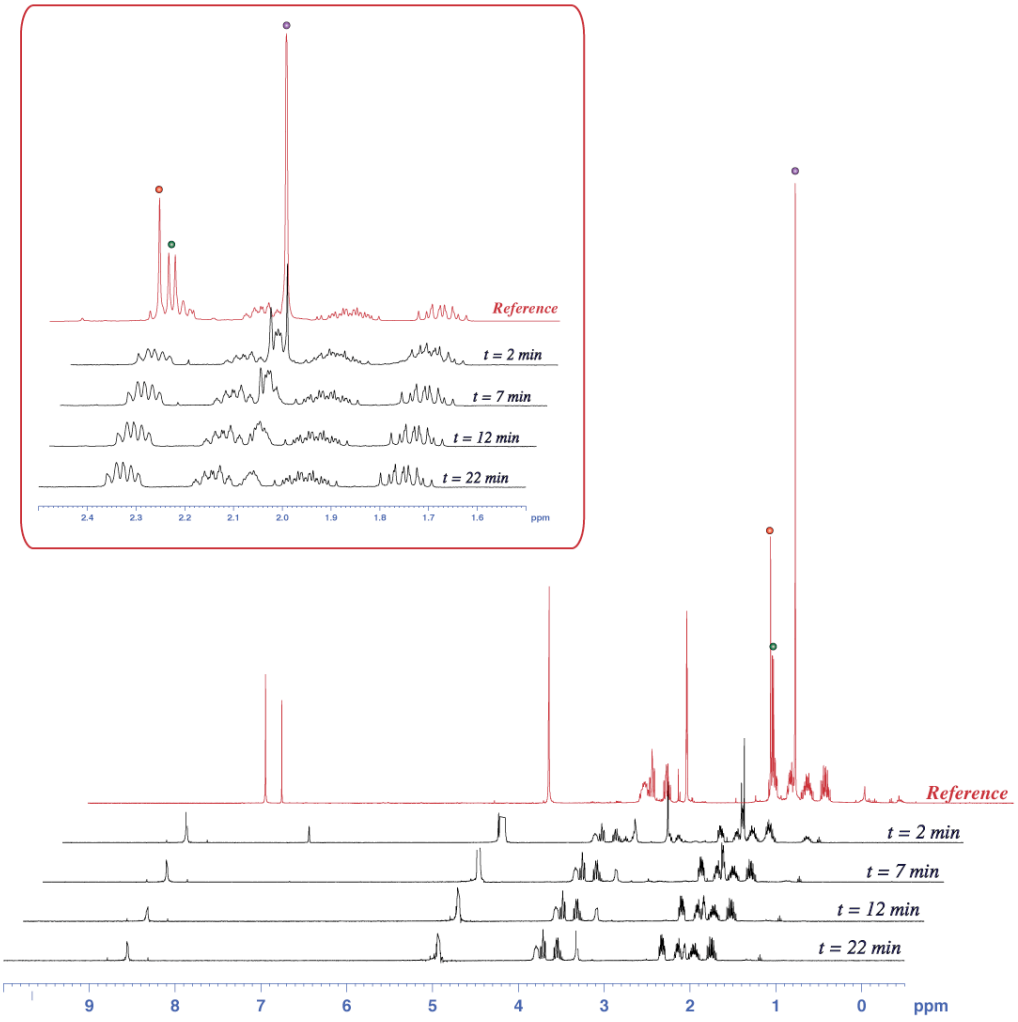

Note: Peaks @ 8.55, 4.95 and 3.3 ppm were graphically suppressed for clarity.

EXPERIMENT 3: PHENYLYNONE CYCLIZATION.

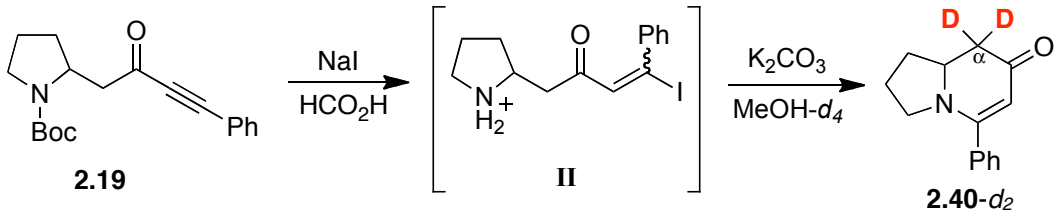

Vinyl iodide **II** was prepared from ynone **2.19** (25 mg, 0.080 mmol) according to Method B. Following evaporation of HCO_2H, the residue containing vinyl iodide **II** was dissolved in CD_3OD (2.0 mL) and added (0.60 mL) to an NMR tube. To the NMR tube was added 0.30 mL of a saturated solution of K_2CO_3 in CD_3OD and the NMR tube was rigorously agitated. NMR spectra were recorded at various time increments from 2.0 min to 70.0 min. Deuteration of the α-position was rapid and complete.

EXPERIMENT 3: NMR

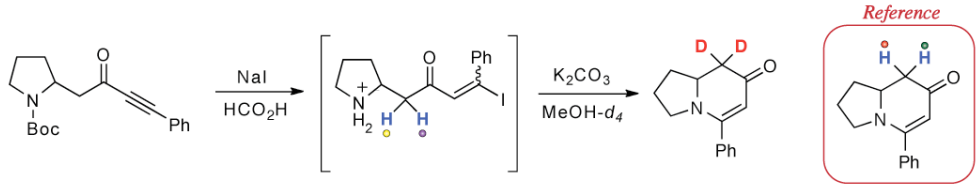

Spectra expansion

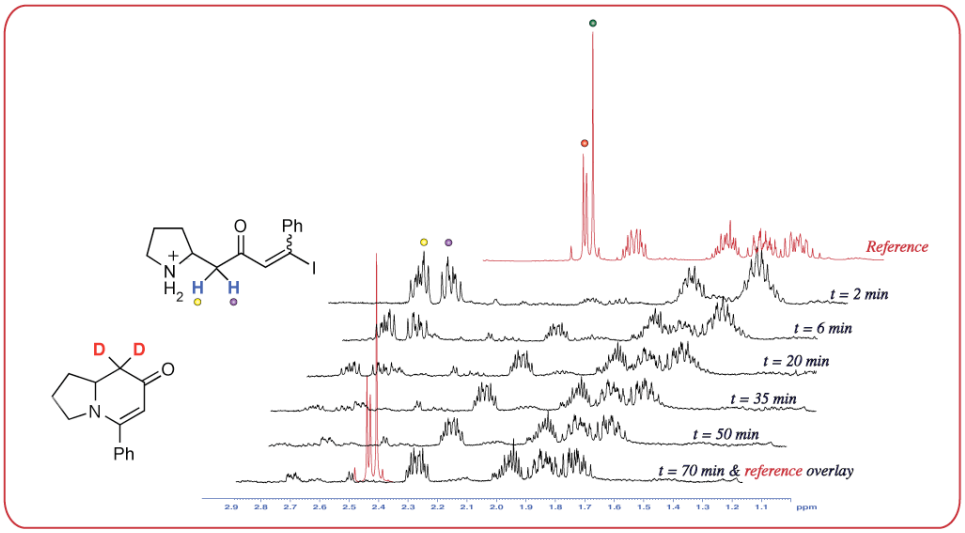

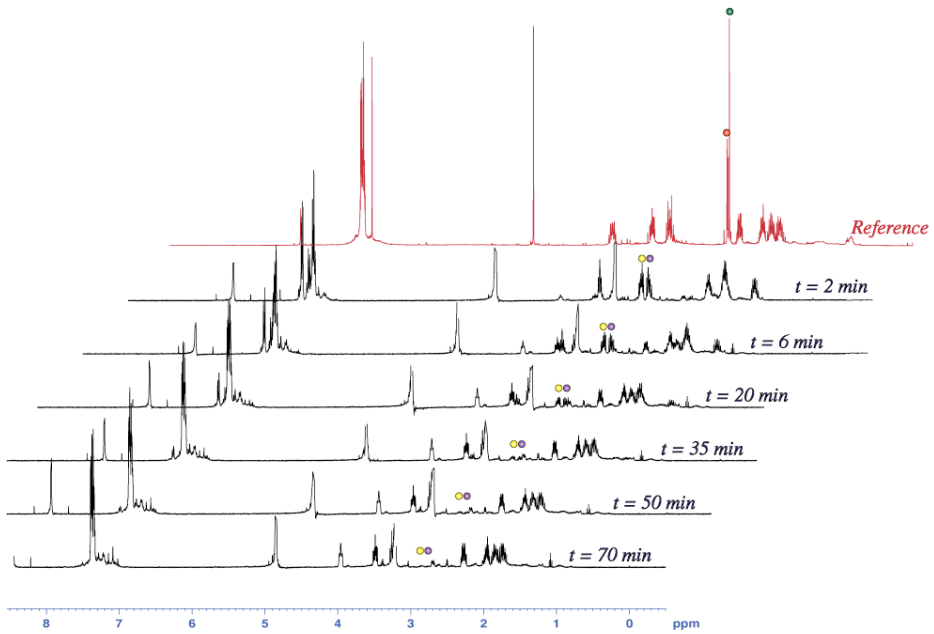

Note: Peaks @ 4.95 and 3.3 ppm were graphically suppressed for clarity.

EXPERIMENT 4: POST-CYCLIZATION DEUTERIUM EXCHANGE.

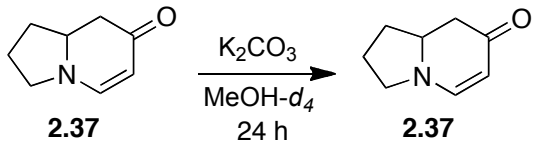

2.37 **2.37**

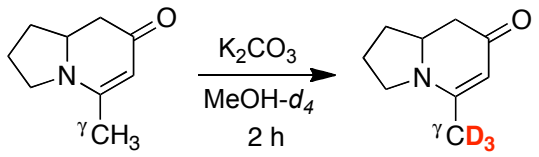

2.39 **2.39-*d*3**

Enaminone **2.37** (10 mg, 0.070 mmol) and **2.39** (11 mg, 0.070 mmol) were dissolved in CD_3OD (1.0 mL) each and added (0.60 mL of each solution) to separate NMR tubes. An initial NMR spectrum was obtained. To each NMR tube was added 0.30 mL of a saturated solution of K_2CO_3 in CD_3OD and the NMR tubes were rigorously agitated. NMR spectra were recorded at various increments over 24 h. Enaminone **2.37** was completely intact at 24 h, whereas, enaminone **2.39** underwent > 95% γ-deuteration after 2 h.

EXPERIMENT 4: NMR

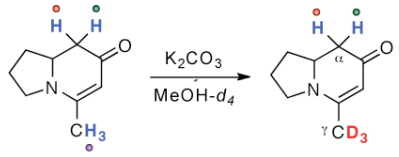

Spectra expansion

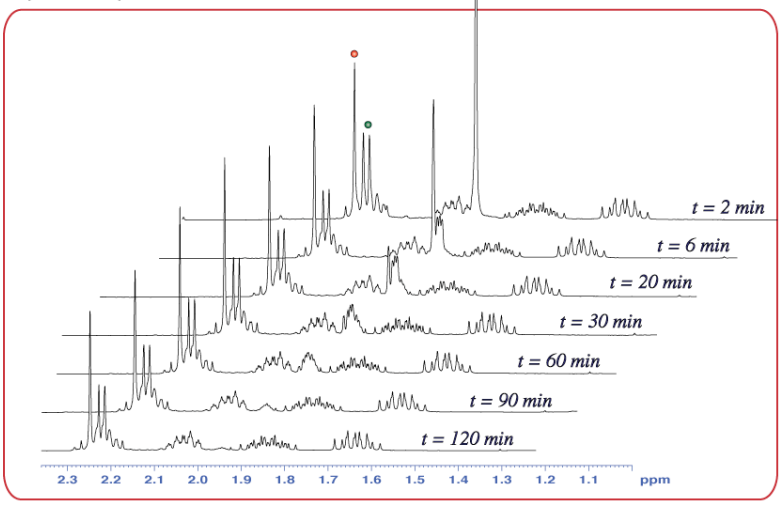

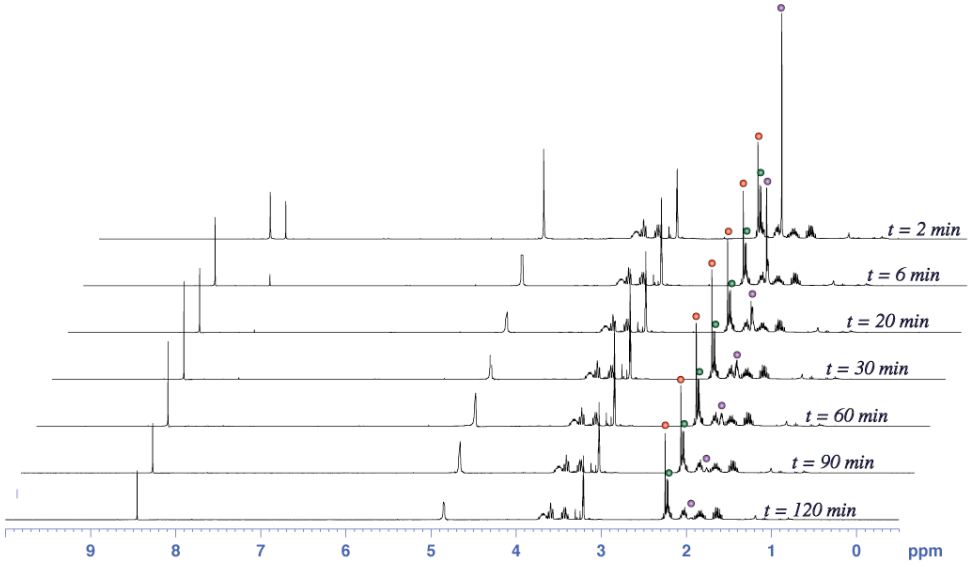

Note: Peak @ 4.95 ppm was graphically suppressed for clarity.

STUDIES OF YNONE AND VINYL CHLORIDE REACTIVITY IN ABSENCE OF AN INTERNAL NUCLEOPHILE

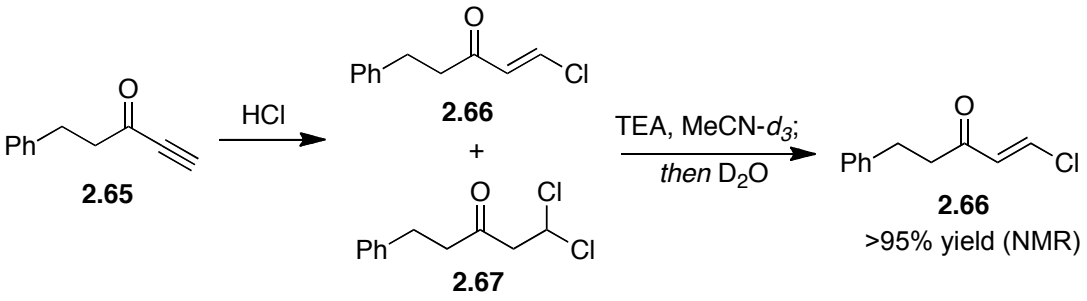

The ynone **2.65** (79 mg, 0.50 mmol) was dissolved in a 4N HCl/dioxane solution (1.5 mL) and allowed to react for 15 min. After this time the dioxane and excess HCl were allowed to evaporate while passing air over the reaction mixture. A 1:6 mixture of **2.66** and **2.67** was obtained. From the residue containing **2.66** and **2.67** 10 mg was taken and dissolved in MeCN-d_3 (1.0 mL) and added (0.60 mL) to an NMR tube. After an NMR spectra was obtained for the mixture, one drop of TEA was added and NMR spectra were recorded at various intervals over 2 h. Dichloride **2.67** had completely reacted to form vinyl chloride **2.66** in less than 2 min. After 2 h, a drop of D_2O was added to the reaction mixture and the NMR tube was vigorously shaken. NMR spectra were recorded at various interval over another 2 h. The vinylchloride moiety remained intact over this period of time.

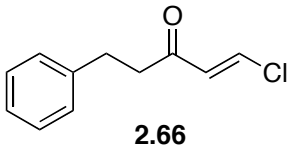

2.66

(*E*)-1-Chloro-5-phenylpent-1-en-3-one (2.66). The title compound was isolated as a colorless oil: ^{1}H NMR (400 MHz, $CDCl_3$) δ2.76-2.80 (m, 2H), 2.85-2.90 (m, 2H), 6.45 (d, *J* = 13.6 Hz, 1H), 7.11 (m, 3H), 7.19-7.23 (m, 3H); ^{13}C NMR (100 MHz, $CDCl_3$) δ29.6, 42.9, 126.3, 128.3, 128.6, 132.3, 136.8, 140.6, 196.2; IR (neat) 2926, 1682, 1586, 1454, 1169, 942 cm^{-1}; HRMS (EI+) *m/e* calc'd for $[M+H]^+$ $C_{11}H_{12}ClO$: 194.0498, found 194.0479.

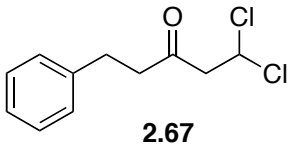

2.67

1,1-Dichloro-5-phenylpentan-3-one (2.67). The title compound was isolated as a colorless oil upon evaporation of HCl: ^{1}H NMR (400 MHz, $CDCl_3$) δ2.72 (t, *J* = 7.5 Hz, 2H), 2.86 (t, *J* = 7.5 Hz, 2H), 3.25 (d, *J* = 6.4 Hz, 2H), 6.05 (t, *J* = 6.4 Hz, 1H), 7.10-7.16 (m, 3H), 7.20-7.24 (m, 2H); ^{13}C NMR (100 MHz, $CDCl_3$) δ29.2, 45.0, 55.5, 67.2, 126.4, 128.3, 128.6, 140.3, 203.4; IR (neat) 2925, 1721, 1454, 1405, 1371, 1092 cm^{-1}; HRMS (EI+) *m/e* calc'd for $[M+H]^+$ $C_{11}H_{13}Cl_2O$: 230.0265, found 230.0276.

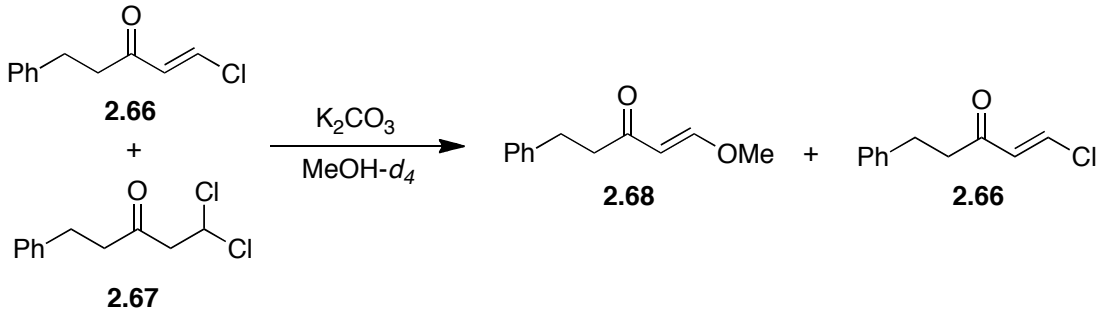

The mixture of chlorides **2.66** and **2.67** (10 mg) were dissolved in methanol-d_4 (1.0 mL) and added (0.60 mL) to an NMR tube. An initial NMR spectrum was recorded as a reference. A saturated solution of K_2CO_3 in methanol-d_4 (0.30 mL) was added to the NMR tube and the tube was vigorously agitated. NMR spectra were recorded at various intervals. After 2 h the spectra showed complete consumption of dichloroketone **2.67** and a 1:2 mixture of ether **2.68** and vinyl chloride **2.66**, respectively. NMR spectra for vinyl ether **2.68** matched those found in the literature.[349]

6.3 Chapter 3

6.3.1 Preparation of starting materials

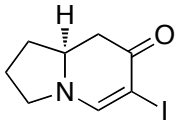

3.1

(*S*)-6-iodo-2,3,8,8a-tetrahydroindolizin-7(1*H*)-one (3.1). Enaminone **2.37** (421 mg, 3.07 mmol, 1.00 equiv) and DMAP (751 mg, 6.15 mmol, 2.00 equiv) were dissolved in CH_2Cl_2 (45 mL). To this flask I_2 (73.8 mL, 3.69 mmol, 1.2 equiv, 0.05M in CH_2Cl_2) was added

dropwise over 20 min and the reaction mixture was stirred for 5 h. The reaction mixture was poured into a saturated solution of $Na_2S_2O_3$ (200 mL) and vigorously stirred for 5 min. The product was extracted with CH_2Cl_2 (3x), dried over Na_2SO_4 and purified via SiO_2 flash chromatography (100% EtOAc). The title compound was isolated as a yellow solid (782 mg, 92%). Spectral data matched those found in the literature.[213]

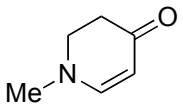

3.18

Compound **3.18** was prepared from 4-hydroxypyridine using alkylation/reduction methodology developed by Guerry and Neier.[350] NMR spectra matched those found in the literature.

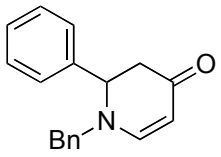

3.19

1-Benzyl-2-phenyl-2,3-dihydropyridin-4(1*H*)-one (3.19) was prepared from 4-hydroxypyridine using *N*-alkylation[351] and conjugate addition of PhMgCl using methodology reported by Klegraf *et al*.[230] NMR spectra matched those found in the literature.[351]

6.3.2 Pd(II)-catalyzed C3-arylation of enaminones

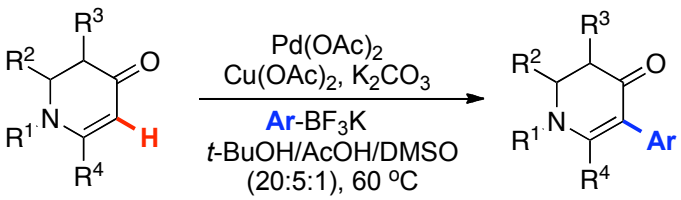

Representative procedure for enaminone arylation:

Enaminone (0.20 mmol), $Pd(OAc)_2$ (14 mg, 0.06 mmol), anhydrous $Cu(OAc)_2$ powder (110 mg, 0.60 mmol) and granular K_2CO_3 (55 mg, 0.40 mmol,)[5] were combined in a 20:5:1 mixture of *t*-BuOH/AcOH/DMSO (2.0 mL) under N_2[6] and stirred for 5 min (*Note: Solvents were used without purification or degassing*). The reaction mixture was heated to 60 °C and the potassium trifluoroborate (0.40-0.60 mmol) was added slowly over 5 h as a solid. The amount of trifluoroborate needed depends on the rate of addition. Typically 0.20 equivalents of trifluoroborate were added every 30 minutes. The reaction was stirred for an additional h and was monitored by TLC using 100% EtOAc as the mobile phase. The reaction mixture was diluted with EtOAc (8 mL) and excess K_2CO_3 (~1 g) was added to neutralize the AcOH. After stirring this mixture for 5 min the precipitate was filtered over Celite using EtOAc as the eluent. The filtrate was concentrated and purified by chromatography on SiO_2 (EtOAc/ hexanes).

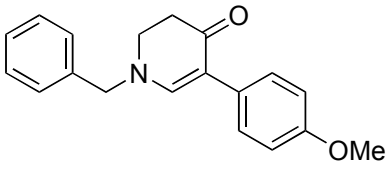

3.4

1-Benzyl-5-(4-methoxyphenyl)-2,3-dihydropyridin-4(1*H*)-one (3.4). Potassium (4-methoxyphenyl)trifluoroborate was added slowly over 6 h and the reaction was stirred for an additional hour. The title compound was isolated as a yellowish oil. (^{1}H NMR (400 MHz, $CDCl_3$) δ 2.60 (t, 2H, *J* = 7.8 Hz), 3.44 (t, 2H, *J* = 7.8 Hz), 3.80 (s, 3H), 4.43 (s, 2H), 6.87 (d, 2H, *J* = 8.8 Hz), 7.29-7.42 (m, 8H); ^{13}C NMR (100 MHz, $CDCl_3$) δ 36.4, 46.9, 55.34, 60.2, 111.1, 113.7 (2C), 127.7 (2C), 128.4, 128.8, 129.0 (2C), 129.1 (2C), 135.8, 152.8, 157.8, 188.9; IR (neat) 2835, 1629, 1595, 1298, 1245, 1126 cm^{-1}; HRMS (ESI+) *m/e* calc'd for $[M+H]^+$ $C_{19}H_{20}NO_2$: 294.1494, found 294.1482.

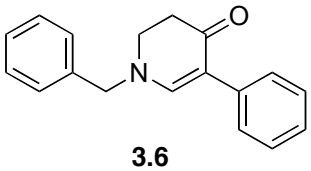

3.6

1-Benzyl-5-phenyl-2,3-dihydropyridin-4(1*H*)-one (3.6). Potassium phenyltrifluoroborate was added slowly over 6 h and the reaction was stirred for an additional hour. The title compound was isolated as a colorless oil. ^{1}H NMR (400 MHz, $CDCl_3$) δ 2.60 (t, 2H, *J* = 7.8 Hz), 3.45 (t, 2H, *J* = 7.8 Hz), 4.43 (s, 2H), 7.16 (tt, 1H, *J* = 1.4, 3.7 Hz), 7.29-7.42 (m, 10H);

^{13}C NMR (100 MHz, $CDCl_3$) δ 36.3, 46.8, 60.2, 111.2, 125.7, 127.7 (2C), 127.8 (2C), 128.2 (2C), 128.4, 129.1 (2C), 135.7, 136.3, 153.2, 188.6; IR (neat) 3029, 1628, 1595, 1495, 1299, 1127 cm^{-1}; HRMS (ESI+) *m/e* calc'd for $[M+H]^+$ $C_{18}H_{18}NO$: 264.1383, found 264.1388.

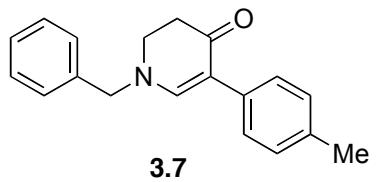

3.7

1-Benzyl-5-(4-tolyl)-2,3-dihydropyridin-4(1*H*)-one (3.7). Potassium (4-tolyl)-trifluoroborate was added slowly over 4 h and the reaction was stirred for an additional hour. The title compound was isolated as a colorless oil. ^{1}H NMR (400 MHz, $CDCl_3$) δ 2.32 (s, 3H), 2.60 (t, 2H, *J* = 7.8 Hz), 3.44 (t, 2H, *J* = 7.8 Hz), 4.42 (s, 2H), 7.12 (d, 2H, *J* = 8.0 Hz), 7.28-7.42 (m, 8H); ^{13}C NMR (100 MHz, $CDCl_3$) δ 21.1, 36.3, 46.8, 60.2, 111.3, 127.7 (2C), 127.8 (2C), 128.4, 128.9 (2C), 129.1 (2C), 133.3, 135.3, 135.8, 152.9, 188.7; IR (neat) 2919, 1634, 1595, 1382, 1298, 1125 cm^{-1}; HRMS (ESI+) *m/e* calc'd for $[M+H]^+$ $C_{19}H_{20}NO$: 278.1539, found 278.1551.

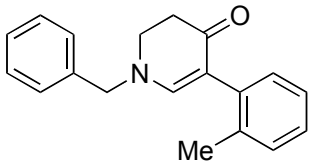

3.8

1-Benzyl-5-(2-tolyl)-2,3-dihydropyridin-4(1*H*)-one (3.8). Potassium (2-tolyl)trifluoroborate was added slowly over 12 h and the reaction was stirred for an additional

12 h. The title compound was isolated as a white solid (mp 94-97 °C). ^{1}H NMR (400 MHz, $CDCl_3$) δ 2.22 (s, 3H), 2.60 (t, 2H, *J* = 7.8 Hz), 3.45 (t, 2H, *J* = 7.8 Hz), 4.37 (s, 2H), 7.07-7.42 (m, 10H); ^{13}C NMR (100 MHz, $CDCl_3$) δ 20.4, 36.0, 47.1, 60.0, 112.2, 125.6, 127.1, 127.7 (2C), 128.4, 129.1 (2C), 130.0, 130.6, 135.8, 136.1, 137.9, 153.9, 188.3; IR (neat) 2960, 1635, 1595, 1322, 1303, 1135 cm^{-1}; HRMS (ESI+) *m/e* calc'd for $[M+H]^+$ $C_{19}H_{20}NO$: 278.1539, found 278.1547.

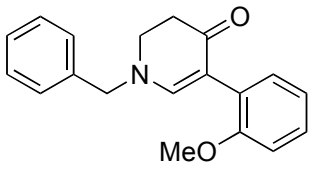

3.9

1-Benzyl-5-(2-methoxyphenyl)-2,3-dihydropyridin-4(1*H*)-one (3.9). Potassium (2-methoxyphenyl)trifluoroborate was added slowly over 12 h and the reaction was stirred for an additional 12 h. The title compound was isolated as a colorless oil. ^{1}H NMR (400 MHz, $CDCl_3$) δ 2.63 (t, 2H, *J* = 7.8 Hz), 3.46 (t, 2H, *J* = 7.8 Hz), 3.79 (s, 3H) 4.41 (s, 2H), 6.90 (dd, 1H, *J* = 1.1, 8.2 Hz), 6.93 (ddd, 1H, *J* = 1.1, 7.4, 7.4 Hz), 7.19 (ddd, 1H, *J* = 1.8, 7.4, 8.2 Hz), 7.28-7.42 (m, 7H); ^{13}C NMR (100 MHz, $CDCl_3$) δ 36.1, 46.9, 55.7, 60.2, 107.2, 111.3, 120.5, 125.0, 127.5, 127.7 (2C), 128.3, 129.0 (2C), 132.0, 135.9, 154.9 157.0, 188.3; IR (neat) cm^{-1} 2960, 1631, 1593, 1302, 1132, 1028; HRMS (ESI+) *m/e* calc'd for $[M+H]^+$ $C_{19}H_{20}NO_2$: 294.1494, found 194.1504.

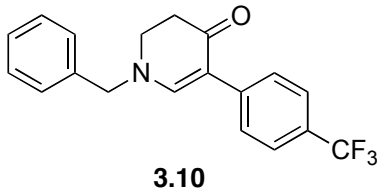

3.10

1-Benzyl-5-(4-(trifluoromethyl)phenyl)-2,3-dihydropyridin-4(1*H*)-one (3.10). Potassium (4-trifluoromethylphenyl)trifluoroborate was added slowly over 12 h and the reaction was stirred for an additional 12 h. The title compound was isolated as a white solid (mp 118-119 ^{o}C). NMR (400 MHz, $CDCl_3$) δ 2.61 (t, 2H, *J* = 7.8 Hz), 3.49 (t, 2H, *J* = 7.8 Hz), 4.45 (s, 2H), 7.29-7.44 (m, 5H), 7.48 (s, 1H), 7.54 (s, 4H); ^{19}F NMR (377 MHz, $CDCl_3$) δ -65.9; ^{13}C NMR (100 MHz, $CDCl_3$) δ 36.2, 46.8, 60.5, 109.8, 124.6 (q, *J* = 271.7 Hz), 125.2 (q, 2C, *J* = 3.8 Hz), 127.5 (q, *J* = 32.3 Hz), 127.6 (2C), 127.8 (2C), 128.7, 129.3 (2C), 135.4, 140.2, 153.5, 188.36; IR (neat) 3032, 1637, 1599, 1327, 1113, 1068 cm^{-1}; HRMS (ESI+) *m/e* calc'd for $[M+H]^+$ $C_{19}H_{17}F_3NO$: 332.1257, found 332.1259.

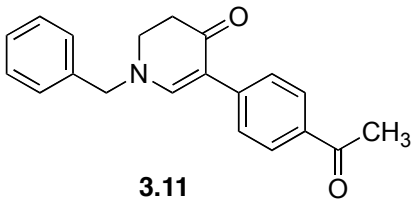

3.11

1-Benzyl-5-(4-acetylphenyl)-2,3-dihydropyridin-4(1*H*)-one (3.11). Potassium (4-acetylphenyl)trifluoroborate was added slowly over 12 h and the reaction was stirred for an additional 12 h. The title compound was isolated as a colorless oil. ^{1}H NMR (400 MHz, $CDCl_3$) δ 2.58 (s, 3H), 2.62 (t, 2H, *J* = 7.8 Hz), 3.50 (t, 2H, *J* = 7.8 Hz), 4.50 (s, 2H),

7.30-7.42 (m, 5H), 7.54 (s, 1H), 7.55 (d, 2H, J = 8.6 Hz), 7.90 (d, 2H, J = 8.6 Hz); ^{13}C NMR (100 MHz, $CDCl_3$) δ 26.5, 36.2, 46.6, 60.5, 109.7, 127.0 (2C), 127.7 (2C), 128.4 (2C), 128.6, 129.2 (2C), 134.1, 135.2, 141.6, 153.5, 188.2, 197.8; IR (neat) 3030, 1672, 1635, 1592, 1271, 1129 cm^{-1}; HRMS (ESI+) *m/e* calc'd for $[M+H]^+$ $C_{20}H_{20}NO_2$: 306.1489, found 306.1503.

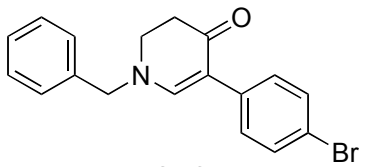

3.12

1-Benzyl-5-(4-bromophenyl)-2,3-dihydropyridin-4(1*H*)-one (3.12). Potassium (4-bromophenyl)trifluoroborate was added slowly over 5 h and the reaction was stirred for an additional hour. The title compound was isolated as a yellowish oil. ^{1}H NMR (400 MHz, $CDCl_3$) δ 2.59 (t, 2H, J = 7.8 Hz), 3.46 (t, 2H, J = 7.8 Hz), 4.45 (s, 2H), 7.27-7.43 (m, 10H); ^{13}C NMR (100 MHz, $CDCl_3$) δ 36.2, 46.7, 60.3, 109.9, 119.3, 127.6 (2C), 128.5, 129.1 (2C), 129.3 (2C), 131.2 (2C), 135.3, 135.5, 152.9, 188.3; IR (neat) 3029, 1631, 1598, 1378, 1293, 1127 cm^{-1}; HRMS (ESI+) *m/e* calc'd for $[M+H]^+$ $C_{18}H_{17}BrNO$: 342.0488, found 342.0483.

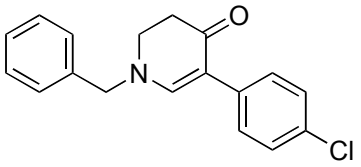

3.13

1-Benzyl-5-(4-chlorophenyl)-2,3-dihydropyridin-4(1*H*)-one (3.13). Potassium (4-chlorophenyl)trifluoroborate was added slowly over 7 h and the reaction was stirred for an additional hour. The title compound was isolated as a yellowish oil. ^{1}H NMR (400 MHz, $CDCl_3$) δ 2.59 (t, 2H, *J* = 7.8 Hz), 3.4 (t, 2H, *J* = 7.8 Hz), 4.45 (s, 2H), 7.25-7.43 (m, 10H); ^{13}C NMR (100 MHz, $CDCl_3$) δ 36.2, 46.7, 60.3, 109.9, 127.7 (2C), 128.2 (2C), 128.5, 128.9 (2C), 129.1 (2C), 131.2, 134.8, 135.5, 153.0, 188.4; IR (neat) 3030, 1632, 1599, 1493, 1294, 1128 cm^{-1}; HRMS (ESI+) *m/e* calc'd for $[M+H]^+$ $C_{18}H_{17}ClNO$: 298.0993, found 298.0996.

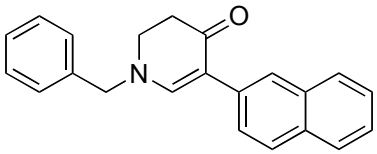

3.14

1-Benzyl-5-(naphthalen-2-yl)-2,3-dihydropyridin-4(1*H*)-one (3.14). Potassium (2-naphthalene)trifluoroborate was added slowly over 3 h and the reaction was stirred for an additional hour. The title compound was isolated as a colorless oil. ^{1}H NMR (400 MHz, $CDCl_3$) δ 2.63 (t, 2H, *J* = 7.8 Hz), 3.46 (t, 2H, *J* = 7.8 Hz), 4.45 (s, 2H), 7.30-7.43 (m, 7H), 7.52 (s, 1H), 7.59 (dd, 1H, *J* = 1.9, 8.7 Hz), 7.76-7.80 (m, 3H), 7.83 (d, 1H, *J* = 1.2 Hz); ^{13}C NMR (100 MHz, $CDCl_3$) δ 36.4, 46.7, 60.3, 111.0, 125.0, 125.5, 125.7, 126.9, 127.4, 127.5,

127.7 (2C), 127.7, 128.4, 129.1 (2C), 131.9, 133.7, 134.1, 135.7, 153.5, 188.7; IR (neat) 3055, 1636, 1600, 1320, 1297, 1135 cm^{-1}; HRMS (ESI+) *m/e* calc'd for $[M+H]^+$ $C_{22}H_{20}NO$: 314.1539, found 314.1545.

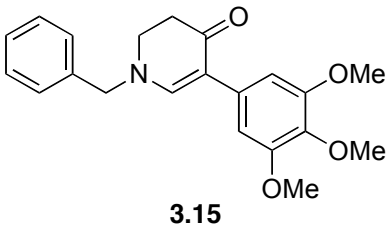

3.15

1-Benzyl-5-(3,4,5-trimethoxyphenyl)-2,3-dihydropyridin-4(1*H*)-one (3.15). Potassium (3,4,5-trimethoxyphenyl)trifluoroborate was added slowly over 5 h and the reaction was stirred for an additional hour. The title compound was isolated as a yellowish oil. ^1H NMR (400 MHz, $CDCl_3$) δ 2.60 (t, 2H, *J* = 7.8 Hz), 3.46 (t, 2H, *J* = 7.8 Hz), 3.83 (s, 3H), 3.86 (s, 6H), 4.45 (s, 2H), 6.64 (s, 2H), 7.29-7.44 (m, 6H); ^{13}C NMR (100 MHz, $CDCl_3$) δ 36.3, 46.7, 56.1, 60.2, 60.8, 105.3, 111.1, 127.7 (2C), 128.4, 129.1 (2C), 132.1, 135.7, 136.4, 152.9, 153.1, 188.6; IR (neat) 2937, 1630, 1596, 1453, 1328, 1239, 1125 cm^{-1}; HRMS (ESI+) *m/e* calc'd for $[M+H]^+$ $C_{21}H_{24}NO_4$: 354.1700, found 354.1702.

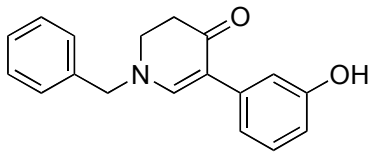

3.16

1-Benzyl-5-(3-hydroxyphenyl)-2,3-dihydropyridin-4(1*H*)-one (3.16). Potassium (3-hydroxyphenyl)trifluoroborate was added slowly over 2 h and the reaction was stirred for an additional h. The title compound was isolated as white solid which later turned pink (mp 145-155 ^{o}C). ^{1}H NMR (400 MHz, $CDCl_3$) δ 2.64 (t, 2H, *J* = 7.9 Hz), 3.44 (t, 2H, *J* = 7.9 Hz), 4.45 (s, 2H), 6.69 (ddd, 1H, *J* = 1.0, 2.5, 8.0 Hz) 6.72 (ddd, 1H, *J* = 1.0, 1.5, 8.0 Hz), 7.15 (t, 1H, *J* = 8.0 Hz), 7.27-7.42 (m, 5H), 7.46 (dd, 1H, *J* = 1.5, 2.5 Hz), 7.50 (s, 1H), 8.1 (s, 1H); ^{13}C NMR (100 MHz, $CDCl_3$) δ 36.0, 46.5, 60.5, 110.3, 113.3, 115.8, 117.8, 127.8 (2C), 128.6, 129.3 (2C), 129.4, 135.5, 137.4, 154.5, 156.8, 189.3; IR (neat) 3168, 1594, 1452, 1324, 1303, 1126 cm^{-1}; HRMS (ESI+) *m/e* calc'd for $[M+H]^+$ $C_{18}H_{18}NO_2$: 280.1332, found 280.1339.

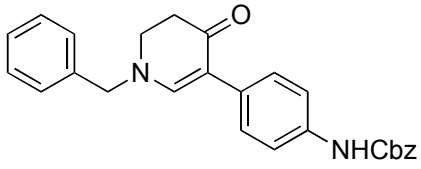

3.17

1-Benzyl-5-(4-aminobenzyloxycarbonyl)-2,3-dihydropyridin-4(1*H*)-one (3.17). Potassium (4-Cbz-aminophenyl)trifluoroborate was added slowly over 4 h and the reaction was stirred for an additional hour. The title compound was isolated as a pale yellow solid (mp 153.5-155 ^{o}C). ^{1}H NMR (400 MHz, $CDCl_3$) δ 2.58 (t, 2H, *J* = 7.8 Hz), 3.43 (t, 2H, *J* = 7.8 Hz), 4.43 (s, 2H), 5.19 (s, 2H), 6.71 (s, 1H), 7.30-7.40 (m, 15H); ^{13}C NMR (100 MHz, $(CD_3)_2CO$) δ 37.2, 47.3, 60.2, 66.8, 110.3, 118.7, 128.5 (2C), 128.8 (2C), 128.8 (2C), 128.8 (2C), 128.9 (2C), 129.3 (2C), 129.7 (2C), 132.9, 137.2, 137.8, 138.0 153.9, 154.4, 188.4; IR (neat) 3316, 3031,

1724, 1593, 1529, 1220 cm^{-1}; HRMS (ESI+) *m/e* calc'd for $[M+H]^+$ $C_{26}H_{25}N_2O_3$: 413.1860, found 413.1874.

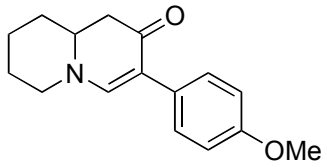

3.20

3-(4-Methoxyphenyl)-7,8,9,9a-tetrahydro-1*H*-quinolizin-2(6*H*)-one (3.20). Trifluoroborate **3.3** was added slowly over 2 h and the reaction was stirred for an additional h. **4a** was isolated as a pale yellow solid (mp 97-99 °C). ^{1}H NMR (400 MHz, $CDCl_3$) δ 1.35-1.68 (m, 3H), 1.76-1.89 (m, 3H), 2.45-2.62 (m, 2H), 3.01 (dt, 1H, *J* = 2.6, 6.3 Hz), 3.32-3.45 (m, 2H), 3.78 (s, 3H), 6.85 (d, 2H, *J* = 8.8 Hz), 7.05 (s, 1H), 7.29 (d, 2H, *J* = 8.8 Hz); ^{13}C NMR (100 MHz, $CDCl_3$) δ 20.7, 23.2, 29.2, 41.4, 50.7, 52.9, 54.8, 109.5, 111.1 (2C), 126.1, 126.6 (2C), 151.3, 155.3, 187.4; IR (neat) 2937, 1636, 1596, 1511, 1243, 1133 cm^{-1}; HRMS (ESI+) *m/e* calc'd for $[M+H]^+$ $C_{16}H_{20}NO_2$: 258.1494, found 258.1488.

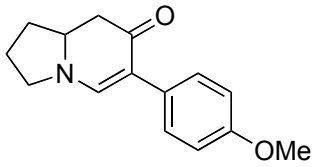

3.2

6-(4-Methoxyphenyl)-2,3,8,8a-tetrahydroindolizin-7(1*H*)-one (3.2). Trifluoroborate **3.3** was added slowly over 8 h and the reaction was stirred for an additional hour. The title

compound was isolated as a pale yellow solid (mp 118-119 °C). *Note: See Section 6.4 for a more detailed description of the preparation of enantiomerically pure* ***3.2***. ^{1}H NMR (400 MHz, $CDCl_3$) δ 1.68-1.76 (m, 1H), 1.92-2.02 (m, 1H), 2.11-2.15 (m, 1H), 2.28-2.33 (m, 1H), 2.49 (t, 1H, *J* = 16.0 Hz), 2.58 (dd, 1H, *J* = 5.0, 16.0 Hz), 3.53-3.63 (m, 2H), 3.79-3.87 (m, 1H), 3.79 (s, 3H), 6.85 (d, 2H, *J* = 8.8 Hz), 7.30 (d, 2H, *J* = 8.8 Hz), 7.38 (s, 1H); ^{13}C NMR (100 MHz, $CDCl_3$) δ 24.4, 33.1, 42.4, 49.8, 55.4, 57.8, 109.5, 113.5 (2C), 128.8 (2C), 129.6, 148.8, 157.4, 189.0; IR (neat) 2953, 2885, 2833, 1620, 1574, 1510, 1277, 837, 733 cm^{-1}; HRMS (ESI+) *m/e* calc'd for $[M+H]^+$ $C_{15}H_{18}NO_2$: 244.1338, found 244.1327.

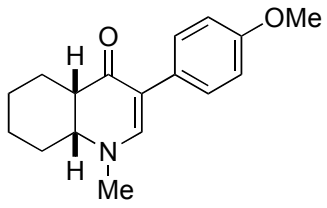

3.21

(*cis*)-3-(4-Methoxyphenyl)-1-methyl-4a,5,6,7,8,8a-hexahydroquinolin-4(1*H*)- one (3.21). Trifluoroborate **3.3** was added slowly over 6 h and the reaction was stirred for an additional h. The title compound was isolated as a colorless oil. ^{1}H NMR (400 MHz, $CDCl_3$) δ 1.31-1.54 (m, 4H), 1.60-1.75 (m, 2H), 1.85-1.96 (m, 1H), 2.22-2.33 (m, 1H), 2.73-2.77 (m, 1H), 3.08 (s, 3H), 3.45 (ddd, 1H, *J* = 3.5, 5.5, 9.0 Hz), 3.78 (s, 3H), 6.84 (d, 2H, *J* = 8.8 Hz), 7.05 (s, 1H), 7.31 (d, 2H, *J* = 8.8 Hz); ^{13}C NMR (100 MHz, $CDCl_3$) δ 22.8, 23.5, 23.7, 24.5, 40.7, 45.7, 55.3, 60.1, 109.2, 113.6 (2C), 128.8 (2C), 129.2, 151.9, 157.5, 190.7; IR (neat)

2932, 1629, 1599, 1512, 1243, 1035 cm^{-1}; HRMS (ESI+) *m/e* calc'd for $[M+H]^+$ $C_{17}H_{22}NO_2$: 272.1645, found 272.1652.

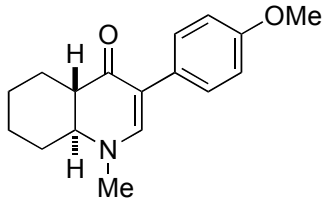

3.22

***(trans)*-3-(4-Methoxyphenyl)-1-methyl-4a,5,6,7,8,8a-hexahydroquinolin-4(1*H*)-one (3.22).** Trifluoroborate **3.3** was added slowly over 6 h and the reaction was stirred for an additional h. The title compound was isolated as an off-white solid (mp 151-152.5 °C). ^1H NMR (400 MHz, $CDCl_3$) δ 1.08-1.47 (m, 4H), 1.83-1.90 (m, 2H), 2.15-2.25 (m, 2H), 2.46-2.50 (m, 1H), 3.00 (s, 3H), 3.09 (ddd, 1H, *J* = 3.6, 11.3, 14.8 Hz), 3.78 (s, 3H), 6.84 (d, 2H, *J* = 8.8 Hz), 7.16 (s, 1H), 7.31 (d, 2H, *J* = 8.8 Hz); ^{13}C NMR (100 MHz, $CDCl_3$) δ 24.4, 24.9, 25.0, 30.4, 39.6, 48.7, 55.3, 62.0, 110.9, 113.5 (2C), 128.9, (2C) 129.1, 153.7, 157.7, 191.2; IR (neat) 2919, 1621, 1591, 1513, 1247, 1159 cm^{-1}; HRMS (ESI+) *m/e* calc'd for $[M+H]^+$ $C_{17}H_{22}NO_2$: 272.1645, found 272.1651.

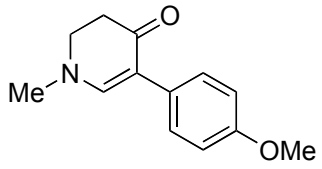

3.23

5-(4-Methoxyphenyl)-1-methyl-2,3-dihydropyridin-4(1*H*)-one (3.23). Trifluoroborate **3.3** was added slowly over 5 h and the reaction was stirred for an additional h. The title compound was isolated as a yellowish oil. ^{1}H NMR (400 MHz, $CDCl_3$) δ 2.62 (t, 2H, *J* = 7.8 Hz), 3.08 (s, 3H), 3.47 (t, 2H, *J* = 7.8 Hz), 3.78 (s, 3H), 6.85 (d, 2H, *J* = 8.8 Hz), 7.13 (s, 1H), 7.28 (d, 2H, *J* = 8.8 Hz); ^{13}C NMR (100 MHz, $CDCl_3$) δ 36.3, 43.5, 49.3, 55.5, 110.8, 113.8 (2C), 129.1 (2C), 129.1, 153.8, 157.9, 188.7; IR (neat) 2957, 1626, 1598, 1512, 1299, 1245 cm^{-1}; HRMS (ESI+) *m/e* calc'd for $[M+H]^+$ $C_{13}H_{16}NO_2$: 218.1181, found 218.1176.

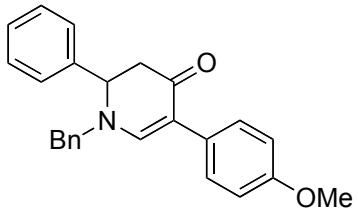

3.24

1-Benzyl-5-(4-methoxyphenyl)-2-phenyl-2,3-dihydropyridin-4(1*H*)-one (3.24). Trifluoroborate **3.3** was added slowly over 6 h and the reaction was stirred for an additional h. The title compound was isolated as a yellowish oil. ^{1}H NMR (400 MHz, $CDCl_3$) d 2.83 (dd, 1H, *J* = 7.5, 16.3 Hz), 2.98 (dd, 1H, *J* = 7.5, 16.3 Hz), 3.80 (s, 3H), 4.19 (d, 1H, *J* = 15.1 Hz), 4.41 (d, 1H, *J* = 15.1 Hz), 4.56 (t, 1H, *J* = 7.5 Hz), 6.89 (d, 2H, *J* = 8.8 Hz), 7.16-7.38

(m, 12H), 7.49 (s, 1H); ^{13}C NMR (100 MHz, $CDCl_3$) d 44.4, 55.3, 57.5, 61.0, 111.3, 113.8 (2C), 127.1 (2C), 127.8 (2C), 128.3, 128.4, 128.6, 128.9 (2C), 129.0 (2C), 129.1 (2C), 136.0, 138.5, 152.6, 157.9, 187.8; IR (neat) 3030, 1634, 1595, 1512, 1245, 1178 cm^{-1}; HRMS (ESI +) *m/e* calc'd for $[M+H]^+$ $C_{25}H_{24}NO_2$: 370.1802, found 370.1811.

Oxidative Heck coupling:

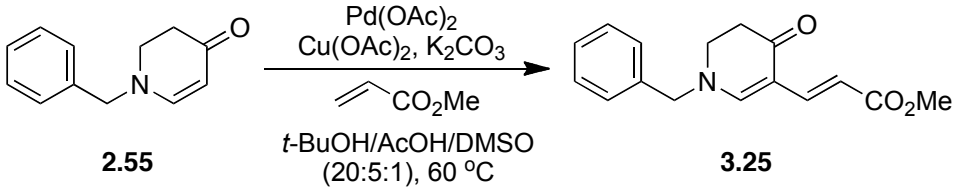

2.55 **3.25**

(*E*)-Methyl 3-(1-Benzyl-4-oxo-1,4,5,6-tetrahydropyridin-3-yl)acrylate (3.25). Enaminone **2.55** (37 mg, 0.20 mmol), methylacrylate (34 mg, 0.40 mmol), $Pd(OAc)_2$ (14 mg, 0.06 mmol), $Cu(OAc)_2$ (110 mg, 0.60 mmol) and K_2CO_3 (55 mg, 0.40 mmol) combined in a 20:5:1 mixture of *t*-BuOH/AcOH/DMSO (2.0 mL) and stirred for 5 min. The reaction mixture was heated to 80 °C and stirred until judged complete by TLC. The reaction mixture was diluted with EtOAc (8 mL) and excess K_2CO_3 (~1 g) was added to neutralize the AcOH. After stirring this mixture for 5 min the precipitate was filtered over Celite using EtOAc as the eluent. The filtrate was concentrated and purified by chromatography on SiO_2 (65% EtOAc/ hexanes). The title compound was isolated as a waxy yellow solid. ^{1}H NMR (400 MHz, $CDCl_3$) δ 2.53 (t, 2H, *J* = 7.8 Hz), 3.46 (t, 2H, *J* = 7.8 Hz), 3.71 (s, 3H), 4.51 (s, 2H), 6.66 (d, 1H, *J* = 15.6 Hz), 7.22 (d, 1H, *J* = 15.6 Hz), 7.26-7.28 (m, 2H), 7.36-7.43 (m, 3H),

7.51 (s, 1H); ^{13}C NMR (100 MHz, $CDCl_3$) δ 35.9, 46.2, 51.1, 60.7, 106.0, 110.9, 127.8 (2C), 128.9, 129.3 (2C), 134.4, 140.4, 156.9, 169.6, 188.7; IR (neat) 2948, 1696, 1653, 1596, 1436, 1224 cm^{-1}; HRMS (ESI+) *m/e* calc'd for $[M+H]^+$ $C_{16}H_{18}NO_3$: 272.1287, found 272.1275.

6.4 Chapter 4

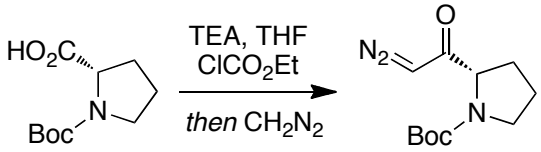

Boc-L-proline **4.3**

(*S*)-*tert*-butyl 2-(2-diazoacetyl)pyrrolidine-1-carboxylate (4.3). *Warning: Large amounts of diazomethane were used for this transformation. Proper care should be taken when handling this highly explosive reagent. All glassware used was free of cracks, scratches or ground-glass joints and a blast shield was used.* Boc-L-proline (10.8 g, 50.0 mmol, 1.00 equiv) was taken into THF (100 mL) with stirring and cooled to 0 ºC with an ice bath. The reaction solution was treated with TEA (7.66 mL, 55.0 mmol, 1.10 equiv) and allowed to react for 15 min to fully deprotonate the carboxylic acid. With the addition of ethyl chloroformate (5.23 mL, 55.0 mmol, 1.10 equiv), a thick white precipitate formed. Stirring was continued for 15 min then stopped. In a separate flask, an ice-cold ethereal solution of diazomethane was prepared and, without stirring, was carefully decanted into the freshly prepared anhydride reaction flask using a glass funnel. The reaction solution was lightly stirred for 4 seconds then stirring was stopped. The mixture was allowed to warm to room

temperature and react overnight. Any additional diazomethane was carefully quenched with 0.5 N acetic acid (100 mL). The drop-wise addition of saturated sodium bicarbonate regulated the solution back to a basic pH 8-9 with gentle stirring. The organic and aqueous layers were separated. The organic phase was washed twice each with saturated sodium bicarbonate and brine then dried over sodium sulfate. The solvent was evaporated under reduced pressure. At this point the crude diazoketone could be used for subsequent Wolff rearrangement reactions. Alternatively, the diazoketone could also be purified by chromatography on SiO_2 (15% EtOAc/hexanes) to provide the title compound as a yellow oil (72%). The spectral data matched that in the literature.[352, 353]

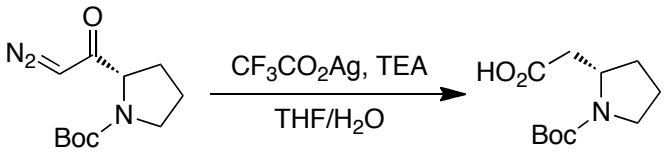

4.3 **4.4**

(*S*)-2-(1-(*tert*-butoxycarbonyl)pyrrolidin-2-yl)acetic acid (4.4). Diazoketone **4.3** (8.61 g, 36.0 mmol, 1.00 equiv) was dissolved in 220 mL of a 1:10 mixture of water and THF and cooled to –25 ºC and stirred for 30 minutes. Foil was used to cover the reaction flask so as to exclude light from the reaction solution. In a separate foil covered flask, silver trifluoroacetate (795 mg, 3.60 mmol, 0.10 equiv) was dissolved in TEA (110 mL). This solution was added dropwise to the diazoketone mixture over 30 min. The reaction temperature was allowed to slowly warm to room temperature and the solution was stirred overnight. To the reaction mixture was added activated carbon (~2 g) and the reaction mixture was stirred for 5 min and filtered. The filtrate was concentrated and the residue

redissolved in EtOAc. To this was added activated carbon (~2 g) and the process repeated. When the filtrate had been concentrated a second time the residue was purified via SiO_2 flash chromatography (30% EtOAc/hexanes) affording the title compound (68%) as a white solid. The spectral data matched that in the literature.[353]

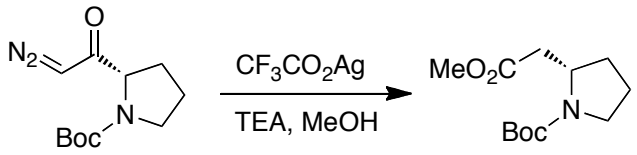

4.3 **4.5**

(*S*)-*tert*-butyl 2-(2-methoxy-2-oxoethyl)pyrrolidine-1-carboxylate (4.5). Diazoketone **4.3** (2.53 g, 10.6 mmol, 1.00 equiv) was dissolved in 45 mL of MeOH and the reaction flask was covered with foil to exclude light from the reaction solution. In a separate foil covered flask, silver trifluoroacetate (240 mg, 1.4 mmol, 0.13 equiv) was dissolved in TEA (30 mL). This solution was added dropwise to the diazoketone mixture over 30 min. The reaction temperature was allowed to slowly warm to room temperature and the solution was stirred overnight. To the reaction mixture was added activated carbon (~1 g) and the reaction mixture was stirred for 5 min and filtered. The filtrate was concentrated and the residue redissolved in EtOAc. To this was added activated carbon (~1 g) and the process repeated. When the filtrate had been concentrated a second time the residue was purified via SiO_2 flash chromatography (15% EtOAc/hexanes) affording the title compound (86%) as a clear oil. The spectral data matched that in the literature.[354]

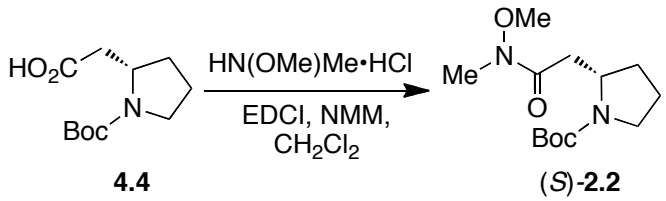

4.4 (*S*)-**2.2**

(*S*)-*tert*-Butyl 2-(2-(Methoxy(methyl)amino)-2-oxoethyl)pyrrolidine-1-carboxylate (2.2). Amino acid **4.4** (920 mg, 4.0 mmol, 1.0 equiv) was dissolved in anhydrous CH_2Cl_2 (100 mL) under an argon atmosphere and cooled to –15 °C. To this solution was added *N*,*O*-dimethylhydroxylamine•HCl (430 mg, 4.4 mmol, 1.1 equiv) and *N*-methylmorpholine (0.49 mL, 4.4 mmol, 1.1 equiv) followed by EDCI (810 mg 4.2 mmol, 1.1 equiv). The reaction mixture was then allowed to come to room temperature. After 2 h the reaction was again cooled to 0 °C and quenched by the addition of an ice cold 10% HCl solution (25 mL) and allowed to stir at this temperature for 5 min. The reaction was diluted with water (50 mL) and extracted with CH_2Cl_2 (x3). The combined organic layers were washed with saturated $NaHCO_3$ (x1), dried over Na_2SO_4, filtered and concentrated. Purification via SiO_2 flash chromatography (50% EtOAc/hexane) afforded the title compound as a clear oil (98%). See Section 6.2 for spectral data.

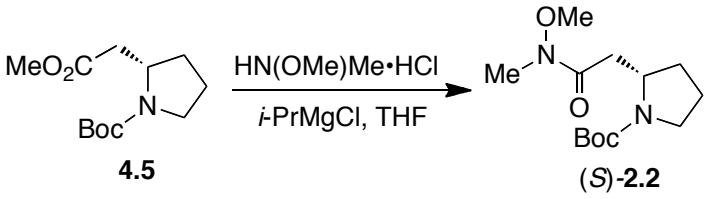

4.5 (*S*)-**2.2**

Methyl ester **4.5** was converted to the Weinreb amide **2.2** using the procedure reported by Williams *et al*.[279] The crude product was purified via SiO_2 flash chromatography (50%

EtOAc in hexanes) to give the Weinreb amide (86%) as a clear viscous oil. See Section 6.2 for spectral data.

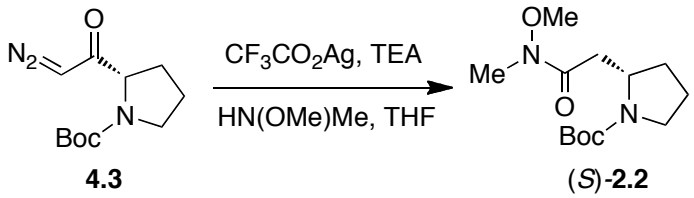

4.3 (*S*)-**2.2**

Diazoketone **4.4** (7.37 g, 30.8 mmol, 1.00 equiv)was taken into THF (130 mL) and cooled to 0 ºC. Foil was used to cover the reaction flask so as to exclude light from the reaction solution. To this was added freshly distilled *N,O*-dimethylhydroxylamine (4.00 g, 92.4 mmol, 3.00 equiv).[344] In a separate foil covered flask, silver trifluoroacetate (1.37 g, 6.20 mmol, 0.20 equiv) was dissolved in TEA (86 mL). This solution was added to the diazoketone mixture over 30 min. The reaction temperature was allowed to slowly warm to room temperature and the solution was stirred overnight. To the reaction mixture was added activated charcoal (~2 g) and the reaction mixture was stirred for 5 min and filtered. The filtrate was concentrated and the residue redissolved in EtOAc. To this was added activated charcoal (~2 g) and the process repeated. When the filtrate had been concentrated a second time the residue was purified via SiO_2 flash chromatography (50% EtOAc/hexanes) affording the pure Weinreb amide as a clear oil (97%). See Section 6.2 for spectral data.

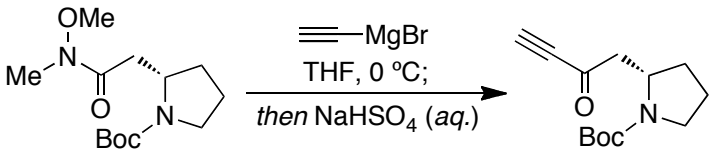

(*S*)-**2.2** (*S*)-**2.17**

(*S*)-*tert*-butyl 2-(2-oxobut-3-yn-1-yl)pyrrolidine-1-carboxylate (2.17). The Weinreb amide (4.66 g, 17.1 mmol, 1.0 equiv) was dissolved in anhydrous THF (200 mL) under nitrogen atmosphere and cooled to 0 °C. To this reaction vessel, was added dropwise, a solution of ethynyl magnesium bromide reagent (171 mL, 85.6 mmol, 5.0 equiv, 0.5 M in THF) and allowed to come to room temperature. After the reaction was judged complete by TLC it was quenched by the addition of an ice cold 10% HCl solution (15 mL) and allowed to stir at this temperature for 5 minutes. The reaction was diluted with water and extracted with EtOAc (x3). The combined organic layers were washed with saturated $NaHCO_3$ (x1), dried over Na_2SO_4, filtered and concentrated. The title compound was obtained as a clear oil (3.94 g, 97% yield) after SiO_2 flash chromatography (20% EtOAc/Hexanes): Spectral data was identical to that reported.[255]

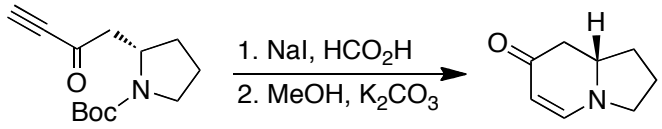

(*S*)-**2.17** (*S*)-**2.37**

(*S*)-2,3,8,8a-tetrahydroindolizin-7(1H)-one (2.37). Ynone **2.17** (3.74 g, 15.8 mmol, 1.0 equiv) was dissolved in formic acid (50 mL) solution under a N_2 atmosphere and NaI (7.09 g,

47.3 mmol, 3.0 equiv) was added. The reaction was left stirring for 6 h at room temperature. The solvent was removed by passing N_2 over the reaction mixture. The remaining residue was placed under vacuum for 15 minutes and then dissolved in MeOH (100 mL). A separate flask was charged with 700 mL of MeOH and K_2CO_3 (10.9 g, 79.0 mmol, 5.0 equiv). To this flask was added the solution of deprotected ynone over 15 minutes. The reaction was stirred for 1 h and the solvent was evaporated. At this time CH_2Cl_2 was added to redissolve the product (but not the inorganic salts), the slurry was suction filtered, and the filtrate concentrated. To the solid residue was added more CH_2Cl_2 and the precipitates were once again filtered away. This residue after removal of solvent was purified via SiO_2 flash chromatography to provide the title compound as an off-white solid (2.05 g, 95% yield) after SiO_2 flash chromatography (100% acetone): See Section 6.2 for spectral data.

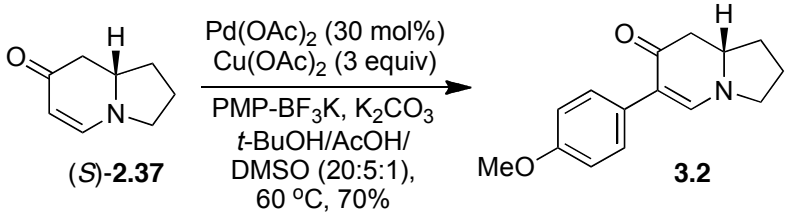

(*S*)-6-(4-methoxyphenyl)-2,3,8,8a-tetrahydroindolizin-7(1*H*)-one (3.2). Freshly purified enaminone (750 mg, 5.5 mmol, 1.0 equiv), $Pd(OAc)_2$ (370 mg, 1.7 mmol, 0.30 equiv), anhydrous $Cu(OAc)_2$ powder (3.0 g, 17 mmol, 3.0 equiv) and granular K_2CO_3 (1.5 g, 11 mmol, 2.0 equiv) were combined in a 20:5:1 mixture of degassed *t*-BuOH/AcOH/DMSO (55 mL) under N_2 and stirred for 5 min (*Note: Solvents were used without purification*). The reaction mixture was heated to 60 °C and the potassium trifluoroborate (3.5 g, 17 mmol, 3.0

equiv) was added slowly over 5 h as a solid. Approximately, 0.20 equivalents of trifluoroborate were added every 30 min. The reaction was stirred for an additional hour and was monitored by TLC using 100% EtOAc as the mobile phase. The reaction mixture was diluted with EtOAc and added to a separatory funnel containing brine. The product was extracted with EtOAc (3x). The combined organic layers were washed brine (2x) and sat. $NaHCO_3$ (*aq*.) (2x), dried over Na_2SO_4 and concentrated *in vacuo*. The title compound was obtained as a pale yellow solid (930 mg, 70% yield) after SiO_2 flash chromatography (80% EtOAc/hexanes). The spectral data was identical to that of (±)-**3.2** (See Section 6.2). $[\alpha]_D^{22}$ = –97.5 (*c* 1.00, $CHCl_3$).

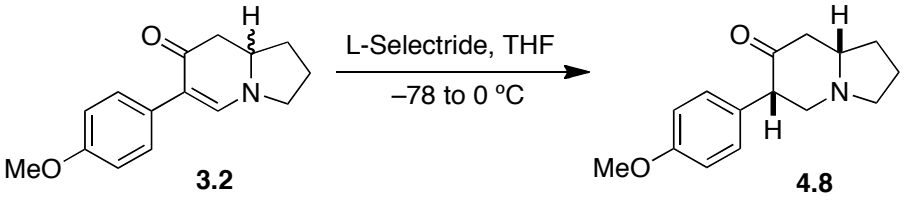

(6*S,8a*S**)-6-(4-methoxyphenyl)hexahydroindolizin-7(1*H*)-one (4.8).** Enaminone **3.2** (120 mg, 0.50 mmol, 1.0 equiv) was dissolved in anhydrous THF (5 mL) under a N_2 atmosphere. The solution was cooled to –78 ºC at which point L-Selectride (0.55 mL, 0.55 mmol, 1.1 equiv, 1.0 M in THF) was added over 15 minutes. After stirring for 1 h, the reaction was slowly warmed to 0 ºC over 1.5 h and stirred at room temperature for an additional 2 h. The reaction was quenched with a saturated solution of $NaHCO_3$ (*aq*.) and added to a separatory funnel. The product was extracted with EtOAc (3x). The combined organic layers were dried over Na_2SO_4 and concentrated *in vacuo*. The title compound (110 mg, 90% yield) was obtained as a white crystalline solid (mp 118–120 ºC) after SiO_2 flash

chromatography [60% EtOAc/hexanes (1% TEA)]. Spectral data was identical to that reported.[318] $[\alpha]_D^{22} = +6.05$ (c 1.14, $CHCl_3$).

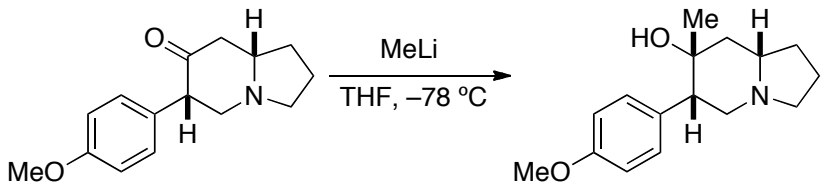

4.8 **4.9**

(6*S*,7*R*,8a*S*)-6-(4-methoxyphenyl)-7-methyloctahydroindolizin-7-ol (4.9). Ketone **4.8** (105 mg, 0.43 mmol, 1.00 equiv) taken in anhydrous THF (3.5 mL) in a flame dried RBF and cooled to –78 ºC. Methyl lithium (0.32 mL, 0.52 mmol, 1.2 equiv, 1.6 M in Et_2O) was added dropwise and stirred for 45 min at –78 ºC. The reaction was quenched with MeOH (1 mL) and allowed to warm to room temperature. The quenched reaction mixture was added to a separatory funnel containing 10% NaOH (*aq*.) and the product was extracted with EtOAc (3x). The combined organic layers were dried over Na_2SO_4 and concentrated *in vacuo*. The title compound (85 mg, 75% yield) was obtained as a white crystalline solid (mp 92–96 ºC) after SiO_2 flash chromatography [50% EtOAc/hexanes (1% TEA)]. ^{1}H NMR (400 MHz, $CDCl_3$) δ 1.05 (s, 3H), 1.37–1.49 (m, 2H), 1.71–1.78 (m, 1H), 1.81–1.91 (m, 2H), 1.97 (dd, J = 13.2, 2.5 Hz, 1H), 2.23 (dd, J = 17.9, 8.9 Hz, 1H), 2.34–2.39 (m, 1H), 2.67 (dd, J = 11.3, 11.3 Hz, 1H), 2.83 (dd, J = 11.9, 3.8 Hz, 1H), 2.94 (dd, J = 10.6, 3.9 Hz, 1H), 3.07 (dd, J = 8.6, 8.6 Hz, 1H), 3.8 (s, 3H), 6.86 (d, J = 8.5 Hz, 2H), 7.20 (d, J = 8.6 Hz, 2H); ^{13}C NMR (100 MHz, $CDCl_3$) δ 21.3, 29.6, 30.1, 44.3, 51.4, 53.7, 53.7, 55.2, 59.4, 70.4, 113.7, 130.3,

131.9, 158.6 ; IR (neat) 3416, 2961, 1611, 1512, 1246, 1178, 833 cm^{-1} ; HRMS (ESI+) *m/e* calc'd for $[M+H]^+ C_{16}H_{24}NO_2$: 262.1807, found 262.1790. $[\alpha]_D^{22} = -6.54$ (*c* 1.10, $CHCl_3$).

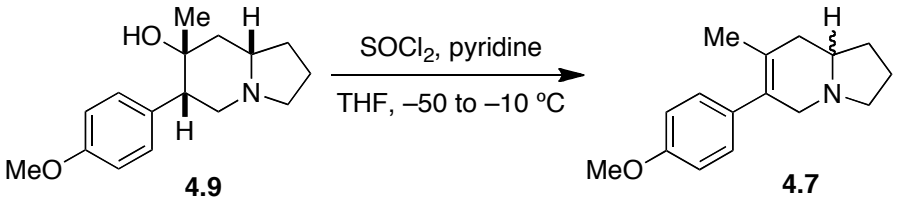

6-(4-Methoxyphenyl)-7-methyl-1,2,3,5,8,8a-hexahydroindolizine (4.7). Indolizidine **4.9** (62 mg, 0.24 mmol, 1.0 equiv) was dissolved in anhydrous THF (4.0 mL) and cooled to –50 ºC. Pyridine (0.1 mL) followed by $SOCl_2$ (0.043 mL, 0.59 mmol, 2.5 equiv) in 0.5 mL THF was added dropwise to the reaction mixture. The reaction mixture was kept between –30 and –10 ºC for 1.5 h. The reaction was quenched with 10% NaOH (*aq*.). The quenched reaction mixture was added to a separatory funnel containing 10% NaOH (*aq*.) and the product was extracted with EtOAc (3x). The combined organic layers were dried over Na_2SO_4 and concentrated *in vacuo*. The title compound was obtained as a colorless oil (51 mg, 88% yield) after SiO_2 flash chromatography [20% EtOAc/hexanes (1% TEA)]. See below for spectral data.

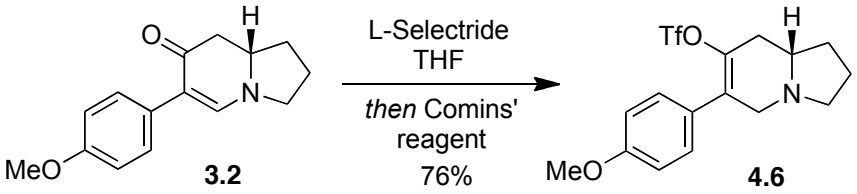

(*S*) - 6 - (4-Methoxyphenyl) - 1, 2, 3, 5, 8, 8a – hexahydroindolizin – 7 – yl – trifluoromethanesulfonate (4.6). Enaminone **3.2** (590 mg, 2.4 mmol, 1.0 equiv) was dissolved in anhydrous THF (30 mL) under a N_2 atmosphere. The solution was cooled to –78 ºC at which point L-Selectride (0.23 mL, 0.23 mmol, 1.0 equiv, 1.0 M in THF) was added over 15 min. After stirring for 1 h, the reaction was slowly warmed to 0 ºC over 2 h. The reaction mixture was once again cooled to –78 ºC and Comins' reagent (1.1 g, 2.7 mmol, 1.1 equiv) was added all at once. The mixture was stirred for another hour at –78 ºC and then slowly warmed to 0 ºC over 2 h. The reaction was quenched with a saturated solution of $NaHCO_3$ (*aq*.) and added to a separatory funnel. The product was extracted with EtOAc (3x). The combined organic layers were dried over Na_2SO_4 and concentrated *in vacuo*. The title compound was obtained as a colorless oil (690 mg, 76% yield) after SiO_2 flash chromatography (10% EtOAc/hexanes (1% TEA): ^{1}H NMR (500 MHz, $CDCl_3$) δ 1.49-1.57 (m, 1H), 1.76-1.84 (m, 1H), 1.87-1.96 (m, 1H), 2.00-2.07 (m, 1H), 2.22 (dd, *J* = 18.1, 9.2 Hz, 1H), 2.47-2.62 (m, 3H), 3.06 (d, *J* = 15.8 Hz, 1H), 3.18 (dt, *J* = 4.4, 2.1 Hz, 1H), 3.72-3.75 (m, 1H), 3.74 (s, 3H), 6.83 (d, *J* = 8.8 Hz, 2H), 7.14 (d, *J* = 8.8 Hz, 2H); ^{13}C NMR (125 MHz, $CDCl_3$) δ 22.2, 30.5, 35.2, 53.4, 55.3, 55.6, 60.5, 113.9, 118.1 (q, J_{CF} = 320 Hz), 126.6, 129.2, 129.5, 142.0, 159.5 ; IR (neat) 2959, 1610, 1512, 1416, 1209, 1146 cm^{-1}; HRMS (ESI +) *m/e* calc'd for $[M+H]^+$ $C_{16}H_{19}F_3NO_4S$: 378.0987, found 378.0974; $[\alpha]_D^{22}$ = +66.3 (*c* 1.00, $CHCl_3$).

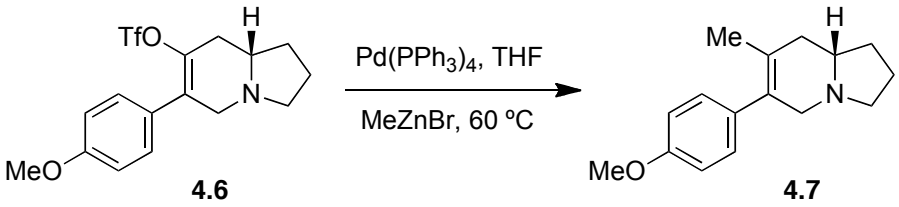

4.6 **4.7**

(*S*)-6-(4-Methoxyphenyl)-7-methyl-1,2,3,5,8,8a-hexahydroindolizine (4.7). *Preparation of organo zinc reagent*. A flame dried RBF under N_2 was charged with anhydrous THF (10.0 mL) and cooled to –78 ºC. Methyl lithium (1.6 mL, 2.5 mmol, 5.0 equiv, 1.6M in Et_2O) was added and the solution was allowed to sit. A separate RBF was charged with anhydrous $ZnBr_2$ (590 mg, 2.6 mmol, 5.2 equiv). The $ZnBr_2$ was dried by heating the RBF under a vacuum with a heat gun for 5 min. When the $ZnBr_2$ had cooled to room temperature it was dissolved in anhydrous THF (6.0 mL) under N_2. This $ZnBr_2$ solution was slowly cannulated into the methyl lithium solution and the resulting solution was stirred at –78 ºC for 5 min and then allowed to warm to room temperature.

Triflate **4.6** (190 mg, 0.50 mmol, 1.0 equiv), dissolved in a minimal amount of THF, and $Pd(PPh_3)_4$ (29 mg, 0.025 mmol, 5.0 mol%) were added sequentially to the zinc reagent. If the reaction had not gone to completion after 1 h at room temperature, the reaction mixture was heated to 50 ºC. Upon consumption of the triflate starting material (as judged by TLC) SiO_2 was added to the reaction mixture and the solvent was evaporated to leave a free flowing powder. Following flash chromatography (20% EtOAc/hexanes (1% TEA)) 110 mg (91%) of the title compound was obtained as a colorless oil: ^{1}H NMR (400 MHz, $CDCl_3$) δ 1.46-1.54 (m, 1H), 1.60 (s, 3H), 1.73-1.81 (m, 1H), 1.85-1.94 (m, 1H), 2.00-2.32 (m, 5H), 2.91 (d, *J* = 15.4 Hz, 1H), 3.22 (dd, *J* = 3.2, 3.2 Hz, 1H), 3.62 (d, *J* = 15.4 Hz, 1H), 3.82 (s, 3H), 6.86 (d, *J* = 8.7 Hz, 2H), 7.10 (d, *J* = 8.7 Hz, 2H); ^{13}C NMR (100 MHz, $CDCl_3$) δ 20.0,

21.4, 30.8, 38.5, 54.2, 55.2, 57.8, 60.2, 113.5, 127.9, 130.0, 130.3, 133.8, 158.1; IR (neat) 2907, 1609, 1510, 1244, 1175, 831 cm^{-1}; HRMS (ESI+) *m/e* calc'd for $[M+H]^+$ $C_{16}H_{22}NO$: 244.1701, found 244.1688; $[\alpha]_D^{22} = +142$ (*c* 1.00, $CHCl_3$).

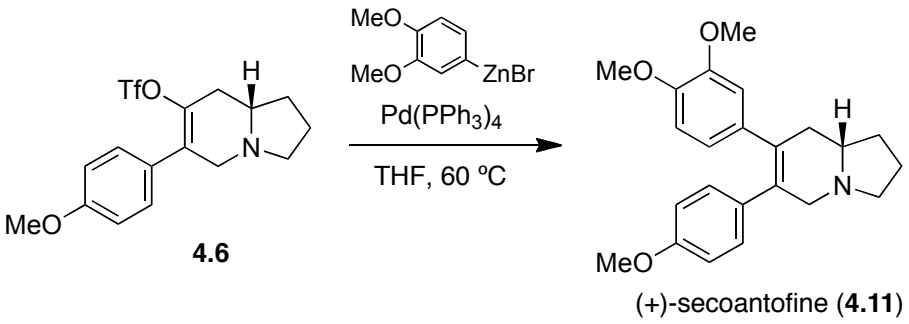

(+)-Secoantofine (4.11). *Preparation of organo zinc reagent*. A flame dried RBF under N_2 was charged with anhydrous THF (15.0 mL) and cooled to –78 ºC. *tert*-Butyllithium (6.6 mL, 11 mmol, 11 equiv, 1.7 M in pentane) was added carefully and the solution was allowed to sit for 5 min at –78 ºC. 4-Bromoveratrole (1.2 g, 5.4 mmol, 5.0 equiv) was then added dropwise and the resulting reaction mixture was stirred for 2 h and –78 ºC. A different RBF was charged with anhydrous $ZnBr_2$ (1.3 g, 5.6 mmol, 5.2 equiv). The $ZnBr_2$ was dried by heating the RBF under a vacuum with a heat gun for 5 min. When the $ZnBr_2$ had cooled to room temperature it dissolved in anhydrous THF (12.0 mL) under N_2. This $ZnBr_2$ solution was slowly cannulated into the yellow aryllithium reagent solution. The resulting cloudy white solution was stirred at –78 ºC for 5 min and then allowed to warm to room temperature. Upon warming the solution became clear. Triflate **4.6** (400 mg, 1.1 mmol, 1.0 equiv) (dissolved in a minimal amount of THF) and $Pd(PPh_3)_4$ (62 mg, 0.054 mmol, 5.0 mol %) were added sequentially to the zinc reagent. If the reaction had not gone to completion

after 1 h at room temperature, the reaction mixture was heated to 50 ºC. Upon consumption of the triflate starting material (as judged by TLC) SiO_2 was added to the reaction mixture and the solvent was evaporated to leave a free flowing powder. Following flash chromatography [40% EtOAc/hexanes (1% TEA)] 380 mg (96%) of the title compound was obtained as a yellow oil: ^{1}H NMR (400 MHz, $CDCl_3$) δ 1.51-1.63 (m, 1H), 1.78-2.01 (m, 2H), 2.06-2.14 (m, 1H), 2.25 (dd, *J* = 9.0, 9.0 Hz, 1H), 2.36-2.45 (m, 2H), 2.69-2.77 (m, 1H), 3.07 (td, *J* = 16.0, 3.1 Hz, 1H), 3.29 (dt, *J* = 4.3, 2.0 Hz, 1H), 3.54 (s, 3H), 3.72 (s, 3H), 3.81 (s, 3H), 3.86 (d, *J* = 15.8 Hz, 1H), 6.47 (d, *J* = 1.1 Hz, 1H), 6.66-6.69 (m, 4H), 6.97 (d, *J* = 8.8 Hz, 2H); ^{13}C NMR (100 MHz, $CDCl_3$) δ 21.5, 30.8, 38.6, 54.3, 55.1, 55.5, 55.7, 57.9, 60.4, 110.4, 113.1, 113.4, 120.7, 130.2, 132.6, 132.7, 133.6, 135.1, 147.1, 147.9, 158.0; IR (neat) 2955, 1607, 1511, 1245, 1030, 755 cm^{-1}; HRMS (ESI+) *m/e* calc'd for $[M+H]^+$ $C_{23}H_{28}NO_3$: 366.2064, found 366.2068; $[\alpha]_D^{22} = +169$ (*c* 1.00, $CHCl_3$).

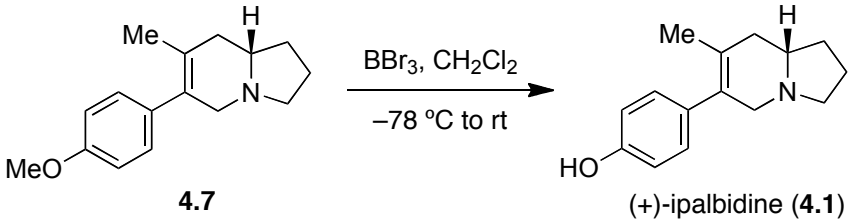

(+)-Ipalbidine (4.1). *O*-Methylipalbidine (**4.7**) (56 mg, 0.23 mmol, 1.0 equiv) was dissolved in CH_2Cl_2 (1.0 mL) and cooled to –78 ºC under N_2. To this solution was added BBr_3 (0.23 mL, 0.23 mmol, 1.0 M in CH_2Cl_2). The reaction was allowed to warm to room temperature over night. The reaction was quenched with water (1.0 mL) and then 5.0 mL of a saturated solution of $NaHCO_3$ (*aq*.). The product was extracted from the aqueous layer with CH_2Cl_2

(3x). The combined organic layers were dried with Na_2SO_4, concentrated and purified *via* flash chromatography [80% EtOAc/hexane (1% TEA)] to provide 42 mg (80%) of (+)-ipalbidine as a white crystalline solid (mp 122.2-124.6 ºC). ^{1}H NMR (500 MHz, $CDCl_3$) δ 1.60 (s, 3H), 1.75-1.84 (m, 1H), 1.91-1.99 (m, 1H), 2.06-2.23 (m, 2H), 2.35-2.45 (m, 2H), 2.54-2.61 (m, 1H), 2.79-2.87 (m, 1H), 3.21 (d, *J* = 14.7 Hz, 1H), 3.45-3.50 (m, 1H), 3.77 (d, *J* = 15.5 Hz, 1H), 6.83 (d, *J* = 8.5 Hz, 2H), 6.95 (d, *J* = 8.5 Hz, 2H); ^{13}C NMR (100 MHz, $CDCl_3$) δ 20.0, 21.0, 29.7, 36.0, 53.4, 55.9, 61.0, 115.6, 127.9, 128.6, 129.8, 130.9, 155.7; IR (neat) 2913, 1609, 1513, 1445, 1269, 1169 cm^{-1}; HRMS (ESI+) *m/e* calc'd for $[M+H]^+$ $C_{15}H_{20}NO$: 230.1545, found 230.1531; $[\alpha]_D^{22} = +202$ (*c* 1.00, $CHCl_3$). [Lit. *S-enantiomer:* +233.5 (*c* 1, $CHCl_3$); *R-enantiomer:* –237 (*c* 1, $CHCl_3$), –190.5 (*c* 1, MeOH)].[326]

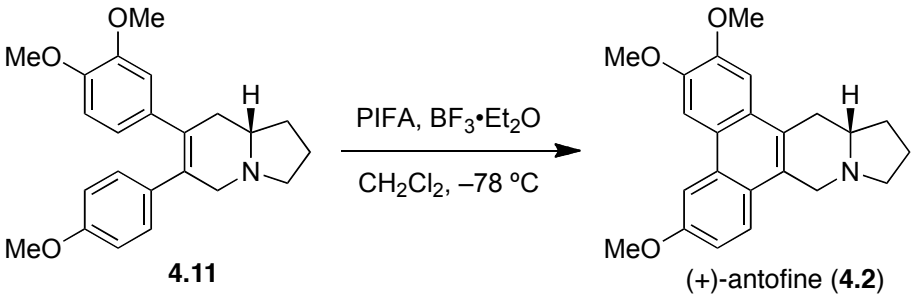

4.11 (+)-antofine (**4.2**)

(+)-Antofine (4.2). Secoantofine (**4.11**) (48 mg, 0.13 mmol, 1.0 equiv) was dissolved in CH_2Cl_2 (2.0 mL) and cooled to –78 ºC. To this solution was added PIFA (62 mg, 0.14 mmol, 1.1 equiv) and BF_3•Et_2O (16 mg, 0.14 mmol, 1.1 equiv) sequentially. The solution was stirred for 4 h while being monitored by TLC. A solution of PIFA (62 mg in 2.0 mL CH_2Cl_2) was added dropwise to the reaction mixture until the reaction had gone to completion. Upon consumption of starting material the reaction was quenched with 10% NaOH (*aq*.) and the

mixture was vigorously stirred for 1 h. The product was extracted from the aqueous layer with CH_2Cl_2 (3x). The combined organic layers were dried with Na_2SO_4, concentrated and purified *via* flash chromatography [70% EtOAc/hexane (1% TEA)] to provide 34 mg (70%) of (+)-antofine as a white crystalline solid: mp 226-227 °C (decomp.) ^{1}H NMR (400 MHz, $CDCl_3$) δ 1.65-1.75 (m, 1H), 1.80-2.02 (m, 2H), 2.13-2.22 (m, 1H), 2.35-2.46 (m, 2H), 2.79-2.86 (m, 1H), 3.28 (ddd, *J* = 15.8, 3.7, 1.5 Hz, 1H), 3.38 (dt, *J* = 4.3, 2.1 Hz, 1H), 3.63 (d, *J* = 14.9 Hz, 1H), 3.95 (s, 3H), 3.99 (s, 3H), 4.04 (s, 3H), 4.63 (d, *J* = 14.9 Hz, 1H), 7.13 (dd, *J* = 9.0, 2.5 Hz, 1H), 7.25 (s, 1H), 7.75 (d, *J* = 9.0 Hz, 1H), 7.83 (d, *J* = 2.5 Hz, 1H), 7.85 (s, 1H); ^{13}C NMR (100 MHz, $CDCl_3$) δ 21.6, 31.3, 33.7, 53.8, 55.0, 55.5, 55.9, 56.0, 60.3, 104.0, 104.7, 114.9, 123.5, 124.1, 124.2, 125.5, 126.7, 127.0, 130.2, 148.4, 149.4, 157.5; HRMS (ESI+) *m/e* calc'd for $[M+H]^+$ $C_{23}H_{26}NO_3$: 364.1913, found 364.1909; $[\alpha]_D^{22} = +111$ (*c* 1.00, $CHCl_3$). [Lit. *R-enantiomer*: –113.4 (*c* 1.23, $CHCl_3$),[149] –125.2 (*c* 1.27, $CHCl_3$),[184] –108.2 (*c* 0.71, $CHCl_3$);[171] *S-enantiomer*: +66 ($CHCl_3$)[355]].

6.5 Chapter 5

6.5.1 Preparation of tylocrebrine and analogs

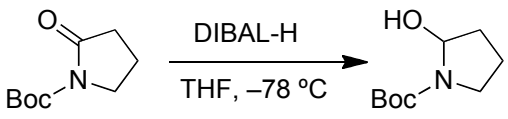

5.6 **5.7**

***tert*-butyl 2-(2-ethoxy-2-oxoethyl)pyrrolidine-1-carboxylate (5.7).** Pyrrolidinone **5.6**

(4.21g, 22.7 mmol, 1.0 equiv) was dissolved in THF (65 mL) under a N_2 atmosphere and cooled to –78 ºC. DIBAL-H (32.0 mL, 32.0 mmol, 1.4 equiv, 1.0 M in hexanes) was added slowly (over 15 minutes) and reaction mixture was stirred for 1 h. The reaction was quenched with saturated NH_4Cl (80 mL) and warmed to room temperature. The quenched reaction was then treated with 10% Na_2CO_3 (60 mL) and vigorously stirred for 20 minutes. The product was then extracted with CH_2Cl_2 (3x) and the combined organic layers were dried over Na_2SO_4 and concentrated *in vacuo*. The title compound was obtained as a clear oil (3.92 g, 92% yield) after SiO_2 flash chromatography (30% EtOAc/Hexanes): Spectral data was identical to that reported.[356]

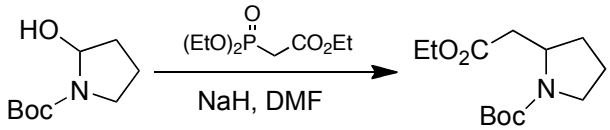

5.7 **5.8**

***tert*-butyl 2-(2-ethoxy-2-oxoethyl)pyrrolidine-1-carboxylate (5.8).** To a flame-dried flask was added anhydrous DMF (100 mL) and the flask was purged with N_2. Sodium hydride (1.01 g, 25.2 mmol, 1.2 equiv, 60% in mineral oil) was added to the flask followed by triethylphosphonoacetate (5.0 mL, 25.2 mmol, 1.2 equiv). The mixture was stirred for 1 h at room temperature. To this solution was added hemiaminal **5.7** (3.92 g, 21.0 mmol, 1.0 equiv) in a solution of DMF (100 mL). The reaction was stirred for 12 h at room temperature and quenched with saturated NH_4Cl (80 mL). The product was then extracted with EtOAc (3x) and washed with brine (2x). The combined organic layers were dried over Na_2SO_4 and concentrated *in vacuo*. The title compound was obtained as a clear oil (4.65 g, 86% yield)

after SiO_2 flash chromatography (25% EtOAc/Hexanes): Spectral data was identical to that reported.[357]

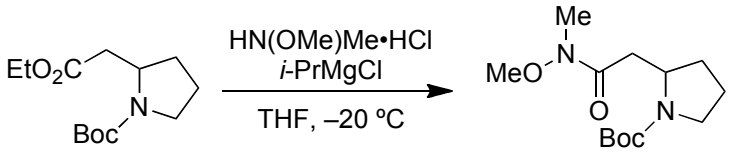

5.8 (±)-**2.2**

***tert*-butyl 2-(2-(methoxy(methyl)amino)-2-oxoethyl)pyrrolidine-1-carboxylate (2.2).** Ester **5.8** (4.65 g, 18.1 mmol, 1.0 equiv) and HN(OMe)Me•HCl (2.65 g, 27.1 mmol, 1.5 equiv) were dissolved in anhydrous THF (55 mL) and cooled to –30 ºC under a N_2 atmosphere. To a flame dried dropping funnel was added *i*-PrMgCl (27.0 mL, 54.3 mmol, 3.0 equiv, 2.0 M in THF). This Grignard reagent was added dropwise to the reaction mixture over 15 minutes and the reaction was stirred for 30 minutes at –15 ºC. The reaction was quenched with saturated NH_4Cl (80 mL) and the product was extracted with EtOAc (3x). The combined organic layers were dried over Na_2SO_4 and concentrated *in vacuo*. The title compound was obtained as a clear oil (4.18 g, 85% yield) after SiO_2 flash chromatography (50% EtOAc/Hexanes): See Section 6.2 for spectral data.

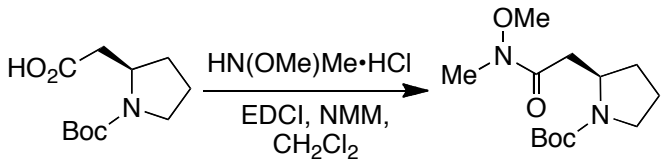

Boc-D-β-homoproline (*R*)-**2.2**

(*R*)-*tert*-butyl 2-(2-(methoxy(methyl)amino)-2-oxoethyl)pyrrolidine-1-carboxylate [(*R*)-2.2]. Boc-D-β-homoproline (4.0 g, 17.4 mmol, 1.0 equiv) was dissolved in anhydrous CH_2Cl_2 (50 mL) under argon atmosphere and cooled to –0 °C. To this solution was added *N*,*O*-dimethylhydroxylamine•HCl (1.87 g, 19.2 mmol, 1.1 equiv) and *N*-methylmorpholine (2.1 mL, 19.2 mmol, 1.1 equiv) followed by EDCI (3.68 g, 19.2 mmol, 1.05 equiv). The reaction mixture was then allowed to come to room temperature. After 2 hours the reaction was again cooled to 0 °C and quenched by the addition of an ice cold 10% HCl solution (50 mL) and allowed to stir at this temperature for 5 minutes. The reaction was diluted with water (100 mL) and extracted with CH_2Cl_2 (x3). The combined organic layers were washed with saturated $NaHCO_3$ (x1), dried over Na_2SO_4, filtered and concentrated. The title compound was obtained as a clear oil (4.66 g, 98% yield) after SiO_2 flash chromatography (40% EtOAc/ Hexanes): See Section 6.2 for spectral data.

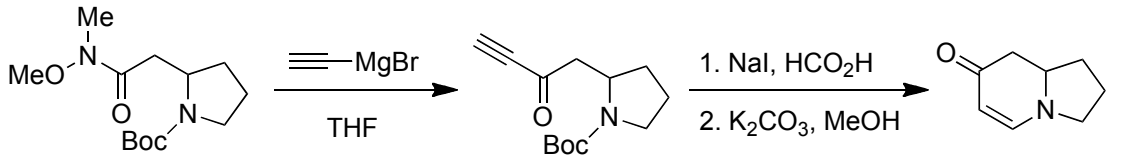

(*R*)-**2.2**, (*S*)-**2.2**, (±)-**2.2**

(*R*)-**2.17**, (*S*)-**2.17**, (±)-**2.17**

(*R*)-**2.37**, (*S*)-**2.37**, (±)-**2.37**

Compounds **2.17** and **2.37** were prepared according the procedure in Section 6.2 Optical rotations for the *R*-enantiomers can be found below.

(*R*)-tert-butyl 2-(2-oxobut-3-yn-1-yl)pyrrolidine-1-carboxylate (*R*-2.17). $[\alpha]_D^{22} = +21.3$ (*c* 1.00, $CHCl_3$).

(*R*)-2,3,8,8a-tetrahydroindolizin-7(1H)-one (*R*-2.37). $[\alpha]_D^{22} = +770$ (*c* 1.00, $CHCl_3$).

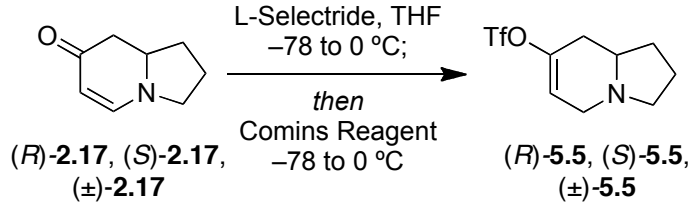

(*R*)-**2.17**, (*S*)-**2.17**, (±)-**2.17**

(*R*)-**5.5**, (*S*)-**5.5**, (±)-**5.5**

(*R*)-1,2,3,5,8,8a-hexahydroindolizin-7-yl trifluoromethanesulfonate (*R*-5.5). Enaminone (*R*)-**2.17** (1.35 g, 9.81 mmol, 1.0 equiv) was dissolved in anhydrous THF (30 mL) under a N_2 atmosphere. The solution was cooled to –78 ºC at which point L-Selectride (10.8 mL, 10.8 mmol, 1.1 equiv, 1.0 M in THF) was added over 15 minutes. After stirring for 1 h, the reaction was slowly warmed to 0 ºC over 2 hours. The reaction mixture was once again cooled to –78 ºC and Comins' reagent (4.24 g, 10.8 mmol, 1.1 equiv) was added all at once.

The mixture was stirred for another hour at –78 ºC and then slowly warmed to 0 ºC over 2 hours. The reaction was quenched with a saturated solution of $NaHCO_3$ (*aq.*) and added to a separatory funnel. The product was extracted with ethyl acetate (3x). The combined organic layers were dried over Na_2SO_4 and concentrated *in vacuo*. The title compound was obtained as a colorless oil (2.67 g, 73% yield) after SiO_2 flash chromatography (20% EtOAc/Hexanes (1% TEA): ^{1}H NMR (400 MHz, $CDCl_3$) δ; 1.40-1.49 (m, 1H), 1.70-2.01 (m, 3H), 2.14 (dd, *J* = 17.9, 8.9 Hz, 1H), 2.27-2.46 (m, 3H), 2.82 (d, *J* = 16.3 Hz, 1H), 3.11 (dt, *J* = 4.3, 2.3 Hz), 3.51 (dd, 16.3, 4.8 Hz, 1H), 5.72-5.73 (m, 1H); ^{13}C NMR (100 MHz, $CDCl_3$) δ 22.1, 30.4, 35.0, 49.6, 53.3, 60.2, 116.7, 118.5 (q, *J* = 320 Hz), 147.8; IR (neat) 2794, 1689, 1419, 1210, 1143, 1024, 879 cm^{-1}; HRMS (ESI+) *m/e* calc'd for $[M+H]^+$ $C_9H_{13}F_3NO_3S$: 272.0568, found 272.0574; (*R*)-Enantiomer: $[\alpha]_D^{22} = -74.5$ (*c* 1.00, $CHCl_3$). (*S*)-Enantiomer: $[\alpha]_D^{22} = +75.2$ (*c* 1.00, $CHCl_3$).

SUZUKI COUPLINGS

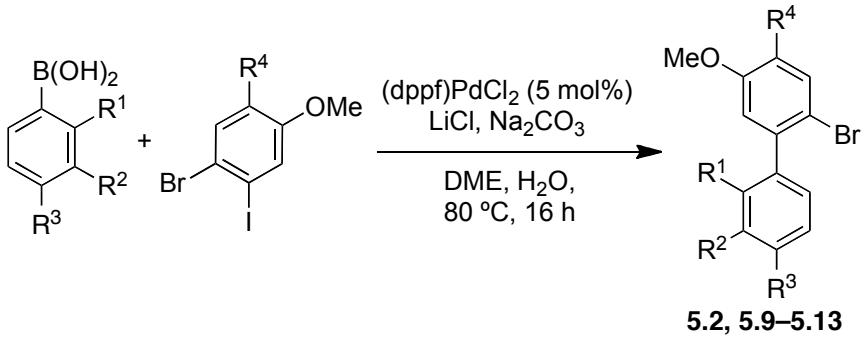

5.2, 5.9–5.13

Compounds **5.4**, **5.9, 5.10, 5.11, 5.12 and 5.13** were prepared according the procedure shown for compound **5.4**.

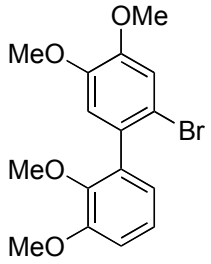

5.4

2'-bromo-2,3,4',5'-tetramethoxy-1,1'-biphenyl (5.4). DME (60 mL) and Na_2CO_3 (21.1 mL, 42.3 mmol, 5.0 equiv, 2.0 M *aq.* solution) were added to a round-bottomed flask and degassed under reduced pressure for 30 minutes. Iodobromoveratrole (2.90 g, 8.45 mmol, 1.0 equiv), arylboronic acid (2.0 g, 11.0 mmol, 1.3 equiv), LiCl (1.07 g, 25.4 mmol, 3.0 equiv) and (dppf)$PdCl_2$ (310 mg, 0.42 mmol, 0.05 equiv) were added all at once and the reaction mixture was heated to 80 ºC under a N_2 atmosphere. After 16 h the reaction was quenched with a saturated solution of NH_4Cl (*aq.*) and added to a separatory funnel. The product was extracted with ethyl acetate (3x). The combined organic layers were dried over Na_2SO_4 and concentrated *in vacuo*. The title compound was obtained as a colorless oil (2.15 g, 72% yield) after SiO_2 flash chromatography (20% EtOAc/Hexanes): ^{1}H NMR (400 MHz, $CDCl_3$) δ 3.63 (s, 3H), 3.83 (s, 3H), 3.91 (s, 3H), 3.91 (s, 3H), 6.82 (dd, *J* = 7.6, 1.5 Hz, 1H), 6.83 (s, 1H), 6.96 (dd, *J* = 8.2, 1.5 Hz, 1H), 7.09 (dd, *J* = 7.9, 7.9 Hz, 1H), 7.12 (s, 1H); ^{13}C NMR (100 MHz, $CDCl_3$) δ 55.8, 56.0, 56.2, 60.7, 111.9, 113.5, 114.2, 115.2, 123.3, 123.4, 131.3, 135.4, 146.7, 147.9, 148.8, 152.8; IR (neat) cm^{-1} 2935, 1579, 1506, 1473, 1262, 1210, 1058, 1007, 941; HRMS (ESI+) *m/e* calc'd for $[M+H]^+$ $C_{16}H_{17}BrO_4$: 353.0388, found 353.0394.

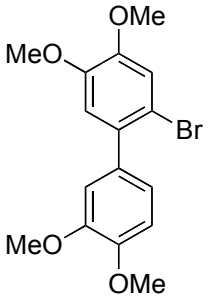

5.9

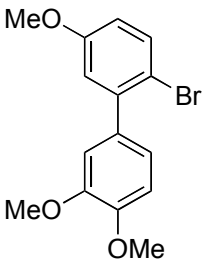

5.13

2-bromo-3',4,4',5-tetramethoxy-1,1'-biphenyl (5.9) and **2-bromo-3',4',5-trimethoxy-1,1'-biphenyl (5.13).** Spectral data was identical to that reported.[149]

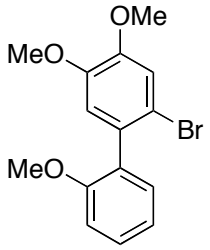

5.10

2-bromo-2',4,5-trimethoxy-1,1'-biphenyl (5.10). ^{1}H NMR (400 MHz, $CDCl_3$) δ 3.81 (s, 3H), 3.85 (s, 3H), 3.91 (s, 3H), 6.81 (s, 1H), 6.99 (d, *J* = 8.3 Hz, 1H), 7.03 (ddd, *J* = 7.4, 7.4, 1.8 Hz, 1H), 7.12 (s, 1H), 7.19 (dd, *J* = 7.4, 1.8 Hz, 1H), 7.38 (ddd, *J* = 8.3, 7.4, 1.7 Hz, 1H); ^{13}C NMR (100 MHz, $CDCl_3$) δ 55.7, 56.0, 56.2, 111.1, 114.2, 114.2, 115.3, 120.3, 129.3, 130.2, 131.2, 131.7, 148.0, 148.7, 156.7; IR (neat) cm^{-1} 2937, 1597, 1490, 1463, 1245, 1207, 1026, 903, 860; HRMS (ESI+) *m/e* calc'd for $[M+Na]^+$ $C_{15}H_{15}BrO_3$: 345.0102, found 345.0071.

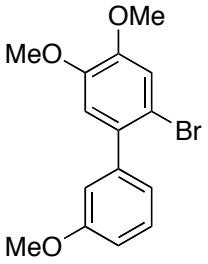

5.11

2-bromo-3',4,5-trimethoxy-1,1'-biphenyl (5.11). ^{1}H NMR (400 MHz, $CDCl_3$) δ 3.85 (s, 3H), 3.86 (s, 3H), 3.91 (s, 3H), 6.84 (s, 1H), 6.90–7.00 (m, 3H), 7.12 (s, 1H), 7.34 (dd, *J* = 7.9, 7.9 Hz, 1H); ^{13}C NMR (100 MHz, $CDCl_3$) δ 55.3, 56.1, 56.2, 112.4, 112.9, 113.8, 115.3, 115.8, 122.0, 129.0, 134.6, 142.4, 148.2, 148.8, 159.1; IR (neat) cm^{-1} 2936, 1602, 1507, 1485, 1464, 1246, 1205, 1028, 932, 857; HRMS (ESI+) *m/e* calc'd for $[M+H]^+$ $C_{15}H_{15}BrO_3$: 322.0205, found 325.1938.

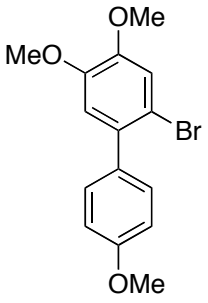

5.12

2-bromo-4,4',5-trimethoxy-1,1'-biphenyl (5.12). ^{1}H NMR (400 MHz, $CDCl_3$) δ 3.85 (s, 3H), 3.86 (s, 3H), 3.91 (s, 3H), 6.82 (s, 1H), 6.96 (d, *J* = 8.7 Hz, 2H), 7.11 (s, 1H), 7.34 (d, *J* = 8.7 Hz, 2H); ^{13}C NMR (100 MHz, $CDCl_3$) δ 55.3, 56.1, 56.2, 112.7, 113.4, 113.9, 115.7,

130.6, 133.6, 134.4, 148.2, 148.6, 158.9; IR (neat) cm^{-1} 2937, 1601, 1507, 1486, 1464, 1205, 1028, 932, 857; HRMS (ESI+) *m/e* calc'd for $[M+H]^+$ $C_{15}H_{15}BrO_3$: 322.0205, found 325.1855.

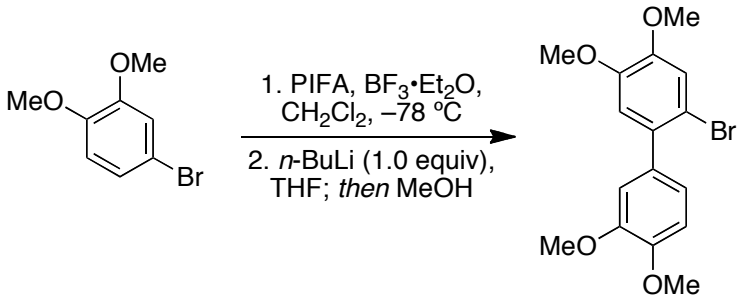

5.9

2-bromo-3',4,4',5-tetramethoxy-1,1'-biphenyl (5.9). *Dimerization:* 4-Bromoveratrole (20.0 g, 92.1 mmol, 1.0 equiv) was dissolved in CH_2Cl_2 (1.0 L) in a 2 L round-bottomed flask and cooled to –78 ºC. To this solution was added dropwise (over 1 h) a pre-mixed solution of PIFA (21.8 g, 50.7 mmol, 0.55 equiv) and BF_3•Et_2O (12.7 mL, 101.4 mmol, 1.1 equiv) in CH_2Cl_2 (500 mL). The reaction mixture was stirred until the starting material was completely consumed (~ 1 h). The reaction was quenched by adding 10% NaOH (500 mL) and the reaction mixture was vigorously stirred for 1 h. The product was extracted with CH_2Cl_2 (3x). The combined organic layers were dried over Na_2SO_4 and concentrated *in vacuo* and recrystallized from EtOH. Veratrole dimer **5.15** was obtained as a white crystalline solid (18.8 g, 95% yield). Spectral data was identical to that reported.[358]

Dehalogenation: Veratrole dimer **5.15** (10.0 g, 23.0 mmol, 1.0 equiv) was dissolved in anhydrous THF (400 mL) and cooled to –78 ºC. To this solution was added *n*-BuLi (9.3 mL,

23.0 mmol, 1.0 equiv, 2.5M in hexanes) dropwise via syringe pump (0.62 mL/min). Upon complete addition of *n*-BuLi the reaction was stirred for another 20 minutes before 2.0 mL of MeOH was added as a proton source. The quenched reaction mixture was stirred for 5 minutes at –78 ºC and then poured into a separatory funnel with 100 mL of H_2O. The product was extracted with ethyl acetate (3x). The combined organic layers were dried over Na_2SO_4 and concentrated *in vacuo* and recrystallized from MeOH. The title compound was obtained as an off-white crystalline solid (6.79 g, 84% yield). Spectral data was identical to that reported.[149]

NEGISHI COUPLINGS

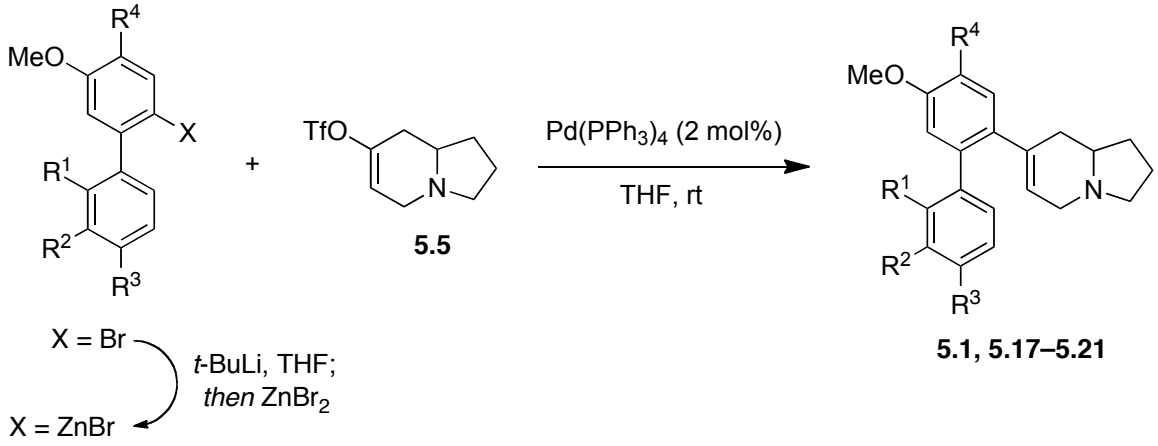

Compounds **5.1**, **5.17, 5.18, 5.19, 5.20 and 5.21** were prepared according the procedure shown for compound **5.1**.

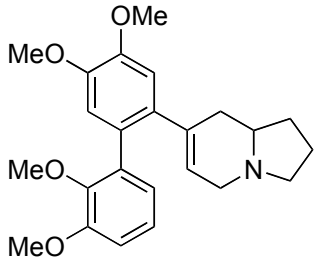

(*R*)-**5.1**, (*S*)-**5.1** and (±)-**5.1**

(*R*)-7-(2',3',4,5-tetramethoxy-[1,1'-biphenyl]-2-yl)-1,2,3,5,8,8a-hexahydroindolizine (*R*-5.1). *Representative procedure for preparing zincate solution:* A dry RBF containing anhydrous $ZnBr_2$ (412 mg, 1.83 mmol, 1.65 equiv) was heated with heat gun under vacuum. The flask was then cooled to 25 °C, and anhydrous THF (15 mL) was added. To a separate flask containing 20 mL of THF at –78 °C was added *tert*-butyllithium (2.06 mL, 3.50 mmol, 3.15 equiv, 1.7 M in THF), and then the biarylbromide **5.4** (590 mg, 1.67 mmol, 1.5 equiv) in a minimal amount of THF (~5 mL) was added dropwise. The mixture was stirred at –78 °C for 2 h, and the solution of $ZnBr_2$ in THF was transferred via a cannula. The resulting zinc reagent was stirred at -78 °C for 10 min and warmed to 25 °C.

Representative procedure for Negishi Coupling: Triflate **5.5** (300 mg, 1.11 mmol, 1.0 equiv) and $Pd(PPh_3)_4$ (26 mg, 0.02 mmol, 0.02 equiv) were added sequentially to the solution of zinc reagent. The resulting yellow mixture was stirred at room temperature until the triflate had been consumed (~1 h). The reaction was quenched with SiO_2 the solvent removed as to provide a free-flowing powder. The SiO_2 was loaded onto a SiO_2 column and purified by flash chromatography (60 % EtOAc/hexanes [1% TEA]). The title compound was obtained as a yellowish foamy solid (415 mg, 95%). ^1H NMR (400 MHz, $CDCl_3$) δ 1.28-1.38 (m, 1H), 1.63-1.73 (m, 1H), 1.75-1.89 (m, 2H), 1.95-2.16 (m, 4H) 2.72 (dd, J = 16.2, 1.5 Hz,

1H), 3.15 (dt, J = 8.6, 2.1 Hz, 1H), 3.50 (dd, J = 16.2, 4.7 Hz, 1H), 3.59 (s, 3H), 3.85 (s, 3H), 3.89 (s, 3H), 3.90 (s, 3H), 5.53 (m, 1H), 6.82 (dd, J = 7.9, 1.4 Hz, 1H), 6.82 (s, 1H), 6.87 (dd, J = 7.9, 1.4 Hz, 1H), 7.00 (dd, J = 7.9, 7.9 Hz, 1H); ^{13}C NMR (100 MHz, $CDCl_3$) δ 21.3, 30.6, 36.4, 52.7, 54.2, 55.8, 55.9, 55.9, 60.1, 60.4, 111.1, 111.9, 113.8, 123.3, 123.6, 124.7, 127.9, 134.9, 135.7, 137.3, 146.4, 147.1, 147.8, 152.8; IR (neat) 2935, 1515, 1469, 1262, 1008, 751 cm^{-1}; HRMS (ESI+) *m/e* calc'd for $[M+H]^+$ $C_{24}H_{30}NO_4$: 396.2175, found 396.2163. (*R*)-Enantiomer: $[\alpha]_D^{22}$ = –62.8 (*c* 1.00, $CHCl_3$).

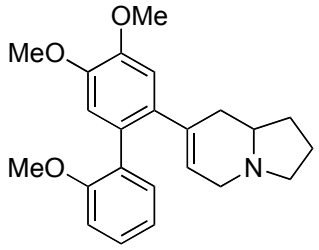

(±)-**5.17**

7-(2',4,5-trimethoxy-[1,1'-biphenyl]-2-yl)-1,2,3,5,8,8a-hexahydroindolizine (±-5.17). Using the same proportions as above, the title compound was obtained after flash chromatography (60 % EtOAc/hexanes [1% TEA]) as a yellowish foamy solid (467 mg, 97%). ^{1}H NMR (400 MHz, $CDCl_3$) δ 1.30-1.40 (m, 1H), 1.63-1.73 (m, 2H), 1.76-1.97 (m, 3H), 2.03-2.16 (m, 3H), 2.64 (d, J = 16.2 Hz, 1H), 3.14 (dt, J = 8.6, 2.0 Hz, 1H), 3.46 (ddd, J = 16.2, 4.6, 1.7 Hz, 1H), 3.75 (s, 3H), 3.86 (s, 3H), 3.88 (s, 3H), 5.43-5.44 (m, 1H), 6.81 (d, J = 8.1 Hz, 2H), 6.91 (d, J = 8.1 Hz, 1H), 6.95 (dt, J = 7.4, 1.0 Hz, 1H), 7.19 (dd, J = 7.4, 1.7 Hz, 1H), 7.28 (ddd, J = 8.1, 7.4, 1.7 Hz, 1H); ^{13}C NMR (100 MHz, $CDCl_3$) δ 21.3, 30.7, 36.4, 52.8, 54.2, 55.4, 55.8, 55.9, 60.1, 110.5, 111.6, 113.9, 120.2, 124.2, 128.2, 128.5, 130.6,

131.5, 135.4, 137.1, 147.2, 147.8, 156.4; IR (neat) 2935, 1515, 1491, 1246, 1028, 753 cm^{-1}; HRMS (ESI+) *m/e* calc'd for $[M+H]^+$ $C_{23}H_{28}NO_3$: 366.2069, found 366.2067.

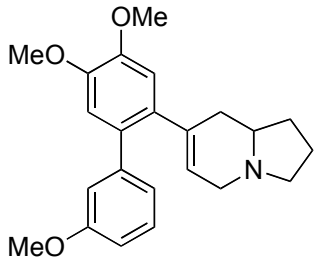

(±)-**5.18**

7-(3',4,5-trimethoxy-[1,1'-biphenyl]-2-yl)-1,2,3,5,8,8a-hexahydroindolizine (±-5.18). Using the same proportions as above, the title compound was obtained after flash chromatography (60 % EtOAc/hexanes [1% TEA]) as a yellowish foamy solid (432 mg, 95%). ^1H NMR (400 MHz, $CDCl_3$) δ ;1.24-1.34 (m, 1H), 1.64-1.87 (m, 3H), 1.91-2.00 (m, 3H), 2.11 (dd, *J* = 18.0, 9.0 Hz, 1H), 2.84 (dd, *J* = 16.3, 1.8 Hz, 1H), 3.18 (dt, *J* = 8.6, 2.1 Hz, 1H), 3.59 (dd, *J* = 16.3, 4.7 Hz, 1H), 3.82 (s, 3H), 3.89 (s, 3H), 3.89 (s, 3H), 5.70-5.71 (m, 1H), 6.81 (s, 1H), 6.82-6.85 (m, 1H), 6.84 (s, 1H), 6.96-7.00 (m, 2H), 7.27 (dd, *J* = 7.9, 7.9 Hz, 1H); ^{13}C NMR (100 MHz, $CDCl_3$) δ 21.3, 30.6, 36.6, 52.9, 54.2, 55.2, 55.9, 56.0, 60.3, 112.3, 113.0, 113.2, 114.4, 121.5, 125.1, 129.0, 131.8, 134.3, 138.5, 143.1, 147.8 147.9, 159.2; IR (neat) 2956, 1502, 1464, 1238, 1040, 753 cm^{-1}; HRMS (ESI+) *m/e* calc'd for $[M+H]^+$ $C_{23}H_{28}NO_3$: 366.2069, found 366.2068.

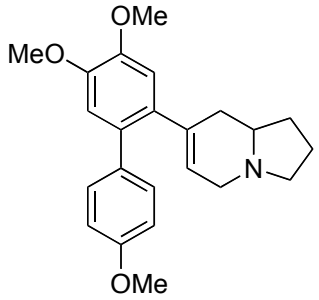

(±)-**5.19**

7-(4,4',5-trimethoxy-[1,1'-biphenyl]-2-yl)-1,2,3,5,8,8a-hexahydroindolizine (±-5.19). Using the same proportions as above, the title compound was obtained after flash chromatography (60 % EtOAc/hexanes [1% TEA]) as a yellowish foamy solid (444 mg, 98%). ^{1}H NMR (400 MHz, $CDCl_3$) δ 1.24-1.34 (m, 1H), 1.63-1.73 (m, 2H), 1.75-2.02 (m, 3H), 2.12 (dd, *J* = 17.9, 9.0 Hz, 1H), 2.84 (dd, *J* = 16.3, 1.8 Hz, 1H), 3.19 (dt, *J* = 8.5, 2.0 Hz, 1H), 3.59 (ddd, *J* = 16.3, 4.7, 1.6 Hz, 1H), 3.84 (s, 3H), 3.88 (s, 3H), 3.89 (s, 3H), 5.69-5.70 (m, 1H), 6.80 (s, 1H), 6.81 (s, 1H), 6.90 (d, *J* = 8.8 Hz, 2H), 7.33 (d, *J* = 8.8 Hz, 1H); ^{13}C NMR (100 MHz, $CDCl_3$) δ; 21.3, 30.6, 36.6, 52.9, 54.3, 55.3, 55.9, 56.0, 60.2, 113.0, 113.2, 113.5, 125.1, 128.5, 129.9, 131.6, 134.2, 138.5, 147.6, 147.8, 158.4; IR (neat) 2956, 1514, 1464, 1249, 1045, 772 cm^{-1}; HRMS (ESI+) *m/e* calc'd for $[M+H]^+$ $C_{23}H_{28}NO_3$: 366.2069, found 366.2074.

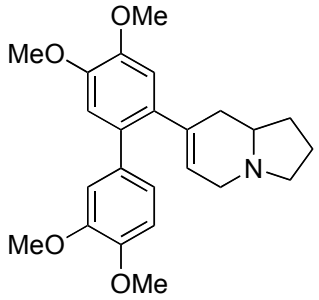

(*R*)-**5.20** and (±)-**5.20**

(*R*)-7-(3',4',5-tetramethoxy-[1,1'-biphenyl]-2-yl)-1,2,3,5,8,8a-hexahydroindolizine. (*R*-5.20) Using the same quantities and proportions as above, the title compound was obtained as a yellowish foamy solid (429 mg, 98%). ^{1}H NMR (400 MHz, $CDCl_3$) δ 1.23-1.32 (m, 1H), 1.62-1.72 (m, 1H), 1.74-1.85 (m, 2H), 1.87-2.98 (m, 3H), 2.09 (dd, *J* = 9.0 Hz, 1H), 2.82 (dd, *J* = 16.3, 1.8 Hz, 1H), 3.17 (dt, *J* = 8.5, 1.8 Hz, 1H), 3.60 (dd, *J* = 16.3, 4.6 Hz, 1H), 3.87 (s, 3H), 3.87 (s, 3H), 3.88 (s, 3H), 3.91 (s, 3H), 5.73-5.74 (m, 1H), 6.81 (d, *J* = 6.0 Hz, 1H), 6.87 (d, *J* = 8.2 Hz, 1H), 6.94 (dd, *J* = 8.2, 1.9 Hz, 1H), 6.98 (d, *J* = 1.9 Hz, 1H); ^{13}C NMR (100 MHz, $CDCl_3$) δ21.3, 30.6, 36.6, 53.0, 54.3, 55.8, 55.9, 56.0, 56.0, 60.4, 110.9, 112.3, 113.1, 113.2, 120.9, 124.9, 131.6, 134.1, 134.5, 138.9, 147.7, 147.8, 147.8, 148.2; IR (neat) 2954, 1504, 1464, 1249, 1028, 762 cm^{-1}; HRMS (ESI+) *m/e* calc'd for $[M+H]^+$ $C_{24}H_{30}NO_4$: 396.2175, found 396.2177. (*R*)-Enantiomer: $[\alpha]_D^{22} = -138$ (*c* 1.00, $CHCl_3$).

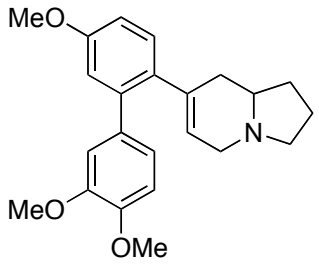

(±)-**5.21**

7-(3',4',5-trimethoxy-[1,1'-biphenyl]-2-yl)-1,2,3,5,8,8a-hexahydroindolizine (5.21). Using the same proportions as above, the title compound was obtained after flash chromatography (60 % EtOAc/hexanes [1% TEA]) as a yellowish foamy solid (485 mg, 98%). ^{1}H NMR (400 MHz, $CDCl_3$) δ 1.22-1.32 (m, 1H), 1.63-1.98 (m, 6H), 2.09 (dd, *J* = 17.9, 8.9 Hz, 1H), 2.83 (dd, *J* = 16.2, 1.6 Hz, 1H), 3.18 (dt, *J* = 8.5, 1.9 Hz, 1H), 3.61 (ddd, *J* = 16.2, 4.5, 1.1 Hz, 1H), 3.83 (s, 3H), 3.87 (s, 3H), 3.92 (s, 3H), 5.69-5.70 (m, 1H), 6.82 (dd, *J* = 8.4, 2.7 Hz, 1H), 6.86 (d, *J* = 2.7 Hz, 1H), 6.89 (d, *J* = 8.2 Hz, 1H), 6.98 (dd, *J* = 8.2, 2.0 Hz, 1H), 7.01 (d, *J* = 2.0 Hz, 1H), 7.20 (d, *J* = 8.4 Hz, 1H); ^{13}C NMR (100 MHz, $CDCl_3$) δ 21.3, 30.6, 36.5, 53.0, 54.3, 55.3, 55.8, 55.9 60.3, 110.9, 112.1, 112.2, 115.5, 120.9, 124.7, 130.9, 134.4, 134.5, 138.5, 140.4, 148.0, 148.3, 158.6; IR (neat) 2955, 1517, 1464, 1248, 1029, 754 cm^{-1}; HRMS (ESI+) *m/e* calc'd for $[M+H]^+$ $C_{23}H_{28}NO_3$: 366.2069, found 366.2069.

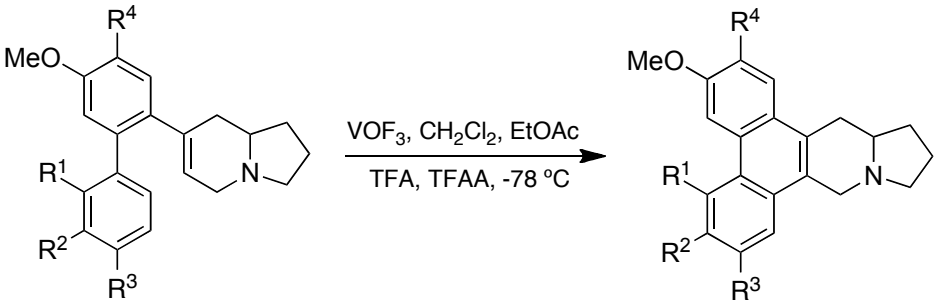

5.1, 5.17–5.21 **1.1, 1.4, 4.2, 5.22–5.24**

Compounds **1.1**, **1.4**, **4.2**, **5.22**, **5.23** and **5.24** were prepared according the procedure shown for compound **1.4**.

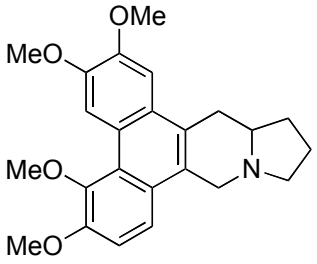

tylocrebrine
(*R*)-**1.4**, (*S*)-**1.4** and (±)-**1.4**

(*R*)-Tylocrebrine (*R*-1.4). Indolizidine **5.1** (400 mg, 1.01 mmol, 1.0 equiv) was dissolved in anhydrous CH_2Cl_2 (100 mL) and cooled to –78 °C. Two drops of TFAA was then added to this solution. In a separate flask containing VOF_3 (500 mg, 4.04 mmol, 4.0 equiv) was added anhydrous CH_2Cl_2 (10 mL), anhydrous EtOAc (5 mL), TFA (0.5 mL) and TFAA (2 drops). The VOF_3 solution was then added over 20 minutes to the solution of indolizidine **5.1**. The

reaction mixture was stirred for 1 h at –78 ºC and then slowly warmed over 3 h to ~ –15 ºC or until the starting material had been consumed. To the reaction mixture was added 10% NaOH (50 mL) and the biphasic mixture was vigorously stirred for 1 h at room temperature. The product was extracted with CH_2Cl_2. The combined organic layers were washed with brine and dried over anhydrous Na_2SO_4. Filtration and concentration *in vacuo* gave the crude product. Purification by flash chromatography (80 % EtOAc/hexanes [1% TEA]) provided the title compound as white crystalline solid (247 mg, 62%): mp 227–229 ºC (decomp.) [Lit. mp 218–220 ºC];[20] ^{1}H NMR (400 MHz, $CDCl_3$) δ 1.73-1.83 (m, 1H), 1.87-1.96 (m, 1H), 1.99-2.10 (m, 1H), 2.19-2.31 (m, 1H), 2.42-2.52 (m, 2H), 2.91 (dd, *J* = 14.8, 11.3 Hz, 1H), 3.33 (dd, *J* = 15.8, 3.5 Hz, 1H), 3.46 (t, *J* = 8.2 Hz, 1H), 3.68 (d, *J* = 14.7 Hz, 1H), 3.92 (s, 3H), 4.03 (s, 3H), 4.07 (s, 3H), 4.07 (s, 3H), 4.66 (d, *J* = 14. 8 Hz, 1H), 7.28 (d, *J* = 9.1 Hz, 1H), 7.33 (s, 1H), 7.65 (d, *J* = 9.1 Hz, 1H), 9.33 (s, 1H); ^{13}C NMR (100 MHz, $CDCl_3$) δ 21.6, 31.3, 34.0, 54.2, 55.1, 55.7, 56.5, 60.0, 60.2, 103.5, 109.1, 112.1, 118.8, 123.3, 123.6, 125.8, 126.5, 127.9, 146.3, 147.7, 148.7, 150.6; IR 2936, 1601, 1514, 1467, 1255, 1114, 1033, 913 (neat) cm^{-1}; HRMS (ESI+) *m/e* calc'd for $[M+H]^+$ $C_{24}H_{28}NO_4$: 394.2013, found 394.2021. $[\alpha]_D^{22} = -105$ (*c* 1.00, $CHCl_3$). [Lit. –45 (*c* 0.74, $CHCl_3$)][20]

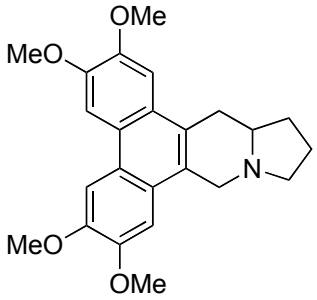

tylophorine
(*R*)-**1.1** and (±)-**1.1**

(*R*)-Tylophorine (*R*-1.1). Using the same quantities and proportions as above, the title compound was obtained after flash chromatography (5% MeOH/CH_2Cl_2) as a white crystalline solid (354 mg, 89%). mp 284–285 ºC (decomp.) [Lit. mp 274–276 ºC,[359, 360] 275 ºC[11, 14]] ; ^{1}H NMR (400 MHz, $CDCl_3$) δ 1.72-1.97 (m, 2H), 1.99-2.10 (m, 1H), 2.20-2.28 (m, 1H), 2.43 (m, 2H), 2.90 (dd, *J* = 15.6, 10.6 Hz, 1H), 3.35 (dd, *J* = 15.8, 2.5 Hz, 1H), 3.46 (dt, *J* = 4.2, 1.6 Hz, 1H), 3.65 (d, *J* = 14.6 Hz, 1H), 4.05 (s, 3H), 4.05 (s, 3H), 4.11 (s, 6H), 4.61 (d, *J* = 14.6 Hz, 1H), 7.15 (s, 1H), 7.30 (s, 1H), 7.81 (s, 1H), 7.82 (s, 1H); ^{13}C NMR (100 MHz, $CDCl_3$) δ 21.6, 31.3, 33.8, 54.1, 55.2, 55.9, 55.9, 56.1, 60.3, 103.2, 103.4, 103.5, 104.0, 123.5, 123.6, 124.4, 125.9, 126.0, 126.3, 148.4, 148.5, 148.7, 148.7; IR (neat) 2960, 1619, 1515, 1248, 1151, 1017, 841 cm^{-1}; HRMS (ESI+) *m/e* calc'd for $[M]^+$ $C_{24}H_{24}NO_4^+$: 394.2013, found 394.2011. $[\alpha]_D^{22} = -99.0$ (*c* 1.00, $CHCl_3$) [Lit. –76.5 (*c* 0.04, $CHC1_3$),[360] –77.6 (*c* 0.65, $CHCl_3$)[149]].

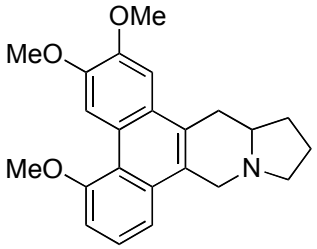

6-desmethoxytylocrebrine
(±)-**5.22**

(±)-6-Desmethoxytylocrebrine (5.22). Using the same proportions as above, the title compound was obtained after flash chromatography (5% MeOH/CH_2Cl_2) as a white crystalline solid (28 mg, 28%). ^{1}H NMR (400 MHz, $CDCl_3$) δ 1.72-1.82 (m, 1H), 1.87–1.97 (m, 1H), 1.98-2.10 (m, 1H), 2.42-2.52 (m, 2H), 2.94 (dd, *J* = 15.8, 10.5 Hz, 1H), 3.38 (dd, *J* = 16.0, 2.2 Hz, 1H), 3.48 (dt, *J* = 4.3, 2.0 Hz, 1H), 3.70 (d, *J* = 14.9 Hz, 1H), 4.07 (s, 3H), 4.09 (s, 3H), 4.12 (s, 3H), 4.68 (d, *J* = 14.9 Hz, 1H), 7.11 (d, *J* = 7.7, 1H), 7.36 (s, 1H), 7.48 (dd, *J* = 8.0, 8.0 Hz, 1H), 7.54 (dd, *J* = 8.3, 1.1 Hz, 1H); HRMS (ESI+) *m/e* calc'd for $[M+H]^+$ $C_{23}H_{28}NO_3$: 364.1913, found 364.1898. ^{13}C NMR and IR data could not be obtained, because the sample prepared degraded in $CDCl_3$.

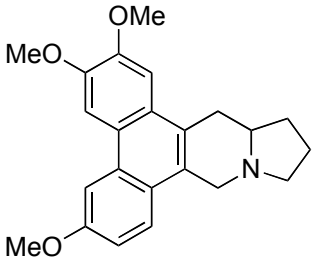

antofine
(±)-**4.2**

(±)-Antofine (4.2). Using the same proportions as above, the title compound was obtained after flash chromatography (5% MeOH/CH_2Cl_2) as a white crystalline solid (141 mg, 70%). See Section 6.4 for spectral data.

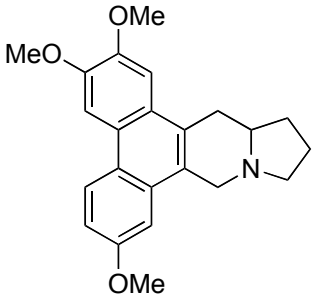

6-desmethoxytylophorine
(±)-**5.23**

(±)-Desmethoxytylophorine (5.23). Using the same proportions as above, the title compound was obtained after flash chromatography (5% MeOH/CH_2Cl_2) as a white crystalline solid (190 mg, 85%). mp 203–205 ºC (decomp.) ^{1}H NMR (400 MHz, $CDCl_3$) δ 1.72-1.96 (m, 2H), 1.98-2.09 (m, 1H), 2.20-2.28 (m, 1H), 2.42–2.54 (m, 2H), 2.90 (dd, J = 15.6, 10.5 Hz, 1H), 3.33 (dd, J = 15.8, 2.4 Hz, 1H), 3.46 (dt, J = 8.6, 1.7 Hz, 1H), 3.69 (d, J = 14.8 Hz, 1H), 4.01 (s, 3H), 4.06 (s, 3H), 4.10 (s, 3H), 4.69 (d, J = 14.9 Hz, 1H), 7.20 (dd, J =

9.0, 2.5 Hz, 1H), 7.30 (s, 1H), 7.81 (d, J = 9.0 Hz, 1H), 7.89 (d, J = 2.5 Hz, 1H) 7.91 (s, 1H); ^{13}C NMR (100 MHz, $CDCl_3$) δ 21.6, 31.3, 33.6, 53.8, 55.0, 55.5, 55.9, 56.0, 60.2, 103.8, 104.0, 104.7, 114.9, 123.5, 124.1, 124.2, 125.5, 126.5, 127.1, 130.2, 148.4, 149.4, 157.5; IR (neat) 2914, 1615, 1512, 1257, 1033, 912, 843 cm^{-1}; HRMS (ESI+) *m/e* calc'd for $[M+H]^+$ $C_{23}H_{28}NO_3$: 364.1913, found 364.1909.

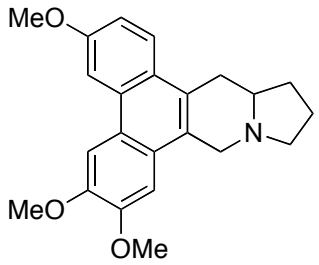

deoxypergularinine
(±)-**5.24**

(±)-Deoxypergularinine (5.24). Using the same proportions as above, the title compound was obtained after flash chromatography (5% MeOH/CH_2Cl_2) as a white crystalline solid (170 mg, 68%). mp 221–222 ºC (decomp.) ^{1}H NMR (400 MHz, $CDCl_3$) δ 1.71-1.81 (m, 1H), 1.87–1.97 (m, 1H), 1.98-2.09 (m, 1H), 2.20-2.28 (m, 1H), 2.46 (dd, J = 18.0, 9.0 Hz, 1H), 2.43–2.52 (m, 1H), 2.94 (dd, J = 16.0, 10.6 Hz, 1H), 3.41–3.50 (m, 2H), 3.66 (d, J = 14.7 Hz, 1H), 4.02 (s, 3H), 4.06 (s, 3H), 4.10 (s, 3H), 4.61 (d, J = 14.6 Hz, 1H), 7.17 (s, 1H), 7.22 (dd, J = 9.0, 2.5 Hz, 1H), 7.90 (d, J = 2.5 Hz, 1H), 7.92 (s, 1H), 7.95 (d, J = 9.1 Hz, 1H); ^{13}C NMR (100 MHz, $CDCl_3$) δ 21.6, 31.3, 33.7, 54.0, 55.2, 55.5, 55.9, 56.0, 60.2, 103.2, 104.0, 104.6, 114.8, 123.3, 125.2, 125.4, 125.6, 125.7, 127.1, 130.4, 148.3, 149.4, 157.6; IR (neat) cm^{-1}

2928, 1604, 1528, 1468, 1205, 1165, 1031, 913 HRMS (ESI+) *m/e* calc'd for $[M+H]^+$ $C_{23}H_{28}NO_3$: 364.1913, found 394.1910.

6.5.2 Biological procedures

6.5.2.1 Anti-proliferation assay

MCF-7, COLO-205 and NCI-ADR-RES cancer cells were harvested (125 G centrifuge for 5 min) from a exponential-phase maintenance culture. The cells were resuspended in a new culture medium (RPMI Medium 1640) and the cell density was adjusted to 10^5 cells/mL and dispensed in 96-well culture plates at a density 5,000 cells per well (50 μL). The cells were incubated overnight growth to allow cells to adhere to the wells. The culture medium in each well was replaced with fresh culture medium (50 μL) containing varying concentrations (50, 12.5, 3.125, 0.8, 0.2, 0.05, 0.0125, 0.003 μL) of the test and control (Taxol) compounds. The cultures were grown for an additional 48 h and alamarBlue® (20ul) was added. After 1–2 h, the fluorescence excitation (530 nm) and emission (590 nm) of each well were measured to determine the optical density. *(This assay was performed by Dr. Harry Tian at the ITDD)*

6.5.2.2 MOA assay

The following stock solutions were prepared: MAO-A (5 mg/mL, 75 U/mg), MAO-B (5 mg/mL, 58 U/mg), *p*-tyramine (100 mM), Amplex® Red reagent (20 mM), HRP (200 U/mL),

reaction buffer. Amplex® Red reagent solution (400 µL) was prepared that consisted of Amplex® Red (50 µL, 20 mM stock solution), *p*-tyramine (50 µL, 100 mM stock solution) and HRP (2 U/mL). Varying concentrations (100, 20, 4, 0.8, 0.16, 0.032, 0.0064, 0.0013 µM) of test and control compounds were added wells in a 360-well plate using the ECHO 550 acoustic liquid handler. MAO-A or MAO-B stock solutions (25 µL) were added to the appropriate wells by hand and the plate was incubated at room temperature for 15 min. Amplex® Red solution (25 µL) was added to the appropriate wells by hand and the plate was incubated at room temperature for 30 minutes. The fluorescence excitation (530 nm) and emission (590 nm) were measured for each well. *(This assay was performed by Dr. Jonothan Soldberg at the ITDD)*

6.5.2.3 Comprehensive CNS target screen and binding assays

Receptor binding profiles and K_D determinations were generously provided by the National Institute of Mental Health's Psychoactive Drug Screening Program, Contract # HHSN-271-2008-00025-C (NIMH PDSP). The NIMH PDSP is Directed by Bryan L. Roth MD, PhD at the University of North Carolina at Chapel Hill and Project Officer Jamie Driscol at NIMH, Bethesda MD, USA. For experimental details please refer to the PDSP web site http://pdsp.med.unc.edu.

6.6 X-Ray crystal structure

REFERENCE NUMBER: 08053a
CRYSTAL STRUCTURE REPORT
[C8 H13 I N O]+ IReport
prepared for:
M. Niphakis / Prof. G. Georg
March 25, 2008
Victor G. Young, Jr.
X-Ray Crystallographic Laboratory
Department of Chemistry
University of Minnesota
207 Pleasant St. S.E.
Minneapolis, MN 55455

DATA COLLECTION

A crystal (approximate dimensions 0.45 x 0.20 x 0.05 mm^3) was placed onto the tip of a 0.1 mm diameter glass capillary and mounted on a CCD area detector diffractometer for a data collection at 173(2) K.[1] A preliminary set of cell constants was calculated from reflections harvested from three sets of 20 frames. These initial sets of frames were oriented such that orthogonal wedges of reciprocal space were surveyed. This produced initial orientation matrices determined from 122 reflections. The data collection was carried out using MoKα radiation (graphite monochromator) with a frame time of 10 seconds and a detector distance of 4.9 cm. A randomly oriented region of reciprocal space was surveyed to the extent of one sphere and to a resolution of 0.77 Å. Four major sections of frames were collected with 0.30º steps in ω at four different ϕ settings and a detector position of -28º in 2θ. The intensity data were corrected for absorption and decay (SADABS).[2] Final cell constants were calculated from 2533 strong reflections from the actual data collection after integration (SAINT).[3] Please refer to Table 1 for additional crystal and refinement information.

STRUCTURE SOLUTION AND REFINEMENT

The structure was solved using Bruker SHELXTL[4] and refined using Bruker SHELXTL.[4] The space group P21 was determined based on systematic absences and intensity statistics. A direct methods solution was calculated which provided most non-hydrogen atoms from the E-map. Full matrix least squares / difference Fourier cycles were performed which located the remaining non-hydrogen atoms. All non-hydrogen atoms were refined with anisotropic displacement parameters. All hydrogen atoms were placed in ideal positions and refined as riding atoms with relative isotropic displacement parameters. The final full matrix least squares refinement converged to $R1 = 0.0192$ and $wR2 = 0.0483$ (F_2, all data).

STRUCTURE DESCRIPTION

The structure is the one suggested. CHECKCIF determined the P21 structure to be pseudo-centric (83%), but the structure is clearly chiral with the absolute configuration at C4 being S. Data collection and structure solution were conducted at the X-Ray Crystallographic Laboratory, 192C Kolthoff Hall, Department of Chemistry, University of Minnesota. All calculations were performed using Pentium computers using the current SHELXTL suite of programs.

References:

1. SMART V5.054, Bruker Analytical X-ray Systems, Madison, WI (2001).

2. An empirical correction for absorption anisotropy, R. Blessing, *Acta Cryst*. **A51**, 33-38 (1995).

3. SAINT+ V6.45, Bruker Analytical X-Ray Systems, Madison, WI (2003).

4. SHELXTL V6.14, Bruker Analytical X-Ray Systems, Madison, WI (2000).

Some equations of interest:

$$R_{\text{int}} = \sum \left| F_o^2 - < F_o^2 > \right| / \sum \left| F_o^2 \right|$$

$$R_1 = \sum \left\| F_o^2 - F_c^2 \right\| / \sum \left| F_o \right|$$

$$wR2 = \left[\sum \left[w \left(F_o^2 - F_c^2 \right)^2 \right] / \sum \left[w \left(F_o^2 \right)^2 \right] \right]^{1/2}$$

$$\text{where} \quad w = q / \left[\sigma^2 \left(F_o^2 \right) + \left(a * P \right)^2 + b * P + d + e * \sin(\theta) \right]$$

$$GooF = S = \left[\sum \left[w \left(F_o^2 - F_c^2 \right)^2 \right] / (n - p) \right]^{1/2}$$

Table 1. Crystal data and structure refinement for 08053a.

Identification code	08053a	
Empirical formula	$C_8H_{13}I_2NO$	
Formula weight	392.99	
Temperature	173(2) K	
Wavelength	0.71073 Å	
Crystal system	Monoclinic	
Space group	$P2_1$	
Unit cell dimensions	a = 8.7128(13) Å	α = 90°
	b = 7.4839(11) Å	β = 96.339(2)°
	c = 9.3223(13) Å	γ = 90°
Volume	604.15(15) Å3	
Z	2	
Density (calculated)	2.160 Mg/m^3	
Absorption coefficient	5.168 mm^{-1}	
F(000)	364	
Crystal color, morphology	Colorless, Plate	
Crystal size	0.45 x 0.20 x 0.05 mm3	
Theta range for data collection	2.20 to 27.46°	
Index ranges	$-11 \le h \le 11, -9 \le k \le 9, 0 \le l \le 12$	
Reflections collected	6149	
Independent reflections	2704 [R(int) = 0.0252]	
Observed reflections	2619	
Completeness to theta = 27.46‘	99.00%	
Absorption correction	Multi-scan	
Max. and min. transmission	0.7821 and 0.2045	
Refinement method	Full-matrix least-squares on F2	

Identification code	08053a
Data / restraints / parameters	2704 / 1 / 109
Goodness-of-fit on F^2	1.025
Final R indices [I>2sigma(I)]	$R1 = 0.0192$, $wR2 = 0.0479$
R indices (all data)	$R1 = 0.0203$, $wR2 = 0.0483$
Absolute structure parameter	0.00(3)
Largest diff. peak and hole	0.570 and –0.438 e.Å^{-3}

Table 2. Atomic coordinates (x10^4) and equivalent isotropic displacement parameters (Å^2 x 10^3) for 08053a. U_{eq} is defined as one third of the trace of the orthogonalized U_{ij} tensor.

	x	y	z	U_{eq}
N1	6388(3) 3	088(3)	4160(3)	24(1)
C1	8059(4)	2548(5)	4568(4)	34(1)
C2	8981(4)	4079(6)	4066(4)	43(1)
C3	8007(3)	4677(7)	2684(4)	38(1)
C4	6372(3)	4679(5)	3141(3)	28(1)
C5	5083(3)	4517(6)	1903(3)	27(1)
C6	3522(3)	4553(6)	2435(3)	32(1)
O1	3376(2)	4524(5)	3716(2)	40(1)
C7	2115(3)	4615(7)	1377(3)	35(1)
C8	2079(3)	4606(6)	-25(3)	32(1)
I1	-43(1)	4668(1)	-1311(1)	36(1)
I2	4346(1)	-506(1)	2402(1)	29(1)

Table 3. Bond lengths [Å] and angles [°] for 08053a.

N(1)-C(4)	1.522(4)
N(1)-C(1)	1.519(4)
N(1)-H(1A)	0.9200
N(1)-H(1B)	0.9200
C(1)-C(2)	1.503(5)
C(1)-H(1C)	0.9900
C(1)-H(1D)	0.9900
C(2)-C(3)	1.530(5)
C(2)-H(2A)	0.9900
C(2)-H(2B)	0.9900
C(3)-C(4)	1.532(4)
C(3)-H(3A)	0.9900
C(3)-H(3B)	0.9900
C(4)-C(5)	1.524(4)
C(4)-H(4A)	1.0000
C(5)-C(6)	1.498(4)
C(5)-H(5A)	0.9900
C(5)-H(5B)	0.9900
C(6)-O(1)	1.215(3)
C(6)-C(7)	1.487(4)
C(7)-C(8)	1.304(4)
C(7)-H(7A)	0.9500
C(8)-I(1)	2.090(3)
C(8)-H(8A)	0.9500
C(4)-N(1)-C(1)	107.9(2)

N(1)-C(4)	1.522(4)
C(4)-N(1)-H(1A)	110.1
C(1)-N(1)-H(1A)	110.1
C(4)-N(1)-H(1B)	110.1
C(1)-N(1)-H(1B)	110.1
H(1A)-N(1)-H(1B)	108.4
C(2)-C(1)-N(1)	104.5(3)
C(2)-C(1)-H(1C)	110.9
N(1)-C(1)-H(1C)	110.9
C(2)-C(1)-H(1D)	110.9
N(1)-C(1)-H(1D)	110.9
H(1C)-C(1)-H(1D)	108.9
C(1)-C(2)-C(3)	102.7(3)
C(1)-C(2)-H(2A)	111.2
C(3)-C(2)-H(2A)	111.2
C(1)-C(2)-H(2B)	111.2
C(3)-C(2)-H(2B)	111.2
H(2A)-C(2)-H(2B)	109.1
C(2)-C(3)-C(4)	102.3(3)
C(2)-C(3)-H(3A)	111.3
C(4)-C(3)-H(3A)	111.3
C(2)-C(3)-H(3B)	111.3
C(4)-C(3)-H(3B)	111.3
H(3A)-C(3)-H(3B)	109.2
N(1)-C(4)-C(5)	111.4(3)
N(1)-C(4)-C(3)	103.2(3)
C(5)-C(4)-C(3)	114.8(3)

N(1)-C(4)	1.522(4)
N(1)-C(4)-H(4A)	109.1
C(5)-C(4)-H(4A)	109.1
C(3)-C(4)-H(4A)	109.1
C(6)-C(5)-C(4)	111.6(2)
C(6)-C(5)-H(5A)	109.3
C(4)-C(5)-H(5A)	109.3
C(6)-C(5)-H(5B)	109.3
C(4)-C(5)-H(5B)	109.3
H(5A)-C(5)-H(5B)	108.0
O(1)-C(6)-C(7)	119.0(3)
O(1)-C(6)-C(5)	121.5(3)
C(7)-C(6)-C(5)	119.5(3)
C(8)-C(7)-C(6)	126.3(3)
C(8)-C(7)-H(7A)	116.9
C(6)-C(7)-H(7A)	116.9
C(7)-C(8)-I(1)	119.8(2)
C(7)-C(8)-H(8A)	120.1
I(1)-C(8)-H(8A)	120.1

Symmetry transformations used to generate equivalent atoms

Table 4. Anisotropic displacement parameters ($Å^2$ x 10^3) for 08053a. The anisotropic displacement factor exponent takes the form: $-2\pi^2[h^2 a^{*2}U_{11} + ... + 2 h k a^* b^* U_{12}]$

	U_{11}	U_{22}	U_{33}	U_{23}	U_{13}	U_{12}
N1	22(1)	27(1)	22(1)	-1(1)	4(1)	-3(1)
C1	21(2)	43(2)	37(2)	6(2)	3(1)	4(1)
C2	26(2)	62(3)	39(2)	10(2)	3(2)	-8(2)
C3	24(1)	48(2)	44(2)	14(2)	7(1)	-6(2)
C4	25(1)	29(2)	30(1)	5(2)	2(1)	0(2)
C5	27(1)	30(2)	25(1)	2(2)	5(1)	5(2)
C6	27(1)	37(2)	30(1)	-3(2)	2(1)	8(2)
O1	32(1)	64(2)	25(1)	2(2)	6(1)	8(2)
C7	22(1)	50(2)	32(1)	0(2)	5(1)	4(2)
C8	27(1)	32(2)	35(1)	1(2)	1(1)	-2(2)
I1	32(1)	43(1)	32(1)	1(1)	-4(1)	0(1)
I2	32(1)	29(1)	25(1)	1(1)	3(1)	-6(1)

Table 5. Hydrogen coordinates (x 10^4) and isotropic displacement parameters (Å^2 x 10^3) for 08053a.

	x	y	z	U_{eq}
H1A	5842	2152	3713	28
H1B	5938	3394	4973	28
H1C	8277	2380	5624	41
H1D	8299	1425	4078	41
H2A	10020	3683	3866	51
H2B	9091	5051	4791	51
H3A	8097	3827	1884	46
H3B	8312	5884	2385	46
H4A	6217	5799	3693	34
H5A	5162	5514	1217	33
H5B	5206	3384	1379	33
H7A	1149	4667	1759	42
H8A	3014	4570	-461	38

Table 6. Torsion angles [°] for 08053a.

C4-N1-C1-C2	12.8(3)
N1-C1-C2-C3	-35.3(4)
C1-C2-C3-C4	44.7(4)
C1-N1-C4-C5	138.4(3)
C1-N1-C4-C3	14.7(3)
C2-C3-C4-N1	-36.0(4)
C2-C3-C4-C5	-157.5(4)
N1-C4-C5-C6	63.9(4)
C3-C4-C5-C6	-179.3(4)
C4-C5-C6-O1	-7.2(6)
C4-C5-C6-C7	173.2(4)
O1-C6-C7-C8	-178.1(5)
C5-C6-C7-C8	1.5(8)
C6-C7-C8-I1	179.2(4)

Symmetry transformations used to generate equivalent atoms.

Table 7. Hydrogen bonds for 08053a [Å and °].

D-H...A	d(D-H)	d(H...A)	d(D...A)
N1-H1B...I2#1	0.92	2.62	3.498(2)
N1-H1A...I2	0.92	2.61	3.528(3)

Symmetry transformations used to generate equivalent atoms:
#1 -x+1,y+1/2,-z+1

checkCIF/PLATON report

No syntax errors found. CIF dictionary Interpreting this report

Datablock: 08053a

Bond precision: C-C = 0.0044 A Wavelength=0.71073

Cell: a=8.7128(13) b=7.4839(11) c=9.3223(13)
alpha=90 beta=96.339(2) gamma=90

Temperature: 173 K

	Calculated	Reported
Volume	604.15(15)	604.15(15)
Space group	P 21	P2(1)
Hall group	P 2yb	?
Moiety formula	$C_8H_{13}INO$, I	$C_8H_{13}INO$, I
Sum formula	$C_8H_{13}I_2NO$	$C_8H_{13}I_2NO$
Mr	392.99	392.99
Dx,g cm^{-3}	2.160	2.160
Z	2	2
Mu (mm^{-1})	5.168	5.168
F000	364.0	364.0
F000’	362.24	
h,k,lmax	11,9,12 11,9,12	
N_{ref} 1488(2761) 2704		
Tmin,Tmax	0.301,0.772	0.205,0.782
Tmin’	0.094	

Correction method = AbsCorr = MULTI-SCAN
Data completeness = 1.82(0.98) Theta(max) = 27.460
R(reflections) = 0.0192(2619) wR2 (reflections) = 0.0483(2704)
S = 1.025 Npar = 109

The following ALERTS were generated. Each ALERT has the format **test-name_ALERT_alert-type_alert-level.**

Alert level B

PLAT111_ALERT_2_B ADDSYM Detects (Pseudo) Centre of Symmetry ..... 83 PerFi

Alert level C

PLAT850_ALERT_2_C Check Flack Parameter Exact Value 0.00 and su .. 0.03

Alert level G

REFLT03_ALERT_4_G Please check that the estimate of the number of Friedel pairs is correct. If it is not, please give the correct count in the _publ_section_exptl_refinement section of the submitted CIF.

From the CIF: _diffrn_reflns_theta_max	27.46
From the CIF: _reflns_number_total	2704
Count of symmetry unique reflns	1488
Completeness (_total/calc)	181.72%
TEST3: Check Friedels for noncentro structure	
Estimate of Friedel pairs measured	1216
Fraction of Friedel pairs measured	0.817
Are heavy atom types Z>Si present	yes

PLAT791_ALERT_1_G Confirm the Absolute Configuration of C4 … S

PLAT860_ALERT_3_G Note: Number of Least-Squares Restraints … 1

0 **ALERT level A** = In general: serious problem
1 **ALERT level B** = Potentially serious problem
1 **ALERT level C** = Check and explain
3 **ALERT level G** = General alerts; check
1 ALERT type 1 CIF construction/syntax error, inconsistent or missing data
2 ALERT type 2 Indicator that the structure model may be wrong or deficient
1 ALERT type 3 Indicator that the structure quality may be low
1 ALERT type 4 Improvement, methodology, query or suggestion
0 ALERT type 5 Informative message, check

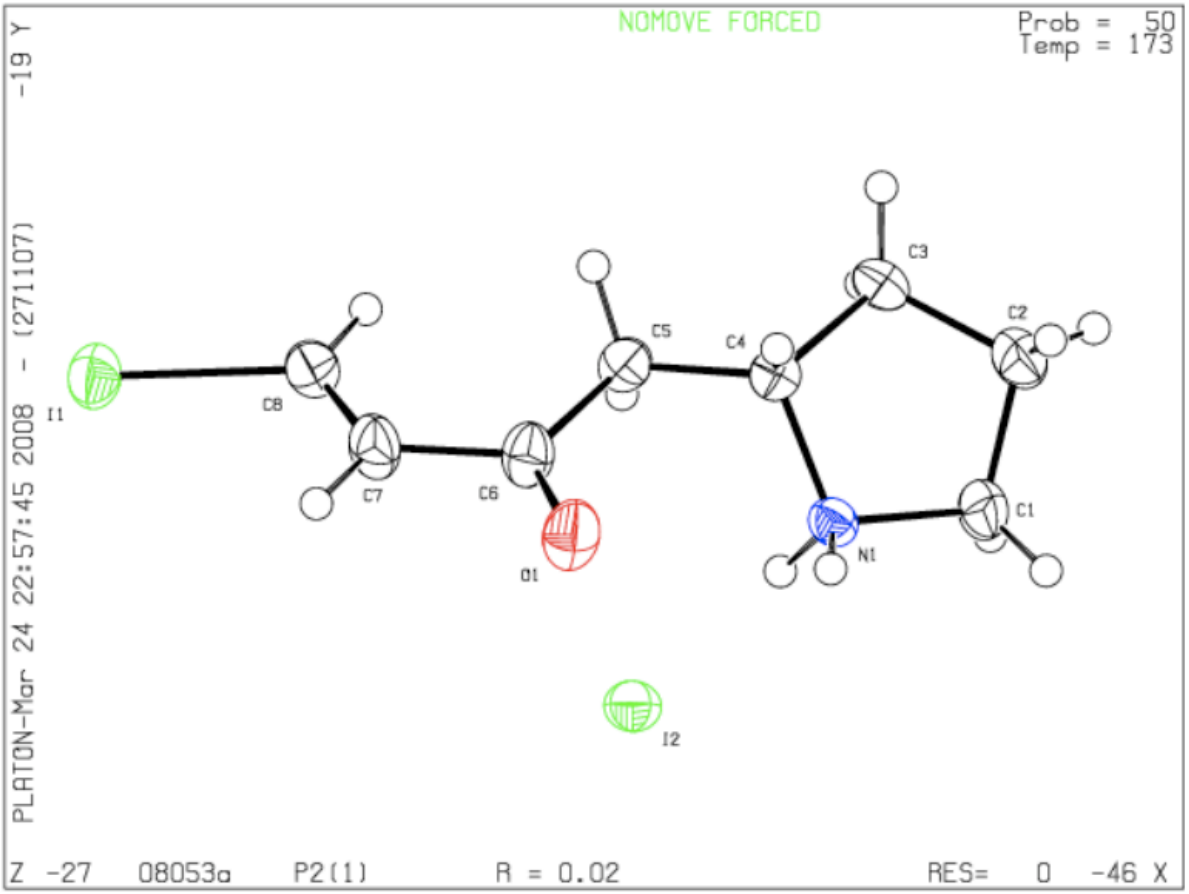
NOMOVE FORCED
Prob = 50
Temp = 173
-19 Y
PLATON-Mar 24 22:57:45 2008 - (271107)
I1
C8
C7
C6
O1
C5
C4
C3
C2
C1
N1
I2
Z -27 08053a P2(1) R = 0.02 RES= 0 -46 X

BIBLIOGRAPHY

1. Bhavan, B. V., In *Selected Medicinal Plants of India*, Tata Press: Bombay, India, 1992; pp 333-336.

2. Suffness, M.; Cordell, G. A., In The Alkaloids: Chemistry and Pharmacology. In *The Alkaloids*, Brossi, A., Ed. Academic Press: Orlando, FL, 1985; Vol. 25, pp 156-163.

3. Chemler, S. R. Phenanthroindolizidines and phenanthroquinolizidines: promising alkaloids for anti-cancer therapy. *Curr. Bioact. Compd.* **2009,** *5* (1), 2-19.

4. Li, Z.; Jin, Z.; Huang, R. Isolation, total synthesis and biological activity of phenanthroindolizidine and phenanthroquinolizidine alkaloids. *Synthesis* **2001,** (16), 2365-2378.

5. Gellert, E. The indolizidine alkaloids. *J. Nat. Prod.* **1982,** *45* (1), 50-73.

6. Chopra, R. N.; Chopra, I. C.; Handa, K. L.; Kapur, L. D., *Tylophora asthmatica*. In *Indigenous drugs of India*, Academic Publishers: Calcutta, 1958; pp 431-433.

7. Ratnagiriswaran, A. N.; Venkatachalam, K. The chemical examination of *Tylophora asthmatica* and the isolation of the alkaloids tylophorine and tylophorinine. *Indian J. Med. Res.* **1935,** *22*, 433-441.

8. Govindachari, T. R.; Lakshmikantham, M. V.; Pai, B. R.; Rajappa, S. Chemical examination of *Tylophora asthmatica*. III. Complete structure of tylophorine. *Tetrahedron* **1960,** *9*, 53-57.

9. Govindachari, T. R.; Lakshmikantham, M. V.; Nagarajan, N.; Pai, B. R. Chemical examination of *Tylophora asthmatica*. II. *Tetrahedron* **1958,** *4*, 311-324.

10. Govindachari, T. R.; Lakshmikantham, M. V.; Nagarajan, K.; Pai, B. R. Structure of tylophorine. *Chem. Ind.* **1957**, 1484-1485.

11. Govindachari, T. R.; Pai, B. R.; Nagarajan, K. Chemical examination of *Tylophora asthmatica* I. *J. Chem. Soc.* **1954**, 2801-2803.

12. Govindachari, T. R.; Pai, B. R.; Ragade, I. S.; Rajappa, S.; Viswanathan, N. Chemical examination of *Tylophora asthmatica*. V. Structure of tylophorinine. *Tetrahedron* **1961,** *14*, 288-295.

13. Govindachari, T. R.; Lakshmikantham, M. V.; Rajadurai, S. Chemical Examination of *Tylophora asthmatica* - IV. Synthesis of Tylophorine. *Tetrahedron* **1961,** *14*, 284-287.

14. Gellert, E.; Rudzats, R.; Craig, J. C.; Roy, S. K.; Woodard, R. W. The absolute configuration of cryptopleurine and tylocrebrine. *Aust. J. Chem.* **1978,** *31* (9), 2095-2097.

15. Buckley, T. F., III; Henry, R. Amino acids as chiral educts for asymmetric products. Chirally specific syntheses of tylophorine and cryptopleurine. *J. Org. Chem.* **1983,** *48* (23), 4222-4232.

16. de la Lande, I. S. The alkaloids of Cryptocarya pleurosperma. *Aust. J. Exp. Biol. Med. Sci.* **1948,** *26*, 181-187.

17. Fridrichsons, J.; Mathieson, A. M. Structure of a derivative of cryptopleurine. *Nature* **1954,** *173*, 732-733.

18. Gellert, E. Structure of cryptopleurine and Hofmann degradation of some quinolizidine alkaloids. *Aust. J. Chem.* **1956,** *9*, 489-496.

19. Gellert, E. The Hofmann degradation of some quinolizidine alkaloids. *Chem. Ind.* **1955**, 983-984.

20. Gellert, E.; Govindachari, T. R.; Lakshmikantham, M. V.; Ragade, I. S.; Rudzats, R.; Viswanathan, N. Alkaloids of *Tylophora crebriflora*: Structure and synthesis of tylocrebrine, a new phenanthroindolizidine alkaloid. *J. Chem. Soc.* **1962**, 1008-1014.

21. Gellert, E.; Rudzats, R. Antileukemia activity of tylocrebrine. *J. Med. Chem.* **1964,** *7* (3), 361-362.

22. Damu, A. G.; Kuo, P.-C.; Shi, L.-S.; Li, C.-Y.; Kuoh, C.-S.; Wu, P.-L.; Wu, T.-S. Phenanthroindolizidine alkaloids from the stems of *Ficus septica*. *J. Nat. Prod.* **2005,** *68* (7), 1071-1075.

23. Damu, A. G.; Kuo, P. C.; Shi, L. S.; Li, C. Y.; Su, C. R.; Wu, T. S. Cytotoxic phenanthroindolizidine alkaloids from the roots of *Ficus septica*. *Planta Med.* **2009,** *75* (10), 1152-1156.

24. Stærk, D.; Christensen, J.; Lemmich, E.; Duus, J. O.; Olsen, C. E.; Jaroszewski, J. W. Cytotoxic activity of some phenanthroindolizidine *N*-oxide alkaloids from *Cynanchum vincetoxicum*. *J. Nat. Prod.* **2000,** *63* (11), 1584-1586.

25. Johns, S. R.; Lamberton, J. A.; Sioumis, A. A.; Willing, R. I. New alkaloids from *Cryptocarya pleurosperma*: Structures of cryptopleuridine and cryptopleurospermine. *Aust. J. Chem.* **1970,** *23* (2), 353-361.

26. Bhutani, K. K.; Ali, M.; Atal, C. K. Alkaloids from *Tylophora hirsuta*. *Phytochemistry* **1984,** *23* (8), 1765-1769.

27. Ali, M.; Bhutani, K. K. Investigations of medicinal plants. Part 9. Minor alkaloids of *Tylophora hirsuta*. *Phytochemistry* **1987,** *26* (7), 2089-2092.

28. Pettit, G. R.; Goswami, A.; Cragg, G. M.; Schmidt, J. M.; Zou, J.-C. Antineoplastic agents, 103. The isolation and structure of hypoestestatins 1 and 2 from the East African *Hypoestes verticillaris*. *J. Nat. Prod.* **2004,** *47* (6), 913-919.

29. Bhutani, K. K.; Ali, M.; Atal, C. K. 13a-Hydroxytylophorine from *Tylophora hirsuta*. *Phytochemistry* **1985,** *24* (11), 2778-2780.

30. Ali, M.; Ansari, S. H.; Qadry, J. S. Rare phenanthroindolizidine alkaloids and a substituted phenanthrene, tyloindane, from *Tylophora indica*. *J. Nat. Prod.* **1991,** *54* (5), 1271-1278.

31. Loder, J. W. Synthesis of pleurospermine, the leaf alkaloid of *Cryptocarya pleurosperma*. *Aust. J. Chem.* **1962,** *15*, 296-300.

32. Mulchandani, N. B.; Iyer, S. S.; Badheka, L. P. Biosynthesis of tylophorine. I. Incorporation of tyrosine-2-14C into tylophorine. *Phytochemistry* **1969,** *8* (10), 1931-1935.

33. Mulchandani, N. B.; Iyer, S. S.; Badheka, L. P. Biosynthesis of tylophorine. II. Incorporation of phenylalanine-2-14C into tylophorine. *Phytochemistry* **1971,** *10* (5), 1047-1050.

34. Mulchandani, N. B.; Iyer, S. S.; Badheka, L. P. Incorporation of cinnamic acid-2-14C into tylophorine. *Phytochemistry* **1976,** *15* (11), 1697-1699.

35. Hedges, S. H.; Herbert, R. B.; Knagg, E.; Pasupathy, V. The implication of phenylacetaldehydes in the biosynthesis of the phenanthroindolizidine alkaloid, tylophorine. *Tetrahedron Lett.* **1988,** *29* (7), 807-810.

36. Barton, D. H. R. The biogenesis of phenolic alkaloids. *Proc. Chem. Soc., London* **1963,** 293-299.

37. Chitnis, M. P.; Khandalekar, D. D.; Adwankar, M. K.; Sahasrabudhe, M. B. Anti-cancer activity of the extracts of stem and leaf of *Tylophora indica*. *Indian J. Med. Res.* **1972,** *60* (3), 359-362.

38. Shivpuri, D. N.; Menon, M. P.; Parkash, D. Preliminary studies in *Tylophora indica* in the treatment of asthma and allergic rhinitis. *J. Assoc. Physicians India* **1968,** *16* (1), 9-15.

39. Shivpuri, D. N.; Menon, M. P.; Prakash, D. A crossover double-blind study on *Tylophora indica* in the treatment of asthma and allergic rhinitis. *J. Allergy* **1969,** *43* (3), 145-150.

40. Shivpuri, D. N.; Singhal, S. C.; Parkash, D. Treatment of asthma with an alcoholic extract of tylophora indica: a cross-over, double-blind study. *Ann. Allergy* **1972,** *30* (7), 407-412.

41. Gupta, S.; George, P.; Gupta, V.; Tandon, V. R.; Sundaram, K. R. *Tylophora indica* in bronchial asthma—a double blind study. *Indian J. Med. Res.* **1979,** *69*, 981-989.

42. Thiruvengadam, K. V.; Haranath, K.; Sudarsan, S.; Sekar, T. S.; Rajagopal, K. R.; Zacharian, M. G.; Devarajan, T. V. *Tylophora indica* in bronchial asthma (a controlled comparison with a standard anti-asthmatic drug). *J. Indian Med. Assoc.* **1978,** *71* (7), 172-176.

43. Mathew, K. K.; Shivpuri, D. N. Treatment of asthma with alkaloids of *Tylophora indica*: a double-blind study. *Aspects Allergy Appl. Immunol.* **1974,** *7*, 166-179.

44. Gore, K. V.; Rao, A. K.; Guruswamy, M. N. Physiological studies with *Tylophora asthmatica* in bronchial asthma. *Indian J. Med. Res.* **1980,** *71*, 144-148.

45. Tillie-Leblond, I.; Montani, D.; Crestani, B.; De Blic, J.; Humbert, M.; Tunon-de-Lara, M.; Magnan, A.; Roche, N.; Ostinelli, J.; Chanez, P. Relation between inflammation and symptoms in asthma. *Allergy* **2009,** *64* (3), 354-367.

46. Huntley, A.; Ernst, E. Herbal medicines for asthma: a systematic review. *Thorax* **2000,** *55* (11), 925-929.

47. Ernst, E. Complementary therapies for asthma: what patients use. *J. Asthma* **1998,** *35* (8), 667-671.

48. Haranath, P. S.; Shyamalakumari, S. Experimental study on mode of action of *Tylophora asthmatica* in bronchial asthma. *Indian J. Med. Res.* **1975,** *63* (5), 661-670.

49. Atal, C. K.; Sharma, M. L.; Kaul, A.; Khajuria, A. Immunomodulating agents of plant origin. I: Preliminary screening. *J. Ethnopharmacol.* **1986,** *18* (2), 133-141.

50. Udupa, A. L.; Udupa, S. L.; Guruswamy, M. N. The possible site of anti-asthmatic action of *Tylophora asthmatica* on pituitary-adrenal axis in albino rats. *Planta Med.* **1991,** *57* (5), 409-413.

51. Ganguly, T.; Sainis, K. B. Inhibition of cellular immune responses by *Tylophora indica* in experimental models. *Phytomedicine* **2001,** *8* (5), 348-355.

52. Ganguly, T.; Badheka, L. P.; Sainis, K. B. Immunomodulatory effect of *Tylophora indica* on Con A induced lymphoproliferation. *Phytomedicine* **2001,** *8* (6), 431-437.

53. Hoffman, H. Acceleration and retardation of the process of axon-sprouting in partially devervated muscles. *Aust. J. Exp. Biol. Med. Sci.* **1952,** *30* (6), 541-566.

54. Chopra, R. N.; Ghosh, N. N.; Bose, J. B.; Ghosh, S. Chemical and pharmacological investigation of *Tylophora asthmatica*. *Arch. Pharm. Ber. Dtsch. Pharm. Ges.* **1937,** *275*, 236-242.

55. Donaldson, G. R.; Atkinson, M. R.; Murray, A. W. Inhibition of protein synthesis in Ehrlich ascites-tumour cells by the phenanthrene alkaloids tylophorine, tylocrebrine and cryptopleurine. *Biochem. Biophys. Res. Commun.* **1968,** *31* (1), 104-109.

56. Su, C.-R.; Damu Amooru, G.; Chiang, P.-C.; Bastow Kenneth, F.; Morris-Natschke Susan, L.; Lee, K.-H.; Wu, T.-S. Total synthesis of phenanthroindolizidine alkaloids (±)-antofine, (±)-deoxypergularinine, and their dehydro congeners and evaluation of their cytotoxic activity. *Bioorg. Med. Chem.* **2008,** *16* (11), 6233-6241.

57. Stærk, D.; Lykkeberg, A. K.; Christensen, J.; Budnik, B. A.; Abe, F.; Jaroszewski, J. W. *In vitro* cytotoxic activity of phenanthroindolizidine alkaloids from *Cynanchum incetoxicum* and *Tylophora tanakae* against drug-sensitive and multidrug-resistant cancer cells. *J. Nat. Prod.* **2002,** *65* (9), 1299-1302.

58. Gao, W.; Lam, W.; Zhong, S.; Kaczmarek, C.; Baker, D. C.; Cheng, Y.-C. Novel mode of action of tylophorine analogs as antitumor compounds. *Cancer Res.* **2004,** *64* (2), 678-688.

59. Paull, K. D.; Hamel, E.; Malspeis, L. Prediction of biochemical mechanism of action from the *in vitro* antitumor screen of the National Cancer Institute. *Cancer Chemother. Agents* **1995**, 9-45.

60. Gao, W.; Bussom, S.; Grill, S. P.; Gullen, E. A.; Hu, Y.-C.; Huang, X.; Zhong, S.; Kaczmarek, C.; Gutierrez, J.; Francis, S.; Baker, D. C.; Yu, S.; Cheng, Y.-C. Structure-activity studies of phenanthroindolizidine alkaloids as potential antitumor agents. *Bioorg. Med. Chem. Lett.* **2007,** *17* (15), 4338-4342.

61. Huang, X.; Gao, S.; Fan, L.; Yu, S.; Liang, X. Cytotoxic alkaloids from the roots of *Tylophora atrofolliculata*. *Planta Med.* **2004,** *70* (5), 441-445.

62. Gao, W.; Chen, A. P.-C.; Leung, C.-H.; Gullen, E. A.; Fuerstner, A.; Shi, Q.; Wei, L.; Lee, K.-H.; Cheng, Y.-C. Structural analogs of tylophora alkaloids may not be functional analogs. *Bioorg. Med. Chem. Lett.* **2008,** *18* (2), 704-709.

63. Fu, Y.; Lee Sang, K.; Min, H.-Y.; Lee, T.; Lee, J.; Cheng, M.; Kim, S. Synthesis and structure-activity studies of antofine analogues as potential anticancer agents. *Bioorg. Med. Chem. Lett.* **2007,** *17* (1), 97-100.

64. Yang, C.-W.; Chuang, T.-H.; Wu, P.-L.; Huang, W.-H.; Lee, S.-J. Anti-inflammatory effects of 7-methoxycryptopleurine and structure-activity relations of phenanthroindolizidines and phenanthroquinolizidines. *Biochem. Biophys. Res. Commun.* **2007,** *354* (4), 942-948.

65. Abe, F.; Hirokawa, M.; Yamauchi, T.; Honda, K.; Hayashi, N.; Ishii, M.; Imagawa, S.; Iwahana, M. Further investigation of phenanthroindolizidine alkaloids from *Tylophora tanakae*. *Chem. Pharm. Bull.* **1998,** *46* (5), 767-769.

66. Fu, Y.; Lee, S. K.; Min, H. Y.; Lee, T.; Lee, J.; Cheng, M.; Kim, S. Synthesis and structure-activity studies of antofine analogues as potential anticancer agents. *Bioorg Med. Chem. Lett.* **2007,** *17* (1), 97-100.

67. *Data acquired from Developmental Therapeutics Program NCI/NIH.* http://dtp.nci.nih.gov/

68. Chuang, T. H.; Lee, S. J.; Yang, C. W.; Wu, P. L. Expedient synthesis and structure-activity relationships of phenanthroindolizidine and phenanthroquinolizidine alkaloids. *Org. Biomol. Chem.* **2006,** *4* (5), 860-867.

69. Wei, L.; Brossi, A.; Kendall, R.; Bastow, K. F.; Morris-Natschke, S. L.; Shi, Q.; Lee, K.-H. Antitumor agents 251: Synthesis, cytotoxic evaluation, and structure-activity relationship studies of phenanthrene-based tylophorine derivatives (PBTs) as a new class of antitumor agents. *Bioorg. Med. Chem.* **2006,** *14* (19), 6560-6569.

70. Zhang, S. X.; Wei, L. Y.; Bastow, K.; Zheng, W. F.; Brossi, A.; Lee, K. H.; Tropsha, A. Antitumor Agents 252. Application of validated QSAR models to database mining: discovery of novel tylophorine derivatives as potential anticancer agents. *J. Comput. Aided Mol. Des.* **2007,** *21* (1-3), 97-112.

71. Lin, J. C.; Yang, S. C.; Hong, T. M.; Yu, S. L.; Shi, Q.; Wei, L.; Chen, H. Y.; Yang, P. C.; Lee, K.-H. Phenanthrene-based tylophorine-1 (PBT-1) inhibits lung cancer cell growth through the Akt and NF-κB pathways. *J. Med. Chem.* **2009,** *52* (7), 1903-1911.

72. Donaldson, G. R.; Atkinson, M. R.; Murray, A. W. Inhibition of protein biosynthesis in Ehrlich ascites-tumor cells by the phenanthrene alkaloids tylophorine, tylocrebrine, and cryptopleurine. *Biochem. Biophys. Res. Commun.* **1968,** *31*, 104-109.

73. Haslam, J. M.; Davey, P. J.; Linnane, A. W. Differentiation *in vitro* by phenanthrene alkaloids of yeast mitochondria protein synthesis from ribosomal systems of both yeast and bacteria. *Biochem. Biophys. Res. Commun.* **1968,** *33*, 368-373.

74. Huang, M. T.; Grollman, A. P. Mode of action of tylocrebrine: Effects on protein and nucleic acid synthesis. *Mol. Pharmacol.* **1972,** *8*, 583-550.

75. Bucher, K.; Skogerson, L. Cryptopleurine - An inhibitor of translocation. *Biochemistry (Mosc)*. **1976,** *15*, 4755-4759.

76. Skogerson, L.; McLaughlin, C.; Wakatama, E. Modification of ribosomes in cryptopleurine-resistant mutants of yeast. *J. Bacteriol.* **1973,** *116* (2), 818-822.

77. Grant, P.; Sánchez, L.; Jiménez, A. Cryptopleurine resistance: Genetic locus for a 40S ribosomal componenet in *Saccharomyces cerevisiae*. *J. Bacteriol.* **1974,** *120*, 1308-1314.

78. Entner, N.; Grollman, A. P. Inhibition of protein synthesis. Mechanism of amebicide action of emetine and other structurally related compounds. *J. Protozool.* **1973,** *20* (1), 160-163.

79. Gupta, R. S.; Krepinsky, J. J.; Siminovitch, L. Structural determinants responsible for the biological activity of (–)-emetine, (–)-cryptopleurine, and (–)-tylocrebrine: structure-activity relationship among related compounds. *Mol. Pharmacol.* **1980,** *18* (1), 136-143.

80. Gupta, R. S.; Siminovich, L. Mutants of CHO cells resistant to the protein synthesis inhibitors, cryptopleurine and tylocrebrine: Genetic and biochemical evidence for common site of action of emetin, cryptopleurine, tylocrebrine, and tubulosine. *Biochemistry (Mosc)*. **1977,** *16*, 3209-3214.

81. Sollhuber, M.; Grande, M. T.; Trigo, G. G.; Vazquez, D.; Jimenez, A. Structure-activity relationships between cryptopleurine and related compounds acting on yeast cell-free systems. *Curr. Microbiol.* **1980,** *4* (2), 81-84.

82. Dolz, H.; Sollhuber, M.; Trigo, G. G.; Vazquez, D.; Jimenez, A. Synthesis and biological activity of [14a-3H]-cryptopleurine. *Anal. Biochem.* **1980,** *108* (2), 215-219.

83. Dölz, D.; Vázquez, D.; Jiménez, A. Quantitation of the specific interaction of [14a-^{3}H]-cryptopleurine with 80S and 40S ribosomal species from the yeast *Saccharomyces cerevisiae*. *Biochemistry (Mosc)*. **1982,** *21*, 3181-3187.

84. Pestka, S. Inhibitors of ribosome functions. *Annu. Rev. Microbiol.* **1971,** *25*, 487-562.

85. Chan, J.; Khan, S. N.; Harvey, I.; Merrick, W.; Pelletier, J. Eukaryotic protein synthesis inhibitors identified by comparison of cytotoxicity profiles. *RNA* **2004,** *10* (3), 528-543.

86. Watkins, S. J.; Norbury, C. J. Translation initiation and its deregulation during tumorigenesis. *Br. J. Cancer* **2002,** *86* (7), 1023-1027.

87. Graff, J. R.; Zimmer, S. G. Translational control and metastatic progression: enhanced activity of the mRNA cap-binding protein eIF-4E selectively enhances translation of metastasis-related mRNAs. *Clin. Exp. Metastasis* **2003,** *20* (3), 265-273.

88. Rinehart, K. L. Antitumor compounds from tunicates. *Med. Res. Rev.* **2000,** *20* (1), 1-27.

89. Ottenheijm, H. C.; Van den Broek, L. A. The development of sparsomycin as an anti-tumour drug. *Anticancer. Drug Des.* **1988,** *2* (4), 333-337.

90. Kantarjian, H. M.; Talpaz, M.; Santini, V.; Murgo, A.; Cheson, B.; O'Brien, S. M. Homoharringtonine: history, current research, and future direction. *Cancer* **2001,** *92* (6), 1591-1605.

91. Ganguly, T.; Khar, A. Induction of apoptosis in a human erythroleukemic cell line K562 by Tylophora alkaloids involves release of cytochrome c and activation of caspase 3. *Phytomedicine* **2002,** *9* (4), 288-295.

92. Lee, S. K.; Nam, K. A.; Heo, Y. H. Cytotoxic activity and G2/M cell cycle arrest mediated by antofine, a phenanthroindolizidine alkaloid isolated from *Cynanchum paniculatum*. *Planta Med.* **2003,** *69* (1), 21-25.

93. Wu, C. M.; Yang, C. W.; Lee, Y. Z.; Chuang, T. H.; Wu, P. L.; Chao, Y. S.; Lee, S. J. Tylophorine arrests carcinoma cells at G1 phase by downregulating cyclin A2 expression. *Biochem. Biophys. Res. Commun.* **2009,** *386* (1), 140-145.

94. Yan, J.; Luo, D.; Luo, Y.; Gao, X.; Zhang, G. Induction of G1 arrest and differentiation in MDA-MB-231 breast cancer cell by boehmeriasin A, a novel compound from plant. *Int. J. Gynecol. Cancer* **2006,** *16* (1), 165-170.

95. Hochegger, H.; Takeda, S.; Hunt, T. Cyclin-dependent kinases and cell-cycle transitions: Does one fit all? *Nat. Rev. Mol. Cell Biol.* **2008,** *9* (11), 910-916.

96. Sherr, C. J. Cancer cell cycles. *Science* **1996,** *274* (5293), 1672-1677.

97. Sherr, C. J. The Pezcoller lecture: cancer cell cycles revisited. *Cancer Res.* **2000,** *60* (14), 3689-3695.

98. Sherr, C. J.; Roberts, J. M. CDK inhibitors: Positive and negative regulators of G1-phase progression. *Genes Dev.* **1999,** *13* (12), 1501-1512.

99. Hanahan, D.; Weinberg, R. A. The hallmarks of cancer. *Cell* **2000,** *100* (1), 57-70.

100. Cai, X. F.; Jin, X. J.; Lee, D. H.; Yang, Y. T.; Lee, K.; Hong, Y. S.; Lee, J. H.; Lee, J. J. Phenanthroquinolizidine alkaloids from the roots of *Boehmeria pannosa* potently inhibit hypoxia-inducible factor-1 in AGS human gastric cancer cells. *J. Nat. Prod.* **2006,** *69* (7), 1095-1097.

101. Giaccia, A.; Siim, B. G.; Johnson, R. S. HIF-1 as a target for drug development. *Nat. Rev. Drug Discov.* **2003,** *2* (10), 803-811.

102. Semenza, G. L. Targeting HIF-1 for cancer therapy. *Nat. Rev. Cancer* **2003,** *3* (10), 721-732.

103. Banwell, M. G.; Bezos, A.; Burns, C.; Kruszelnicki, I.; Parish, C. R.; Su, S.; Sydnes, M. O. C8c-C15 Monoseco-analogues of the phenanthroquinolizidine alkaloids julandine and cryptopleurine exhibiting potent anti-angiogenic properties. *Bioorg. Med. Chem. Lett.* **2006,** *16* (1), 181-185.

104. Sydnes, M. O.; Bezos, A.; Burns, C.; Kruszelnicki, I.; Parish, C. R.; Su, S.; Rae, A. D.; Willis, A. C.; Banwell, M. G. Synthesis and biological evaluation of some enantiomerically pure C8c-C15 monoseco analogues of the phenanthroquinolizidine-type alkaloids cryptopleurine and julandine. *Aust. J. Chem.* **2008,** *61* (7), 506-520.

105. Luo, Y.; Liu, Y.; Luo, D.; Gao, X.; Li, B.; Zhang, G. Cytotoxic alkaloids from *Boehmeria siamensis*. *Planta Med.* **2003,** *69* (9), 842-845.

106. Wei, H.; Yan, J.; Liu, J.; Luo, D.; Zhang, J.; Gao, X. Genes involved in the anti-cancer effect of a potent new compound boehmeriasin A on breast cancer cell. *J. Med. Plants Res.* **2009,** *3* (1), 35-44.

107. Hayden, M. S.; Ghosh, S. Shared principles in NF-κB signaling. *Cell* **2008,** *132* (3), 344-362.

108. Hayden, M. S.; Ghosh, S. Signaling to NF-κB. *Genes Dev.* **2004,** *18* (18), 2195-2224.

109. Giuliani, C.; Napolitano, G.; Bucci, I.; Montani, V.; Monaco, F. NF-κB transcription factor: Role in the pathogenesis of inflammatory, autoimmune, and neoplastic diseases and therapy implications. *Clin. Ter.* **2001,** *152* (4), 249-253.

110. Xi, Z.; Zhang, R.; Yu, Z.; Ouyang, D.; Huang, R. Selective interaction between tylophorine B and bulged DNA. *Bioorg. Med. Chem. Lett.* **2005,** *15* (10), 2673-2677.

111. Turner, D. H. Bulges in nucleic acids. *Curr. Opin. Struct. Biol.* **1992,** *2* (3), 334-337.

112. Xi, Z.; Hwang, G. S.; Goldberg, I. H.; Harris, J. L.; Pennington, W. T.; Fouad, F. S.; Qabaja, G.; Wright, J. M.; Jones, G. B. Targeting DNA bulged microenvironments with synthetic agents: lessons from a natural product. *Chem. Biol.* **2002,** *9* (8), 925-931.

113. Xi, Z.; Zhang, R.; Yu, Z.; Ouyang, D. The interaction between tylophorine B and TMV RNA. *Bioorg. Med. Chem. Lett.* **2006,** *16* (16), 4300-4304.

114. Rao, K. N.; Bhattacharya, R. K.; Venkatachalam, S. R. Thymidylate synthase activity and the cell growth are inhibited by the β-carboline-benzoquinolizidine alkaloid deoxytubulosine. *J. Biochem. Mol. Toxicol.* **1998,** *12* (3), 167-173.

115. Rao, K. N.; Bhattacharya, R. K.; Veankatachalam, S. R. Inhibition of thymidylate synthase by pergularinine, tylophorinidine and deoxytubulosine. *Indian J. Biochem. Biophys.* **1999,** *36* (6), 442-448.

116. Rao, K. N.; Venkatachalam, S. R. Inhibition of dihydrofolate reductase and cell growth activity by the phenanthroindolizidine alkaloids pergularinine and tylophorinidine: *In vitro* cytotoxicity of these plant alkaloids and their potential as antimicrobial and anticancer agents. *Toxicol. In Vitro* **2000,** *14* (1), 53-59.

117. Gopalakrishnan, C.; Shankaranarayan, D.; Kameswarn, L.; Natarajan, S. Pharmacological investigations of tylophorine, the major alkaloid of *Tylophora indica*. *Indian J. Med. Res.* **1979,** *69* (3), 513-520.

118. Gopalakrishnan, C.; Shankaranarayanan, D.; Nazimudeen, S. K.; Kameswaran, L. Effect of tylophorine, a major alkaloid of *Tylophora indica*, on immunopathological and inflammatory reactions. *Indian J. Med. Res.* **1980,** *71* (June), 940-948.

119. You, X.; Pan, M.; Gao, W.; Shiah, H. S.; Tao, J.; Zhang, D.; Koumpouras, F.; Wang, S.; Zhao, H.; Madri, J. A.; Baker, D.; Cheng, Y. C.; Yin, Z. Effects of a novel tylophorine analog on collagen-induced arthritis through inhibition of the innate immune response. *Arthritis Rheum.* **2006,** *54* (3), 877-886.

120. Yang, C. W.; Chen, W. L.; Wu, P. L.; Tseng, H. Y.; Lee, S.-J. Anti-inflammatory mechanisms of phenanthroindolizidine alkaloids. *Mol. Pharmacol.* **2006,** *69* (3), 749-758.

121. Barnard, C. The c-mitotic activity of cryptopleurine. *Aust. J. Sci.* **1949,** *12*, 30-31.

122. Cleland, K. W. Effect of cryptopleurine on cell division. *Aust. J. Sci.* **1950,** *12*, 144-145.

123. Foldeak, S. Synthesis of analogs of cryptopleurine. *Tetrahedron* **1971,** *27* (15), 3465-3476.

124. Bhutani, K. K.; Sharma, G. L.; Ali, M. Plant based antiamoebic drugs; Part I. Antiamoebic activity of phenanthroindolizidine alkaloids; common structural determinants of activity with emetine. *Planta Med.* **1987,** *53* (6), 532-536.

125. Shimizu, T. Tylophorine insecticide. *Nogyo oyobi Engei* **1988,** *63* (1), 49-50.

126. Tripathi, A. K.; Singh, D.; Jain, D. C. Persistency of tylophorine as an insect antifeedant against *Spilosoma obliqua* Walker. *Phytother. Res.* **1990,** *4* (4), 144-147.

127. Krmpotic, E.; Farnsworth, N. R.; Messmer, W. M. Cryptopleurine, an active antiviral alkaloid from *Boehmeria cylindrica* (Urticaceae). *J. Pharm. Sci.* **1972,** *61* (9), 1508-1509.

128. Yao, Y. C.; Zhao, Y. G.; Gao, J.; An, T. Y.; Yu, X. S.; Li, G. R.; Huang, R. Q. Studies on bioactivities of *Cynanchum komarovii al*. as inhibiter against plant viruses. *J. Inner Mongolia Polytech. Univ. (Nat. Sci. Ed.)* **2002,** *21* (1), 1-4.

129. Wang, K.; Su, B.; Wang, Z.; Wu, M.; Li, Z.; Hu, Y.; Fan, Z.; Mi, N.; Wang, Q. Synthesis and antiviral activities of phenanthroindolizidine alkaloids and their derivatives. *J. Agric. Food Chem.* **2009**.

130. Hollingshead, M. G.; Alley, M. C.; Kaur, G.; Pacula-Cox, C. M.; Stinson, S. F., NCI Specialized Procedures in Preclinical Drug Evaluations. In *Anticancer Drug Development Guide: Preclinical Screening, Clinical Trials, and Approval, Second Edition*, Teicher, B. A.; Andrews, P. A., Eds. 2004; pp 153-156.

131. Dikshith, T. S.; Raizada, R. B.; Mulchandani, N. B. Toxicity of pure alkaloid of *Tylophora asthamatica* in male rat. *Indian J. Exp. Biol.* **1990,** *28* (3), 208-212.

132. Hitchcock, S. A.; Pennington, L. D. Structure-brain exposure relationships. *J. Med. Chem.* **2006,** *49* (26), 7559-7583.

133. Lovering, F.; Bikker, J.; Humblet, C. Escape from flatland: Increasing saturation as an approach to improving clinical success. *J. Med. Chem.* **2009,** *52* (21), 6752-6756.

134. Bradsher, C. K.; Berger, H. Aromatic cyclodehydration. XXXVI. The synthesis of (±)-cryptopleurine. *J. Am. Chem. Soc.* **1958,** *80*, 930-932.

135. Bradsher, C. K.; Berger, H. Synthesis of DL-cryptopleurine. *J. Am. Chem. Soc.* **1957,** *79*, 3287-3288.

136. McIver, A.; Young, D. D.; Deiters, A. A general approach to triphenylenes and azatriphenylenes: Total synthesis of dehydrotylophorine and tylophorine. *Chem. Commun.* **2008,** (39), 4750-4752.

137. Zeng, W.; Chemler, S. R. Total synthesis of (*S*)-(+)-tylophorine via enantioselective intramolecular alkene carboamination. *J. Org. Chem.* **2008,** *73* (15), 6045-6047.

138. Rossiter, L. M.; Slater, M. L.; Giessert, R. E.; Sakwa, S. A.; Herr, R. J. A concise palladium-catalyzed carboamination route to (±)-tylophorine. *J. Org. Chem.* **2009**. *74* (24), 9554-9557.

139. Pearson, W. H.; Walavalkar, R. Synthesis of (±)-tylophorine by the intramolecular cycloaddition of an azide with an ω-chloralkene. *Tetrahedron* **1994,** *50* (43), 12293-12304.

140. Comins, D. L.; Morgan, L. A. *N*-Acyldihydropyridones as synthetic intermediates: Synthesis of (±)-septicine and (±)-tylophorine. *Tetrahedron Lett.* **1991,** *32* (42), 5919-5922.

141. Comins, D. L.; Chen, X.; Morgan, L. A. Enantiopure *N*-acyldihydropyridones as synthetic intermediates: Asymmetric synthesis of (–)-septicine and (–)-tylophorine. *J. Org. Chem.* **1997,** *62* (21), 7435-7438.

142. Sheehan, S. M.; Padwa, A. New synthetic route to 2-pyridones and its application toward the synthesis of (±)-ipalbidine. *J. Org. Chem.* **1997,** *62* (3), 438-439.

143. Wang, K. L.; Lue, M. Y.; Wang, Q.-M.; Huang, R.-Q. Iron(III) chloride-based mild synthesis of phenanthrene and its application to total synthesis of phenanthroindolizidine alkaloids. *Tetrahedron* **2008,** *64* (32), 7504-7510.

144. Iida, H.; Kibayashi, C. Synthesis of (±)-julandine and (±)-cryptopleurine. *Tetrahedron Lett.* **1981,** *22* (20), 1913-1914.

145. Iida, H.; Tanaka, M.; Kibayashi, C. Synthesis of (±)-septicine and (±)-tylophorine by regioselective [3+2]-cycloaddition. *J. Chem. Soc., Chem. Commun.* **1983,** (6), 271-272.

146. Chauncy, B.; Gellert, E. Synthesis of phenanthroindolizidines. II. Synthesis of (±)-tylocrebrine, (±)-tylophorine, (±)-antofine, and (±)-2,3-dimethoxyphenanthroindolizidine. *Aust. J. Chem.* **1970,** *23* (12), 2503-2516.

147. Suzuki, H.; Aoyagi, S.; Kibayashi, C. Asymmetric Total synthesis of (*R*)-(–)-cryptopleurine and (*R*)-(–)-julandine via highly enantioselective amidoalkylations with *N*-acylhydrazonium salts. *J. Org. Chem.* **1995,** *60*, 6614-6122.

148. Suzuki, H.; Aoyagi, S.; Kibayashi, C. Enantioselective synthesis of (*R*)-(–)-cryptopleurine. *Tetrahedron Lett.* **1995,** *36*, 935-936.

149. Fürstner, A.; Kennedy, J. W. J. Total syntheses of the tylophora alkaloids cryptopleurine, (–)-antofine, (–)-tylophorine, and (–)-ficuseptine C. *Chem. Eur. J.* **2006,** *12* (28), 7398-7410.

150. Camacho-Davila, A.; Herndon James, W. Total synthesis of antofine using the net [5+5]-cycloaddition of γ, δ-unsaturated carbene complexes and 2-alkynylphenyl ketones as a key step. *J. Org. Chem.* **2006,** *71* (17), 6682-6685.

151. Kimball, F. S.; Tunoori, A. R.; Victory, S. F.; Dutta, D.; White, J. M.; Himes, R. H.; Georg, G. I. Synthesis, *in vitro*, and *in vivo* cytotoxicity of 6,7-diaryl-2,3,8,8a-tetrahydroindolizin-5(1H)-ones. *Bioorg. Med. Chem. Lett.* **2007,** *17*, 4703-4707.

152. Kimball, F. S.; Turunen, B. J.; Ellis, K. C.; Himes, R. H.; Georg, G. I. Enantiospecific synthesis and cytotoxicity of 7-(4-methoxyphenyl)-6-phenyl-2,3,8,8a-tetrahydroindolizin-5(1H)-one enantiomers. *Biorg. Med. Chem.* **2008,** *16* (8), 4367-4377.

153. Kimball, S. F.; Himes, R. H.; Georg, G. I. Synthesis and evaluation of heteroaromatic 6,7-diaryl-2,3,8,8a-tetrahydroindolizin-5(1H)-ones for cytotoxicity against the HCT-116 colon cancer cell line. *Bioorg. Med. Chem. Lett.* **2008,** *18* (11), 3248-3250.

154. Li, H.; Hu, T.; Wang, K.; Liu, Y.; Fan, Z.; Huang, R.; Wang, Q. Total synthesis and antiviral activity of enantio-enriched (+)-deoxytylophorinine. *Lett. Org. Chem.* **2006,** *3* (11), 806-810.

155. Sharma, V. M.; Adi Seshu, K. V.; Vamsee Krishna, C.; Prasanna, P.; Chandra, S. V.; Venkateswarlu, A.; Rajagopal, S.; Ajaykumar, R.; Deevi, D. S.; Rao Mamidi, N. V. S.; Rajagopalan, R. Novel 6,7-diphenyl-2,3,8,8a-tetrahydro-1H-indolizin-5-one analogues as cytotoxic agents. *Bioorg. Med. Chem. Lett.* **2003,** *13* (10), 1679-1682.

156. Suzuki, H.; Aoyagi, S.; Kibayashi, C. Asymmetric total synthesis of (*R*)-(–)-cryptopleurine and (*R*)-(–)-julandine via highly enantioselective amidoalkylations with *N*-acylhydrazonium salts. *J. Org. Chem.* **1995,** *60* (19), 6114-6122.

157. Suzuki, H.; Aoyagi, S.; Kibayashi, C. Enantioselective synthesis of (*R*)-(–)-cryptopleurine. *Tetrahedron Lett.* **1995,** *36* (6), 935-936.

158. Cragg, J. E.; Hedges, S. H.; Herbert, R. B. Synthesis of the alkaloids julandine and ipalbidine. Use of silicon(IV) chloride. *Tetrahedron Lett.* **1981,** *22* (22), 2127-2130.

159. Cragg, J. E.; Herbert, R. B. Synthesis of the alkaloids, 3',4'-dimethoxy-2-(2-piperidyl)acetophenone, julandine, and cryptopleurine. *J. Chem. Soc., Perkin Trans. 1* **1982,** (10), 2487-2490.

160. Herbert, R. B.; Knagg, E.; Organ, H. M.; Pasupathy, V.; Towlson, D. S. A biogenetically patterned synthesis of deoxycryptopleuridine. *Heterocycles* **1987,** *25* (1), 409-418.

161. Baxter, G.; Melville, J. C.; Robins, D. J. Stabilization of 3,4-dihydro-2H-pyrrole (1-Pyrroline) by complexation with zinc iodide. *Synlett* **1991**, 359-360.

162. Iida, H.; Watanbe, Y.; Tanaka, M.; Kibayashi, C. General synthesis of phenanthroindolizidine, phenanthroquinolizidine, and related alkaloids: Preparation of (±)-tylophorine, (±)-cryptopleurine, (±)-septicine, and (±)-julandine. *J. Org. Chem.* **1984,** *49*, 2412-2418.

163. Mangla, V. K.; Bhakuni, D. S. A new synthesis of septicine, a secophenanthroindolizidine alkaloid. *Indian J. Chem., Sect. B* **1980,** *19* (9), 748-749.

164. Mangla, V. K.; Bhakuni, D. S. Synthesis of substituted 6,7-diphenyl-1,2,3,5,8,8a-hexahydroindolizines. *Indian J. Chem., Sect. B* **1980,** *19* (11), 931-937.

165. Mangla, V. K.; Bhakuni, D. S. Synthesis of tylophorine. *Tetrahedron* **1980,** *36*, 2489-2490.

166. Cragg, J. E.; Herbert, R. B.; Jackson, F. B.; Moody, C. J.; Nicolson, I. T. Phenanthroindolizidine and related alkaloids: synthesis of tylophorine, septicine, and deoxytylophorinine. *J. Chem. Soc., Perkin Trans. 1* **1982,** (10), 2477-2485.

167. Iwasa, K.; Kamigauchi, M.; Takao, N.; Wiegrebe, W. The preparation of the biosynthetic precursor 3,7-dihydroxy-2,6-dimethoxyphenanthroindolizidine. *J. Nat. Prod.* **1988,** *51* (1), 172-175.

168. Padwa, A.; Sheehan, S. M.; Straub, C. S. An isomunchnone-based method for the synthesis of highly substituted 2(1H)-pyridones. *J. Org. Chem.* **1999,** *64* (23), 8648-8659.

169. Yamashita, S.; Kurono, N.; Senboku, H.; Tokuda, M.; Orito, K. Synthesis of phenanthro[9,10-b]indolizidin-9-ones, phenanthro[9,10-b]quinolizidin-9-one, and related benzolactams by Pd(OAc)2-catalyzed direct aromatic carbonylation. *Eur. J. Org. Chem.* **2009,** (8), 1173-1180.

170. Kim, S.; Lee, Y. M.; Lee, J.; Lee, T.; Fu, Y.; Song, Y.; Cho, J.; Kim, D. Expedient Syntheses of antofine and cryptopleurine via intramolecular 1,3-dipolar cycloaddition. *J. Org. Chem.* **2007,** *72* (13), 4886-4891.

171. Kim, S.; Lee, J.; Lee, T.; Park, H. G.; Kim, D. First asymmetric total synthesis of (–)-antofine by using an enantioselective catalytic phase transfer alkylation. *Org. Lett.* **2003,** *5* (15), 2703-2706.

172. Lebrun, S.; Couture, A.; Deniau, E.; Grandelaudon, P. Total syntheses of (±)-cryptopleurine, (±)-antofine and (±)-deoxypergularinine. *Tetrahedron* **1999,** *55* (9), 2659-2670.

173. Nordlander, J. E.; Njoroge, F. G. A short synthesis of (*S*)-(+)-tylophorine. *J. Org. Chem.* **1987,** *52* (8), 1627-1630.

174. Khatri, N. A.; Schmitthenner, H. F.; Shringarpure, J.; Weinreb, S. M. Synthesis of indolizidine alkaloids via the intramolecular imino Diels-Alder reaction. *J. Am. Chem. Soc.* **1981,** *103* (21), 6387-6393.

175. Bremmer, M. L.; Khatri, N. A.; Weinreb, S. M. Quinolizidine alkaloid synthesis via the intramolecular imino Diels-Alder reaction. *Epi*-Lupinine and cryptopleurine. *J. Org. Chem.* **1983,** *48* (21), 3661-3666.

176. Grieco, P. A.; Parker, D. T. Quinolizidine synthesis via intramolecular immonium ion based Diels-Alder reactions: Total synthesis of (±)-lupinine, (±)-epilupinine, (±)-cryptopleurine, and (±)-julandine. *J. Synth. Org. Chem. Jpn.* **1988,** *53*, 3325-3330.

177. Ihara, M.; Tsuruta, M.; Fukumoto, K.; Kametani, T. A versatile and stereocontrolled synthesis of quinolizidines and indolizidines using trialkylsilyl trifluoromethanesulfonate: total synthesis of (±)-tylophorine. *J. Chem. Soc., Chem. Commun.* **1985,** (17), 1159-1161.

178. Ihara, M.; Takino, Y.; Fukumoto, K.; Kametani, T. Enantioselective synthesis of naturally occurring (–)-tylophorine by way of an asymmetric intramolecular double Michael reaction. *Heterocycles* **1989,** *28* (1), 63-65.

179. Jin, Z.; Li, S. P.; Wang, Q. M.; Huang, R. Q. A concise total synthesis of *S*-(+)-tylophorine. *Chin. Chem. Lett.* **2004,** *15* (10), 1164-1166.

180. Gross, M.; Meienhofer, J. *The Peptides*. Academic Press: New York, 1979.

181. Iwao, M.; Mahalanabis, K. K.; Watanabe, M.; De Silva, S. O.; Snieckus, V. Directed ortho metalation of tertiary aromatic amides. A new N-hetero ring annelation method and synthesis of phenanthroquinolizidine and -indolizidine alkaloids. *Tetrahedron* **1983,** *39* (12), 1955-1962.

182. Iwao, M.; Watanabe, M.; De Silva, S. O.; Snieckus, V. Directed metalation of tertiary benzamides. Abbreviated syntheses of phenanthroquinolizidine and indolizidine alkaloids. *Tetrahedron Lett.* **1981,** *22* (25), 2349-2352.

183. Ciufolini, M. A.; Roschangar, F. A Unified strategy for the synthesis of phenanthroizidine alkaloids: Preparation of sterically congested pyridines. *J. Am. Chem. Soc.* **1996,** *118* (48), 12082-12089.

184. Kim, S.; Lee, T.; Lee, E.; Lee, J.; Fan, G.-J.; Lee, S. K.; Kim, D. Asymmetric total syntheses of (−)-antofine and (−)-cryptopleurine using (*R*)-(*E*)-4-(tributylstannyl)but-3-en-2-ol. *J. Org. Chem.* **2004,** *69* (9), 3144-3149.

185. Liepa, A. J.; Summons, R. E. An improved phenanthrene synthesis: A simple route to (±)-tylophorine. *J. Chem. Soc., Chem. Commun.* **1977**, 826.

186. Yerxa, B. R.; Yang, K.; Moore, H. W. Synthesis of (±)-septicine. *Tetrahedron* **1994,** *50* (21), 6173-6180.

187. Takeuchi, K.; Ishita, A.; Matsuo, J. I.; Ishibashi, H. Synthesis of 13a-methylphenanthroindolizidines using radical cascade cyclization: synthetic studies toward (±)-hypoestestatin 1. *Tetrahedron* **2007,** *63* (45), 11101-11107.

188. Ali, M.; Ansari, S. H.; Qadry, J. S. Rare phenanthroindolozidine alkaloids and a substituted phenanthrene tyloindane, from *Tylophora Indica*. *J. Nat. Prod.* **1991,** *54*, 1271-1278.

189. Michael, J. P.; De Koning, C. B.; Gravestock, D.; Hosken, G. D.; Howard, A. S.; Jungmann, C. M.; Krause, R. W. M.; Parsons, A. S.; Pelly, S. C.; Stanbury, T. V. Enaminones: versatile intermediates for natural product synthesis. *Pure Appl. Chem.* **1999,** *71* (6), 979-988.

190. Elassar, A. Z. A.; El-Khair, A. A. Recent developments in the chemistry of enaminones. *Tetrahedron* **2003,** *59* (43), 8463-8480.

191. Edafiogho, I. O.; Alexander, M. S.; Moore, J. A.; Farrar, V. A.; Scott, K. R. Anticonvulsant enaminones with emphasis on methyl 4-[(*p*-chlorophenyl)amino]-6-methyl-2-oxocyclohex-3-en-1-oate (ADD 196022). *Curr. Med. Chem.* **1994,** *1* (2), 159-175.

192. Edafiogho, I. O.; Kombian, S. B.; Ananthalakshmi, K. V. V.; Salama, N. N.; Eddington, N. D.; Wilson, T. L.; Alexander, M. S.; Jackson, P. L.; Hanson, C. D.; Scott, K. R. Enaminones: Exploring additional therapeutic activities. *J. Pharm. Sci.* **2007,** *96* (10), 2509-2531.

193. Eddington, N. D.; Cox, D. S.; Roberts, R. R.; Stables, J. P.; Powell, C. B.; Scott, K. R. Enaminones-versatile therapeutic pharmacophores. Further advances. *Curr. Med. Chem.* **2000,** *7* (4), 417-436.

194. Salama, N. N.; Eddington, N. D.; Payne, D.; Wilson, T. L.; Scott, K. R. Multidrug resistance and anticonvulsants: New studies with some enaminones. *Curr. Med. Chem.* **2004,** *11* (15), 2093-2103.

195. Cordell, G. A., *The Alkaloids: Chemistry and Biology*. Elsevier: Amsterdam, The Netherlands, 2003; Vol. 60, p 404.

196. Michael, J. P. Indolizidine and quinolizidine alkaloids. *Nat. Prod. Rep.* **2008,** *25* (1), 139-165.

197. Michael, J. P. Indolizidine and quinolizidine alkaloids. *Nat. Prod. Rep.* **2007,** *24* (1), 191-222.

198. Michael, J. P. Indolizidine and quinolizidine alkaloids. *Nat. Prod. Rep.* **2005,** *22* (5), 603-626.

199. Michael, J. P. Indolizidine and quinolizidine alkaloids. *Nat. Prod. Rep.* **2004,** *21* (5), 625-649.

200. Ege, M.; Wanner, K. T. Synthesis of β-amino acids based on oxidative cleavage of dihydropyridone derivatives. *Org. Lett.* **2004,** *6* (20), 3553-3556.

201. Garcia Mancheno, O.; Gomez Arrayas, R.; Adrio, J.; Carretero, J. C. Catalytic enantioselective approach to the stereodivergent synthesis of (+)-lasubines I and II. *J. Org. Chem.* **2007,** *72* (26), 10294-10297.

202. Shintani, R.; Tokunaga, N.; Doi, H.; Hayashi, T. A new entry of nucleophiles in rhodium-catalyzed asymmetric 1,4-addition reactions: Addition of organozinc reagents for the synthesis of 2-aryl-4-piperidones. *J. Am. Chem. Soc.* **2004,** *126* (20), 6240-6241.

203. Klegraf, E.; Knauer, S.; Kunz, H. Stereoselective synthesis of benzomorphan derivatives with perpivaloylated galactose as the chiral auxiliary. *Angew. Chem., Int . Ed.* **2006,** *45* (16), 2623-2626.

204. Knauer, S.; Kunz, H. Palladium-catalysed C-C coupling reactions in the enantioselective synthesis of 2,4-disubstituted 4,5-dehydropiperidines using galactosylamine as a stereodifferentiating auxiliary. *Tetrahedron: Asymmetry* **2005,** *16* (2), 529-539.

205. Kitagawa, H.; Kumura, K.; Atsumi, K. A novel synthesis of 2,3-disubstituted-4-pyridones from 4-methoxypyridine. *Chem. Lett.* **2006,** *35* (7), 712-713.

206. Donohoe, T. J.; Johnson, D. J.; Mace, L. H.; Thomas, R. E.; Chiu, J. Y. K.; Rodrigues, J. S.; Compton, R. G.; Banks, C. E.; Tomcik, P.; Bamford, M. J.; Ichihara, O. The

ammonia-free partial reduction of substituted pyridinium salts. *Org. Biomol. Chem.* **2006,** *4* (6), 1071-1084.

207. Lim, S. H.; Curtis, M. D.; Beak, P. Asymmetric syntheses of fused bicyclic compounds by conjugate additions of allylic organolithium species to activated olefins and subsequent cyclizations. *Org. Lett.* **2001,** *3* (5), 711-714.

208. Di Bussolo, V.; Fiasella, A.; Romano, M. R.; Favero, L.; Pineschi, M.; Crotti, P. Stereoselective synthesis of 2,3-unsaturated-aza-*O*-glycosides via new diastereoisomeric *N*-Cbz-imino glycal-derived allyl epoxides. *Org. Lett.* **2007,** *9* (22), 4479-4482.

209. Comins, D. L.; Killpack, M. O. Stereoselective addition of (triphenylsilyl)magnesium bromide to chiral 1-acyl-4-methoxypyridinium salts. Synthesis and reactions of enantiopure 1-acyl-2-(triphenylsilyl)-2,3-dihydro-4-pyridones. *J. Am. Chem. Soc.* **1992,** *114* (27), 10972-10974.

210. Thiel, J.; Wysocka, W.; Boczon, W. The steric structure of multiflorine methylation products. *Monatsh. Chem.* **1995,** *126* (2), 233-239.

211. Meyers, A. I.; Singh, S. Chemistry of enamino ketones. V. Addition of organometallic reagents and the formation of alkylated pyridinium and pyrrolinium salts. *Tetrahedron* **1969,** *25* (18), 4161-4166.

212. Ge, H.; Niphakis, M. J.; Georg, G. I. Palladium(II)-catalyzed direct arylation of enaminones using organotrifluoroborates. *J. Am. Chem. Soc.* **2008,** *130* (12), 3708-3709.

213. Wang, X.; Turunen, B. J.; Leighty, M. W.; Georg, G. I. Microwave-assisted Suzuki-Miyaura couplings on α-iodoenaminones. *Tetrahedron Lett.* **2007,** *48* (50), 8811-8814.

214. Felpin, F.-X. Practical and efficient Suzuki-Miyaura cross-coupling of 2-iodocycloenones with arylboronic acids catalyzed by recyclable Pd(0)/C. *J. Org. Chem.* **2005,** *70* (21), 8575-8578.

215. Sebesta, R.; Pizzuti, M. G.; Boersma, A. J.; Minnaard, A. J.; Feringa, B. L. Catalytic enantioselective conjugate addition of dialkylzinc reagents to *N*-substituted-2,3-dehydro-4-piperidones. *Chem. Commun.* **2005,** (13), 1711-1713.

216. Nakao, Y.; Chen, J.; Imanaka, H.; Hiyama, T.; Ichikawa, Y.; Duan, W.-L.; Shintani, R.; Hayashi, T. Organo[2-(hydroxymethyl)phenyl]dimethylsilanes as mild and reproducible agents for rhodium-catalyzed 1,4-addition reactions. *J. Am. Chem. Soc.* **2007,** *129* (29), 9137-9143.

217. Gini, F.; Hessen, B.; Minnaard, A. J. Palladium-catalyzed enantioselective conjugate addition of arylboronic acids. *Org. Lett.* **2005,** *7* (23), 5309-5312.

218. Jagt, R. B. C.; De Vries, J. G.; Feringa, B. L.; Minnaard, A. J. Enantioselective synthesis of 2-aryl-4-piperidones via rhodium/phosphoramidite-catalyzed conjugate addition of arylboroxines. *Org. Lett.* **2005,** *7* (12), 2433-2435.

219. Furman, B.; Lipner, G. Rhodium-catalyzed intramolecular conjugate addition of vinylstannanes to dihydro-4-pyridones: A simple method for stereoselective construction of 1-azabicyclic alkaloids. *Tetrahedron* **2008,** *64* (16), 3464-3470.

220. Focken, T.; Charette, A. B. Stereoselective synthesis of pyridinones: Application to the synthesis of (–)-barrenazines. *Org. Lett.* **2006,** *8* (14), 2985-2988.

221. Comins, D. L.; Zheng, X.; Goehring, R. R. Total synthesis of the putative structure of the lupin alkaloid plumerinine. *Org. Lett.* **2002,** *4* (9), 1611-1613.

222. Comins, D. L.; Brown, J. D. Addition of Grignard reagents to 1-acyl-4-methoxypyridinium salts. An approach to the synthesis of quinolizidinones. *Tetrahedron Lett.* **1986,** *27* (38), 4549-4552.

223. Comins, D. L.; Libby, A. H.; Al-awar, R. S.; Foti, C. J. Asymmetric synthesis of the lycopodium alkaloid, *N*-α-Acetyl-*N*-β-methylphlegmarine. *J. Org. Chem.* **1999,** *64* (7), 2184-2185.

224. Comins, D. L.; Zhang, Y. M. Anionic Cyclizations of chiral 2,3-dihydro-4-pyridones: A five-step, asymmetric synthesis of indolizidine 209D. *J. Am. Chem. Soc.* **1996,** *118* (48), 12248-12249.

225. Comins, D. L.; Hong, H. The addition of metallo enolates to chiral 1-acylpyridinium salts. An asymmetric synthesis of (–)-sedamine. *J. Org. Chem.* **1993,** *58* (19), 5035-5036.

226. Comins, D. L.; Benjelloun, N. R. Enantiopure *N*-acyldihydropyridones as synthetic intermediates. An asymmetric synthesis of solenopsin A. *Tetrahedron Lett.* **1994,** *35* (6), 829-832.

227. Comins, D. L.; Sahn, J. J. A Six-step asymmetric synthesis of (+)-hyperaspine. *Org. Lett.* **2005,** *7* (23), 5227-5228.

228. Comins, D. L.; Sandelier, M. J.; Grillo, T. A. Asymmetric synthesis of (+)-deoxoprosopinine. *J. Org. Chem.* **2001,** *66* (20), 6829-6832.

229. Comins, D. L.; Zhang, Y. M.; Joseph, S. P. Enantiopure *N*-acyldihydropyridones as synthetic intermediates: Asymmetric synthesis of benzomorphans. *Org. Lett.* **1999,** *1* (4), 657-659.

230. Klegraf, E.; Follmann, M.; Schollmeyer, D.; Kunz, H. Stereoselective synthesis of enantiomerically pure piperidine derivatives by *N*-galactosylation of pyridones. *Eur. J. Org. Chem.* **2004,** (15), 3346-3360.

231. Comins, D. L.; Goehring, R. R.; Joseph, S. P.; O'Connor, S. Asymmetric synthesis of 2-alkyl(aryl)-2,3-dihydro-4-pyridones by addition of Grignard reagents to chiral 1-acyl-4-methoxypyridinium salts. *J. Org. Chem.* **1990,** *55* (9), 2574-2576.

232. Hoesl, C. E.; Maurus, M.; Pabel, J.; Polborn, K.; Wanner, K. T. Generation of chiral *N*-acylpyridinium ions by means of silyl triflates and their diastereoselective trapping reactions: formation of *N*-acyldihydropyridines and *N*-acyldihydropyridones. *Tetrahedron* **2002,** *58* (33), 6757-6770.

233. Streith, J.; Boiron, A.; Paillaud, J. L.; Rodriguez-Perez, E. M.; Strehler, C.; Tschamber, T.; Zehnder, M. Chelate-controlled asymmetric synthesis of 2-substituted 2,3-dihydropyridin-4(1H)-ones: synthesis of D- and L-aminodeoxyaltrose derivatives. *Helv. Chim. Acta* **1995,** *78* (1), 61-72.

234. Comins, D. L.; Hong, H. Chiral dihydropyridones as synthetic intermediates. Asymmetric synthesis of (+)-elaeokanine A and (+)-elaeokanine C. *J. Am. Chem. Soc.* **1991,** *113* (17), 6672-6673.

235. Follmann, M.; Kunz, H. Desymmetrization reactions on 4-pyridone using carbohydrate templates. *Synlett* **1998,** (9), 989-990.

236. Comins, D. L.; Joseph, S. P.; Goehring, R. R. Asymmetric synthesis of 2-alkyl(aryl)-2,3-dihydro-4-pyridones by addition of Grignard reagents to chiral 1-acyl-4-methoxypyridinium salts. *J. Am. Chem. Soc.* **1994,** *116* (11), 4719-4728.

237. Zech, G.; Kunz, H. Synthesis of a polymer-bound galactosylamine and its application as an immobilized chiral auxiliary in stereoselective syntheses of piperidine and amino acid derivatives. *Chem. Eur. J.* **2004,** *10* (17), 4136-4149.

238. Alcaide, B.; Almendros, P.; Alonso, J. M.; Aly, M. F. Useful dual Diels-Alder behavior of 2-azetidinone-tethered aryl imines as azadienophiles or azadienes: A β -lactam-based stereocontrolled access to optically pure, highly functionalized indolizidine systems. *Chem. Eur. J.* **2003,** *9* (14), 3415-3426.

239. Badorrey, R.; Cativiela, C.; Diaz-de-Villegas, M. D.; Galvez, J. A. Highly convergent stereoselective synthesis of chiral key intermediates in the synthesis of Palinavir from imines derived from L-glyceraldehyde. *Tetrahedron* **2002,** *58* (2), 341-354.

240. Andreassen, T.; Haaland, T.; Hansen, L. K.; Gautun, O. R. Asymmetric aza-Diels-Alder reactions of an *N*-*tert*-butanesulfinyl α-imino ester. *Tetrahedron Lett.* **2007,** *48* (48), 8413-8415.

241. Kranke, B.; Hebrault, D.; Schultz-Kukula, M.; Kunz, H. Arabinosylamine in asymmetric syntheses of chiral piperidine alkaloids. *Synlett* **2004,** (4), 671-674.

242. Kranke, B.; Kunz, H. Stereoselective synthesis of chiral piperidine derivatives employing arabinopyranosylamine as the carbohydrate auxiliary. *Can. J. Chem.* **2006,** *84* (4), 625-641.

243. Newman, C. A.; Antilla, J. C.; Chen, P.; Predeus, A. V.; Fielding, L.; Wulff, W. D. Regulation of orthogonal functions in a dual catalyst system. Subservient role of a nonchiral Lewis acid in an asymmetric catalytic heteroatom Diels-Alder reaction. *J. Am. Chem. Soc.* **2007,** *129* (23), 7216-7217.

244. Josephsohn, N. S.; Snapper, M. L.; Hoveyda, A. H. Efficient and practical Ag-catalyzed cycloadditions between arylimines and the Danishefsky diene. *J. Am. Chem. Soc.* **2003,** *125* (14), 4018-4019.

245. Shang, D.; Xin, J.; Liu, Y.; Zhou, X.; Liu, X.; Feng, X. Enantioselective aza-Diels-Alder reaction of aldimines with "Danishefsky-type diene" catalyzed by chiral Scandium(III)-*N*,*N*'-dioxide complexes. *J. Org. Chem.* **2008,** *73* (2), 630-637.

246. Yao, S.; Johannsen, M.; Hazell, R. G.; Jorgensen, K. A. Catalytic enantioselective aza Diels-Alder reactions of imino dienophiles. *Angew. Chem., Int. Ed.* **1998,** *37* (22), 3121-3124.

247. Kobayashi, S.; Komiyama, S.; Ishitani, H. The first enantioselective aza-Diels-Alder reactions of imino dienophiles on use of a chiral zirconium catalyst. *Angew. Chem., Int. Ed.* **1998,** *37* (7), 979-981.

248. Jurcik, V.; Arai, K.; Salter, M. M.; Yamashita, Y.; Kobayashi, S. Niobium-catalyzed highly enantioselective aza-Diels-Alder reactions. *Adv. Synth. Catal.* **2008,** *350* (5), 647-651.

249. Cros, J. P.; Perez-Fuertes, Y.; Thatcher, M. J.; Arimori, S.; Bull, S. D.; James, T. D. Non-linear effects operate and dynamic ligand exchange occurs when chiral BINOL-boron Lewis acids are used for asymmetric catalysis. *Tetrahedron: Asymmetry* **2003,** *14* (14), 1965-1968.

250. Friedman, R. K.; Rovis, T. Predictable and regioselective insertion of internal unsymmetrical alkynes in rhodium-catalyzed cycloadditions with alkenyl isocyanates. *J. Am. Chem. Soc.* **2009,** *131* (30), 10775-10782.

251. Lee, E. E.; Rovis, T. Enantioselective synthesis of indolizidines bearing quaternary substituted stereocenters via rhodium-catalyzed [2+2+2]-cycloaddition of alkenyl isocyanates and terminal alkynes. *Org. Lett.* **2008,** *10* (6), 1231-1234.

252. Yu, R. T.; Lee, E. E.; Malik, G.; Rovis, T. Total synthesis of indolizidine alkaloid (–)-209D: Overriding substrate bias in the asymmetric rhodium-catalyzed [2+2+2]-cycloaddition. *Angew. Chem., Int. Ed.* **2009,** *48* (13), 2379-2382.

253. Yu, R. T.; Rovis, T. Enantioselective rhodium-catalyzed [2+2+2]-cycloaddition of alkenyl isocyanates and terminal alkynes: Application to the total synthesis of (+)-lasubine II. *J. Am. Chem. Soc.* **2006,** *128* (38), 12370-12371.

254. Yu, R. T.; Rovis, T. Rhodium-catalyzed [2+2+2]-cycloaddition of alkenyl isocyanates and alkynes. *J. Am. Chem. Soc.* **2006,** *128* (9), 2782-2783.

255. Turunen, B. J.; Georg, G. I. Amino acid-derived enaminones: A study in ring formation providing valuable asymmetric synthons. *J. Am. Chem. Soc.* **2006,** *128* (27), 8702-8703.

256. Cole, D. C. Recent stereoselective synthetic approaches to β-amino acids. *Tetrahedron* **1994,** *50* (32), 9517-9582.

257. Liu, M.; Sibi, M. P. Recent advances in the stereoselective synthesis of β-amino acids. *Tetrahedron* **2002,** *58* (40), 7991-8035.

258. Drexler, H. J.; You, J.; Zhang, S.; Fischer, C.; Baumann, W.; Spannenberg, A.; Heller, D. Chiral β-amino acid derivatives via asymmetric hydrogenation. *Org. Process Res. Dev.* **2003,** *7* (3), 355-361.

259. Ma, J. A. Recent developments in the catalytic asymmetric synthesis of α- and β-amino acids. *Angew. Chem., Int. Ed.* **2003,** *42* (36), 4290-4299.

260. Sewald, N. Synthetic routes towards enantiomerically pure β-amino acids. *Angew. Chem., Int. Ed.* **2003,** *42* (47), 5794-5795.

261. Lelais, G.; Seebach, D. β-2-Amino acids - Syntheses, occurrence in natural products, and components of β-peptides. *Biopolymers* **2004,** *76* (3), 206-243.

262. Seebach, D.; Kimmerlin, T.; Sebesta, R.; Campo, M. A.; Beck, A. K. How we drifted into peptide chemistry and where we have arrived at. *Tetrahedron* **2004,** *60* (35), 7455-7506.

263. Juaristi, E.; Soloshonok, V. A., *Enantioselective Synthesis of Beta-Amino Acids*. 2nd ed.; Wiley: Hoboken, 2005.

264. Baldwin, J. E. Rules for ring closure. *J. Chem. Soc., Chem. Commun.* **1976,** (18), 734-736.

265. Sakai, N.; Annaka, K.; Fujita, A.; Sato, A.; Konakahara, T. $InBr_3$-Promoted divergent approach to polysubstituted indoles and quinolines from 2-ethynylanilines: Switch from an intramolecular cyclization to an intermolecular dimerization by a type of terminal substituent group. *J. Org. Chem.* **2008,** *73* (11), 4160-4165.

266. Ding, Q.; Ye, Y.; Fan, R.; Wu, J. Selective synthesis of 2,3-disubstituted-2H-isoindol-1-ylphosphonate and 2,3-disubstituted-1,2-dihydroiso-quinolin-1-ylphosphonate via metal-tuned reaction of α-amino (2-alkynylphenyl)methylphosphonate. *J. Org. Chem.* **2007,** *72* (14), 5439-5442.

267. Kadzimirsz, D.; Hildebrandt, D.; Merz, K.; Dyker, G. Isoindoles and dihydroisoquinolines by gold-catalyzed intramolecular hydroamination of alkynes. *Chem. Commun.* **2006,** (6), 661-662.

268. Zhou, C.; Dubrovsky, A. V.; Larock, R. C. Diversity-oriented synthesis of 3-iodochromones and heteroatom analogues via ICl-induced cyclization. *J. Org. Chem.* **2006,** *71* (4), 1626-1632.

269. Hessian, K. O.; Flynn, B. L. Selective *endo*- and *exo*-iodocyclizations in the synthesis of quinolines and indoles. *Org. Lett.* **2006,** *8* (2), 243-246.

270. Tsubakiyama, M.; Sato, Y.; Mori, M. Synthesis of bicyclic heterocycles from propargyl esters using a palladium catalyst bearing a bidentate ligand. *Heterocycles* **2004,** *64*, 27-31.

271. Yao, T.; Larock, R. C. Regio- and stereoselective synthesis of isoindolin-1-ones via electrophilic cyclization. *J. Org. Chem.* **2005,** *70* (4), 1432-1437.

272. Mshvidobadze, E. V.; Vasilevsky, S. F.; Elguero, J. A new route to pyrazolo[3,4-c]- and -[4,3-c]pyridinones via heterocyclization of vic-substituted hydroxamic acids of acetylenylpyrazoles. *Tetrahedron* **2004,** *60* (51), 11875-11878.

273. Huang, Q.; Campo, M. A.; Yao, T.; Tian, Q.; Larock, R. C. Synthesis of fused polycycles by 1,4-palladium migration chemistry. *J. Org. Chem.* **2004,** *69* (24), 8251-8257.

274. Lavallee, J. F.; Berthiaume, G.; Deslongchamps, P. Intramolecular Michael addition of cyclic β-keto esters onto conjugated acetylenic ketones. *Tetrahedron Lett.* **1986,** *27* (45), 5455-5458.

275. Dillon, P. W.; Underwood, G. R. Cyclic allenes. I. Electronic structure and probable deformation of the allene linkage when included in a ring. INDO-MO [intermediate

neglect of differential overlap-molecular orbital] study. *J. Am. Chem. Soc.* **1974,** *96* (3), 779-787.

276. Slosse, P.; Hootele, C. Myrtine and epimyrtine, quinolizidine alkaloids from *Vaccinium Myrtillus*. *Tetrahedron* **1981,** *37* (24), 4287-4294.

277. Morley, C.; Knight, D. W.; Share, A. C. Complementary enantioselective approaches to the quinolizidine alkaloids lupinine and epilupinine by enolate Claisen rearrangements or direct allylation of piperidin-2-ylacetic acid derivatives. *J. Chem. Soc., Perkin Trans. 1* **1994,** (20), 2903-2907.

278. Harrison, J. R.; O'Brien, P.; Porter, D. W.; Smith, N. M. Studies towards the preparation of sparteine-like diamines for asymmetric synthesis. *J. Chem. Soc., Perkin Trans. 1* **1999,** (24), 3623-3631.

279. Williams, J. M.; Jobson, R. B.; Yasuda, N.; Marchesini, G.; Dolling, U. H.; Grabowski, E. J. J. A new general method for preparation of *N*-methoxy-*N*-methylamides - Application in direct conversion of an ester to a ketone. *Tetrahedron Lett.* **1995,** *36* (31), 5461-5464.

280. Wei, H.-X.; Timmons, C.; Farag, M. A.; Pare, P. W.; Li, G. MgI_2-Catalyzed halo aldol reaction: A practical approach to (*E*)-β-iodovinyl-β'-hydroxy ketones. *Org. Biomol. Chem.* **2004,** *2* (20), 2893-2896.

281. Wasserman, H. H.; Berger, G. D.; Cho, K. R. Transamidation reactions using β-lactams. The synthesis of homaline. *Tetrahedron Lett.* **1982,** *23* (4), 465-468.

282. Sibgatulin, D. A.; Volochnyuk, D. M.; Rusanov, E. B.; Kostyuk, A. N. Aminoalkylation of 'push-pull' enamines having a methyl group at the α-position with imines of methyl 3,3,3-trifluoropyruvate. *Synthesis* **2006,** (10), 1625-1630.

283. Volochnyuk, D. M.; Kostyuk, A. N.; Sibgatulin, D. A.; Petrenko, A. E. Unexpected addition of methyl 3,3,3-trifluoropyruvate to 'push-pull' enamines having a methyl group at α-position. *Synthesis* **2004,** (15), 2545-2549.

284. Pilli, R. A.; Ferreira de Oliveira, M. C. Recent progress in the chemistry of the Stemona alkaloids. *Nat. Prod. Rep.* **2000,** *17* (1), 117-127.

285. Seger, C.; Mereiter, K.; Kaltenegger, E.; Pacher, T.; Greger, H.; Hofer, O. Two pyrrolo[1,2-a]azepine type alkaloids from *Stemona collinsae* CRAIB: Structure elucidations, relationship to asparagamine A, and a new biogenetic concept of their formation. *Chem. Biodivers.* **2004,** *1* (2), 265-279.

286. *See supporting information in Chapter 6*.

287. Horton Douglas, A.; Bourne Gregory, T.; Smythe Mark, L. The combinatorial synthesis of bicyclic privileged structures or privileged substructures. *Chem. Rev.* **2003,** *103* (3), 893-930.

288. Corbet, J.-P.; Mignani, G. Selected patented cross-coupling reaction technologies. *Chem. Rev.* **2006,** *106* (7), 2651-2710.

289. King, A. O.; Yasuda, N., Organometallics in Process Chemistry. In *Topics in Organometallic Chemistry*, Larsen, R. D., Ed. Springer: Berlin, 2004; Vol. 6, pp 205-245.

290. Barder, T. E.; Walker, S. D.; Martinelli, J. R.; Buchwald, S. L. Catalysts for Suzuki-Miyaura coupling processes: Scope and studies of the effect of ligand structure. *J. Am. Chem. Soc.* **2005,** *127* (13), 4685-4696.

291. Barder, T. E.; Buchwald, S. L. Efficient catalyst for the Suzuki-Miyaura coupling of potassium aryl trifluoroborates with aryl chlorides. *Org. Lett.* **2004,** *6* (16), 2649-2652.

292. Miura, M.; Nomura, M. Direct arylation via cleavage of activated and unactivated C–H bonds. *Top. Curr. Chem.* **2002,** *219* (Cross-Coupling Reactions), 211-241.

293. Kakiuchi, F.; Chatani, N. Catalytic methods for C–H bond functionalization: Application in organic synthesis. *Adv. Synth. Catal.* **2003,** *345* (9+10), 1077-1101.

294. Labinger, J. A.; Bercaw, J. E. Understanding and exploiting C–H bond activation. *Nature* **2002,** *417* (6888), 507-514.

295. Miura, M.; Satoh, T. Arylation reactions via C–H bond cleavage. *Top. Organomet. Chem.* **2005,** *14*, 55-83.

296. Alberico, D.; Scott Mark, E.; Lautens, M. Aryl-aryl bond formation by transition-metal-catalyzed direct arylation. *Chem. Rev.* **2007,** *107* (1), 174-238.

297. Dick, A. R.; Sanford, M. S. Transition metal catalyzed oxidative functionalization of carbon-hydrogen bonds. *Tetrahedron* **2006,** *62* (11), 2439-2463.

298. Goldberg, K. I.; Goldman, A. S., Activation and functionalization of C–H bonds. In *ACS symposium series; 885*, American Chemical Society; Distributed by Oxford University Press: Washington, DC [New York], 2004; p 3.

299. Alberico, D.; Scott, M. E.; Lautens, M. Aryl-aryl bond formation by transition-metal-catalyzed direct arylation. *Chem. Rev.* **2007,** *107* (1), 174-238.

300. Daugulis, O.; Zaitsev, V. G. Anilide ortho-arylation by using C–H activation methodology. *Angew. Chem., Int. Ed.* **2005,** *44* (26), 4046-4048.

301. Shi, Z.; Li, B.; Wan, X.; Cheng, J.; Fang, Z.; Cao, B.; Qin, C.; Wang, Y. Suzuki-Miyaura coupling reaction by Pd(II)-catalyzed aromatic C–H bond activation directed by an *N*-alkyl acetamino group. *Angew. Chem., Int. Ed.* **2007,** *46* (29), 5554-5558.

302. Beccalli, E. M.; Broggini, G.; Martinelli, M.; Sottocornola, S. C–C, C–O, C–N Bond formation on sp^2 carbon by Pd(II)-catalyzed reactions involving oxidant agents. *Chem. Rev.* **2007,** *107* (11), 5318-5365.

303. Ackermann, L.; Vicente, R.; Kapdi, A. R. Transition metal-catalyzed direct arylation of (hetero)arenes by C–H bond cleavage. *Angew. Chem., Int. Ed.* **2009,** *48* (52), 9792-9826.

304. Yang, S. D.; Sun, C. L.; Fang, Z.; Li, B. J.; Li, Y. Z.; Shi, Z. J. Palladium-catalyzed direct arylation of (hetero)arenes with aryl boronic acids. *Angew. Chem., Int. Ed.* **2008,** *47* (8), 1473-1476.

305. Joucla, L.; Djakovitch, L. Transition metal-catalysed, direct and site-selective N1-, C2-or C3-arylation of the indole nucleus: 20 Years of improvements. *Adv. Synth. Catal.* **2009,** *351* (5), 673-714.

306. Lane, B. S.; Brown, M. A.; Sames, D. Direct palladium-catalyzed C-2 and C-3 arylation of indoles: A mechanistic rationale for regioselectivity. *J. Am. Chem. Soc.* **2005,** *127* (22), 8050-8057.

307. Garg, N. K.; Caspi, D. D.; Stoltz, B. M. The total synthesis of (+)-dragmacidin F. *J. Am. Chem. Soc.* **2004,** *126* (31), 9552-9553.

308. Jia, C.; Lu, W.; Oyamada, J.; Kitamura, T.; Matsuda, K.; Irie, M.; Fujiwara, Y. Novel Pd(II)- and Pt(II)-catalyzed regio- and stereoselective *trans*-hydroarylation of alkynes by simple arenes. *J. Am. Chem. Soc.* **2000,** *122* (30), 7252-7263.

309. Molander, G. A.; Ellis, N. Organotrifluoroborates: Protected boronic acids that expand the versatility of the Suzuki coupling reaction. *Acc. Chem. Res.* **2007,** *40* (4), 275-286.

310. Keith, J. A.; Henry, P. M. The mechanism of the Wacker reaction: A tale of two hydroxypalladations. *Angew. Chem., Int. Ed.* **2009,** *48* (48), 9038-9049.

311. Muzart, J. Palladium-catalysed oxidation of primary and secondary alcohols. *Tetrahedron* **2003,** *59* (31), 5789-5816.

312. Pelletier, G.; Larivee, A.; Charette, A. B. Highly regioselective intermolecular arylation of 1,2,3,4-tetrahydropyridines. *Org. Lett.* **2008,** *10* (21), 4791-4794.

313. Chen, X.; Chu, Y. Inhibitory effects of ipalbidine on respiratory burst and oxygen free radicals of leukocytes. *Zhongguo Yaolixue Tongbao* **1998,** *14* (3), 243-244.

314. Chen, X.; Chu, Y.; Han, G. Anti-inflammatory effect of ipalbidine. *Zhongguo Yaolixue Tongbao* **1998,** *14* (2), 167-169.

315. Wang, L.; Chu, Y. Effect of norepinephrinergic system on ipalbidine analgesia. *Yaoxue Xuebao* **1996,** *31* (11), 806-811.

316. Honda, T.; Namiki, H.; Nagase, H.; Mizutani, H. Enantiospecific synthesis of an indolizidine alkaloid, (+)-ipalbidine. *Tetrahedron Lett.* **2003,** *44* (15), 3035-3038.

317. Ikeda, M.; Shikaura, J.; Maekawa, N.; Daibuzono, K.; Teranishi, H.; Teraoka, Y.; Oda, N.; Ishibashi, H. A synthesis of (±)-ipalbidine using sulfur-controlled 6-exo selective radical cyclization of α-phenylthio amide. *Heterocycles* **1999,** *50* (1), 31-34.

318. Jefford, C. W.; Kubota, T.; Zaslona, A. Intramolecular carbenoid reactions of pyrrole derivatives. A total synthesis of (±)-ipalbidine. *Helv. Chim. Acta* **1986,** *69* (8), 2048-2061.

319. Danishefsky, S. J.; Vogel, C. A concise total synthesis of (±)-ipalbidine by application of the aldimine-diene cyclocondensation reaction. *J. Org. Chem.* **1986,** *51* (20), 3915-3916.

320. Liu, Z.; Lu, R.; Chen, Q.; Hong, H. Total synthesis of (*S*)-(+)-ipalbidine. *Huaxue Xuebao* **1985,** *43* (10), 992-995.

321. Iida, H.; Watanabe, Y.; Kibayashi, C. A formal total synthesis of ipalbidine. *J. Chem. Soc., Perkin Trans. 1* **1985,** (2), 261-266.

322. Iida, H.; Watanabe, Y.; Kibayashi, C. Formal synthesis of (±)-ipalbidine. *Chem. Lett.* **1983,** (8), 1195-1196.

323. Howard, A. S.; Gerrans, G. C.; Michael, J. P. Use of vinylogous urethanes in alkaloid synthesis: formal synthesis of ipalbidine. *J. Org. Chem.* **1980,** *45* (9), 1713-1715.

324. Hedges, S. H.; Herbert, R. B. An economical, biogenetically patterned synthesis of the alkaloid (±)-ipalbidine. *J. Chem. Res.* **1979,** (1), 1.

325. Stevens, R. V.; Luh, Y. General methods of alkaloid synthesis. XIII. The total synthesis of (±)-ipalbidine and (±)-septicine. *Tetrahedron Lett.* **1977,** (11), 979-982.

326. Wick, A. E.; Bartlett, P. A.; Dolphin, D. Total synthesis of ipalbidine and ipalbine. *Helv. Chim. Acta* **1971,** *54* (2), 513-522.

327. Govindachari, T. R.; Sidhaye, A. R.; Viswanathan, N. Synthesis of ipalbidine. *Tetrahedron* **1970,** *26* (15), 3829-3831.

328. Bhakuni, D. S.; Gupta, P. K. Synthesis of (±)-antofine and (±)-alkaloid C. *Indian J. Chem.* **1982,** *21B* (5), 393-395.

329. Pirc, S.; Bevk, D.; Golobic, A.; Stanovnik, B.; Svete, J. Transformation of amino acids into nonracemic 1-(heteroaryl)ethanamines by the enamino ketone methodology. *Helv. Chim. Acta* **2006,** *89* (1), 30-44.

330. Bidros, D. S.; Vogelbaum, M. A. Novel drug delivery strategies in neuro-oncology. *Neurotherapeutics* **2009,** *6* (3), 539-546.

331. Nagano, Y. Standard enthalpies of formation of phenanthrene and naphthacene. *J. Chem. Thermodyn.* **2002,** *34* (3), 377-383.

332. Nagano, Y.; Nakano, M. Strain energy of phenanthrene. *J. Chem. Thermodyn.* **2003,** *35* (9), 1403-1412.

333. Lapouyade, R.; Villeneuve, P.; Nourmamode, A.; Morand, J. P. The one-electron oxidation of biphenyl-2-ylethylenes - Subsequent chemical reactivity controlled by electron return or proton transfer. *J. Chem. Soc., Chem. Commun.* **1987,** (10), 776-778.

334. Speciale, S. G. MPTP: Insights into parkinsonian neurodegeneration. *Neurotoxicol. Teratol.* **2002,** *24* (5), 607-620.

335. Chuck, T. L.; McLaughlin, P. J.; Arizzi-LaFrance, M. N.; Salamone, J. D.; Correa, M. Comparison between multiple behavioral effects of peripheral ethanol administration in rats: sedation, ataxia, and bradykinesia. *Life Sci.* **2006,** *79* (2), 154-161.

336. Zhang, J.; Xiong, B.; Zhen, X.; Zhang, A. Dopamine D1 receptor ligands: Where are we now and where are we going. *Med. Res. Rev.* **2009,** *29* (2), 272-294.

337. Miyamoto, S.; Duncan, G. E.; Marx, C. E.; Lieberman, J. A. Treatments for schizophrenia: a critical review of pharmacology and mechanisms of action of antipsychotic drugs. *Mol. Psychiatry* **2005,** *10* (1), 79-104.

338. Hill, S. J. Distribution, properties, and functional characteristics of three classes of histamine receptor. *Pharmacol. Rev.* **1990,** *42* (1), 45-83.

339. Papay, R.; Gaivin, R.; Jha, A.; McCune, D. F.; McGrath, J. C.; Rodrigo, M. C.; Simpson, P. C.; Doze, V. A.; Perez, D. M. Localization of the mouse α1A-adrenergic receptor (AR) in the brain: α1AAR is expressed in neurons, GABAergic interneurons, and NG2 oligodendrocyte progenitors. *J. Comp. Neurol.* **2006,** *497* (2), 209-222.

340. Stone, E. A.; Lin, Y.; Itteera, A.; Quartermain, D. Pharmacological evidence for the role of central α1B-adrenoceptors in the motor activity and spontaneous movement of mice. *Neuropharmacology* **2001,** *40* (2), 254-261.

341. Shah, N.; Khurana, S.; Cheng, K.; Raufman, J. P. Muscarinic receptors and ligands in cancer. *Am. J. Physiol. Cell Physiol.* **2009,** *296* (2), 221-232.

342. Abrams, P.; Andersson, K. E.; Buccafusco, J. J.; Chapple, C.; De Groat, W. C.; Fryer, A. D.; Kay, G.; Laties, A.; Nathanson, N. M.; Pasricha, P. J.; Wein, A. J. Muscarinic receptors: their distribution and function in body systems, and the implications for treating overactive bladder. *Br. J. Pharmacol.* **2006,** *148* (5), 565-578.

343. Servent, D.; Fruchart-Gaillard, C. Muscarinic toxins: Tools for the study of the pharmacological and functional properties of muscarinic receptors. *J. Neurochem.* **2009,** *109* (5), 1193-1202.

344. Woo, J. C. S.; Fenster, E.; Dake, G. R. A Convenient Method for the Conversion of Hindered Carboxylic Acids to *N*-Methoxy-*N*-methyl (Weinreb) Amides. *J. Org. Chem.* **2004,** *69* (25), 8984-8986.

345. Epperson, M. T.; Gin, D. Y. Enantiospecific synthesis of the bridged pyrrolizidine core of asparagamine A: Dipolar cycloadditions of azomethine ylides derived from the sulfonylation of vinylogous amides. *Angew. Chem., Int. Ed.* **2002,** *41* (10), 1778-1780.

346. Amore, K. M.; Leadbeater, N. E.; Miller, T. A.; Schmink, J. R. Fast, easy, solvent-free, microwave-promoted Michael addition of anilines to α, β-unsaturated alkenes: synthesis of *N*-aryl functionalized β-amino esters and acids. *Tetrahedron Lett.* **2006,** *47* (48), 8583-8586.

347. Poon, C. Y.; Chiu, P. A synthesis of the tetracyclic carboskeleton of isaindigotidione. *Tetrahedron Lett.* **2004,** *45* (14), 2985-2988.

348. Ge, H.; Niphakis, M. J.; Georg, G. I. Palladium(II)-catalyzed direct arylation of enaminones using organotrifluoroborates. *J. Am. Chem. Soc.* **2008,** *130* (12), 3708-3709.

349. Hudlicky, T.; Olivo, H. F.; Natchus, M. G.; Umpierrez, E. F.; Pandolfi, E.; Volonterio, C. Synthesis of β-methoxy enones via a new 2-carbon extension of carboxylic acids. *J. Org. Chem.* **1990,** *55* (15), 4767-4770.

350. Guerry, P.; Neier, R. Reduction of 4-pyridinones. *Synthesis* **1984,** (6), 485-488.

351. Hattori, K.; Yamamoto, H. Asymmetric aza-Diels-Alder reaction: Enantio- and diastereoselective reaction of imine mediate by chiral Lewis acid. *Tetrahedron* **1993,** *49* (9), 1749-1760.

352. Plucinska, K.; Liberek, B. Synthesis of diazoketones derived from α-amino acids - Problem of side reactions. *Tetrahedron* **1987,** *43* (15), 3509-3517.

353. Vasanthakumar, G. R.; Patil, B. S.; Babu, V. V. S. Homologation of α-amino acids to β-amino acids using Boc_2O. *J. Chem. Soc., Perkin Trans. 1* **2002,** (18), 2087-2089.

354. Mahboobi, S.; Popp, A.; Burgemeister, T.; Schollmeyer, D. Diastereoselective synthesis of (–)-1-methyl-(3*S*,4*R*)-3,4-bis((2*S*)-*N*-(*tert*-butyloxycarbonyl)pyrrolidin-2-yl)-2-pyrrolidinone by an asymmetric Michael reaction. *Tetrahedron: Asymmetry* **1998,** *9* (13), 2369-2376.

355. Faber, L.; Wiegrebe, W. Stereospecific synthesis of a 9,11,12,13,13a,14-hexahydrodibenzo(*f*,*h*)pyrrolo(1,2-*b*)isoquinoline alkaloid. *Helv. Chim. Acta* **1973,** *56* (8), 2882-2884.

356. Dieter, R. K.; Sharma, R. R. A facile preparation of enecarbamates. *J. Org. Chem.* **1996,** *61* (12), 4180-4184.

357. Knight, D. W.; Share, A. C.; Gallagher, P. T. Homoproline homologation by enolate Claisen rearrangement or direct allylation: Syntheses of (–)-trachelanthamidine, (–)-isoretronecanol and (±)-turneforcidine. *J. Chem. Soc., Perkin Trans. 1* **1997,** (14), 2089-2097.

358. Tohma, H.; Morioka, H.; Takizawa, S.; Arisawa, M.; Kita, Y. Efficient oxidative biaryl coupling reaction of phenol ether derivatives using hypervalent iodine(III) reagents. *Tetrahedron* **2001,** *57* (2), 345-352.

359. Ihara, M.; Takino, Y.; Fukumoto, K.; Kametani, T. Asymmetric total syntheses of (–)-tylophorine via the highly enantioselective intramolecular double Michael reaction. *Tetrahedron Lett.* **1988,** *29* (33), 4135-4138.

360. Ihara, M.; Takino, Y.; Tomotake, M.; Fukumoto, K. Asymmetric total synthesis of the naturally occurring (*R*)-(–)-enantiomer of tylophorine via intramolecular double Michael reaction. *J. Chem. Soc., Perkin Trans. 1* **1990,** (8), 2287-2292.

361. *Modified from dissertation of Brandon Turunen.*